

Matching of Electroweak Parameters for the Parity Violating Interaction

Dissertation

zur Erlangung des Grades
„Doktor der Naturwissenschaften“
am Fachbereich Physik, Mathematik und Informatik
der Johannes Gutenberg-Universität in Mainz

Stephan Wezorke

geboren in Frankfurt am Main
Mainz, den 24. März 2023

1. Gutachter:
2. Gutachter:

Datum der mündlichen Prüfung: 25. Mai 2023

Acknowledgment

This work was supported by the Deutsche Forschungsgemeinschaft (DFG) in the framework of the collaborative research center SFB1044 “The Low-Energy Frontier of the Standard Model: From Quarks and Gluons to Hadrons and Nuclei”.

Abstract

This thesis investigates the formalism of matching in the electroweak sector of the Standard Model in the minimal modified subtraction scheme. Two different effective models are used to derive an expression of the weak mixing angle below the particle threshold of the W -boson at one-loop order. One model is based on a four-fermion contact interaction, while the other one resembles the electroweak sector of the Standard Model due to the introduction of a pseudo gauge boson Z' , whose mass is not generated by the Higgs mechanism. The findings are compared to already published results and shortcomings in the existing literature are pointed out. It is demonstrated that the previously published matching condition of the weak mixing angle for integrating out the W -boson is not based on a well-defined effective theory and needs to be replaced, for example by a formula derived in this thesis.

The related concept of running coupling parameters in terms of the renormalization group equation is discussed in addition. The perturbative treatment of the running electromagnetic coupling as can be found in the literature is presented in detail.

The overarching goal is the precise determination of the parity violating interaction at zero momentum transfer for which electroweak one-loop corrections are discussed including the role of the weak mixing angle. It can be used to derive the parity violating asymmetry of elastic electron-proton-scattering which is going to be measured in the P2 experiment in Mainz to determine the weak mixing angle.

Zusammenfassung

In dieser Arbeit wird der Formalismus des „Matching“ im elektroschwachen Sektor des Standardmodells in $\overline{\text{MS}}$ -Renormierung untersucht. Zwei verschiedene effektive Modelle werden verwendet um einen Ausdruck des schwachen Mischungswinkels unterhalb der Teilchenschwelle des W -Bosons in Einschleifenordnung herzuleiten. Das eine Modell basiert auf einer vier-Fermion-Kontaktwechselwirkung, während das andere dem elektroschwachen Sektor des Standardmodells aufgrund der Einführung eines Pseudo-Eichbosons Z' , dessen Masse nicht durch den Higgs-Mechanismus generiert wird, ähnelt. Die Ergebnisse werden mit bereits publizierten Resultaten verglichen und Mängel in der bestehenden Literatur werden benannt. Es wird aufgezeigt, dass die zuvor publizierte „Matching“-Bedingung des schwachen Mischungswinkels für das Ausintegrieren des W -Bosons nicht auf einer wohldefinierten effektiven Theorie basiert und ersetzt werden muss, zum Beispiel durch eine in dieser Arbeit hergeleitete Formel.

Das verwandte Konzept der laufenden Kopplung im Rahmen der Renormierungsgruppengleichung wird diskutiert. Die störungstheoretische Behandlung der laufenden elektromagnetischen Kopplung, wie sie in der Literatur zu finden ist, wird im Detail dargelegt.

Das übergeordnete Ziel ist die präzise Bestimmung der paritätsverletzenden Wechselwirkung bei verschwindendem Impulsübertrag für welche elektroschwache Einschleifen-Korrekturen inklusive der Rolle des schwachen Mischungswinkels diskutiert werden. Diese kann verwendet werden um die paritätsverletzende Asymmetrie der elastischen Elektron-Proton-Streuung zu berechnen, welche am Mainzer P2 Experiment zur Bestimmung des schwachen Mischungswinkels gemessen werden soll.

Contents

1. Introduction	11
1.1. Experimental Motivation	11
1.2. Theoretical Motivation	13
1.3. Outline	14
2. Theoretical Background	17
2.1. Electroweak Sector of the Standard Model	17
2.2. Regularization and Renormalization	23
2.3. Notation	26
2.3.1. $\overline{\text{MS}}$ Renormalization	26
2.3.2. Matching	26
2.3.3. Abbreviations	27
2.3.4. Neutral Current Interactions and Vector-Axial Vector Coupling Constants	28
2.4. Fermi Constant	29
2.5. Coupling Parameters	31
2.5.1. Running Coupling Parameters	31
2.5.2. Renormalization Group Equation	36
2.5.3. Renormalization Group Evolution	38
2.5.4. Matching Conditions	40
3. Electromagnetic Coupling in the Modified Minimal Subtraction Scheme	45
3.1. Dispersion Relation Approach to the Vacuum Polarization Function	47
3.1.1. Fixed-Order Integration of the Contour Integral	50
3.1.2. Contour Improved Perturbation Theory	58

3.2.	Non-hadronic Contributions	60
3.3.	Perturbative Expression of the Vacuum Polarization Function	62
3.4.	Electromagnetic Renormalization Group Equation	66
3.4.1.	Intermediate Solution	69
3.4.2.	Running of the Strong Coupling	72
3.4.3.	Solution of the Auxiliary Function Parametrizing the Strong Interaction	74
3.5.	Matching Conditions	75
4.	Parity Violating Interaction and the Weak Mixing Angle	79
4.1.	Irreducible Vertex Functions	80
4.1.1.	Bosonic Two-Point Functions	80
4.1.2.	Fermionic Two-Point Functions	84
4.1.3.	Three-Point Functions	86
4.2.	Parity Violating Fermion–Fermion Interaction	90
4.2.1.	Contribution of Scalar and Pseudo-Scalar Terms	92
4.2.2.	General Structure	94
4.2.3.	$\overline{\text{MS}}$ -Coupling Parameters in the Standard Model	97
4.3.	The β -Function of the Weak Mixing Angle	107
4.4.	Solution of the Weak Mixing Angle’s β -Function	108
5.	Matching Conditions	113
5.1.	Introduction	113
5.1.1.	Concept	113
5.1.2.	Published Calculations	114
5.1.3.	Outline	116
5.2.	Calculation in the Context of a Grand Unified Theory	116
5.2.1.	Heavy Particles at Zero Momentum Transfer	116
5.2.2.	Effective Theory	118
5.2.3.	Application to the Fundamental Gauge Bosons of the Electroweak Sector	121
5.2.4.	Derivation of the Electromagnetic Coupling and the Weak Mixing Angle Via the Fundamental Gauge Couplings	122

5.2.5. Matching of Electromagnetic Coupling in Terms of the Photonic Self-Energy Function	123
5.3. Z as a Pseudo Gauge Boson	125
5.3.1. Lagrangian	125
5.3.2. Irreducible Vertex Functions	127
5.3.3. Matching Conditions of Two- and Three-Point Functions	129
5.3.4. Parity Violating Fermion–Fermion Interaction	142
5.3.5. Matching of the Weak Mixing Angle	145
5.4. Contact Interaction Model	148
5.4.1. Lagrangian	148
5.4.2. Irreducible Vertex Functions	150
5.4.3. Matching Conditions of Two and Three Point Functions	152
5.4.4. Parity Violating Fermion–Fermion Interaction	157
5.4.5. Matching of the Weak Mixing Angle	163
5.4.6. Matching at a Fermion Threshold	165
6. Conclusion	169
6.1. Summary	169
6.2. Discussion of the Electromagnetic Matching Condition	171
6.3. Outlook	172
A. Illustration of the RG-Running and Matching Conditions in a Simple Model	175
B. Feynman Rules	179
C. One-Loop Functions at Zero Momentum Transfer	181
C.1. Bosonic Self-Energies	182
C.2. Fermionic Self-Energies	184
C.3. Vertex Functions	184
C.3.1. Function Values at Zero Momentum Transfer	185
C.3.2. Derivative of the Axial Fermion-Fermion-Photon–Vertex	185
C.4. Passarino–Veltman Functions	189

C.5. Propagators	190
D. LSZ Reduction Formula for Fermions in the EWSM	191
D.1. In- and Out-fields	191
D.2. Reduction Formula	194
D.3. Normalization	196
D.4. Amputation of Green Functions	197
Bibliography	199

1. Introduction

1.1. Experimental Motivation

In the past century, particle physicists made great progress in describing the behavior of particles that are thought to be fundamental. The discovery of quarks and the development of the associated gauge theory of the strong interaction, quantum chromodynamics (QCD), as well as the discovery of the heavy W^\pm - and Z-bosons and the unification of the electromagnetic and weak forces led to a compound theory of elementary particles. This theory was successful in describing virtually all phenomena occurring in high energy physics and hence established as the Standard Model of particle physics over the course of the years. The Higgs particle that was detected in 2012 at the Large Hadron Collider was said to be the last missing piece predicted by the Standard Model and required for its completion, as the masses of all other particles are generated via the Higgs mechanism.

Besides its great success in describing experimental observations, people hope for a grand unification of the three distinct gauge groups $SU(3)$, $SU(2)$ and $U(1)$. In particular, the unification of the electromagnetic and weak sector in terms of the electroweak gauge group $SU(2)\times U(1)$ was a great theoretical success and a lot of effort was made in order to find a grand unification consistent with observations. This led to an uncounted number of unifying theories of which Supersymmetry, for example, is probably one of the most known ones. A unification of the gauge groups would reduce the number of free parameters, as the current gauge couplings would be related to a set of group theoretical constants. Despite the theoretical beauty of some of these theories, no reliable experimental evidence was found for any of the proposed extensions of the Standard Model up to date.

Extensions and alternative models were not more successful than the Standard Model itself, but the Standard Model is not the end of the story. Even though it predicts almost all observations in experiment, it is known to be incomplete. A wide range of experiments confirmed that neutrino oscillations, predicted already in 1957 by Bruno Pontecorvo, occur. That is, a neutrino of a given flavor may alter to a neutrino of another flavor when propagating at macroscopic distances. The physical mechanism describing this effect requires a non-vanishing mass difference between the three neutrino flavors, while the Standard Model describes neutrinos as massless particles. The masses of the neutrinos may be incorporated into the Standard Model easily, but other deviations, like the anomalous magnetic moment of the muon hint at the necessity of a new theory. In addition, certain observations like the matter–antimatter asymmetry in the observable universe can not be explained within the Standard Model.

On top of that, the Standard Model does not contain a description of gravity. When matter is in a state of ultra-high density, for instance shortly after the big bang or in neutron stars or black holes, gravitational effects become significant on the scale of particle physics. In this regime, the Standard Model can not be applied and hence needs to be understood as an effective model with a particular scope of applicability. Furthermore, there is no explanation of dark matter or the hypothetical dark energy within the Standard Model, up to now. Although there is no satisfying explanation for dark matter, ultra-precise experiments probing the Standard Model might be sensitive to some kind of proposed force between dark and visible matter, like a dark photon.

All these flaws of the existing model, commonly summarized as “New Physics”, suggest that the Standard Model is just an effective part of a greater unified theory. In order to search for or get a better understanding of new physics, it is necessary to probe the Standard Model to the greatest possible extent, to see at which point – if at all – its predictions fail. One possibility to do so is by performing scattering experiments at high energies, to be sensitive to resonances of hypothetical new heavy particles. One famous facility performing high energy experiments is the CERN at which the Higgs boson was discovered in 2012, and the W^\pm and Z bosons in the eighties of the past century.

Measurements at the Z-pole also allowed to obtain a precise value of the weak mixing angle, which parametrizes the relation between the fields of the physically observable photon and Z-boson and the fundamental $SU(2) \times U(1)$ -gauge fields. The value obtained at the Large Electron-Positron Collider, that is in the high energy regime, is the most precise determination of the weak mixing angle to date. This value also fixes the prediction of the Standard model for the weak mixing angle at low energies. However, some types of new interactions (like a dark photon) might give a measurable contribution to the weak mixing angle at low energies only and thus evade the discovery of new physics at high energies. This makes the low energy regime an excellent place to look for new physics.

Thus, a complementary approach to experimental high energy physics is, to study new physics at medium or low energies. Since, the effects of new physics are still small, low energy measurements have to be exceedingly precise in order to be sufficiently sensitive. A particular example of a low energy precision experiment is the upcoming P2 experiment in Mainz. Its aim is to measure the weak mixing angle at low momentum transfer ($Q^2 \approx 4.5 \cdot 10^{-3} \text{ GeV}^2$) with much higher precision than previous low energy experiments. The goal is to obtain a value with 0.15 % relative accuracy [1].

1.2. Theoretical Motivation

The accuracy of an experiment is meaningless without a precise theoretical prediction of the measured observable within the Standard Model to see whether the Standard Model fails and if one of its extensions or a different model is in better agreement with the experimental outcome. Precise theoretical predictions require the calculation of loop diagrams; in this context, the renormalization group equation is a particularly useful tool, as it allows resumming large logarithmic corrections up to any order by solving a differential equation. The corresponding solution describes the running of coupling parameters with respect to the energy scale. This formalism can be used to obtain a low energy prediction within the Standard Model itself. However, at low energies it is more convenient to use an effective model that does not incorporate heavy particles which are

insignificant at low energies. The parameters of the effective model can be obtained by matching it with the Standard Model, the corresponding equations are called matching conditions.

By construction, the matching conditions depend on the formulation of the effective model and are not applicable without a precise definition thereof. In QCD, the construction of an effective model is apparent since one can omit heavy fermions without altering the fundamental properties of the strong interaction. This is a consequence of the gluons being massless and avoids a model ambiguity in the context of matching conditions. In the electroweak sector of the Standard Model on the other hand, the gauge bosons carry a mass and should be removed in the transition to an effective model, too. This does change the underlying forces and allows choosing different types of effective models that correspond to potentially unequal matching conditions. All these matching conditions are valid within their respective model, but a direct comparison is inadequate.

In addition, the weak mixing angle is a property of the fundamental gauge group of the Standard Model $SU(2) \times U(1)$ and its definition within an effective model is not evident, initially. It is easy to write down an effective parameter and the relation to the weak mixing angle in the Standard Model is obtained via the matching. However, the physical interpretation of the effective parameter remains unobvious, as the fundamental fields that are mixed according to the weak mixing angle are not present in the effective model.

In this thesis, the matching condition of the weak mixing angle is studied within the minimal modified subtraction scheme \overline{MS} in two different effective models. This requires a discussion of the renormalization group equation of the weak mixing angle and the electromagnetic coupling in addition. A detailed outline of the following chapters is given in Section 1.3.

1.3. Outline

Chapter 2 defines the Lagrangian of the Standard Model's electroweak sector in Section 2.1 and gives a brief introduction to the concept of renormalization in Section 2.2. Conventions used throughout the thesis are defined in Sec-

tion 2.3. Finally, Section 2.5 gives a short introduction to the basic ideas of running coupling parameters, the renormalization group equation and matching conditions.

In Chapter 3, the running of the $\overline{\text{MS}}$ -renormalized electromagnetic coupling $\hat{\alpha}$ is discussed, as it is required for a calculation of the weak mixing angle at low energies. This chapter includes the derivation of the coupling above the non-perturbative regime using an unsubtracted dispersion relation approach in Section 3.1 and its running in terms of the electromagnetic renormalization group equation in Section 3.4. Eventually, a simple derivation of the matching condition of the electromagnetic coupling is presented in Section 3.5, which is based on a calculation of the vacuum polarization in perturbation theory in Section 3.3.

In Chapter 4, the parity violating interaction required for the measurement in the P2 experiment is calculated within the Standard Model, with the final result given in Section 4.2. This requires the derivation of the irreducible vertex functions in Section 4.1 that also serve as a basis for the matching conditions later on. The chapter is closed by a discussion of the β -function of the weak mixing angle in Sections 4.3 and 4.4, which builds upon the running of the electromagnetic coupling discussed in Chapter 3.

Chapter 5 is dedicated to a concise derivation of the matching conditions of the electromagnetic coupling and the weak mixing angle. First, basic ideas and previously published results are presented in Sections 5.1 and 5.2. The matching condition of the weak mixing angle found in the literature is based on a method that is not convincing when applied to the electroweak sector of the Standard Model; the shortcomings are pointed out. In Section 5.3 the matching conditions are calculated for an effective model in which the Higgs and W-boson are missing, but neutral current interactions are mediated by a pseudo gauge boson. This calculation is repeated in Section 5.4 in the context of an effective contact interaction model, in which the neutral current interactions of the Standard Model are effectively described by a four-fermion vertex.

Finally, the thesis is summarized in Section 6.1 in which the main results of the previous chapters are highlighted. An outlook over possible future work and improvements is given in Section 6.3.

2. Theoretical Background

2.1. Electroweak Sector of the Standard Model

The Standard Model of particle physics is a non-abelian quantum field theory that is invariant under a transformation according to its fundamental gauge group $SU(3) \times SU(2) \times U(1)$. The subgroup $SU(3)$ is the gauge group associated with the sector of the strong interaction, while the remaining $SU(2) \times U(1)$ is the unbroken gauge group of the weak sector that historically emerged from the effective Fermi interaction theory. The gauge groups determine the number of gauge bosons that mediate the interaction of the three forces that are combined in the Standard Model. There are eight bosons in the strong sector, the gluons, and 3+1 bosons in the electroweak sector. The gauge bosons of the electroweak sector are organized in an isotriplet and one isosinglet, commonly referred to as $W_\mu^a, a = 1, 2, 3$ and B_μ , respectively. A quantum field theory with $SU(N)$ as the fundamental gauge group is called a Yang-Mills theory, for which the Lagrangian of the self-interacting gauge fields A_μ^a reads

$$\mathcal{L}_{\text{YM}} = -\frac{1}{4} \left(\partial_\mu A_\nu^a - \partial_\nu A_\mu^a + g_{\text{YM}} \sum_{b,c} f^{abc} A_\mu^b A_\nu^c \right)^2, \quad a, b, c = 1, \dots, N^2 - 1. \quad (2.1)$$

The number of fields $N^2 - 1$ of the theory is the number of generators of the Lie-group and g_{YM} is the coupling constant of the theory. The structure constants f^{abc} are not present in a theory with an abelian gauge group, but give rise to the self-interaction in theories with non-abelian gauge groups via three- and four-point interaction terms; ultimately, this self-interaction is the reason for confinement and asymptotic freedom in quantum chromodynamics.

2. Theoretical Background

The dynamics of the gluon fields and the isotriplet in the electroweak sector are determined by two different Yang-Mills terms of the form (2.1), while the isosinglet is described by a term of the non-selfinteracting field B_μ ,

$$\mathcal{L}_B = -\frac{1}{4} (\partial_\mu B_\nu - \partial_\nu B_\mu)^2, \quad (2.2)$$

similar to the photon field in quantum electrodynamics. The part of the Standard Model that describes the dynamics of the gauge bosons is the sum of these three pieces,

$$\begin{aligned} \mathcal{L}_{\text{Bosons}} = \mathcal{L}_B &- \frac{1}{4} \left(\partial_\mu \tilde{A}_\nu^a - \partial_\nu \tilde{A}_\mu^a + \tilde{g} \sum_{b,c=1}^8 f^{abc} \tilde{A}_\mu^b \tilde{A}_\nu^c \right)^2 \\ &- \frac{1}{4} \left(\partial_\mu W_\nu^i - \partial_\nu W_\mu^i + g_2 \sum_{j,k=1}^3 \varepsilon^{ijk} W_\mu^j W_\nu^k \right)^2, \end{aligned} \quad (2.3)$$

with $i = 1, 2, 3$; $a = 1, \dots, 8$ and where \tilde{A} refers to the gluon field. The tensors f^{abc} and ε^{abc} are the structure constants of the gauge groups SU(3) and SU(2), respectively, and \tilde{g} and g_2 are the corresponding coupling constants. As local gauge invariance prohibits the insertion of mass terms for the gauge bosons, the masses of the physical W- and Z-bosons are generated by the Higgs mechanism. The Higgs field $\Phi(x)$ is a complex scalar doublet and the associated Lagrangian of the Higgs sector reads

$$\mathcal{L}_{\text{Higgs}} = (D_\mu \Phi)^\dagger (D^\mu \Phi) - V(\Phi), \quad (2.4)$$

with the covariant derivative

$$D_\mu = \partial_\mu - ig_2 \frac{\sigma^i}{2} W_\mu^i + ig_1 \frac{Y}{2} B_\mu \quad (2.5)$$

and the Higgs potential

$$V(\Phi) = \frac{\lambda}{4} |\Phi|^4 - \mu^2 |\Phi|^2, \quad \lambda, \mu^2 > 0, \quad (2.6)$$

where σ^i , $i = 1, 2, 3$ are the Pauli matrices, Y is the hypercharge and g_1 is the coupling constant of the U(1) gauge group. Equation (2.6) defines a Mexican hat potential with a continuous global minimum off the origin. Following the notation of Reference [2], the Higgs doublet $\Phi(x)$ may be parametrized as

$$\Phi(x) = \langle \Phi \rangle + \begin{pmatrix} \phi^+(x) \\ \frac{1}{\sqrt{2}} (\eta(x) + i\xi(x)) \end{pmatrix}, \quad (2.7)$$

where $\langle \Phi \rangle^\dagger = \left(0, \frac{v}{\sqrt{2}}\right)$ is a vacuum expectation value of the Higgs field, whose absolute value is determined by $v = \frac{2\mu}{\sqrt{\lambda}}$. The value v is fixed by the minimum of the Higgs potential, but the orientation of $\langle \Phi \rangle^\dagger$ in the SU(2) space is arbitrary. Inserting the parametrization (2.7) into Equation (2.4) yields kinetic and various interaction terms for the fields $\phi^+(x)$, $\eta(x)$ and $\xi(x)$ as well as the mass terms

$$\begin{aligned} \left[(D_\mu \langle \Phi \rangle)^\dagger (D^\mu \langle \Phi \rangle) \right]_{\text{mass terms}} &= \frac{v^2}{8} \left[g_2^2 (W_\mu^1 + iW_\mu^2) (W^{1\mu} - iW^{2\mu}) \right. \\ &\quad \left. + (g_1 B_\mu + g_2 W_\mu^3) (g_1 B^\mu + g_2 W^{3\mu}) \right] \\ &= \frac{1}{2} M_W^2 W_\mu^\dagger W^\mu + \frac{1}{2} M_Z^2 Z_\mu^\dagger Z^\mu. \end{aligned} \quad (2.8)$$

The masses of the physical W- and Z-boson emerge from the vacuum expectation value of the Higgs field; they read $M_W = \frac{1}{2} v g_2$ and $M_Z = \frac{1}{2} v \sqrt{g_1^2 + g_2^2}$ in terms of the fundamental coupling constants and the vacuum expectation value of the Higgs field. The corresponding fields are defined as

$$W_\mu^\pm = \frac{1}{\sqrt{2}} (W_\mu^1 \mp iW_\mu^2), \quad (2.9a)$$

$$Z_\mu = \frac{1}{\sqrt{g_1^2 + g_2^2}} (g_2 W_\mu^3 + g_1 B_\mu) = \cos \theta_W W_\mu^3 + \sin \theta_W B_\mu \quad (2.9b)$$

2. Theoretical Background

in terms of the weak mixing angle θ_W . It is defined by a ratio of the fundamental gauge couplings,¹

$$\sin^2 \theta_W = \frac{g_1^2}{g_1^2 + g_2^2}, \quad (2.10)$$

and serves as a parametrization of the mixing of the W_μ^3 and B_μ gauge fields into the physical Z_μ and A_μ fields. The latter one remains massless after the spontaneous symmetry breaking and reads

$$A_\mu = \frac{1}{\sqrt{g_1^2 + g_2^2}} \left(-g_1 W_\mu^3 + g_2 B_\mu \right) = -\sin \theta_W W_\mu^3 + \cos \theta_W B_\mu. \quad (2.11)$$

Solving Equation (2.10) for the weak mixing angle, one finds at tree-level

$$\cos^2 \theta_W = \frac{M_W^2}{M_Z^2}, \quad \sin^2 \theta_W = 1 - \frac{M_W^2}{M_Z^2} \quad (2.12)$$

as the relation between weak mixing angle and masses of the massive gauge bosons. The cosine and sine of the weak mixing angle are commonly abbreviated with c and s , respectively. A definition including arguments and accents will be given in Section 2.3.

The previous introduction covers the essential properties of the Standard Model in the fundamental basis of the W_μ^i - and B_μ -fields and is required to understand the origin of the weak mixing angle. For the discussion of matching conditions later on, it is convenient to work in the physical basis of the W_μ^\pm -, Z_μ - and A_μ -fields. And since the strong interaction is not directly relevant for the matching of electroweak parameters, it is sufficient to only discuss the electroweak sector of the Standard Model (EWSM). The results of QCD calculations are taken from the literature where needed, but the strong sector of the Standard Model will not be discussed.

The starting point for the discussion of matching conditions is the Lagrangian of the EWSM in terms of the physical fields. For brevity, terms involving

¹Although less precise, the term “weak mixing angle” is often used as a synonym for $\sin^2 \theta_W$, too.

the physical Higgs boson η and interaction terms that do not contain either the photon or Z-boson are not given explicitly, as these are not required for the calculation of the parity violating interaction at one-loop order, which is the main goal of this thesis. The WW-box graph does contribute to the parity violating interaction, but the corresponding terms can not be absorbed into universal parameters and do not contribute to the matching conditions, consequently. The full EWSM Lagrangian may be separated into several pieces according to

$$\mathcal{L} = \mathcal{L}_f + \mathcal{L}_b + \mathcal{L}_{bs} + \mathcal{L}_H + \mathcal{L}_Y + \mathcal{L}_{\text{fix}} + \mathcal{L}_g, \quad (2.13)$$

where \mathcal{L}_f contains the kinetic terms of fermions and their interaction with the gauge bosons and \mathcal{L}_b constitutes the free gauge boson Lagrangian as well as the couplings among gauge bosons. The kinetic terms of the scalar fields and the interaction terms that involve gauge bosons and scalar fields are combined in \mathcal{L}_{bs} . The pieces \mathcal{L}_H and \mathcal{L}_Y describe the interaction between the scalar fields and the Yukawa couplings, respectively; they contribute to the gauge boson's self-energies only at higher loop order. The two remaining pieces \mathcal{L}_{fix} and \mathcal{L}_g are the gauge-fixing Lagrangian and the Lagrangian of the Faddeev–Popov ghosts, respectively. The exact definition of all pieces except for \mathcal{L}_H and \mathcal{L}_Y is given in the following.

The fermionic piece reads [3]

$$\begin{aligned} \mathcal{L}_f = \mathcal{L}_{fW} + \sum_f \left[\bar{f} (i\cancel{\partial} - m_f) f - eQ_f \bar{f} \gamma^\mu f A_\mu \right] \\ + \sum_f g_Z \left[T_f^3 \bar{f}_i^L \gamma^\mu f_i^L - s^2 Q_f \bar{f} \gamma^\mu f \right] Z_\mu, \end{aligned} \quad (2.14)$$

where \mathcal{L}_{fW} describes the interaction between fermions and the W-bosons and $g_Z = \frac{e}{cs}$ is used as an abbreviation for the coupling constant of the Z-boson. Conventionally, the masses of the fermions are generated by introducing a Yukawa-coupling between Higgs and fermion fields. Here, they are introduced as independent parameters of the theory for simplicity. The purely gauge bosonic terms in the Lagrangian are

2. Theoretical Background

$$\begin{aligned}
\mathcal{L}_b = & -\frac{1}{4} \left| \partial_\mu A_\nu - \partial_\nu A_\mu - ie \left(W_\mu^- W_\nu^+ - W_\nu^- W_\mu^+ \right) \right|^2 \\
& -\frac{1}{4} \left| \partial_\mu Z_\nu - \partial_\nu Z_\mu + ig_Z \left(W_\mu^- W_\nu^+ - W_\nu^- W_\mu^+ \right) \right|^2 \\
& -\frac{1}{2} \left| \partial_\mu W_\nu^+ - \partial_\nu W_\mu^+ - ie \left(W_\mu^+ A_\nu - W_\nu^+ A_\mu \right) \right. \\
& \quad \left. + ig_Z \left(W_\mu^+ Z_\nu - W_\nu^+ Z_\mu \right) \right|^2
\end{aligned} \tag{2.15}$$

and \mathcal{L}_{bs} is given by

$$\begin{aligned}
\mathcal{L}_{bs} = & \frac{1}{2} \left| i\partial_\mu \chi - i\frac{e}{s} W_\mu^- \phi^+ + iM_Z Z_\mu - \frac{g_Z}{2} Z_\mu \chi \right|^2 \\
& + \left| \partial_\mu \phi^+ + ie A_\mu \phi^+ - ie \frac{c^2 - s^2}{2cs} Z_\mu \phi^+ - iM_W W_\mu^+ + \frac{e}{2s} W_\mu^+ \chi \right|^2 + \dots;
\end{aligned} \tag{2.16}$$

the ellipsis represents kinetic and interaction terms of the physical Higgs η . The gauge-fixing Lagrangian in 't Hooft gauge reads

$$\begin{aligned}
\mathcal{L}_{\text{fix}} = & -\frac{1}{2\xi_A} (\partial^\mu A_\mu) (\partial^\nu A_\nu) - \frac{1}{2\xi_Z} (\partial^\mu Z_\mu) (\partial^\nu Z_\nu) + M_Z \partial^\mu Z_\mu \chi \\
& -\frac{\xi_Z}{2} M_Z^2 \chi^2 - \frac{1}{\xi_W} (\partial^\mu W_\mu^+) (\partial^\nu W_\nu^-) \\
& - iM_W (\partial^\mu W_\mu^+ \phi^- - \partial^\mu W_\mu^- \phi^+) - \xi_W M_W^2 \phi^+ \phi^-,
\end{aligned} \tag{2.17}$$

where ξ_A, ξ_Z and ξ_W are the gauge fixing parameters, and the Lagrangian of the Faddeev-Popov ghosts is

$$\begin{aligned}
\mathcal{L}_g = & -\bar{u}^+ (\partial^\mu \partial_\mu + M_W^2) u^+ - \bar{u}^- (\partial^\mu \partial_\mu + M_W^2) u^- \\
& + ie (\partial^\mu \bar{u}^+) \left(A_\mu - \frac{c}{s} Z_\mu \right) u^+ - ie (\partial^\mu \bar{u}^-) \left(A_\mu - \frac{c}{s} Z_\mu \right) u^- + \dots
\end{aligned} \tag{2.18}$$

The ellipsis stands for the kinetic terms of u^A and u^Z and for interaction terms between the ghost particles and scalars and W-bosons.

The Lagrangian defined above is not yet renormalized even though a special index indicating bare quantities was omitted for readability. Calculations beyond tree-level require a renormalization of the Standard Model, which is obtained by replacing the bare fields and parameters by renormalized ones. For the following discussion, it is sufficient to only introduce renormalization of the neutral gauge and fermion fields by means of the replacement

$$\begin{aligned} \begin{pmatrix} A^\mu \\ Z^\mu \end{pmatrix} &\rightarrow \begin{pmatrix} A_0^\mu \\ Z_0^\mu \end{pmatrix} = X \begin{pmatrix} A^\mu \\ Z^\mu \end{pmatrix}, & X &= \begin{pmatrix} \sqrt{1 + \delta Z_A} & \delta Z_{AZ} \\ \delta Z_{ZA} & \sqrt{1 + \delta Z_Z} \end{pmatrix}, \\ f_i^{L/R} &\rightarrow f_i^{L/R} \sqrt{1 + \delta Z_{L/R}^f}. \end{aligned} \quad (2.19)$$

Masses need to be renormalized, too, but will be expressed in terms of the bare masses denoted by a subscript “0” in the following.

2.2. Regularization and Renormalization

The above definitions determine the theory unambiguously only at tree-level. The computation of diagrams containing loops requires an integration over all possible loop momenta, which diverges due to the lack of an upper bound of the integration variable. Since the divergences stem from the integration over unbounded momenta, they are commonly referred to as ultraviolet divergences (UV-divergences). Regularization techniques can be used to quantify the divergence which is a mandatory step for making physically meaningful predictions.

The most common technique for regularizing the integrals is dimensional regularization, as it preserves all the symmetries of the underlying theory, including gauge symmetry. The divergent integrals are dimensionally regularized by replacing the four-dimensional integration with a D -dimensional one,

$$\int \frac{d^4 q}{(2\pi)^4} \rightarrow \mu^{4-D} \int \frac{d^D q}{(2\pi)^D}, \quad (2.20)$$

2. Theoretical Background

where μ is an arbitrary mass scale that is introduced to keep the mass dimension of the integral fixed. This way, the integral becomes a meromorphic function with a pole at $D = 4$. The one-loop divergences that occur after integration are of the form

$$\Delta_M = \Delta + \log \frac{\mu^2}{M^2}, \quad (2.21a)$$

$$\Delta = \frac{2}{4-D} - \gamma_{\text{EM}} + \log 4\pi, \quad (2.21b)$$

where M is a particle mass and $\gamma_{\text{EM}} = 0.577215\dots$ is the Euler–Mascheroni constant. Only the first term in the definition of Δ is divergent in the physical limit $D = 4$, but conventionally, the entire expression Δ is referred to as a UV-singular piece.

The constants and fields that appear in the Lagrangian have no precise physical meaning as they are not measurable. The observable quantities like cross sections are functions of these constants and fields as well as the meromorphic loop functions in the limit $D = 4$. Since the observables have to be finite, the terms that arise from the constants and fields of the Lagrangian have to cancel the poles of the loop integrals such that the theoretical prediction of the observable is finite, eventually. In addition, different choices of regularization will lead to different results for the loop integrals that may or may not depend on an unphysical scale parameter or cutoff. However, physical observables and the theoretical predictions for these observables must not depend on an unphysical scale or a particular choice of regularization prescription. To work around these issues, the theory needs to be renormalized, which allows obtaining physical meaningful predictions.

The theory is renormalized by rescaling the bare fields and constants with appropriate renormalization constants and requiring that these renormalization constants cancel the divergences of the space-time integrals. This requirement fixes the singular parts of the renormalization constants; however, the finite parts of the renormalization constants are arbitrary and one particular choice of a system of equations that determines all renormalization constants is called a renormalization scheme.

The on-shell renormalization scheme (OS) constrains the renormalization constants such that the renormalized coupling constants and masses coincide with the experimentally measured ones. The fields are renormalized by setting the residue of the corresponding particle's propagator to unity. This is not strictly necessary but allows avoiding the computation of self interactions of the external particles when calculating matrix elements. The OS scheme is appealing, as it gives physical meaning to the constants in the theory, but is not universally applicable. For instance, the mass parameters are set equal to the experimentally determined pole masses, but since light quarks do not exist as free particles at low energy due to confinement, the OS scheme is not applicable to QCD.

In the minimal subtraction scheme (MS), the renormalization constants do not contain any finite terms, but only the terms proportional to $(4 - D)^{-1}$. They are defined such that they cancel precisely the corresponding poles emerging from the loop integrals. The MS renormalization constants can be obtained from the OS ones by keeping only the $\frac{2}{4-D}$ -terms and correspondingly, the renormalized MS loop expressions are derived from the unrenormalized ones by removing these singular terms. A similar scheme is the modified minimal subtraction scheme ($\overline{\text{MS}}$), in which the renormalization constants also include the finite terms $-\gamma_{\text{EM}} + \log 4\pi$ (see Section 2.3.1). The MS and $\overline{\text{MS}}$ scheme are particularly useful in QCD, as the OS scheme can not be applied. Due to the simplicity of the renormalization prescription, it is technically possible to avoid renormalization constants altogether and just omit the UV singular terms when evaluating Feynman loops.

The bare parameters of an unrenormalized theory are unphysical, as they can not be determined in experiments. The measurable quantities are combinations of the bare parameters and parts of the singular loop corrections. As these combinations are finite, the bare parameters need to be singular themselves, in order to cancel the singularities of the loop corrections. The process of renormalization replaces the combination of loop singularities and bare parameters by a new set of renormalized parameters such that all singularities in the renormalized theory cancel. Eventually, all observable quantities are rendered finite.

2. Theoretical Background

The scale dependent logarithms $\log \frac{\mu^2}{M^2}$ arising in dimensional regularization are absorbed into the renormalization constants in the on-shell scheme the same way the singular terms are absorbed. Consequently, the OS-renormalized parameters are independent of the renormalization scale. In schemes like MS and $\overline{\text{MS}}$, in which the logarithms are not separated from the one-loop corrections, the logarithms remain a part of the renormalized theory, rendering the renormalized parameters scale dependent.

2.3. Notation

The physical setup described above closely follows the one outlined in Reference [2]. Accordingly, the one-loop results presented therein can be adopted. The notation that differs and other conventions are described in the following subsections.

2.3.1. $\overline{\text{MS}}$ Renormalization

The $\overline{\text{MS}}$ -renormalized one-loop functions are obtained from the unrenormalized ones by subtracting the UV-divergent terms $\frac{2}{4-D}$, where D is the dimension of space-time in dimensional regularization, as well as the Euler-Mascheroni constant and $\log 4\pi$ that arise with every UV-divergent term. $\overline{\text{MS}}$ -renormalized quantities can be obtained from the unrenormalized ones by applying the following rule to the singular quantities Δ_M introduced above,

$$\Delta_M = \frac{2}{4-D} - \gamma_{\text{EM}} + \log 4\pi + \log \frac{\mu^2}{M^2} \xrightarrow{\overline{\text{MS}}} \hat{\Delta}_M = \log \frac{\mu^2}{M^2}. \quad (2.22)$$

As in case of $\hat{\Delta}_M$, the $\overline{\text{MS}}$ -renormalization of one-loop functions is indicated by a hat in the following.

2.3.2. Matching

Matching is the process of determining effective model parameters by comparison with a theory that is less approximate than the effective model; the details are

laid out in Chapter 5. Since the more complete theory could be an effective one itself and because the Standard Model is considered an effective theory nowadays, it is misleading to refer to the two models as effective and complete ones. Instead, the model with reduced degrees of freedom will be referred to as child theory; in analogy, the other model is called parent theory. This reflects the fact that the child model inherits some properties regarding renormalization when performing the matching.

2.3.3. Abbreviations

- As will be described in Section 2.5.4, subsequently integrating out particles from a theory allows defining the $\overline{\text{MS}}$ -renormalized quantities as piecewise functions. These functions exhibit discontinuities in the scale parameter μ at matching thresholds. Consequently, $\hat{\alpha}(M)$ is ambiguous if M is a point of discontinuity. To avoid ambiguity, the superscripts “+” and “−” are commonly used in the literature to denote the right- and left-handed limits of the $\overline{\text{MS}}$ -renormalized coupling parameters, respectively. This shadows the fact that the two limits are not calculated within the same model of the interacting theory. In light of the findings of Chapter 5, the notation

$$\hat{\alpha}^{\text{p}}(M) = \lim_{\varepsilon \rightarrow 0} \hat{\alpha}(M + \varepsilon), \quad \hat{\alpha}^{\text{c}}(M) = \lim_{\varepsilon \rightarrow 0} \hat{\alpha}(M - \varepsilon) \quad (2.23)$$

is used to highlight that the two numbers stem from a child (c) and a parent (p) model.

- When appropriate, a is used as a short form of the fraction $\frac{\alpha}{\pi}$,

$$a = \frac{\alpha}{\pi}. \quad (2.24)$$

Super- and subscripts as well as arguments are understood as decorations of α ; for instance, $\hat{\alpha}_s(\mu)$ denotes the $\overline{\text{MS}}$ -renormalized strong coupling constant α_s at scale μ divided by π .

- The common short notation c and s for $\cos \theta_W$ and $\sin \theta_W$, respectively, is used. Similarly, $\hat{s}^2(\mu)$ reads $\sin^2 \hat{\theta}_W(\mu)$ and so forth.

- Transverse and longitudinal parts of self-energy and irreducible two-point functions are denoted by a subscript “ T ” and “ L ”. The applied convention for the decomposition reads

$$\Sigma_{\mu\nu}(q^2) = \left(-g_{\mu\nu} + \frac{q_\mu q_\nu}{q^2} \right) \Sigma_T(q^2) - \frac{q_\mu q_\nu}{q^2} \Sigma_L(q^2) \quad (2.25)$$

for a generic self-energy function.

- A subscript “fin” is used to denote finite terms of a self-energy function, that is all terms remaining when dropping the Δ_M defined in Equation (2.21). The piece Δ_M contains finite terms which are also not part of a self-energy with subscript “fin”.
- The operators \Re and \Im are used to denote the real and imaginary parts of complex numbers, respectively.

2.3.4. Neutral Current Interactions and Vector-Axial Vector Coupling Constants

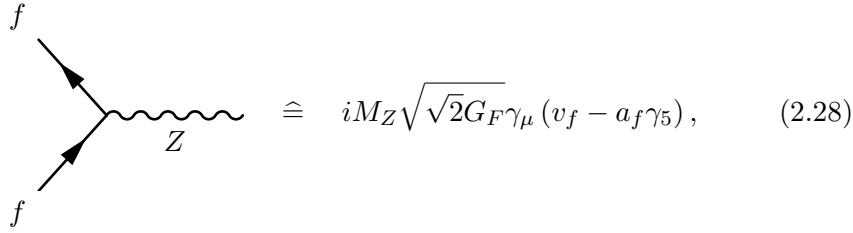
There are different options to parametrize the coupling of the neutral current. In Reference [2], the coupling of a fermion to the Z-boson is expressed in terms of the electric charge $e = \sqrt{4\pi\alpha}$ and the vector and axial vector couplings

$$v_f^{\text{BHS}} = \frac{T_3^f - 2s^2 Q_f}{2cs} \quad \text{and} \quad a_f^{\text{BHS}} = \frac{T_3^f}{2cs}, \quad (2.26)$$

where Q_f and T_3^f denote the charge and the third component of the weak isospin of a fermion, respectively. As will be described later, in Section 4.2.3, one can absorb certain loop corrections in the weak mixing angle that occurs in the numerator of the vector coupling constant. However, these correction terms leave the denominator of Equation (2.26) unaltered, making it more difficult to redefine $\sin^2 \theta_W$ consistently. Therefore, it is convenient to express the fermion–neutral current interaction in terms of the Fermi constant

$$G_F = \frac{\pi\alpha}{\sqrt{2}c^2 s^2 M_Z^2} + \mathcal{O}(\alpha^2). \quad (2.27)$$

Using the Fermi constant is also favorable, as it is known much more precisely than the mass of the W-boson. The Feynman rule of the fermion–Z-boson vertex that reads $ie\gamma_\mu (v_f^{\text{BHS}} - a_f^{\text{BHS}}\gamma_5)$ in Reference [2] then changes to



$$\cong iM_Z\sqrt{\sqrt{2}G_F}\gamma_\mu(v_f - a_f\gamma_5), \quad (2.28)$$

where

$$v_f = T_3^f - 2s^2Q_f, \quad (2.29a)$$

$$a_f = T_3^f \quad (2.29b)$$

are the vector and axial vector coupling constants that are used instead of the ones in Equation (2.26) in the following.

2.4. Fermi Constant

As stated before, using the Fermi constant G_F is beneficial, as it can be determined accurately by measuring the lifetime of the muon. The Fermi constant is defined by the relation

$$\frac{1}{\tau_\mu} = \frac{G_F^2 m_\mu^5}{192\pi^3} \left(1 - 8\frac{m_e^2}{m_\mu^2}\right) \left[1 - \frac{3}{5}\frac{m_\mu^2}{M_W^2} + \frac{\alpha}{2\pi} \left(\frac{25}{4} - \pi^2\right)\right], \quad (2.30)$$

where τ_μ is the muon's lifetime and m_e and m_μ are the masses of the electron and muon, respectively. This formula stems from a leading order calculation of the muon decay in the Fermi interaction model plus photonic one-loop corrections that could already be calculated within this model. These corrections include the emission of real bremsstrahlung photons and a virtual photon line between

2. Theoretical Background

the muon and the electron. For historical reasons, these photonic corrections are part of the definition of G_F . At one-loop order, the Fermi model is insufficient to describe the muon decay properly and several additional diagrams have to be taken into account in the Standard Model.

In the Standard Model, the virtual photon correction that is included in Equation (2.30) is in fact a part of the γW -box graph. The remaining part of this box graph has to be combined with the vertex and external leg corrections as well as the massive box diagrams and the W-boson's self-energy diagram. This calculation was first done in Reference [4], where it was shown that the combination of all one-loop corrections factorize as

$$G_F = \frac{\pi\alpha}{\sqrt{2}c^2s^2M_Z^2} \frac{1}{1 - \Delta r}, \quad (2.31)$$

where Δr accounts for the corrections. In the OS scheme, the correction reads [5]

$$\Delta r = \Pi_T^{WW}(0) + \frac{\alpha}{4\pi s^2} \left(6 + \frac{7 - 4s^2}{2s^2} \log c^2 \right), \quad (2.32)$$

where $\Pi_T^{WW}(0)$ is the transverse part of the OS renormalized self-energy of the W-boson evaluated at zero momentum transfer. In the $\overline{\text{MS}}$ scheme, the relation (2.31) holds with a different correction term $\Delta\hat{r}$. The corresponding calculation of $\Delta\hat{r}$ in the $\overline{\text{MS}}$ scheme was performed some time later [6] with the result² [7]

$$\begin{aligned} \Delta\hat{r} = \Re \left(\frac{\hat{\Sigma}_T^{WW}(0)}{\hat{M}_W^2} - \frac{\hat{\Sigma}_T^{ZZ}(\hat{M}_Z^2)}{\hat{M}_Z^2} \right) \\ - 2 \frac{\delta\hat{e}}{\hat{e}} + \frac{\alpha}{4\pi\hat{s}^2} \left[4 \log \frac{\mu^2}{M_Z^2} + \left(\frac{7}{2\hat{s}^2} - 6 \right) \log \hat{c}^2 + 6 \right]. \end{aligned} \quad (2.33)$$

Equation (2.33) is expressed in terms of the $\overline{\text{MS}}$ renormalization constant of the electric charge $\frac{\delta\hat{e}}{\hat{e}}$. Due to the simple prescription of $\overline{\text{MS}}$, the renormalization

²Note that the expression given explicitly in Reference [6] was obtained using $\mu = M_Z$ and is less general than Equation (2.33)

constant can be obtained from the OS one by dropping the UV divergent pieces according to Equation (2.22); It reads [2]

$$-2 \frac{\delta \hat{e}}{\hat{e}} \Big|_{\mu=M_Z} = \frac{\alpha}{4\pi} \left[\frac{4}{3} \sum_f Q_f^2 \log \frac{m_f^2}{M_Z^2} - 7 \log c^2 \right]. \quad (2.34)$$

As the Fermi constant is an observable, the one-loop expressions of Δr or $\Delta \hat{r}$ can be used with Equation (2.31) and the mass of the Z-boson to determine the mass of the W-boson, for which the experimentally determined value is less precise than the value of the other observables.

2.5. Coupling Parameters

This section is dedicated to an introduction of the concept of running coupling parameters, the renormalization group equation and matching conditions. The following subsections are organized as follows: The energy dependence, that is the “running” of coupling parameters, is discussed in Section 2.5.1, which is followed by an introduction of the renormalization group equation in Section 2.5.2. The latter can be used to rescale a coupling parameter by solving a differential equation as discussed in Section 2.5.3. Last, the concept of matching two different theories to integrate out heavy particles and create effective low energy models is presented in Section 2.5.4. An example of how to apply the methods described in the following can be found in Appendix A.

2.5.1. Running Coupling Parameters

Coupling parameters, as all other parameters of a given model, are obtained by measurements of an observable at a certain energy scale, making them momentum transfer dependent. “Coupling constant” refers to such a parameter for a fixed momentum transfer, which could in principle be addressed as normalization scale or normalization point of the theory. For instance, the electromagnetic coupling constant α is measured in the Thomson limit; experimental difficulties

2. Theoretical Background

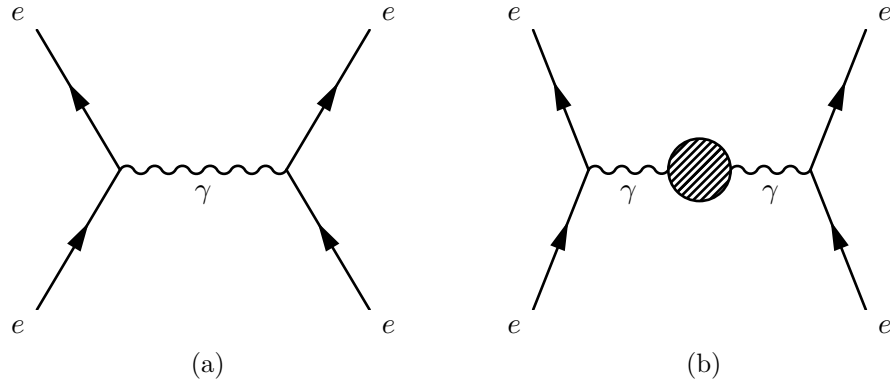


Figure 2.1.: Leading order and next-to-leading order Feynman diagrams of electron-electron scattering.

left aside, it could also be obtained from scattering experiments with momentum transfer close to the Z-pole. But regardless of whether $\alpha \equiv \alpha(q^2 = 0)$ or $\alpha(q^2 = -M_Z^2)$ is used, the theoretical predictions for any observable need to agree up to a certain level of precision. In a less precise manner, “coupling constant” is also used for parameters that “run” due to the momentum dependence. To avoid ambiguities, “coupling constant” is to be understood as usual, while “coupling parameter” refers to the more general momentum dependent coupling strength in this section.

Linking the initially undetermined coupling parameter of a given theory with experimental data requires a theoretical prediction for the outcome of the experiment, which can be inverted in order to compute the coupling parameter within this theory. For instance, the electromagnetic fine-structure constant in QED can be measured in an electron–electron scattering experiment. The leading order diagram of Møller scattering is depicted in Figure 2.1a; the corresponding theoretical cross section $\sigma_{(0)}^{\text{Møller}}(q^2)$ can be obtained using Feynman rules, depends on the squared momentum transfer q^2 and is proportional to the coupling constant $\alpha_{(0)}^2$, where the subscript “(0)” indicates that $\alpha_{(0)}$ and $\sigma_{(0)}^{\text{Møller}}$ are tree-level quantities.

Initially, $\alpha_{(0)}$ is undetermined; it can be obtained at a certain energy scale q^2 by equating the theoretical cross section with the experimentally measured one. This yields

$$\alpha_{(0)}^2(q^2) = \frac{\sigma_{\text{exp}}(q^2)}{\sigma_{(0)}^{\text{th}}(q^2)}, \quad (2.35)$$

where $\sigma_{\text{exp}}(q^2)$ refers to a cross section measurement at momentum transfer q^2 and

$$\sigma_{(0)}^{\text{th}}(q^2) := \frac{\sigma_{(0)}^{\text{Møller}}(q^2)}{\alpha_{(0)}^2} \quad (2.36)$$

is introduced to separate $\alpha_{(0)}$ from the cross section. The common fine-structure constant α that accounts for the coupling strength of charged leptons in the Thomson limit is defined by $\alpha := \alpha_{(0)}(q^2 = 0)$.

At next to leading order, it is necessary to take into account the one-loop diagrams depicted in Figure 2.1b. The self-energy is a tensor that may be decomposed according to Equation (2.25). Using the Feynman rules (B.1) and (B.3), the concatenation of a propagator, the self-energy and another propagator reads

$$\left(-g_{\mu\nu} + \frac{q_\mu q_\nu}{q^2}\right) \frac{-i}{q^2} \Pi_{T,R}^{\gamma\gamma}(q^2) - \frac{q_\mu q_\nu}{q^2} \frac{-i}{q^2} \Pi_{L,R}^{\gamma\gamma}(q^2), \quad (2.37)$$

where $\Pi_{T/L,R}^{\gamma\gamma}(q^2) = \frac{\Sigma_{T/L,R}^{\gamma\gamma}(q^2)}{q^2}$ denotes the vacuum polarization function. The subscript R denotes a certain renormalization scheme, as the evaluation of the loop integral in the self-energy requires the introduction of a regularization and renormalization prescription that cancels the occurring singularities. The terms proportional to $q_\mu q_\nu$ do not contribute to matrix elements due to the conservation of the electromagnetic current. Consequently, the sum of the propagator and the previously determined concatenation may be written only in terms of the transverse piece,

$$\frac{-ig_{\mu\nu}}{q^2} \left(1 - \Pi_{T,R}^{\gamma\gamma}(q^2)\right). \quad (2.38)$$

2. Theoretical Background

Incorporating Diagram 2.1b and omitting terms quadratic in $\Pi_{T,R}^{\gamma\gamma}$, Equation (2.35) becomes³

$$\alpha_R^2(q^2, \mu^2) = \frac{\sigma_{\text{exp}}(q^2)}{\sigma_{(0)}^{\text{th}}(q^2)} \frac{1}{1 - 2\Pi_{T,R}^{\gamma\gamma}(q^2, \mu^2)} = \frac{\alpha_{(0)}^2(q^2)}{1 - 2\Pi_{T,R}^{\gamma\gamma}(q^2, \mu^2)}, \quad (2.39)$$

where μ refers to the renormalization scale and $\Pi_{T,R}^{\gamma\gamma} \propto \alpha_R$ implicitly contains a factor α_R . In case of on-shell renormalization, the renormalization conditions are imposed such that the coupling constant is identical to the tree-level constant,

$$\alpha_{\text{OS}} := \alpha_{\text{OS}}(q^2 = 0, \mu^2) \stackrel{!}{=} \alpha_{(0)} \quad \Leftrightarrow \quad \Pi_{T,\text{OS}}^{\gamma\gamma}(q^2 = 0, \mu^2) = 0. \quad (2.40)$$

It is common to use α without any subscripts to denote the OS coupling constant, which will also be used in the following. On the other hand, the modified minimal subtraction scheme requires subtracting a certain set of terms from the regularized self-energy. Following the prescription outlined in Section 2.3.1, one finds

$$\hat{\Pi}_T^{\gamma\gamma}(q^2 = 0, \mu^2) = \frac{\hat{\alpha}(\mu^2)}{3\pi} \log \frac{\mu^2}{m_e^2}, \quad (2.41)$$

which leads to

$$\hat{\alpha}^2(\mu^2) := \hat{\alpha}^2(q^2 = 0, \mu^2) = \alpha^2 \left(1 - \frac{2\hat{\alpha}(\mu^2)}{3\pi} \log \frac{\mu^2}{m_e^2} \right)^{-1}, \quad (2.42)$$

with an implicit squared charge factor $Q_e^2 = 1$. The $\overline{\text{MS}}$ -renormalization process removed the singularities from the loop integrals but left behind a scale dependence. This dependence of the renormalized coupling constant is necessary, as it precisely cancels the ones of the loop corrections.

The one-loop cross sections in the OS and $\overline{\text{MS}}$ -scheme read

$$\sigma_{\text{OS}}(q^2) = \alpha^2 \sigma_{(0)}^{\text{th}}(q^2) \left[1 + \Pi_{T,\text{OS}}^{\gamma\gamma}(q^2) \right]^{-2}, \quad (2.43a)$$

³This is not Dyson resummed, as the contribution of Diagram 2.1b is added to the theoretical cross section.

$$\Pi_{T,\text{OS}}^{\gamma\gamma}(q^2) = \frac{\Sigma_{T,\text{fin}}^{\gamma\gamma}(q^2)}{q^2} \quad (2.43b)$$

and

$$\sigma_{\overline{\text{MS}}}(q^2) = \hat{\alpha}^2(\mu^2) \sigma_{(0)}^{\text{th}}(q^2) \left[1 + \hat{\Pi}_T^{\gamma\gamma}(q^2, \mu^2) \right]^{-2}, \quad (2.44a)$$

$$\hat{\Pi}_T^{\gamma\gamma}(q^2, \mu^2) = \frac{\alpha}{3\pi} \log \frac{\mu^2}{m_e^2} + \frac{\Sigma_{T,\text{fin}}^{\gamma\gamma}(q^2)}{q^2} \quad (2.44b)$$

after Dyson resumming the reducible higher order contributions, where $\Sigma_{T,\text{fin}}^{\gamma\gamma}$ is the finite part of the self-energy given in Reference [2]. Inserting Equation (2.42) into Equation (2.44) and expanding the fractions in Equations (2.43) and (2.44), one finds that the scale dependence cancels at one-loop order in the $\overline{\text{MS}}$ -prediction,

$$\sigma_{\overline{\text{MS}}}(q^2) = \alpha^2 \sigma_{(0)}^{\text{th}} \left(1 - 2 \frac{\Sigma_{T,\text{fin}}^{\gamma\gamma}(q^2)}{q^2} \right) + \mathcal{O}(\alpha^4), \quad (2.45)$$

and that the OS and $\overline{\text{MS}}$ cross sections are identical, when terms of order $\mathcal{O}(\alpha^4)$ are neglected,

$$\sigma_{\text{OS}}(q^2) = \alpha^2 \sigma_{(0)}^{\text{th}}(q^2) \left(1 - 2 \frac{\Sigma_{T,\text{fin}}^{\gamma\gamma}(q^2)}{q^2} \right) + \mathcal{O}(\alpha^4). \quad (2.46)$$

The electromagnetic coupling constant is defined as the coupling strength in the Thomson limit; consequently it does not depend on the energy scale q^2 . However, Equations (2.45) and (2.46) illustrate that the change in the vacuum polarization corresponding to a change in momentum transfer can be described by an observable modification of the coupling strength, which may be referred to as a running coupling parameter,

$$\sigma_{\text{OS}/\overline{\text{MS}}}(q^2) = \alpha_{\text{run}}^2(q^2) \sigma_{(0)}^{\text{th}}(q^2) + \mathcal{O}(\alpha^4), \quad (2.47a)$$

$$\alpha_{\text{run}}^2(q^2) = \alpha^2 \left(1 - 2 \frac{\Sigma_{T,\text{fin}}^{\gamma\gamma}(q^2)}{q^2} \right). \quad (2.47b)$$

2.5.2. Renormalization Group Equation

The previous section showcased the scale independence of an observable when combining the coupling with the self-energy function. In the simple example in Section 2.5.1 the renormalization scale μ was arbitrary but fixed; the scale that was used when determining $\hat{\alpha}(\mu^2)$ from experiment was the same as the one used in making the prediction (2.44). If two different scales are used, the scale dependent terms do not cancel as before. Using μ_1 to denote the scale that was used to determine coupling parameter $\hat{\alpha}(\mu_1)$ by comparison with experimental data and μ_2 as the scale for which the cross section should be computed yields

$$\begin{aligned}\sigma_{\overline{\text{MS}}}(q^2) &= \hat{\alpha}^2(\mu_1^2) \sigma_{(0)}^{\text{th}}(q^2) \left[1 + \hat{\Pi}_T^{\gamma\gamma}(q^2, \mu_2^2) \right]^{-2} \\ &= \alpha^2 \sigma_{(0)}^{\text{th}} \left(1 - 2 \frac{\alpha}{\pi} \log \frac{\mu_2^2}{\mu_1^2} - 2 \frac{\Sigma_{T,\text{fin}}^{\gamma\gamma}(q^2)}{q^2} + \mathcal{O}(\alpha^2) \right)\end{aligned}\quad (2.48)$$

in a naive calculation. The scales do not cancel, and the result depends on a logarithm of the ratio $\frac{\mu_2}{\mu_1}$. Equation (2.48) is incorrect, as $\hat{\alpha}^2(\mu_2^2)$ must be used instead of $\hat{\alpha}^2(\mu_1^2)$ as first factor. Accordingly, it is necessary to obtain $\hat{\alpha}(\mu_2^2)$ from experimental data itself or derive its value from the experimentally determined $\hat{\alpha}(\mu_1^2)$, that is to rescale the coupling constant. In this section, the renormalization group equation is introduced, which can be used to rescale a coupling parameter and resolve the problem sketched in Equation (2.48). The concrete application of this new technique will be presented in Section 2.5.3.

The starting point for rescaling the coupling is the fact that physical observables must not depend on the particular choice of the scale μ . This can be expressed as

$$\mu^2 \frac{d}{d\mu^2} \mathcal{O}(\alpha, m, \mu^2) = 0, \quad (2.49)$$

where \mathcal{O} is an observable whose expression depends on the coupling, a mass and the renormalization scale. Equation (2.49) is based on the assumption that the theory involves only a single mass m and a single coupling constant α . More general discussions also including anomalous dimensions can be found in textbooks [3, 8]. As shown in Section 2.5.1, the coupling parameter generally

depends on the scale μ , but also on the mass and the coupling itself. The same applies to the renormalized mass, so that the parameters in Equation (2.49) need to be understood as functions of three parameters,

$$\alpha_R = \alpha_R(\alpha, m, \mu^2), \quad m_R = m_R(\alpha, m, \mu^2). \quad (2.50)$$

The subscript R denoting the renormalization scheme is used to highlight that α_R and m_R are functions instead of constants. This allows rewriting Equation (2.49) as

$$\mu^2 \left(\frac{\partial}{\partial \mu^2} + \frac{d\alpha_R}{d\mu^2} \frac{\partial}{\partial \alpha} + \frac{dm_R}{d\mu^2} \frac{\partial}{\partial m} \right) \mathcal{O}(\alpha_R, m_R, \mu^2) = 0, \quad (2.51)$$

which contains the two important derivatives

$$\beta(\alpha, m, \mu^2) := \mu^2 \frac{d}{d\mu^2} \alpha_R(\alpha, m, \mu^2), \quad (2.52)$$

$$\gamma(\alpha, m, \mu^2) := \mu^2 \frac{d}{d\mu^2} m_R(\alpha, m, \mu^2). \quad (2.53)$$

Equation (2.51) is called renormalization group equation (RGE) and implies that a change of the renormalization scale μ induces a shift of the renormalized coupling parameter and mass that compensates for the change in the expression of \mathcal{O} , which is required as the observable must not depend on the unphysical scale, ultimately. This shift is governed by the β - and γ -functions defined in Equations (2.52) and (2.53). Given an expression for β and γ , which can be readily obtained once the theory is properly renormalized, one can solve the differential equations⁴ to find the running mass and coupling parameter.

In a perturbative approach it is convenient to expand Equations (2.52) and (2.53) as a power series in the coupling parameter. This also allows systematically taking into account strong interaction effects that enter via

⁴The associated differential equations are called characteristic equations but will also be referred to as β - and γ -functions throughout this thesis.

2. Theoretical Background

quark loops. For instance, the $\overline{\text{MS}}$ - β -function describing the running of the electromagnetic coupling constant in the Standard Model reads [9]

$$\hat{\beta} = -\frac{\hat{\alpha}^2}{\pi} \sum_{i=0}^{\infty} \left[\hat{\beta}_i \left(\frac{\hat{\alpha}}{\pi} \right)^i + \hat{\delta}_i \left(\frac{\hat{\alpha}_s}{\pi} \right)^i \right] + \mathcal{O}(\hat{\alpha}^3 \hat{\alpha}_s) \quad (2.54)$$

when neglecting mixed terms of the order $\hat{\alpha}\hat{\alpha}_s$ within the brackets. Since the β -function is unambiguously defined as the derivative of the coupling parameter, Equation (2.54) serves as a definition for the coefficients on the right-hand side. Inserting Equation (2.42) into (2.52) allows obtaining the leading order coefficient

$$\hat{\beta}_0 = -\frac{1}{3}. \quad (2.55)$$

The n -th coefficient of the β -function is determined by the result of an $n+1$ -loop calculation. The coefficients are fixed by the scale dependent logarithms, only. Therefore, they can be obtained without evaluating the full integrals.

2.5.3. Renormalization Group Evolution

The scaling behavior of the coupling is given by the RGE introduced in Section 2.5.2 and is a consequence of observables being independent of the scale. In this section, the RGE will be used to rescale the electromagnetic coupling and resolve the issue that was posed in Equation (2.48). To the lowest order in perturbation theory, all terms in the β -function except one may be neglected and one obtains

$$\mu^2 \frac{d\hat{\alpha}}{d\mu^2} = -\frac{\hat{\alpha}^2}{\pi} \hat{\beta}_0 + \mathcal{O}(\alpha^3), \quad (2.56)$$

with the leading coefficient $\hat{\beta}_0$ given in Equation (2.55). Equation (2.56) is an ordinary differential equation that can be solved by imposing an initial value condition, $\hat{\alpha}(\mu_0^2)$, where μ_0^2 is the initial scale. The solution reads

$$\frac{\pi}{\hat{\alpha}(\mu^2)} = \frac{\pi}{\hat{\alpha}(\mu_0^2)} + \hat{\beta}_0 \log \frac{\mu^2}{\mu_0^2}. \quad (2.57)$$

and does not make use of any additional approximations. It can be used to express $\hat{\alpha}^2(\mu_2^2)$ in terms of $\hat{\alpha}(\mu_1^2)$,

$$\begin{aligned}\hat{\alpha}^2(\mu_2^2) &= \left[\frac{1}{\hat{\alpha}(\mu_1^2)} + \frac{\hat{\beta}_0}{\pi} \log \frac{\mu_2^2}{\mu_1^2} \right]^{-2} \\ &= \hat{\alpha}^2(\mu_1^2) \left(1 - 2 \frac{\hat{\alpha}(\mu_1^2)}{\pi} \beta_0 \log \frac{\mu_2^2}{\mu_1^2} \right) + \mathcal{O}(\alpha^4).\end{aligned}\tag{2.58}$$

As stated before, Equation (2.48) is incorrect, as it mixes the coupling parameter at scale μ_1 with the self-energy function at scale μ_2 . The correct cross section in which μ_2 is used in the electromagnetic coupling parameter as well as the self-energy function can now be obtained using Equation (2.58). Combining all pieces, one finds

$$\begin{aligned}\sigma_{\overline{\text{MS}}}(q^2) &= \sigma_{(0)}^{\text{th}}(q^2) \frac{\hat{\alpha}^2(\mu_2^2)}{\left[1 - \hat{\Pi}_T^{\gamma\gamma}(q^2, \mu_2^2) \right]^2} \\ &= \sigma_{(0)}^{\text{th}}(q^2) \hat{\alpha}^2(\mu_1^2) \left[1 - 2 \frac{\alpha}{\pi} \beta_0 \log \frac{\mu_2^2}{\mu_1^2} \right] \\ &\quad \cdot \left[1 + \frac{2\alpha}{3\pi} \log \frac{m_e^2}{\mu_2^2} - 2 \frac{\Sigma_{T,\text{fin}}^{\gamma\gamma}(q^2)}{q^2} \right] + \mathcal{O}(\alpha^4) \\ &= \alpha^2 \sigma_{(0)}^{\text{th}}(q^2) \left[1 - 2 \frac{\Sigma_{T,\text{fin}}^{\gamma\gamma}(q^2)}{q^2} \right] + \mathcal{O}(\alpha^4),\end{aligned}\tag{2.59}$$

where Equation (2.42) was applied to $\hat{\alpha}(\mu_1^2)$ on the last line. The final expression when combining the electromagnetic coupling and self-energy function with the same scale μ_2 is identical to the result of Section 2.5.1 that was obtained using only one scale. This shows that the scale μ is arbitrary to some extent, but one has to be careful to only use quantities with the same scale. The RGE can be used to relate the matching parameter at different scales. Another important observation can be made: The exact solution of the RGE on the first line of

2. Theoretical Background

Equation (2.58) contains not only the leading term that is given explicitly on the second line. Expanding the denominator of Equation (2.58) in $\hat{\alpha}(\mu_1^2)$ yields

$$\hat{\alpha}^2(\mu_2^2) = \hat{\alpha}^2(\mu_1^2) \sum_{n=0}^{\infty} n \left(\frac{\hat{\alpha}^2(\mu_1^2)}{\pi} \beta_0 \log \frac{\mu_1^2}{\mu_2^2} \right)^n, \quad (2.60)$$

which also contains higher order contributions of the scale dependent logarithm. These additional terms correspond to reducible n -loop diagrams that contribute to the photon propagator and are automatically accounted for when the RGE is solved analytically. If the difference of the scales spans several orders of magnitudes, the logarithm becomes large itself leading to a more slowly converging perturbation series. This is the reasons why the use of the RGE is advantageous, as it automatically resums the large logarithms.

Although the coupling parameter as a function of μ is not an observable and the relation to (2.47) is not obvious, it is also referred to as running coupling parameter in the literature. It turns out that the RGE-running as described in this section contains a relevant part of the momentum dependent coupling parameter introduced in Section 2.5.1⁵.

2.5.4. Matching Conditions

The scattering of particles at low energy is dominated by light particles that are sufficiently light to be produced as real particles in the process. Heavier particles may occur in the scattering cross section as virtual particles in loops but play a secondary role, as their numerical contributions are small compared to that of the light particles. This has been proven for any renormalizable theory in terms of the “decoupling theorem” [11], given that the mass of the heavy particle is sufficiently large: The effective theory without the heavy particle is accurate up to order $\frac{p}{M}$, where p is an energy scale and M is the mass of the decoupling particle.

⁵This can be seen when comparing the weak mixing angles as defined in References [9] and [10].

Accordingly, it is desirable to describe scattering processes at low energy using a theory that does not contain the heavy particles, in order to simplify calculations and theoretical predictions for physical observables. The framework of effective theories is the appropriate tool in this context. The effective Lagrangian is derived from the “complete” one by omitting the heavy particle but using a different set of parameters (coupling constants and particle masses) for the effective theory [12]. Then, one has to relate the parameters of both theories in order to construct a physically meaningful effective theory. As will be shown later, the effective model will inherit the renormalization prescription of the “complete” theory. Since the Standard Model has to be considered incomplete and because this concept can also be applied to the removal of heavy particles from an effective model, the term “complete theory” is unsuitable. To highlight the relation between the model including the heavy particles and the one with only light particles, they will be called parent and child model, respectively.

By construction, the child theory will fail at high energies where the heavy particles become active degrees of freedom and can be produced as real particles. However, it needs to be in agreement (up to the accuracy dictated by the perturbative expansion) with the parent theory below the creation threshold of the heavy particles in order to be physically relevant. This requirement allows determining the parameters of the effective theory by equating (matching) it with the parent theory, yielding the so-called “matching conditions”, relations between the parameters of both models.

The derivation of matching conditions in pure QCD has been extensively studied (see References [13–15] and citations therein). While the applicability to the electroweak sector of the Standard Model is not obvious, these results can be directly used in QED. However, in case of the electromagnetic coupling, the matching conditions can be derived in a less systematic but more simple way, which will be briefly illustrated in the following. A more systematic approach to the matching including the weak interaction will be discussed in Chapter 5.

The momentum dependent coupling parameter (2.39) reads

$$\alpha_R^{c/p}(q^2, \mu^2) = \alpha \left(1 + \Pi_{T,R}^{c/p}(q^2, \mu^2) \right), \quad (2.61)$$

2. Theoretical Background

where the superscript “c/p” refers to the parent (p) or child (c) theory, respectively. For readability, the superscript “ $\gamma\gamma$ ” is omitted here and in the remainder of this section. In case of the $\overline{\text{MS}}$ -renormalized QED of an electron and a muon, the vacuum polarization function at one-loop order is given by

$$\hat{\Pi}_T^{e,\mu}(q^2, \mu^2) = \frac{\alpha}{3\pi} \left(\log \frac{\mu^2}{m_e^2} + \log \frac{\mu^2}{m_\mu^2} \right) + \Pi_{T,\text{fin}}^e(q^2) + \Pi_{T,\text{fin}}^\mu(q^2), \quad (2.62)$$

where the terms are separated into pieces originating from the electron and muon, respectively. The effective one-lepton QED can be derived from the two-lepton theory by decoupling the muon. Using α_R^p and α_R^c as an abbreviation for the coupling parameters of the two-lepton and one-lepton QED, respectively, and inserting Equation (2.61) yields

$$\hat{\alpha}^p(q^2, \mu^2) - \hat{\alpha}^c(q^2, \mu^2) = \frac{\alpha^2}{3\pi} \log \frac{\mu^2}{m_\mu^2} + \alpha^2 \Pi_{T,\text{fin}}^\mu(q^2) + \mathcal{O}(\alpha^3) \quad (2.63)$$

for the difference of the coupling parameters, confirming that the coupling parameters of both theories are identical at tree-level. The first term on the right-hand side of Equation (2.63) carries the scale dependence, while the remaining part of the vacuum polarization function contains all terms independent of μ . The electromagnetic coupling constant is determined in the Thomson limit, that is $q^2 = 0$, in which case Equation (2.63) simplifies to

$$\hat{\alpha}^p(\mu^2) - \hat{\alpha}^c(\mu^2) = \frac{\alpha^2}{3\pi} \log \frac{\mu^2}{m_\mu^2} + \mathcal{O}(\alpha^3), \quad (2.64)$$

as $\Pi_{T,\text{fin}}^\mu(q^2)$ vanishes at zero momentum transfer.

A common technique is to define a coupling parameter as a piecewise function of the form

$$\hat{\alpha}(\mu^2) = \begin{cases} \hat{\alpha}^p(\mu^2), & \mu \geq m_\mu \\ \hat{\alpha}^c(\mu^2), & \mu < m_\mu \end{cases} \quad (2.65)$$

and with additional pieces if more particles exist that are removed successively. The definition (2.65) spans several effective models, is discontinuous in general and usually also referred to running coupling parameter.

The scale μ^* at which the theories are matched, that is the scale that determines $\hat{\alpha}^c$ in terms of $\hat{\alpha}^p$, has to be fixed. While the particular choice of the matching scale for each particle is arbitrary, it has a small effect on the numerical value of the coupling parameter at the final scale. In case of QCD, it was shown that a variation of the matching scale by approximately one order of magnitude alters the strong coupling constant at the final scale by less than one percent [15, 16]. It is reasonable to choose μ^* such that no large logarithms occur, $\mu^* \sim m_\mu$, to fully exploit the resumming properties of the RGE. A convenient choice is $\mu^* = m_\mu$ as all scale dependent logarithms vanish in this case and the matching condition is determined by the finite terms, solely. Here, this leads to a continuous coupling parameter (2.65), as the finite part of the vacuum polarization vanishes at one-loop order; at two-loop order, the vacuum polarization contributes to Equation (2.64) inducing a discontinuity at each particle threshold.

A second choice of μ^* that is worth mentioning is the one that is determined by equality of the coupling parameters at the matching scale, $\hat{\alpha}^p(\mu^{*2}) = \hat{\alpha}^c(\mu^{*2})$. Since $\Pi_{\text{fin}}^\mu(q^2)$ is independent of μ , it is possible to tune μ^* such that the terms on the right-hand side of Equation (2.63) cancel. In case of Equation (2.64) it coincides with $\mu^* = m_\mu$ but will differ when two-loop effects are taken into account. This choice is more laborious but has been used for the running of the weak mixing angle in a region where the coupling parameter can be constrained only phenomenologically due to strong interaction effects that break perturbation theory [17, 18].

The matching was introduced in order to decouple a heavy particle, that is to remove a particle and switch over to an effective theory. As indicated before, the matching conditions also need to be applied when switching from an effective theory to another effective theory; both for adding or removing a particle. This allows finding the appropriate coupling parameter of a theory including heavy particles when the parameters have been obtained from experiment using an effective theory without those heavy particles.

The steps that are necessary for the renormalization group evolution of a single coupling parameter including the application of appropriate matching conditions are outlined in the following:

2. Theoretical Background

1. Obtain a numerical value for the coupling constant by comparing a theoretical prediction with experimental data similar to Equations (2.39) and (2.42).
2. Use the RGE to evolve the parameter close to an appropriate matching scale of the next lighter (heavier) particle as done in Equation (2.58).
3. Use the matching conditions to determine the coupling parameter of the theory without (including) this particular particle by equating observables or Green functions similar to Equations (2.61) and (2.64). Go to Step 2 if additional particles need to be decoupled (incorporated).
4. After crossing the last particle threshold, use the RGE to evolve the coupling parameter to the final scale.

Since fermionic matching conditions in QED at one-loop order do not cause a discontinuity at threshold, two-loop effects need to be taken into account to demonstrate above steps in a simple example. The required two-loop expressions are introduced in Chapter 3 so that the applied illustration of this section is postponed till Appendix A.

3. Electromagnetic Coupling in the Modified Minimal Subtraction Scheme

The electromagnetic coupling constant is required for a prediction of the parity violating asymmetry A_{PV} at tree-level which is needed to determine the weak mixing angle in low energy experiments like P2. Since the electromagnetic coupling constant is measured as the strength of charged particle couplings in the Thomson limit, that is at zero momentum transfer, there is no difficulty in obtaining a precise value for the theoretical prediction of the parity violating asymmetry. The most precise determination of the weak mixing angle on the other hand stems from measurements at the Z-pole which can not be directly used in the calculation of a low energy observable. In principle, the weak mixing angle at low energies can be obtained by solving the β -function as shown in Section 2.5.3, but this requires a value of the electromagnetic coupling constant at the same scale as will be seen later. In order to find a prediction of the weak mixing angle at low energies one has to calculate the electromagnetic coupling constant at high energy scales in a first step.

Difficulties arise due to hadronic effects in the low energy regime that can not be treated perturbatively. The electromagnetic coupling is defined unambiguously at tree-level, but becomes renormalization scheme dependent at higher loop orders as described in Section 2.5.1. While the OS scheme is defined such that the vacuum polarization vanishes in the Thomson limit ($\Pi_T^{\gamma\gamma}(0) = 0$), leaving the OS coupling α the same for all orders of perturbation theory, the coupling in the $\overline{\text{MS}}$ -scheme acquires a loop correction and a dependence on the renormalization scale μ induced by $\hat{\Pi}_T^{\gamma\gamma}(0) \neq 0$. The vacuum polarization

3. Electromagnetic Coupling in the Modified Minimal Subtraction Scheme

at zero momentum transfer can be perturbatively derived in the electroweak sector of the Standard Model, but hadronic effects render it impossible to treat quarks and the strong interaction the same way at energy scales less than roughly 1.2 GeV.

One possible solution is the application of an unsubtracted dispersion relation approach allowing the computation of the vacuum polarization - and thus the calculation of the electromagnetic coupling constant - by integrating over experimental data. Choosing appropriate data allows deriving the EM coupling in an energy region, where the strong interaction may be treated perturbatively, too. Utilizing the renormalization group equation, one can then evolve the coupling constant to higher energy scales.

In this chapter, the renormalization group running of the electromagnetic coupling is discussed based on Reference [9]. The starting point is the relation between the electromagnetic coupling in the OS and $\overline{\text{MS}}$ -schemes in terms of the vacuum polarization function, which will be computed in the following. Using Equation (2.39), the relation at leading order, that is without Dyson resumming reducible diagrams, reads¹

$$\hat{\alpha}(\mu) = \frac{\alpha}{1 - \hat{\Pi}_T^{\gamma\gamma}(q^2 = 0, \mu^2)}. \quad (3.1)$$

Apart from Section 3.1.2, this chapter reproduces and verifies the results of Reference [9]. It is organized as follows: An unsubtracted dispersion relation approach to work around hadronic effects is described in Section 3.1 and the non-hadronic effects are discussed in Section 3.2. The results of these two sections are needed to obtain a theoretical value of the electromagnetic coupling just above the non-perturbative energy regime using Equation (3.1). This value can be used as a starting point for the RGE evolution of $\hat{\alpha}(\mu)$ towards the Z-pole. The evolution of the coupling follows the ideas laid out in Sections 2.5.3 and 2.5.4 and requires a solution of the RGE, which is described in Section 3.4. A perturbative expression of the vacuum polarization at large energy scales needed for the RGE

¹The notation of Reference [19] which is used as a source for perturbative QCD expressions and Reference [9] differs from the present one in that a factor of $4\pi\alpha$ is separated from the vacuum polarization function.

as well as the matching conditions is derived in Section 3.3. Based on this, the matching condition for integrating out the W-boson is presented in Section 3.5. A treatment of the non-perturbative regime is required to obtain values of the electromagnetic coupling for scales between the pion creation threshold and the hadronic scale. This is a necessity for the calculation of the weak mixing angle at low energy, as it depends on the electromagnetic coupling at low energy. A method to constrain the electromagnetic coupling phenomenologically and avoid perturbation theory in the non-perturbative regime was investigated in References [9, 18] but will not be discussed in this thesis.

3.1. Dispersion Relation Approach to the Vacuum Polarization Function

As mentioned before, the hadronic contribution $\hat{\Pi}_{T,\text{had}}^{\gamma\gamma}$ to the vacuum polarization function can not be calculated perturbatively. In this section, the unsubtracted dispersion relation approach as applied in Reference² [9] is discussed that allows deriving a numerical value of the electromagnetic coupling constant for the scale μ just above the non-perturbative regime. As this section deals with hadronic effects only, the subscript “had” is omitted in the following and will be put back in Section 3.2. The superscript “ $\gamma\gamma$ ” and subscript “ T ” will be omitted in the entire chapter, as no other self-energies contribute to the electromagnetic coupling when neglecting electroweak two-loop effects.

Employing the analyticity of the vacuum polarization function, its value at the origin can be obtained by means of Cauchy’s integral formula. Avoiding large values of the momentum, $\hat{\Pi}$ can be written as³

$$\hat{\Pi}(0) = \frac{1}{2\pi i} \oint_{|s|=s_0} ds \frac{\hat{\Pi}(s)}{s}, \quad s_0 < 4m_{\pi^\pm}^2, \quad (3.2)$$

with $s_0 < 4m_{\pi^\pm}^2$ arbitrary. The vacuum polarization function contains a branch cut on the real axis above the creation threshold of the pions. Accordingly,

²The dispersion relation approach using subtraction is much older [20].

³The μ dependence is left out for readability in this section.

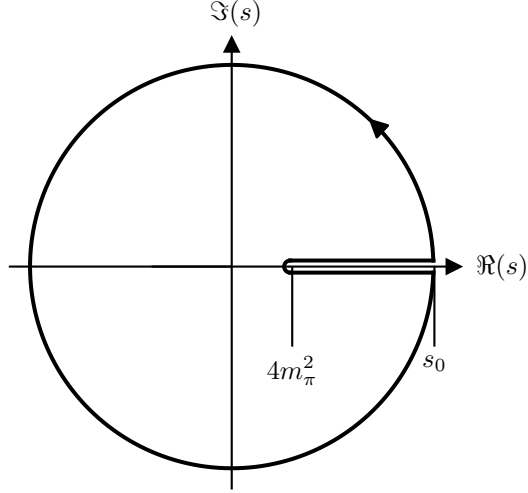


Figure 3.1.: Schematic view of the integration contour for the integral in Equation (3.3). The real axis is excluded for $\Re(q^2) \geq 4m_\pi^2$ and the distance between the two horizontal contour lines is infinitesimal. The arrow on the top right arc indicates the integration direction.

Equation (3.2) only holds for⁴ $s_0 < 4m_{\pi^\pm}^2$. For values of s_0 above this threshold, the integration contour has to be changed in order to exclude the discontinuity on the real axis. Since Cauchy's integral formula can be generalized to non-circular integration contours, this can be achieved by using the integration contour depicted in Figure 3.1, which translates to the contour integral

$$\hat{\Pi}(0) = \frac{1}{2\pi i} \oint_{|s|=s_0} ds \frac{\hat{\Pi}(s)}{s} + \frac{1}{2\pi i} \int_{4m_{\pi^\pm}^2}^{s_0} ds \left(\frac{\hat{\Pi}(s+i\epsilon)}{s+i\epsilon} - \frac{\hat{\Pi}(s-i\epsilon)}{s-i\epsilon} \right). \quad (3.3)$$

⁴The correct threshold is $s_0 < m_{\pi^0}^2$, but the contributions of the process $\gamma^* \rightarrow \pi^0\gamma$ are tiny and negligible compared to the experimental error of the measured cross section.

3.1. Dispersion Relation Approach to the Vacuum Polarization Function

The terms in parentheses account for the part of the integration contour that bends around the branch cut. They can be combined according to

$$\begin{aligned} (\dots) &= \frac{s \left(\hat{\Pi}(s + i\epsilon) - \hat{\Pi}(s - i\epsilon) \right) - i\epsilon \left(\hat{\Pi}(s + i\epsilon) + \hat{\Pi}(s - i\epsilon) \right)}{s^2 + \epsilon^2} \\ &= 2is \frac{\Im \hat{\Pi}(s + i\epsilon)}{s^2 + \epsilon^2} + \mathcal{O}(\epsilon) \approx 2i \frac{\Im \hat{\Pi}(s + i\epsilon)}{s}, \end{aligned} \quad (3.4)$$

where the property $\hat{\Pi}^*(z) = \hat{\Pi}(z^*)$ was used implicitly, by using the relation $\hat{\Pi}(s - i\epsilon) = \Re \hat{\Pi}(s + i\epsilon) - i \Im \hat{\Pi}(s + i\epsilon)$. Inserting the argument of the branch cut integration (3.4) into Equation (3.3) yields⁵

$$\hat{\Pi}(0) = \frac{1}{\pi} \lim_{\epsilon \rightarrow 0} \int_{4m_{\pi^\pm}^2}^{s_0} ds \frac{\Im \hat{\Pi}(s + i\epsilon)}{s} + \frac{1}{2\pi i} \oint_{|s|=s_0} ds \frac{\hat{\Pi}(s)}{s}. \quad (3.5)$$

As mentioned previously, the strong interaction prevents a calculation of the hadronic vacuum polarization in perturbation theory. Accordingly, the first integration of Equation (3.5) has to be evaluated using input from experiments, while the second integral can be treated within the framework of perturbation theory, provided s_0 is well above the hadronic scale. The integration along the real axis can be rewritten using the optical theorem

$$R(s) = \lim_{\epsilon \rightarrow 0} 12\pi \Im \hat{\Pi}(s + i\epsilon), \quad (3.6)$$

where

$$R(s) = \frac{\sigma_{\text{tot}}(e^+e^- \rightarrow \text{hadrons})}{\sigma_0(e^+e^- \rightarrow \mu^+\mu^-)}. \quad (3.7)$$

is the observable hadronic production rate defined as a ratio of cross sections. In the following, I will be used as an abbreviation for the second integral. Using

⁵The author of Reference [9] substituted s with $s - i\epsilon$ but omitted the corresponding change of the integration boundaries. The limit of the integral had been omitted before for the sake of readability, but was introduced back now, to emphasize that $\hat{\Pi}(0)$ does not depend on the auxiliary ϵ .

3. Electromagnetic Coupling in the Modified Minimal Subtraction Scheme

the substitution $s = s_0 e^{i\theta}$, $ds = is d\theta$, with the angle θ bounded by $0 \leq \theta < 2\pi$, to rewrite the contour integration yields

$$\hat{\Pi}(0) = \tilde{R} + I, \quad (3.8a)$$

$$\tilde{R} = \frac{\alpha}{3\pi} \int_{4m_{\pi^\pm}^2}^{s_0} ds \frac{R(s)}{s}, \quad (3.8b)$$

$$I = \frac{1}{2\pi} \int_0^{2\pi} d\theta \hat{\Pi}(s_0 e^{i\theta}). \quad (3.8c)$$

A particular choice of s_0 allows computing the contour integral perturbatively, which is done in Section 3.1.1. The first term of Equation (3.8), the integrated hadronic production rate \tilde{R} , can be evaluated using data from experiments. With the integration boundary $s_0 = (2 \text{ GeV})^2$, a similar quantity can be obtained [18],

$$\tilde{R} \approx \frac{\alpha M_Z^2}{3\pi} \int_{4m_{\pi^\pm}^2}^{4 \text{ GeV}^2} ds \frac{R(s)}{s(M_Z^2 - s)} = (58.71 \pm 0.45) \cdot 10^{-4}, \quad (3.9)$$

which is based on results from References [21] and [22]. The difference of Equation (3.9) and \tilde{R} as defined in Equation (3.8) is [9]

$$\frac{\alpha}{3\pi} \int_{4m_{\pi^\pm}^2}^{s_0} ds R(s) \left[\frac{1}{s} - \frac{M_Z^2}{s(M_Z^2 - s)} \right] \approx -6 \cdot 10^{-7}, \quad (3.10)$$

which is well below the uncertainty of $4.5 \cdot 10^{-5}$ given in Equation (3.9).

3.1.1. Fixed-Order Integration of the Contour Integral

The contour integration of Equation (3.8) requires an analytic expression of the vacuum polarization function $\hat{\Pi}(q)$ as a function of $q^2 = -s_0 = -(2 \text{ GeV})^2$. The exact value is determined by the choice of the boundary for the evaluation of the integrated hadronic production rate that was made above. Because the particular choice $s_0 = (2 \text{ GeV})^2$ is smaller than the charm production-threshold, the vacuum polarization can be computed in an effective QCD with only three light quarks. On the other hand, s_0 is much larger than the masses of the light

3.1. Dispersion Relation Approach to the Vacuum Polarization Function

quarks, so that an expansion of $\hat{\Pi}(q^2)$ in $\frac{\hat{m}_{u,d,s}^2}{q^2}$ is sufficient for the treatment of the light quarks. The vacuum polarization function was derived for a single massive quark up to order $\frac{\hat{m}_q^4}{q^4}$ in Reference [19], with the subscript $1q$ used as an index to indicate that the quantities refer to the contribution of a single quark coupling to the photon. The full vacuum polarization function is then obtained by summing over all quarks of the effective theory and neglecting the mass terms of the quarks that are considered massless. In the three-loop case, the expressions implicitly contain the sum over all quarks in the inner loop, but the masses of these quarks were neglected. The relation between $\hat{\Pi}_{1q}(q^2)$ and the full vacuum polarization function of an effective three-quark QCD is worked out below. The three-loop terms need additional work in order to be applied in the present context and will be discussed in detail, while the one- and two-loop results will be given without comments. Following the notation of Reference [19], a superscript (n) is used to denote terms of $(n+1)$ -loop order. The relevant equations in terms of the $\overline{\text{MS}}$ mass read [19]

$$\hat{\Pi}_{1q}(q^2) = \hat{\Pi}_{1q}^{(0)}(q^2) + \frac{\alpha_s(\mu^2)}{\pi} C_F \hat{\Pi}_{1q}^{(1)}(q^2) + \left(\frac{\alpha_s(\mu^2)}{\pi} \right)^2 \hat{\Pi}_{1q}^{(2)}(q^2) + \mathcal{O}\left(\frac{\hat{\alpha}_s^3}{\pi^3}\right), \quad (3.11a)$$

$$\hat{\Pi}_{1q}^{(0)} = \frac{3\alpha}{4\pi} \left[\frac{20}{9} - \frac{4}{3}L + \frac{8\hat{m}_q^2}{q^2} + \mathcal{O}\left(\frac{\hat{m}_q^4}{q^4}\right) \right], \quad (3.11b)$$

$$\hat{\Pi}_{1q}^{(1)} = \frac{3\alpha}{4\pi} \left[\frac{55}{12} - 4\zeta(3) - L + \frac{4\hat{m}_q^2}{q^2} (4 - 3L) + \mathcal{O}\left(\frac{\hat{m}_q^4}{q^4}\right) \right], \quad (3.11c)$$

with the three-loop order terms

$$\hat{\Pi}_{1q}^{(2)}(q^2) = C_F^2 \hat{\Pi}_{1q,A}^{(2)} + C_A C_F \hat{\Pi}_{1q,NA}^{(2)} + C_F T_F n_l \hat{\Pi}_{1q,l}^{(2)} + C_F T_F \Pi_{1q,F}^{(2)} \quad (3.12a)$$

categorized into the four pieces $\hat{\Pi}_{1q,A}^{(2)}$, $\hat{\Pi}_{1q,NA}^{(2)}$, $\Pi_{1q,F}^{(2)}$ and $\hat{\Pi}_{1q,l}^{(2)}$. The group theoretical constants of SU(3) read $C_F = \frac{4}{3}$, $C_A = 3$, $T_F = \frac{1}{2}$, respectively, and $n_l = n_q - 1$ denotes the number of light quarks, where n_q is the number of all

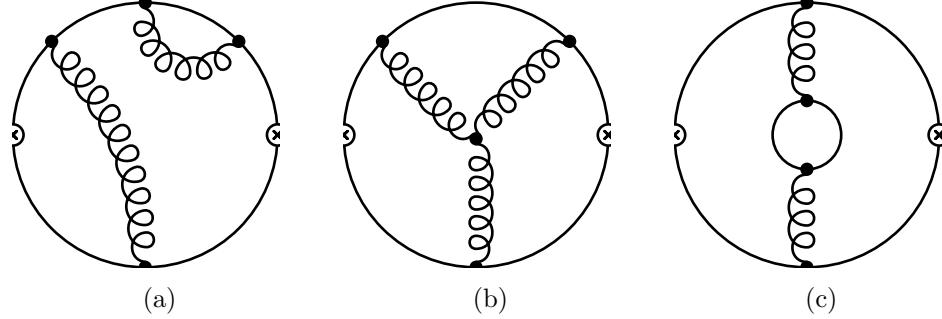


Figure 3.2.: Examples for some of the Feynman diagrams that belong to the three-loop vacuum polarization. The photons coupling to the quark loop at the small crosses are left out. Figure 3.2c stands for all diagrams with an internal quark loop that sum up to $\Pi_{1q,F}^{(2)} + \hat{\Pi}_{1q,l}^{(2)}$, while Figures 3.2a and 3.2b represent the “abelian” and “non-abelian” diagrams that give rise to $\hat{\Pi}_{1q,A}^{(2)}$ and $\hat{\Pi}_{1q,NA}^{(2)}$, respectively.

quarks in the effective theory. The first two pieces correspond to the three-loop Feynman diagrams without internal quark loop, that is diagrams with two gluon lines connected to the outer quark loop and diagrams with an internal gluon loop or a single gluon vertex, respectively. One example of a diagram with two independent gluon lines and no internal quark loop is depicted in Figure 3.2a. These diagrams are part of the abelian part of QCD, as the same diagrams with photons instead of gluons exist and account for the piece $\hat{\Pi}_{1q,A}^{(2)}$ ⁶. The “non-abelian” diagrams that contain gluon-gluon interactions, like Diagram 3.2b, sum up to $\hat{\Pi}_{1q,NA}^{(2)}$. The remaining diagrams contain an internal quark loop like the one shown in Figure 3.2c. They are separated into diagrams in which the inner and outer quark have the same mass \hat{m}_q and diagrams in which the mass \hat{m}_l of the inner quark is negligible. $\Pi_{1q,F}^{(2)}$ corresponds to the first set of diagrams,

⁶The diagrams with an inner quark loop, as the one shown in Figure 3.2c belong to the “abelian” part of QCD, too, but are not included in $\hat{\Pi}_{1q,A}^{(2)}$.

3.1. Dispersion Relation Approach to the Vacuum Polarization Function

while $\hat{\Pi}_{1q,l}^{(2)}$ corresponds to the second. Accordingly, the functions $\hat{\Pi}_{1q,F}^{(2)}$ and $\hat{\Pi}_{1q,l}^{(2)}$ are identical in the limit $\hat{m}_q = 0$. Diagrams with a massive quark in the inner loop and a massless quark in the outer loop were not considered in Reference [19]. For this reason, strange-quarks in the inner loop are considered massless, too, and the contribution of charm- and bottom-quarks that may occur in the inner loop is discussed later on. The explicit expressions for the individual pieces read

$$\begin{aligned} \hat{\Pi}_{1q,A}^{(2)} = \frac{3\alpha}{4\pi} & \left[-\frac{143}{72} - \frac{37}{6}\zeta(3) + 10\zeta(5) + \frac{1}{8}L \right. \\ & + \frac{4\hat{m}_q^2}{q^2} \left(\frac{1667}{96} - \frac{5}{12}\zeta(3) - \frac{35}{6}\zeta(5) - \frac{51}{8}L + \frac{9}{4}L^2 \right) \\ & \left. + \mathcal{O}\left(\frac{\hat{m}_q^4}{q^4}\right) \right], \end{aligned} \quad (3.12b)$$

$$\begin{aligned} \hat{\Pi}_{1q,NA}^{(2)} = \frac{3\alpha}{4\pi} & \left[\frac{44215}{2592} - \frac{227}{18}\zeta(3) - \frac{5}{3}\zeta(5) - \frac{41}{8}L + \frac{11}{24}L^2 + \frac{11}{3}\zeta(3)L \right. \\ & + \frac{4\hat{m}_q^2}{q^2} \left(\frac{1447}{96} + \frac{4}{3}\zeta(3) - \frac{85}{12}\zeta(5) - \frac{185}{24}L + \frac{11}{8}L^2 \right) \\ & \left. + \mathcal{O}\left(\frac{\hat{m}_q^4}{q^4}\right) \right], \end{aligned} \quad (3.12c)$$

$$\begin{aligned} \hat{\Pi}_{1q,l}^{(2)} = \frac{3\alpha}{4\pi} & \left[-\frac{3701}{648} + \frac{38}{9}\zeta(3) + \frac{11}{6}L - \frac{1}{6}L^2 - \frac{4}{3}\zeta(3)L \right. \\ & + \frac{4\hat{m}_q^2}{q^2} \left(-\frac{95}{24} + \frac{13}{16}L - \frac{1}{2}L^2 \right) + \mathcal{O}\left(\frac{\hat{m}_q^4}{q^4}\right) + \mathcal{O}\left(\frac{\hat{m}_l}{\hat{m}_q}\right) \left. \right], \end{aligned} \quad (3.12d)$$

$$\begin{aligned} \Pi_{1q,F}^{(2)} = \frac{3\alpha}{4\pi} & \left[-\frac{3701}{648} + \frac{38}{9}\zeta(3) + \frac{11}{6}L - \frac{1}{6}L^2 - \frac{4}{3}\zeta(3)L \right. \\ & + \frac{4\hat{m}_q^2}{q^2} \left(-\frac{223}{24} + 4\zeta(3) + \frac{13}{16}L - \frac{1}{2}L^2 \right) + \mathcal{O}\left(\frac{\hat{m}_q^4}{q^4}\right) \left. \right], \end{aligned} \quad (3.12e)$$

3. Electromagnetic Coupling in the Modified Minimal Subtraction Scheme

where the abbreviation $L = \log \frac{-q^2}{\mu^2}$ was introduced, terms of order $\frac{\hat{m}_q^4}{q^4}$ were neglected and \hat{m}_l was used to denote the mass of a quark that is light compared to the heaviest one.

Equation (3.12) accounts for the contribution of a single massive quark in the outer loop and $n_l = n_q - 1$ massless quarks in inner loops to the vacuum polarization function. Due to the choice of $s_0 = 2 \text{ GeV}$, it is safe to neglect the masses of the up- and down-quark, which yields

$$\begin{aligned} \hat{\Pi}_{u/d}^{(2)} &= \left[C_F^2 \hat{\Pi}_{1q,A}^{(2)} + C_A C_F \hat{\Pi}_{1q,NA}^{(2)} + C_F T_F \left(n_l \hat{\Pi}_{1q,l}^{(2)} + \Pi_{1q,F}^{(2)} \right) \right]_{\hat{m}_q=0} \\ &= \left[C_F^2 \hat{\Pi}_{1q,A}^{(2)} + C_A C_F \hat{\Pi}_{1q,NA}^{(2)} + C_F T_F (n_l + 1) \hat{\Pi}_{1q,l}^{(2)} \right]_{\hat{m}_q=0} \end{aligned} \quad (3.13)$$

for the contribution of the first generation quarks. The third term accounts for three massless quarks in the inner loop, because a strange-quark in the inner loop is treated as a massless quark as mentioned above. Similarly, the individual contribution of the strange-quarks reads

$$\hat{\Pi}_s^{(2)}(q^2) = \left[C_F^2 \hat{\Pi}_{1q,A}^{(2)} + C_A C_F \hat{\Pi}_{1q,NA}^{(2)} + C_F T_F n_l \hat{\Pi}_{1q,l}^{(2)} + C_F T_F \Pi_{1q,F}^{(2)} \right]_{\hat{m}_q=\hat{m}_s}. \quad (3.14)$$

The polarization function given in (3.11) does not include the electromagnetic charge of the outer quark that stems from the coupling to the photon. Hence, the full three-loop vacuum polarization for all three quarks is obtained by summing the products of the one-quark functions in Equations (3.13) and (3.14) and the appropriate charge factors,

$$\begin{aligned} \hat{\Pi}_{3q}^{(2)} &= Q_u^2 \hat{\Pi}_u^{(2)}(q^2) + Q_d^2 \hat{\Pi}_d^{(2)}(q^2) + Q_s^2 \hat{\Pi}_s^{(2)}(q^2) \\ &= \frac{2}{3} \left[C_F^2 \hat{\Pi}_{1q,A}^{(2)} + C_A C_F \hat{\Pi}_{1q,NA}^{(2)} + C_F T_F (n_l + 1) \hat{\Pi}_{1q,l}^{(2)} \right]_{\hat{m}_q=0} \\ &\quad + \frac{\hat{m}_s^2}{9} \frac{d}{d\hat{m}_q^2} \left[C_F^2 \hat{\Pi}_{1q,A}^{(2)} + C_A C_F \hat{\Pi}_{1q,NA}^{(2)} \right. \\ &\quad \left. + C_F T_F n_l \hat{\Pi}_{1q,l}^{(2)} + C_F T_F \Pi_{1q,F}^{(2)} \right]. \end{aligned} \quad (3.15)$$

3.1. Dispersion Relation Approach to the Vacuum Polarization Function

The first bracket in Equation (3.15), which is proportional to $\frac{2}{3} = Q_u^2 + Q_d^2 + Q_s^2$, accounts for the terms of all three quarks that are independent of mass; the terms on the last line are proportional to m_q^2 . Following the approximations of Reference [9], terms of order $\frac{\hat{m}_q^4}{q^4}$ were neglected, which allows expressing the terms on the last line in terms of a derivative with respect to \hat{m}_q^2 , which automatically removes all terms that are independent of the quark mass.

The integration of I defined in Equation (3.8) requires integrating logarithms of the form $\log\left(-\frac{s_0}{\mu^2}e^{i\theta}\right)$. The branch cut of the logarithm is not crossed because of $0 < \theta < 2\pi$, allowing to simplify the logarithmic terms by using $\log\left(-\frac{s_0}{\mu^2}e^{i\theta}\right) = \log\frac{s_0}{\mu^2} + i(\theta - \pi)$, with a trivial dependence on the integration variable θ . The real part, $\log\frac{s_0}{\mu^2}$, does not depend on the integration variable θ , vanishes when assigning $\mu^2 \rightarrow s_0$, eventually. For this reason, it can be left out immediately. However, the strong coupling constant $\hat{\alpha}_s$ depends on the scale μ , too. Substituting μ^2 with q^2 after the integration, that is assuming $\hat{\alpha}_s$ is constant along the integration contour, is called fixed order perturbation theory (FOPT). Replacing μ^2 with q^2 before the integration and taking into account the running of $\hat{\alpha}_s$ when integrating corresponds to the contour improved perturbation theory (CIPT). The two different integrals are defined as

$$I_{\text{FOPT}} = \frac{1}{2\pi} \left[\int_0^{2\pi} d\theta \hat{\Pi}(q^2 = s_0 e^{i\theta}, \mu^2) \right]_{\mu^2=s_0}, \quad (3.16)$$

$$I_{\text{CIPT}} = \frac{1}{2\pi} \int_0^{2\pi} d\theta \hat{\Pi}(q^2 = s_0 e^{i\theta}, \mu^2 = s_0 e^{i\theta}). \quad (3.17)$$

The FOPT integral can be readily evaluated using the vacuum polarization given above, while the CIPT formalism requires substituting $\hat{\alpha}(\mu)$ with its analytical expression before carrying out the integration. Following the prescription of Reference [9], FOPT is used in this section, but the integration in CIPT and a comparison are given in Section 3.1.2.

The integration of the vacuum polarization function in Equation (3.11) can be divided into three different integrals I_0 , I_1 and \tilde{I}_2 , corresponding to the integration of the pieces $\hat{\Pi}_{1q}^{(0)}$, $\hat{\Pi}_{1q}^{(1)}$ and $\hat{\Pi}_{3q}^{(2)}$, respectively. Since the vacuum

3. Electromagnetic Coupling in the Modified Minimal Subtraction Scheme

polarization $\hat{\Pi}_{1q}$ only accounts for diagrams in which a single quark couples to the photon, one has to sum over all quarks and multiply each term with the appropriate charge factor Q_q^2 . As described above, the correct summation of the three-loop vacuum polarization functions is more involved; making use of the expression in Equation (3.15) one can write

$$I_{\text{FOPT}} = \sum_{q=u,d,s} Q_q^2 [I_0(\hat{m}_q) + I_1(\hat{m}_q)] + \tilde{I}_2. \quad (3.18)$$

Here, the quark sum in the last term is implicitly included in the definition of $\hat{\Pi}_{3q}^{(2)}$, which is the integrand of the integral \tilde{I}_2 ,

$$\tilde{I}_2 = \frac{1}{2\pi} \left[\int_0^{2\pi} d\theta \hat{\Pi}_{3q}^{(2)}(q^2 = s_0 e^{i\theta}, \mu^2) \right]_{\mu^2=s_0}. \quad (3.19)$$

The integrations can be carried out using $\int_0^{2\pi} d\theta(\theta - \pi) = \int_0^{2\pi} d\theta e^{-i\theta} = 0$. Inserting the explicit expressions given above, one finds

$$I_0 = \frac{3\alpha}{4\pi} \frac{20}{9} - \frac{1}{8\pi^3} i \int_0^{2\pi} d\theta(\theta - \pi) + \frac{3}{4\pi^3} \frac{\hat{m}_q^2}{s_0} \int_0^{2\pi} d\theta e^{-i\theta} = \frac{\alpha}{\pi} \frac{5}{3}, \quad (3.20)$$

$$\begin{aligned} I_1 &= \frac{\alpha}{\pi} \frac{\alpha_s}{\pi} \left(\frac{55}{12} - 4\zeta(3) - 12i \frac{\hat{m}_q^2}{s_0} \frac{1}{2\pi} \int_0^{2\pi} d\theta \theta e^{-i\theta} \right) \\ &= \frac{\alpha}{\pi} \frac{\alpha_s}{\pi} \left(\frac{55}{12} - 4\zeta(3) + 12 \frac{\hat{m}_q^2}{s_0} \right), \end{aligned} \quad (3.21)$$

$$\begin{aligned} \tilde{I}_2 &= \frac{2\alpha}{3\pi} \frac{\alpha_s^2}{\pi^2} \left[\frac{118379}{2592} - \frac{31}{12} \zeta(2) - \frac{791}{18} \zeta(3) + \frac{25}{3} \zeta(5) + \frac{403}{36} \frac{\hat{m}_s^2}{s_0} \right. \\ &\quad \left. + n_l \left(-\frac{3701}{1296} + \frac{1}{6} \zeta(2) + \frac{19}{9} \zeta(3) - \frac{7}{18} \frac{\hat{m}_s^2}{s_0} \right) \right] \\ &= \frac{2\alpha}{3\pi} \frac{\alpha_s^2}{\pi^2} \left(\frac{34525}{864} - \frac{9}{4} \zeta(2) - \frac{715}{18} \zeta(3) + \frac{25}{3} \zeta(5) + \frac{125}{12} \frac{\hat{m}_s^2}{s_0} \right), \end{aligned} \quad (3.22)$$

where $n_l = 2$ was used for the number of light quarks on the last line to combine the terms that stem from the Feynman diagrams with an inner quark loop with

3.1. Dispersion Relation Approach to the Vacuum Polarization Function

the remaining ones. The final result of the integration following the FOPT prescription can be found by inserting Equations (3.20), (3.21) and (3.22) into Equation (3.18), which yields⁷

$$\begin{aligned}
 I_{\text{FOPT}} &= \frac{2\alpha}{3\pi} \left\{ \frac{5}{3} + \frac{\alpha_s}{\pi} K_{\text{FOPT}}^{(2)} + \frac{\alpha_s^2}{\pi^2} K_{\text{FOPT}}^{(3)} \right\}, \\
 K_{\text{FOPT}}^{(2)} &= \frac{55}{12} - 4\zeta(3) + 2\frac{\hat{m}_s^2}{s_0}, \\
 K_{\text{FOPT}}^{(3)} &= \frac{34525}{864} - \frac{9}{4}\zeta(2) - \frac{715}{18}\zeta(3) + \frac{25}{3}\zeta(5) + \frac{565}{48}\frac{\hat{m}_s^2}{s_0}.
 \end{aligned} \tag{3.23}$$

The two-loop order terms denoted by $K_{\text{FOPT}}^{(2)}$ stem from a Feynman diagram, in which the quark–antiquark pair exchanges a gluon. The corresponding diagram with a photon instead of a gluon gives the same result but with the coupling $\frac{\alpha_s}{\pi}$ substituted by $\frac{\hat{\alpha}}{4\pi}$ [23] (see also Section 3.3). The additional factor $\frac{1}{4}$ arises, since $C_F^{\text{QCD}} = \frac{4}{3}$ has to be replaced by $C_F^{\text{QED}} = 1$ and the squared charge sum $\sum_{q=u,d,s} Q_q^2 = \frac{2}{3}$ by $\sum_{q=u,d,s} Q_q^4 = \frac{2}{9}$. Modifying Equation (3.23) accordingly to also account for the virtual photon within the fermion loop, the final expression for the nonperturbative part of the vacuum polarization function in fixed order perturbation theory reads [9]

$$\begin{aligned}
 \hat{\Pi}(q^2 = 0, s_0) &= \tilde{R} + \frac{2\alpha}{3\pi} \left\{ \frac{5}{3} + \left(\frac{\alpha_s}{\pi} + \frac{\hat{\alpha}}{4\pi} \right) K_{\text{FOPT}}^{(2)} \right. \\
 &\quad \left. + \frac{\alpha_s^2}{\pi^2} \left[K_{\text{FOPT}}^{(3)} + F\left(\frac{s_0}{\hat{m}_c^2}\right) \right] \right\},
 \end{aligned} \tag{3.24}$$

where F is used to parametrize the effect of massive charm-quarks that may occur in inner loops of Feynman diagrams of the type 3.2c. The corresponding contribution of a heavy quark to a fermion vertex was calculated exactly in Reference [24] and the contribution to the vacuum polarization was given as an

⁷The mass term at two-loop order is neglected in Reference [9].

expansion in terms of the strong coupling constant $\hat{\alpha}_s$ in Reference [25]. The explicit expression for F is given in Reference [9] as

$$F(x) \approx \log x \left[\frac{2}{3} \zeta(3) - \frac{11}{12} + \frac{\log x}{12} \right] - x \left[\frac{2}{25} - \frac{2}{135} \log x \right] + x^2 \left[\frac{1513}{2116800} - \frac{\log x}{5040} \right] - x^3 \left[\frac{1853}{80372250} + \frac{\log x}{127575} \right]. \quad (3.25)$$

3.1.2. Contour Improved Perturbation Theory

As described in Section 3.1.1, the μ -dependence of $\hat{\alpha}_s$ can optionally be taken into account when carrying out the integration of Equation (3.17), which corresponds to the CIPT formalism. It is convenient to express the strong coupling in terms of a power series, as it leads to a straightforward evaluation of the contour integration. The strong coupling constant can be expanded in a power series by solving the β -function iteratively. A higher order solution of the β -function of QCD will be discussed in Section 3.4.2, but the integration in this section will be calculated with the leading solution of the β -function, only. Using the abbreviation $\hat{a}_s = \frac{\hat{\alpha}_s}{\pi}$, the β -function of the strong coupling constant reads [26]

$$\frac{d}{d\mu^2} \hat{a}_s(\mu^2) = - \sum_{k=1}^{\infty} \frac{\hat{\beta}_{k-1}^s}{\mu^2} \hat{a}_s^{k+1}(\mu^2) = - \frac{\hat{\beta}_0^s}{\mu^2} \hat{a}_s^2(\mu^2) + \mathcal{O}(\hat{a}_s^3) \quad (3.26)$$

and can be solved by separation of variables. The leading order solution of the strong coupling constant reads⁸

$$\hat{a}_s(\mu^2) = \left(\frac{\pi}{\hat{\alpha}_s(\mu_0^2)} + \beta_0^{\text{QCD}} \log \frac{\mu^2}{\mu_0^2} \right)^{-1} \quad (3.27)$$

when neglecting higher order contributions beyond the β_0 -term. Expanding Equation (3.27) yields

$$\hat{a}_s(\mu^2) = \hat{a}_s(\mu_0^2) - \hat{a}_s^2(\mu_0^2) \hat{\beta}_0^s \log \frac{\mu^2}{\mu_0^2} + \mathcal{O}(\hat{a}_s^3), \quad (3.28)$$

⁸Terms of order $\mathcal{O}(\hat{a}_s^3)$ were neglected in the β -function, but the solution (3.27) is exact in that sense that it solves the approximated β -function exactly.

3.1. Dispersion Relation Approach to the Vacuum Polarization Function

which will be used for the integration in the following. To that end, $\mu_0^2 = s_0$ is used as initial value condition and $\mu^2 = s_0 e^{i\theta}$ according to the definition of Equation (3.17).

The integral I_0 defined in Equation (3.18) does not contain $\hat{\alpha}_s$ and is the same in FOPT and CIPT, accordingly. I_2 is proportional to α_s^2 , for which reason the additional terms arising from CIPT are of order $\hat{\alpha}_s^3$ and may be neglected. Evaluating I_1 requires the previously used auxiliary integrals

$$\int_0^{2\pi} d\theta i(\theta - \pi) = 0, \quad (3.29)$$

$$\int_0^{2\pi} d\theta e^{-i\theta} = 0, \quad (3.30)$$

$$\int_0^{2\pi} d\theta i(\theta - \pi) e^{-i\theta} = -2\pi, \quad (3.31)$$

as well as

$$\int_0^{2\pi} d\theta i^2(\theta - \pi)^2 = -\frac{2}{3}\pi^3, \quad (3.32)$$

$$\int_0^{2\pi} d\theta i^2(\theta - \pi)^2 e^{-i\theta} = -4\pi \quad (3.33)$$

and yields terms of order α_s^2 that have to be added to I_2 . The additional terms that arise when taking into account the μ -dependence of α_s read

$$\Delta_{I_1} = -\frac{2\alpha}{3\pi} \frac{\alpha_s^2}{\pi} \hat{\beta}_0^s \left(12 \frac{m^2}{s_0} + 3\zeta(2) \right) = -\frac{2\alpha}{3\pi} \frac{\alpha_s^2}{\pi} \left(27 \frac{m^2}{s_0} + \frac{27}{4}\zeta(2) \right), \quad (3.34)$$

where $\hat{\beta}_0^s = \frac{1}{4} \left(11 - \frac{2}{3}n_f \right) = \frac{9}{4}$, was obtained for $n_f = 3$. Summing over the three light quarks results in an additional factor of $\frac{2}{3}$ (or $\frac{1}{9}$ in case of the mass term), leading to the final expression of Equation (3.23) in CIPT. Using $K_{\text{FOPT}}^{(2)}$ to highlight the deviation from the previous calculation, it becomes

$$I^{(3)} = \sum_{i=0}^2 I_i = \frac{2\alpha}{3\pi} \left\{ \frac{5}{3} + \frac{\alpha_s}{\pi} K_{\text{FOPT}}^{(2)} + \frac{\alpha_s^2}{\pi^2} \left[K_{\text{FOPT}}^{(2)} - \frac{9}{2}\zeta(2) + \frac{209}{48} \frac{\hat{m}_s^2}{s_0} \right] \right\}. \quad (3.35)$$

3. Electromagnetic Coupling in the Modified Minimal Subtraction Scheme

Order	FOPT	CIPT	Ratio $\frac{\text{CIPT}}{\text{FOPT}}$
LO	$2.81 \cdot 10^{-2}$	$2.81 \cdot 10^{-2}$	1
NLO	$-0.037 \cdot 10^{-2}$	$-0.037 \cdot 10^{-2}$	1
NNLO	$-0.048 \cdot 10^{-2}$	$-0.173 \cdot 10^{-2}$	3.63
sum	$2.73 \cdot 10^{-2}$	$2.6 \cdot 10^{-2}$	0.95

Table 3.1.: Numerical comparison of Equations (3.23) and (3.35), corresponding to FOPT and CIPT integration of Equation (3.11). The input for the numerical evaluation is $\hat{\alpha}_s = 0.1\pi$, $\hat{m}_s = 0.1 \text{ GeV}$ and $s_0 = (2 \text{ GeV})^2$.

The two formalisms are compared numerically in Table 3.1, where the ratio of the two-loop terms is dominated by the $\zeta(2)$ -term, as the strange quark mass is much smaller than s_0 and all other terms are identical in either formalism. The overall relative difference between the vacuum polarization function obtained using CIPT and FOPT is roughly 4.6 %.

3.2. Non-hadronic Contributions

Section 3.1 dealt with the calculation of the hadronic part of the vacuum polarization function that enters the expression (3.1) of the $\overline{\text{MS}}$ -renormalized electromagnetic coupling. The vacuum polarization also obtains a contribution from charged leptons that needs to be added to the previously determined hadronic contribution and which will be presented in the following.

As mentioned previously, the non-hadronic contributions to the vacuum polarization function can be computed perturbatively. The one-loop expression can be readily obtained from Reference [2] and is given in Appendix C. It reads

$$\hat{\Pi}_{\text{lep}}(q^2 = 0, \mu) = \frac{\alpha}{\pi} \left\{ \frac{1}{3} \left(\sum_l Q_l^2 \log \frac{\mu^2}{m_l^2} \right) - \frac{3}{4} \log \frac{\mu^2}{M_W^2} - \frac{1}{6} \right\} + \mathcal{O}(\alpha^2), \quad (3.36)$$

where the fermion sum is over leptons, only. In order to evaluate this sum within an effective theory at a certain energy scale μ , particles that have been integrated out must not contribute to equation (3.36). For $\mu \lesssim 2 \text{ GeV}$, it is reasonable to not include the contributions of the W-boson; as the scale at which a particle is included into the theory is ambiguous, the terms arising because of the τ -lepton may be included or left out. Following Reference [9], the τ is not included, and one obtains

$$\hat{\Pi}_{\text{lep}}(q^2 = 0, \mu) = \frac{\alpha}{3\pi} \left(\log \frac{\mu^2}{m_e^2} + \log \frac{\mu^2}{m_\mu^2} \right) + \mathcal{O}(\alpha^2). \quad (3.37)$$

The first calculation of leptonic two-loop contributions to the vacuum polarization function was published in Reference [23]. These contributions can also be obtained from the results of Reference [19], in which the contribution of a single heavy quark to vacuum polarization is given. Dividing the expression in terms of the on-shell mass by three to remove the implicit color factor, the leading terms are⁹

$$\hat{\Pi}_{\text{lep}}(q^2 = 0, \mu) = \frac{\alpha}{\pi} \left[\frac{1}{3} \log \frac{\mu^2}{m^2} + \frac{\hat{\alpha}}{4\pi} \left(\frac{15}{4} + \log \frac{\mu^2}{m^2} \right) \right] + \mathcal{O}(\alpha^3), \quad (3.38)$$

where $C_F = 1$ and $Q_f^2 = 1$ was used to adopt the expression to the leptonic case and the strong coupling constant $\hat{\alpha}_s$ was replaced with the electromagnetic coupling $\hat{\alpha}$. Equation (3.38) describes the contribution of a single lepton with its mass defined according to the OS definition. Adding the contributions of the electron and muon yields¹⁰ [9]

$$\hat{\Pi}_{\text{lep}}(q^2 = 0, \mu) = \frac{\alpha}{\pi} \left[\left(\frac{1}{3} + \frac{\hat{\alpha}}{4\pi} \right) \left(\log \frac{\mu^2}{m_e^2} + \log \frac{\mu^2}{m_\mu^2} \right) + \frac{15}{8} \frac{\hat{\alpha}}{\pi} \right] + \mathcal{O}(\alpha^3). \quad (3.39)$$

The last term contributes to the matching conditions which will be discussed in Section 3.5, so it is important to highlight that it is the sum of the identical contributions of the electron and muon.

⁹The complete equation for QCD is given in Equation (3.46).

¹⁰It should read $\frac{15}{8} \frac{\alpha}{\pi}$ instead of $\frac{15}{8}$ in Reference [9].

The relation between the $\overline{\text{MS}}$ -renormalized coupling $\hat{\alpha}$ and the vacuum polarization was given in Equation (3.1). With the hadronic contributions to the vacuum polarization function given in Equation (3.24) and the leptonic terms given in Equation (3.39), the electromagnetic coupling constant for $\mu \gtrsim 1.2 \text{ GeV}$ can be derived using

$$\hat{\alpha}(\mu) = \frac{\alpha}{1 - \hat{\Pi}_{\text{had}}(q^2 = 0, \mu) - \hat{\Pi}_{\text{lep}}(q^2 = 0, \mu)}. \quad (3.40)$$

In a next step, the electromagnetic RGE can be used to evolve the coupling parameter $\hat{\alpha}$ to larger scales $\mu^2 > s_0$; one possible solution of the β -function is discussed in Section 3.4.

3.3. Perturbative Expression of the Vacuum Polarization Function

The previous sections dealt with the calculation of the electromagnetic coupling above the non-perturbative regime. This required a perturbative expression of the leptonic part of the vacuum polarization function which was derived in Section 3.2 as well as the unsubtracted dispersion relation approach of Section 3.1 to handle hadronic effects. In order to obtain a value for the electromagnetic coupling at higher scales, one can make use of the RGE to evolve the coupling by solving the differential equation associated with the β -function. The β -function is determined within the framework of perturbation theory and requires a power series of the vacuum polarization as input, accordingly. The leptonic contribution to this power series was already derived in Section 3.2 but the hadronic contribution needs to be determined in addition. The hadronic contributions that were derived in Section 3.1.1 for the contour integration were obtained assuming small quark masses compared to the momentum transfer, that is the expressions are the leading terms of a power series in $\frac{m_q^2}{q^2}$. This power series can not be used for the derivation of the β -function that requires the contribution to the renormalization constant, which is determined at vanishing momentum transfer. This section deals with the perturbative contribution

3.3. Perturbative Expression of the Vacuum Polarization Function

of quarks to the vacuum polarization at zero momentum transfer, which is required not only for the β -function but also for the derivation of the matching conditions of the heavier quarks.

The vacuum polarization function can be found in Reference [19] in terms of the on-shell mass, but in order to obtain an expression in terms of the $\overline{\text{MS}}$ -mass, one has to express the on-shell mass in terms of the $\overline{\text{MS}}$ -mass as a first step. The relation between the two different mass parameters reads

$$m = \hat{m}(\mu) + m \frac{\hat{\alpha}_s(\mu)}{\pi} C_F \left(1 + \frac{3}{4} L \right) - m \frac{\hat{\alpha}_s^2(\mu)}{\pi^2} N_2 + \mathcal{O}(\hat{\alpha}_s^3), \quad (3.41)$$

where $L = \log \frac{\mu^2}{m^2}$ depends on the scale and the on-shell mass and the second order coefficient is

$$\begin{aligned} N_2 = & C_F T \left(\frac{3}{4} - \frac{3}{2} \zeta(2) \right) + C_F T n_q \left(\frac{71}{96} + \frac{1}{2} \zeta(2) + \frac{13}{24} L + \frac{1}{8} L^2 \right) \\ & + C_F^2 \left(\frac{7}{128} - \frac{15}{8} \zeta(2) - \frac{3}{4} \zeta(3) + \frac{21}{32} L + \frac{9}{32} L^2 + 3 \zeta(2) \log(2) \right) \\ & + C_F C_A \left(-\frac{1111}{384} + \frac{1}{2} \zeta(2) + \frac{3}{8} \zeta(3) - \frac{185}{96} L - \frac{11}{32} L^2 - \frac{3}{2} \zeta(2) \log(2) \right). \end{aligned} \quad (3.42)$$

Neglecting terms of order $\hat{\alpha}_s^2$, it is easily solved for the on-shell mass by replacing the on-shell mass m with the $\overline{\text{MS}}$ -mass \hat{m} on the right-hand side of Equation (3.41). The result in terms of a mass ratio reads

$$\frac{m}{\hat{m}(\mu^2)} = 1 + \frac{\hat{\alpha}_s(\mu)}{\pi} C_F \left(1 + \frac{3}{4} \log \frac{\mu^2}{\hat{m}^2} \right) + \mathcal{O}(\hat{\alpha}_s^2), \quad (3.43)$$

which can now be used to express the logarithm $\log \frac{\mu^2}{m^2}$ in terms of the $\overline{\text{MS}}$ -mass; the result is

$$\log \frac{\mu^2}{m^2} = \log \frac{\mu^2}{\hat{m}^2} - \frac{\hat{\alpha}_s(\mu)}{\pi} C_F \left(2 + \frac{3}{2} \log \frac{\mu^2}{\hat{m}^2} \right) + \mathcal{O}(\hat{\alpha}_s^2). \quad (3.44)$$

3. Electromagnetic Coupling in the Modified Minimal Subtraction Scheme

Substituting equations (3.43) and (3.44) into Equation (3.41) and neglecting terms of order $\hat{\alpha}_s^3$, results in the expression for the OS mass m in terms of the $\overline{\text{MS}}$ mass \hat{m} up to order $\hat{\alpha}_s^2$,

$$\begin{aligned} \frac{m}{\hat{m}(\mu^2)} = 1 + \frac{\hat{\alpha}_s(\mu)}{\pi} \frac{C_F}{4} [4 + 3\hat{L}] \\ + \frac{\hat{\alpha}_s^2(\mu^2)}{\pi^2} \left[\frac{C_F^2}{16} (-8 + 6\hat{L} + 9\hat{L}^2) - N_2 \right] + \mathcal{O}(\hat{\alpha}_s^3), \end{aligned} \quad (3.45)$$

with the scale dependent logarithms abbreviated as $\hat{L} = \log \frac{\mu^2}{\hat{m}^2}$. Here, the explicit C_F^2 -term stems from the substitution of Equations (3.43) and (3.44) into the term of order $\mathcal{O}(\hat{\alpha}_s)$ in Equation (3.41). With Equation (3.45) at hand, it is now possible to derive the vacuum polarization function in terms of the $\overline{\text{MS}}$ -mass.

The vacuum polarization of a single heavy quark with charge Q_f is given in Reference [19], with the mass m as defined in the OS renormalization scheme and reads

$$\frac{\hat{\Pi}(0)}{N_c^f Q_f^2} = \frac{\alpha}{4\pi} \left\{ \frac{4}{3} \log \frac{\mu^2}{m^2} + C_F \frac{\hat{\alpha}_s(\mu^2)}{\pi} \left(\frac{15}{4} + \log \frac{\mu^2}{m^2} \right) + \frac{\hat{\alpha}_s^2(\mu^2)}{\pi^2} K_2 + \mathcal{O}(\hat{\alpha}_s^3) \right\}. \quad (3.46a)$$

The coefficient of the $\hat{\alpha}_s^2$ -term is

$$\begin{aligned} K_2 = C_F T \left(-\frac{23}{8} + 4\zeta(2) + \frac{7}{16}\zeta(3) \right) \\ + C_F T n_q \left(-\frac{917}{648} - \frac{4}{3}\zeta(2) - \frac{14}{9}L - \frac{1}{6}L^2 \right) \\ + C_F^2 \left(\frac{77}{144} + 5\zeta(2) - 8\zeta(2) \log(2) - \frac{1}{8}L + \frac{\zeta(3)}{48} \right) \\ + C_F C_A \left(\frac{14977}{2592} - \frac{4}{3}\zeta(2) + 4\zeta(2) \log 2 + \frac{127}{96}\zeta(3) + \frac{157}{36}L + \frac{11}{24}L^2 \right), \end{aligned} \quad (3.46b)$$

where the abbreviation $L = \log \frac{\mu^2}{m^2}$ for logarithms in terms of the OS mass was used as before. As mentioned in Section 3.2, Equation (3.46) can be also used

3.3. Perturbative Expression of the Vacuum Polarization Function

to derive the vacuum polarization function (3.38) of a single lepton; this is done by dividing by the implicit color factor $N_f = 3$ and inserting $C_F = 1$. Utilizing the mass ratio (3.45), Equation (3.46) can be written up to order $\hat{\alpha}_s^2$ in terms of the $\overline{\text{MS}}$ mass \hat{m} ,

$$\frac{12\pi^2}{N_c^f Q_f^2} \frac{\hat{\Pi}(0)}{4\pi\alpha} = \hat{L} - \frac{\hat{\alpha}_s(\mu^2)}{\pi} C_F \left(\frac{3}{4}\hat{L} - \frac{13}{16} \right) + \frac{\hat{\alpha}_s^2(\mu^2)}{\pi^2} \tilde{K}_2 + \mathcal{O}(\hat{\alpha}_s^3), \quad (3.47a)$$

where the third-order coefficient in terms of $\hat{L} = \log \frac{\mu^2}{\hat{m}^2(\mu^2)}$ reads

$$\begin{aligned} \tilde{K}_2 = & C_F T \left(-\frac{21}{8} + \frac{21}{16} \zeta(3) \right) + C_F T n_q \left(\frac{1}{2} \hat{L}^2 - \frac{1}{3} \hat{L} + \frac{361}{216} \right) \\ & + C_F^2 \left(\frac{27}{8} \hat{L} + \frac{97}{24} - \frac{95}{16} \zeta(3) \right) \\ & + C_F C_A \left(-\frac{11}{8} \hat{L}^2 - \frac{7}{3} \hat{L} + \frac{223}{32} \zeta(3) - \frac{5021}{864} \right). \end{aligned} \quad (3.47b)$$

Equation (3.47) is the vacuum polarization function for a heavy quark coupling to the photon and quarks inside the inner quark loop of the double bubble diagrams¹¹ are treated massless. This expression is required not only in the calculation of the β -function, but also in the derivation of the matching condition for integrating out the heavy quark. Since the quarks in the inner loop are all treated massless, it is not sufficient in this regard. Heavy quarks also appear in the inner loop of a double bubble diagram in which a light quark couples the photon and the vacuum polarization associated with these diagrams enters the matching, too. The corresponding contribution can be reversely extracted from the results of Reference [27], in which the matching condition¹² for integrating out a heavy quark is given. Replacing C_F , C_A and T with their respective numeric values, that is $\frac{4}{3}$, 3 and $\frac{1}{2}$, yields the final expression for the perturbative vacuum polarization function that accounts for all Feynman diagrams containing at least a single heavy quark. Using R_l (R_h) to denote the contributions of

¹¹A double bubble diagram is shown in Figure 3.2c.

¹²The authors of Reference [27] use the term decoupling relation.

three-loop Feynman diagrams in which a light (heavy) quark couples to the photon, it reads [9]

$$\begin{aligned}\hat{\Pi}(0) &= \frac{\alpha}{3\pi^2} N_c^f Q_f^2 \left\{ \hat{L} + \frac{\hat{\alpha}_s(\mu^2)}{\pi} \left(\frac{13}{12} - \hat{L} \right) + \frac{\hat{\alpha}_s^2(\mu^2)}{\pi^2} (R_h + R_l) + \mathcal{O}(\hat{\alpha}_s^3) \right\}, \\ R_h &= \frac{655}{144} \zeta(3) - \frac{3847}{864} - \frac{5}{6} \hat{L} - \frac{11}{8} \hat{L}^2 + n_q \left(\frac{361}{1296} - \frac{1}{18} \hat{L} + \frac{1}{12} \hat{L}^2 \right), \\ R_l &= \sum_l Q_l^2 \left(\frac{295}{1296} - \frac{11}{72} \hat{L} - \frac{1}{12} \hat{L}^2 \right),\end{aligned}\tag{3.48}$$

with the sum evaluated for all $n_l = n_q - 1$ light quarks that are treated massless.

3.4. Electromagnetic Renormalization Group Equation

Using Equation (3.40), the results of Sections 3.1 and 3.2 allow determining the $\overline{\text{MS}}$ -renormalized electromagnetic coupling for scales at the lower end of the perturbative regime $\mu \gtrsim 1.2 \text{ GeV}$; here the particular choice $\mu = 2 \text{ GeV}$ was made. As described in Section 2.5.2, a solution of the β -function can be used to calculate a value at higher energy scales. The derivation of the coefficients in the β -function requires a perturbative expression of the vacuum polarization function that was derived in Section 3.3. In this section, the β -function of the electromagnetic coupling is introduced and the solution of the corresponding differential equation is presented in Section 3.4.1. The solution depends on an auxiliary integral parametrizing strong interaction effects, which is discussed in Section 3.4.3, based on a solution of the β -function of QCD derived in Section 3.4.2.

The β -function describing the running of the electromagnetic coupling constant $\hat{\alpha}$ including higher order terms is determined by the derivative of the coupling with respect to the scale μ . Using the relation between vacuum polarization function and electromagnetic coupling given in Equation (3.1), it may be written as

$$\hat{\beta} = -\frac{\hat{\alpha}^2}{\pi} \mu^2 \frac{d}{d\mu^2} \left[-\frac{\pi}{\alpha} \hat{\Pi}(q^2 = 0, \mu) \right].\tag{3.49}$$

3.4. Electromagnetic Renormalization Group Equation

The definition of the coefficients of the power series of Equation (3.49) is given in Equation (2.54). Since the one-loop diagram is purely electromagnetic, the leading coefficient parametrizing strong interaction effects denoted by $\hat{\delta}_0$, vanishes. The leading $\hat{\beta}_i$ -coefficients can be obtained by differentiating the expressions in Section 3.2. Keeping in mind that Equation (3.39) contains the implicit charge factors Q_f^2 and Q_f^4 , corresponding to the one and two-loop diagrams, one finds

$$\hat{\beta}_0 = -\frac{1}{3} \sum_f N_f Q_f^2, \quad \hat{\beta}_1 = -\frac{1}{4} \sum_f N_f Q_f^4, \quad \hat{\delta}_0 = 0, \quad (3.50)$$

where the sum includes all fermions and the color factor N_f was introduced to account for the multiplicity of quarks.

The higher order coefficients parametrizing strong interaction effects, $\hat{\delta}_i, i > 0$, can be obtained by differentiating the contribution of quarks to the hadronic vacuum polarization with respect to μ^2 . The contribution of a single massive quark is given by the vacuum polarization in Equation (3.48). Computing its derivative also requires differentiating the coupling $\hat{\alpha}_s$ and the mass \hat{m} with respect to μ^2 ; $\hat{\alpha}_s$ is the expansion parameter and the mass occurs in logarithms \hat{L} . The derivatives are the β - and γ -functions of the strong interaction, which can also be expanded as a power series in $\hat{\alpha}_s$. The generic power series in terms of the coefficients β_i^{QCD} and γ_i^{QCD} are similar to the expansion of the electromagnetic beta function. They read [27]

$$\mu^2 \frac{d}{d\mu^2} \frac{\hat{\alpha}_s}{\pi} = - \sum_{i=0}^{\infty} \beta_i^{\text{QCD}} \left(\frac{\hat{\alpha}_s}{\pi} \right)^{i+2} = -\beta_0^{\text{QCD}} \frac{\hat{\alpha}_s^2}{\pi^2} + \mathcal{O}(\hat{\alpha}_s^3), \quad (3.51)$$

$$\frac{1}{\hat{m}} \mu^2 \frac{d}{d\mu^2} \hat{m} = - \sum_{i=0}^{\infty} \gamma_i^{\text{QCD}} \left(\frac{\hat{\alpha}_s}{\pi} \right)^{i+1} = -\gamma_0^{\text{QCD}} \frac{\hat{\alpha}_s}{\pi} - \gamma_1^{\text{QCD}} \frac{\hat{\alpha}_s^2}{\pi^2} + \mathcal{O}(\hat{\alpha}_s^3), \quad (3.52)$$

where only the leading terms that are relevant in the following are kept on the right-hand side. These leading coefficients read [25]

$$\beta_0^{\text{QCD}} = \frac{11}{4} - \frac{1}{6} n_q, \quad \gamma_0^{\text{QCD}} = 1, \quad \gamma_1^{\text{QCD}} = \frac{1}{16} \left(\frac{202}{3} - \frac{20}{9} n_q \right), \quad (3.53)$$

3. Electromagnetic Coupling in the Modified Minimal Subtraction Scheme

with the number of quark flavors denoted by n_q . Neglecting terms of order α_s^3 , the derivative of the scale dependent logarithm is

$$\mu^2 \frac{d}{d\mu^2} \log \frac{\mu^2}{\hat{m}^2} = 1 + 2 \left[\frac{\hat{\alpha}_s}{\pi} + \left(\frac{\hat{\alpha}_s}{\pi} \right)^2 \left(\frac{101}{24} - \frac{5}{36} n_q \right) \right], \quad (3.54)$$

which can be used to find

$$-\frac{\hat{\alpha}^2}{\pi} \mu^2 \frac{d}{d\mu^2} \left[-\frac{\pi}{\alpha} \hat{\Pi}(q^2 = 0, \mu) \right] = -\frac{\hat{\alpha}^2}{\pi} Q_f^2 \left\{ -1 - \frac{\hat{\alpha}_s}{\pi} + \frac{\hat{\alpha}_s^2}{\pi^2} \left[\frac{11}{72} n_q - \frac{125}{48} \right] \right\} \quad (3.55)$$

for the derivative of the vacuum polarization function in Equation (3.48). The leading term accounts for the coefficient $\hat{\beta}_0$ that was already given above, while the remaining ones determine $\hat{\delta}_1$ and $\hat{\delta}_2$. Comparing Equations (2.54) and (3.55) yields

$$\hat{\delta}_1 = -\sum_q Q_q^2 = -N_c C_F \sum_q \frac{Q_q^2}{4}, \quad (3.56)$$

$$\hat{\delta}_2 = \sum_q Q_q^2 \left[\frac{11}{72} n_q - \frac{125}{48} \right] = N_c C_F \sum_q Q_q^2 \left[\frac{11}{144} T_F n_q - \frac{125}{192} \right] \quad (3.57)$$

for the coefficients parametrizing the strong interaction effects on the electromagnetic coupling in agreement with the expressions given in Reference [9].

In order to make use of the renormalization group evolution as was sketched in Section 2.5.3, one has to find a solution of the differential Equation (2.52). Since the coefficients of the β -function can only be obtained perturbatively, one has to restrict the discussion to leading terms in the power series of the β -function. The differential equation that will be discussed in the following accounts for diagrams up to four-loop order and reads¹³

$$\mu^2 \frac{d}{d\mu^2} \hat{\alpha} = -\frac{\hat{\alpha}^2}{\pi} \left(\hat{\beta}_0 + \hat{\beta}_1 \frac{\hat{\alpha}}{\pi} + \hat{\beta}_2 \frac{\hat{\alpha}^2}{\pi^2} + \hat{\delta}_1 \frac{\hat{\alpha}_s(\mu^2)}{\pi} + \hat{\delta}_2 \frac{\hat{\alpha}_s^2(\mu^2)}{\pi^2} + \hat{\delta}_3 \frac{\hat{\alpha}_s^3(\mu^2)}{\pi^3} \right), \quad (3.58)$$

¹³Equation (3.58) includes the $\hat{\beta}_2$ -term but is otherwise identical to the differential equation solved in Reference [9].

with the electromagnetic three-loop coefficient $\hat{\beta}_2$ and the third strong interaction coefficient $\hat{\delta}_3$ given in Reference [9].

Depending on the number of coefficients taken into account, it could be impossible to find a solution in terms of elementary functions, but a series expansion of the solution up to any order¹⁴ can always be obtained by solving the differential equation iteratively. In case of Equation (3.58), it is possible to separate the variables and integrate either side analytically when omitting terms of order $\hat{\alpha}\hat{\alpha}_s$ relative to the $\hat{\beta}_0$ -term that correspond to a product of $\hat{\beta}_1$ - and $\hat{\delta}_1$ -terms. The result is an implicit function of the electromagnetic coupling which can be used for numerical evaluations. An explicit series expansion of the coupling parameter up to any order can then be constructed by iteratively inserting the implicit function into itself.

The differential equation of the electromagnetic coupling depends on the strong coupling due to the non-vanishing coefficients $\hat{\delta}_i, i > 0$. As a consequence, the β -function can only be solved with an expression of the strong coupling at hand, which requires a solution of the β -function of QCD, in turn. It can be obtained from the solution of Equation (3.58), since the β -function of QCD exhibits a similar structure. Therefore, the following discussion is split into three parts: The separation of variables and integration of Equation (3.58) is outlined in Section 3.4.1. The intermediate result will depend on an auxiliary integral of the strong coupling as explained above. In Section 3.4.2, this intermediate result is used to determine an expression of the strong coupling that solves the β -function of QCD. Eventually, the auxiliary integral is solved in Section 3.4.3 by inserting the outcome of Section 3.4.2; the solution can be inserted into the intermediate result of Section 3.4.1 to find the final solution of Equation (3.58).

3.4.1. Intermediate Solution

Terms of order $\mathcal{O}(\hat{\alpha}\hat{\alpha}_s)$ relative to the $\hat{\beta}_0$ -term in Equation (3.58) are denoted by ϵ_i in Reference [9] and account for higher order Feynman diagrams in which

¹⁴The solution may include logarithmic terms stemming from reducible Feynman diagrams up to any order, but will only account for the β -function coefficients that were not omitted in the differential equation.

3. Electromagnetic Coupling in the Modified Minimal Subtraction Scheme

photons and gluons appear side by side. Since these terms were neglected in the differential equation, the product of $\hat{\beta}_1$ and any $\hat{\delta}_i$ can be dropped when solving the differential equation without loosing accuracy. This allows separating the variables $\hat{\alpha}$ and μ^2 . Dividing both sides by the sum of the purely electromagnetic coefficients $\hat{\beta}_i$ times the appropriate power of the coupling constant and dropping $\hat{\beta}_1$ and $\hat{\beta}_2$ in the denominator on the right-hand side yields

$$\frac{d\hat{\alpha}}{\hat{\alpha}^2 \left(\beta_0 + \beta_1 \frac{\hat{\alpha}}{\pi} + \beta_2 \frac{\hat{\alpha}^2}{\pi^2} \right)} = -\frac{1}{\pi} \left[1 + \frac{\mu^2}{\hat{\beta}_0} \frac{d}{d\mu^2} F(\hat{\alpha}_s) + \mathcal{O} \left(\frac{\hat{\alpha} \hat{\alpha}_s}{\pi^2}, \frac{\hat{\alpha}_s^4}{\pi^4} \right) \right] \frac{d\mu^2}{\mu^2}, \quad (3.59)$$

where the auxiliary function F defined as

$$F(\hat{\alpha}_s) = \int_{\mu_0^2}^{\mu^2} \frac{d\mu^2}{\mu^2} \left(\hat{\delta}_1 \frac{\hat{\alpha}_s(\mu^2)}{\pi} + \hat{\delta}_2 \frac{\hat{\alpha}_s^2(\mu^2)}{\pi^2} + \hat{\delta}_3 \frac{\hat{\alpha}_s^3(\mu^2)}{\pi^3} \right) \quad (3.60)$$

accounts for the contribution of the strong interaction coefficients $\hat{\delta}_i$. As explained before, solving the integral in Equation (3.60) requires an expression of the strong coupling constant in terms of the scale μ^2 , which will be derived from an intermediate solution of Equation (3.58) in Section 3.4.2. For the time being, the integral $F(\hat{\alpha}_s)$ is kept as an unknown function and will be calculated in Section 3.4.3, eventually.

Both sides of Equation (3.59) can now be integrated independently. It is convenient to introduce the abbreviations

$$\chi_1 = \beta_1^2 - 2\beta_0\beta_2, \quad (3.61a)$$

$$\chi_2 = \beta_1^2 - 4\beta_0\beta_2, \quad (3.61b)$$

$$B^\pm = -\beta_1 \pm \sqrt{\beta_1^2 - 4\beta_0\beta_2} \frac{\beta_1^2 - 2\beta_0\beta_2}{\beta_1^2 - 4\beta_0\beta_2} = -\beta_1 \pm \frac{\chi_1}{\sqrt{\chi_2}} \quad (3.61c)$$

for combinations of the β -function coefficients that appear in the final solution. The parameters χ_1 and χ_2 are positive because of $\beta_0 < 0$ and $\beta_2 > 0$, and as a

consequence, B^\pm is real valued. Using C to denote the integration constant, the integral of Equation (3.59) can now be written as

$$\begin{aligned} & -\frac{1}{\beta_0 \hat{\alpha}(\mu^2)} - \frac{B^+}{2\pi\beta_0^2} \log\left(\frac{1}{\hat{\alpha}(\mu^2)} + \frac{1}{\pi\chi_1} \left(\beta_1\beta_2 + 2\beta_2 B^+ - \frac{\beta_1^2}{2\beta_0} B^+\right)\right) \\ & - \frac{B^-}{2\pi\beta_0^2} \log\left(\frac{1}{\hat{\alpha}(\mu^2)} + \frac{1}{\pi\chi_1} \left(\beta_1\beta_2 + 2\beta_2 B^- - \frac{\beta_1^2}{2\beta_0} B^-\right)\right) \quad (3.62) \\ & = C - \frac{1}{\pi} \log \frac{\mu^2}{\mu_0^2} - \frac{F(\hat{\alpha}_s)}{\pi\beta_0}. \end{aligned}$$

Since the solution of the differential equation is used to relate the coupling parameter at two different scales, a reasonable choice for the initial value condition is $\lim_{\mu^2 \rightarrow \mu_0^2} \hat{\alpha}(\mu^2) = \hat{\alpha}(\mu_0^2)$, which directly leads to

$$\begin{aligned} C = & -\frac{1}{\beta_0 \hat{\alpha}(\mu_0^2)} - \frac{B^+}{2\pi\beta_0^2} \log\left(\frac{1}{\hat{\alpha}(\mu_0^2)} + \frac{1}{\pi\chi_1} \left(\beta_1\beta_2 + 2\beta_2 B^+ - \frac{\beta_1^2}{2\beta_0} B^+\right)\right) \\ & - \frac{B^-}{2\pi\beta_0^2} \log\left(\frac{1}{\hat{\alpha}(\mu_0^2)} + \frac{1}{\pi\chi_1} \left(\beta_1\beta_2 + 2\beta_2 B^- - \frac{\beta_1^2}{2\beta_0} B^-\right)\right). \quad (3.63) \end{aligned}$$

The logarithms that occur explicitly in Equation (3.62) can be combined with the ones in the integration constant. Introducing $\tilde{L}^\pm(\hat{\alpha}(\mu^2))$ as an abbreviation for the combination of the logarithms as a function of $\hat{\alpha}(\mu^2)$,

$$\tilde{L}^\pm(\hat{\alpha}(\mu^2)) := \log\left(\frac{\frac{\hat{\alpha}(\mu_0^2)}{\hat{\alpha}(\mu^2)} + \frac{\hat{\alpha}(\mu_0^2)}{\pi\chi_1} \left(\beta_1\beta_2 + 2\beta_2 B^\pm - \frac{\beta_1^2}{2\beta_0} B^\pm\right)}{1 + \frac{\hat{\alpha}(\mu_0^2)}{\pi\chi_1} \left(\beta_1\beta_2 + 2\beta_2 B^\pm - \frac{\beta_1^2}{2\beta_0} B^\pm\right)}\right), \quad (3.64)$$

the particular implicit solution reads

$$\begin{aligned} \frac{\hat{\alpha}(\mu_0^2)}{\hat{\alpha}(\mu^2)} = & 1 + F(\hat{\alpha}_s) + \frac{\hat{\alpha}(\mu_0^2)}{\pi} \beta_0 \log \frac{\mu^2}{\mu_0^2} \\ & - \frac{\hat{\alpha}(\mu_0^2)}{2\pi\beta_0} \left[B^+ \tilde{L}^+(\hat{\alpha}(\mu^2)) + B^- \tilde{L}^-(\hat{\alpha}(\mu^2)) \right]. \quad (3.65) \end{aligned}$$

3. Electromagnetic Coupling in the Modified Minimal Subtraction Scheme

When inserting the leading term $\frac{\hat{\alpha}(\mu_0^2)}{\hat{\alpha}(\mu^2)} = 1$ into Equation (3.64), the logarithm vanishes, showing that \tilde{L}^\pm is of order $\mathcal{O}(\alpha)$. This allows deriving an explicit power series of Equation (3.65) by performing a fixed-point iteration up to the desired order. The explicit expression will contain a chain of logarithms, but a simpler expression can be obtained by calculating the corresponding series expansion. Including terms up to four-loop order, the explicit solution of Equation (3.58) reads

$$\begin{aligned} \frac{\hat{\alpha}(\mu_0^2)}{\hat{\alpha}(\mu^2)} = & 1 + \left(\frac{\hat{\alpha}(\mu_0^2)}{\pi} \right) \left(\hat{\beta}_0 L + F(\hat{\alpha}_s) \right) + \left(\frac{\hat{\alpha}(\mu_0^2)}{\pi} \right)^2 \hat{\beta}_1 L \\ & + \left(\frac{\hat{\alpha}(\mu_0^2)}{\pi} \right)^3 L \left(\hat{\beta}_2 - \frac{\hat{\beta}_0 \hat{\beta}_1}{2} L \right) \\ & + \left(\frac{\hat{\alpha}(\mu_0^2)}{\pi} \right)^4 L^2 \left(-\frac{\hat{\beta}_1^2}{2} - \hat{\beta}_0 \hat{\beta}_2 L + \frac{\hat{\beta}_0^2 \hat{\beta}_1}{3} L^2 \right) + \mathcal{O}(\hat{\alpha}^5), \end{aligned} \quad (3.66)$$

where

$$L := \log \frac{\mu^2}{\mu_0^2} \quad (3.67)$$

is used as an abbreviation for the scale dependent logarithms. The terms of order $\mathcal{O}(\hat{\alpha}^4(\mu_0^2))$ contain only logarithms stemming from reducible diagrams, as the coefficient $\hat{\beta}_3$ was omitted in Equation (3.58). Since Equation (3.66) is an expression of the inverse coupling $\hat{\alpha}^{-1}(\mu^2)$, calculating the coupling using this series expansion will include resummed terms beyond the four-loop order.

3.4.2. Running of the Strong Coupling

The expression of the electromagnetic coupling in Equation (3.66) is not complete, as the terms arising from QCD corrections to the vacuum polarization function were collected in the yet undetermined function $F(\hat{\alpha}_s)$ defined in Equation (3.60). Carrying out the integration is only possible when the strong

coupling as a function of the scale parameter μ is known. In order to obtain an expression for $\hat{\alpha}_s(\mu^2)$ one has to solve the β -function of QCD, which is addressed in this section. The final expression of the auxiliary integral will then be determined in Section 3.4.3.

The β -function of QCD reads up to four-loop order [26]

$$\mu^2 \frac{d}{d\mu^2} \frac{\hat{\alpha}_s(\mu^2)}{\pi} = -\frac{\hat{\alpha}_s^2}{\pi^2} \left(\hat{\beta}_0^s + \hat{\beta}_1^s \frac{\hat{\alpha}_s}{\pi} + \hat{\beta}_2^s \frac{\hat{\alpha}_s^2}{\pi^2} + \hat{\beta}_3^s \frac{\hat{\alpha}_s^3}{\pi^3} \right), \quad (3.68)$$

with the leading coefficients

$$\hat{\beta}_0^s = \frac{1}{4} \left(11 - \frac{2}{3} n_q \right), \quad (3.69)$$

$$\hat{\beta}_1^s = \frac{1}{16} \left(102 - \frac{38}{3} n_q \right). \quad (3.70)$$

The variable n_q denotes the number of quarks in the theory and changes when decoupling the heaviest quark. A superscript “s” is used to denote β -function coefficients of QCD in line with the subscript of the strong coupling constant $\hat{\alpha}_s$. The solution of the QCD- β -function is conventionally expressed in terms of the so-called asymptotic scale parameter Λ [28]; it is obtained by performing a series expansion but the final expression of $\hat{\alpha}_s(\mu^2)$ is not given in terms of an initial value $\hat{\alpha}_s(\mu_0^2)$. For the present case, it is more convenient to derive a series expansion of the strong coupling constant similar to Equation (3.66), which is done in the following. The series expansion can then be integrated trivially, as the entire scale dependence is carried by positive powers of the logarithm (3.67).

Equation (3.68) is similar to the β -function of the electromagnetic coupling constant without the QCD terms parametrized by $\hat{\delta}_i$. Not taking into account the four-loop order term $\hat{\beta}_3^s$, Equation (3.68) can be obtained from Equation (3.58) using the substitutions $\hat{\delta}_i \rightarrow 0$, $\hat{\alpha} \rightarrow \hat{\alpha}_s$ and $\hat{\beta}_i \rightarrow \hat{\beta}_i^s$. Accordingly, the three-loop solution may be derived from Equation (3.66) by making the same substitutions. In order to facilitate the integration in Equation (3.60), it is convenient to find a solution of $\hat{\alpha}_s(\mu^2)$ instead of the inverse $\frac{1}{\hat{\alpha}_s(\mu^2)}$. Expanding

the inverse of Equation (3.66), applying the substitutions mentioned above and neglecting terms of order $\mathcal{O}(\hat{\alpha}_s^5)$ yields

$$\begin{aligned} \frac{\hat{\alpha}_s(\mu^2)}{\hat{\alpha}_s(\mu_0^2)} = & 1 - \left(\frac{\hat{\alpha}_s(\mu_0^2)}{\pi} \right) \hat{\beta}_0^s L - \left(\frac{\hat{\alpha}_s(\mu_0^2)}{\pi} \right)^2 L \left[\hat{\beta}_1^s - (\hat{\beta}_0^s)^2 L \right] \\ & - \left(\frac{\hat{\alpha}_s(\mu_0^2)}{\pi} \right)^3 L \left[\hat{\beta}_2^s - \frac{5}{2} \hat{\beta}_0^s \hat{\beta}_1^s L + \hat{\beta}_0^{s3} L^2 \right] \\ & - \left(\frac{\hat{\alpha}_s(\mu_0^2)}{\pi} \right)^4 L^2 \left[\hat{\beta}_3^s - 3 \hat{\beta}_0^s \hat{\beta}_2^s L - \frac{3}{2} \hat{\beta}_1^{s2} L \right. \\ & \quad \left. + \frac{13}{3} \hat{\beta}_0^{s2} \hat{\beta}_1^s L^2 - \hat{\beta}_0^{s4} L \right] + \mathcal{O}(\hat{\alpha}_s^5). \end{aligned} \quad (3.71)$$

The $\hat{\beta}_3^s$ -term on the last line can be guessed by looking at the logarithmic terms stemming from irreducible diagrams at lower orders in the series expansion, but was verified explicitly by inserting the solution (3.71) into the differential Equation (3.68).

3.4.3. Solution of the Auxiliary Function Parametrizing the Strong Interaction

In Section 3.4.1, the solution (3.66) of the electromagnetic β -function was given in terms of the undetermined auxiliary function $F(\hat{\alpha}_s)$, only. Section 3.4.2 was dedicated to the solution of the β -function of QCD in terms of a power series, which is required for the integration of the auxiliary function defined in Equation (3.60). In this section, the result of Section 3.4.2 is utilized to perform the integration, which is the last step required for the final solution of Equation (3.58).

Since the expression of the strong coupling parameter was constructed as a power series that is polynomial in the scale dependent logarithms, the only integral required in this section is

$$\int_{\mu_0^2}^{\mu^2} \frac{d\mu^2}{\mu^2} \log^n \frac{\mu^2}{\mu_0^2} = \frac{1}{n+1} \log^{n+1} \frac{\mu^2}{\mu_0^2}. \quad (3.72)$$

Inserting the expansion of the strong coupling (3.71) into the definition of $F(\hat{\alpha}_s)$ in Equation (3.60) and neglecting terms of order $\mathcal{O}(\hat{\alpha}_s^6)$ yields

$$\begin{aligned}
 F(\hat{\alpha}_s) = & \left(\frac{\hat{\alpha}_s(\mu_0^2)}{\pi} \right) \hat{\delta}_1 L + \left(\frac{\hat{\alpha}_s(\mu_0^2)}{\pi} \right)^2 L \left[\hat{\delta}_2 - \frac{1}{2} \hat{\beta}_0^s \hat{\delta}_1 L \right] \\
 & + \left(\frac{\hat{\alpha}_s(\mu_0^2)}{\pi} \right)^3 L \left[\hat{\delta}_3 - \hat{\beta}_0^s \hat{\delta}_2 L - \frac{\hat{\beta}_1^s \hat{\delta}_1}{2} L + \frac{\hat{\beta}_0^{s2} \hat{\delta}_1}{3} L^2 \right] \\
 & + \left(\frac{\hat{\alpha}_s(\mu_0^2)}{\pi} \right)^4 L^2 c_4 + \left(\frac{\hat{\alpha}_s(\mu_0^2)}{\pi} \right)^5 L^2 c_5 + \mathcal{O}(\hat{\alpha}_s^6),
 \end{aligned} \tag{3.73a}$$

where the coefficients of the fourth and fifth order are

$$\begin{aligned}
 c_4 = & -\frac{3}{2} \hat{\beta}_0^s \hat{\delta}_3 - \hat{\beta}_1^s \hat{\delta}_2 - \frac{\hat{\beta}_2^s \hat{\delta}_1}{2} + \hat{\beta}_0^{s2} \hat{\delta}_2 L + \frac{5}{6} \hat{\beta}_0^s \hat{\beta}_1^s \hat{\delta}_1 L - \frac{\hat{\beta}_0^{s3} \hat{\delta}_1}{4} L^2, \\
 c_5 = & -\frac{3}{2} \hat{\beta}_1^s \hat{\delta}_3 - \hat{\beta}_2^s \hat{\delta}_2 - \frac{\hat{\beta}_3^s \hat{\delta}_1}{2} + 2 \hat{\beta}_0^{s2} \hat{\delta}_3 L + \frac{7}{3} \hat{\beta}_0^s \hat{\beta}_1^s \hat{\delta}_2 L + \frac{\hat{\beta}_1^{s2} \hat{\delta}_1}{2} L \\
 & + \hat{\beta}_0^s \hat{\beta}_2^s \hat{\delta}_1 L - \hat{\beta}_0^{s3} \hat{\delta}_2 L^2 - \frac{13}{12} \hat{\beta}_0^{s2} \hat{\beta}_1^s \hat{\delta}_1 L^2 + \frac{\hat{\beta}_0^{s4} \hat{\delta}_1}{5} L^3.
 \end{aligned} \tag{3.73b}$$

Equation (3.73) coincides with the series expansion of the QCD terms of the solution in Reference [9] when neglecting terms of order $\mathcal{O}(\hat{\alpha}_s^5)$. It can be inserted into (3.66) to obtain the final solution of Equation (3.58).

3.5. Matching Conditions

The concept of matching a child theory onto its parent theory has been outlined in a simplified manner in Section 2.5.4. A more sophisticated formalism will be introduced in Chapter 5, but when neglecting weak interaction effects, the previous concept is sufficient. This section is based on the simplified ansatz in order to reproduce the matching condition for integrating out a heavy fermion that was published in Reference [17].

3. Electromagnetic Coupling in the Modified Minimal Subtraction Scheme

The relation between coupling constant and vacuum polarization function is given in Equation (3.1) and allows expressing the difference of the inverted coupling constants in terms of $\hat{\Pi}^{c/p}$,

$$\frac{1}{\hat{\alpha}^p(\mu^2)} - \frac{1}{\hat{\alpha}^c(\mu^2)} = -\frac{\hat{\Pi}^p(0) - \hat{\Pi}^c(0)}{\alpha}. \quad (3.74)$$

The superscript p (c) introduced in Section 2.5.4 is used to denote the coupling parameter and vacuum polarization of the parent (child) theory. Feynman diagrams that do not contain the heavy fermion are the same in either theory so that the numerator on the right-hand side of Equation (3.74) is precisely given by Equation (3.48) when omitting non-hadronic two-loop effects. The purely electromagnetic terms at two-loop order induced by a single fermion were given in Equation (3.38) and should be added in line with Equation (3.40). The final matching condition becomes [17]

$$\begin{aligned} \frac{\pi}{\hat{\alpha}^p(m_f^2)} - \frac{\pi}{\hat{\alpha}^c(m_f^2)} = & -\frac{\hat{\alpha}}{\pi} N_c^f Q_f^4 \frac{15}{16} - \frac{\hat{\alpha}_s}{\pi} Q_f^2 \frac{13}{12} - \frac{\hat{\alpha}_s^2}{\pi^2} \frac{295}{1296} \sum_l Q_l^2 \\ & - \frac{\hat{\alpha}_s^2}{\pi^2} Q_f^2 \left[\frac{655}{144} \zeta(3) - \frac{3847}{864} + \frac{361}{1296} n_q \right] \end{aligned} \quad (3.75)$$

when choosing $\mu = m_f$ as the matching scale to drop all logarithms and where the terms proportional to $\hat{\alpha}_s$ must be omitted for leptons.

The derivation of Equation (3.75) is simplified by the fact that the strong coupling does not change at fermion threshold when neglecting two-loop contributions. This is used when cancelling the terms stemming from light fermions in Equation (3.74), and it is the reason for omitting the argument of $\hat{\alpha}_s$ in Equation (3.75). To be more precise, the term

$$-4\pi \frac{N_c^f Q_f^2}{12\pi^2} \left(\frac{\hat{\alpha}_s^p(m_f^2)}{\pi} - \frac{\hat{\alpha}_s^c(m_f^2)}{\pi} \right) \frac{13}{12} \quad (3.76)$$

was silently omitted. Since the matching of the strong coupling at one-loop order is proportional to a logarithm of the ratio of fermion mass and scale μ [14],

Equation (3.75) is indeed justified. However, the threshold effects of QCD have to be taken into account at higher loop order. In a sophisticated approach, the child and parent model could be defined including QCD and the matching conditions for the electromagnetic and strong coupling parameters would then be obtained simultaneously. A more systematic ansatz for deriving matching conditions is worked out in Chapter 5, but restricted to a discussion at one-loop order where threshold effects of QCD do not play a role.

4. Parity Violating Interaction and the Weak Mixing Angle

Probing the weak force at low energies is a difficult task due to the suppression of amplitudes by the inverse mass of one of the heavy gauge bosons. Compared to the exchange of a photon, the exchange of a heavy gauge boson is hardly distinguishable from background noise. Hence, the measurement of weak effects on observables at zero or small momentum transfer requires a sophisticated suppression of the electromagnetic interactions, as these dominate parity conserving interactions. A practical solution to this problem is to take advantage of the parity violating property of the weak force. Probing observables that are sensitive to a parity transformation allows discriminating between the weak and the parity conserving electromagnetic force. Measuring a cross section or count rate by scattering particles of opposite polarizations (left- and right-handed) yields tiny differences in a polarization dependent observable. This variation is tiny, but subtracting the “left-handed observable” and “right-handed observable” will cancel all parity conserving effects and the remainder quantifies the parity violation of the observable. An important example is the parity violating left–right asymmetry of electron–proton scattering¹ that is investigated in the P2 experiment to determine the weak mixing angle.

The one-loop corrections to the charged current interaction of muon decay give rise to correction terms that need to be taken into account when expressing neutral-current amplitudes in terms of the Fermi constant. These correction terms may be absorbed in the Fermi constant as described in Section 2.4. Similarly, higher order corrections to the neutral current interaction between

¹In the following, parity violating asymmetry will always refer to the left–right asymmetry of electron–proton scattering.

two fermions contribute to the neutral current interaction and give a correction to the overall coupling strength and the weak mixing angle as will be shown in Section 4.2. Originally, this was used to define an effective weak mixing angle that contains the renormalized one-loop corrections, but will also be used as a basis for the derivation of matching conditions in Chapter 5.

In this chapter, the parity violating interaction is derived in the Standard Model. The Lagrangian of the Standard Model was introduced in Section 2.1, but as described in Section 2.2 the calculation of loop effects requires a renormalization of the theory. In Section 4.1, the irreducible two- and three-point vertex functions of the EWSM are derived, which are required for a systematic renormalization of the model. The renormalized vertex functions are used in the second part, in Section 4.2, to derive the $\overline{\text{MS}}$ -renormalized parity violating interaction. The β -function of the weak mixing angle is derived in Section 4.3 and a possible solution published in Reference [17] is presented in Section 4.4.

4.1. Irreducible Vertex Functions

4.1.1. Bosonic Two-Point Functions

The tree-level two-point functions are determined by the terms in the Standard Model Lagrangian that are bilinear in the respective fields. In case of the bosonic fields, these terms read

$$\mathcal{L}_{bb} = -\frac{1}{4}F_{\mu\nu}F^{\mu\nu} - \frac{1}{4}Z_{\mu\nu}Z^{\mu\nu} + \frac{1}{2}M_{0,Z}Z_\mu Z^\mu - \frac{1}{2\xi_A}(\partial_\mu A_0^\mu)^2 - \frac{1}{2\xi_Z}(\partial_\mu Z_0^\mu)^2. \quad (4.1)$$

The propagator is the two-point function

$$G_{\mu\nu}^{ab}(x_1, x_2) = \frac{(-i)^2 \delta^2}{\delta J_a^\mu(x_1) \delta J_b^\nu(x_2)} \frac{\int \mathcal{D}[\dots] \exp\left(i \int d^4x \left[\mathcal{L} + J_\gamma^\mu A_\mu + J_Z^\mu Z_\mu \right]\right)}{\int \mathcal{D}[\dots] \exp(iS)}, \quad (4.2)$$

where $\int \mathcal{D}[\dots]$ denotes the functional integration over all degrees of freedom and $a, b = \gamma, Z$. In order to evaluate the functional derivative, it is convenient,

to rewrite Equation (4.1) in terms of a matrix multiplication, in which the derivatives of the kinetic terms and counter terms are sandwiched between a vector of the gauge fields. Using X to denote the matrix of renormalization constants defined in Equation (2.19), Equation (4.1) can be written as

$$\mathcal{L}_{bb} = -\frac{i}{2} \begin{pmatrix} A_\mu & Z_\mu \end{pmatrix} \tilde{\Gamma}^{\mu\nu} \begin{pmatrix} A_\nu \\ Z_\nu \end{pmatrix}, \quad (4.3)$$

with

$$\begin{aligned} \tilde{\Gamma}^{\mu\nu} &= iX^T \mathcal{G} X, \\ \mathcal{G} &= \begin{pmatrix} g^{\mu\nu} \partial^2 - \partial^\mu \partial^\nu \left(1 - \frac{1}{\xi_A}\right) & 0 \\ 0 & g^{\mu\nu} (\partial^2 + M_{0,Z}^2) - \partial^\mu \partial^\nu \left(1 - \frac{1}{\xi_Z}\right) \end{pmatrix}. \end{aligned} \quad (4.4)$$

The Lagrangian (4.3) is now expressed in terms of the renormalized fields and the renormalization constants δZ_X are absorbed into the definition of $\tilde{\Gamma}^{\mu\nu}$. The bosonic two-point Green function is related to the inverse $\Delta_{\mu\nu}(x, x')$ of $\tilde{\Gamma}^{\mu\nu}$, defined by

$$\tilde{\Gamma}^{\mu\nu} \Delta_{\nu\rho}(x, x') = \delta^{(4)}(x - x') g^{\mu\rho}, \quad (4.5)$$

which allows determining the Green function by inverting the matrix in Equation (4.4). With the shifted fields

$$\begin{pmatrix} \tilde{A}_\mu \\ \tilde{Z}_\mu \end{pmatrix} = \begin{pmatrix} A_\mu \\ Z_\mu \end{pmatrix} + i \int d^4 x' \Delta_{\mu\rho}(x, x') \begin{pmatrix} J_A^\rho(x') \\ J_Z^\rho(x') \end{pmatrix}, \quad (4.6)$$

where J_A^μ and J_Z^μ are the sources, the bilinear terms read

$$\begin{aligned} &\int d^4 x (\mathcal{L}_{bb} + J_A^\mu A_\mu + J_Z^\mu Z_\mu) \\ &= -\frac{i}{2} \int d^4 x \begin{pmatrix} \tilde{A}_\mu & \tilde{Z}_\mu \end{pmatrix} \tilde{\Gamma}^{\mu\nu} \begin{pmatrix} \tilde{A}_\nu \\ \tilde{Z}_\nu \end{pmatrix} \\ &\quad - \frac{i}{2} \int d^4 x d^4 x' \begin{pmatrix} J_A^\rho(x') & J_Z^\rho(x') \end{pmatrix} \Delta_{\mu\rho}(x, x') \begin{pmatrix} J_A^\mu(x) \\ J_Z^\mu(x) \end{pmatrix}. \end{aligned} \quad (4.7)$$

4. Parity Violating Interaction and the Weak Mixing Angle

Due to translational invariance of the path integral, the fields \tilde{A}_μ and \tilde{Z}_μ can be replaced by A_μ and Z_μ . Equation (4.5) is equivalent to the momentum space expression

$$\tilde{\Gamma}^{\mu\nu}(q^2)\Delta_\nu^\rho(q^2) = g^{\mu\rho}, \quad (4.8)$$

where $\Delta_\nu^\rho(q^2)$ is the Fourier transform of $\Delta_\nu^\rho(x_1, x_2)$,

$$\Delta_\nu^\rho(x_1, x_2) = \int \frac{d^4q}{(2\pi)^4} e^{-iq(x_1-x_2)} \Delta_\nu^\rho(q^2), \quad (4.9)$$

and

$$\begin{aligned} \tilde{\Gamma}^{\mu\nu}(q^2) &= -iX^T \mathcal{G}(q^2) X, \\ \mathcal{G}(q^2) &= \begin{pmatrix} g^{\mu\nu} q^2 - q^\mu q^\nu \left(1 - \frac{1}{\xi_A}\right) & 0 \\ 0 & g^{\mu\nu} (q^2 - M_{0,Z}^2) - q^\mu q^\nu \left(1 - \frac{1}{\xi_Z}\right) \end{pmatrix}. \end{aligned} \quad (4.10)$$

Inserting the bilinear Lagrangian (4.3) instead of the complete Lagrangian of the EWSM into Equation (4.2) yields the tree-level propagator (in matrix notation)

$$G_{\mu\nu}^{\text{tree}}(x_1, x_2) = -\Delta_{\mu\nu}(x_1, x_2), \quad (4.11)$$

which implies

$$\tilde{\Gamma}^{\mu\nu}(q^2) G_{\nu\rho}^{\text{tree}}(q^2) = -g^\mu{}_\rho \quad (4.12)$$

for the tree-level propagator $G_{\nu\rho}^{\text{tree}}(q^2)$ in momentum space. By construction, the tree-level propagator $G_{\nu\rho}^{\text{tree}}(q^2)$ contains the full dependence on the renormalization constants δZ_X . The solution to Equation (4.12) can be easiest found by separating $\tilde{\Gamma}^{\mu\nu}$ into transverse and longitudinal parts. However, for the calculation of the irreducible two-point vertex function, the explicit expression of $G_{\nu\rho}^{\text{tree}}(q^2)$ is not required. The complete propagator including all possible Feynman diagrams can be derived in terms of the self-energy functions $\Sigma_{ab}^{\mu\nu}(q^2)$. Using the matrix $(\tilde{\Sigma}^{\mu\nu}(q^2))_{ab} = \Sigma_{ab}^{\mu\nu}(q^2)$ and omitting the argument q^2 for simplicity, the propagator in matrix notation reads

$$G_{\mu\nu} = G_{\mu\nu}^{\text{tree}} + G_{\mu\alpha}^{\text{tree}} i\tilde{\Sigma}^{\alpha\beta} G_{\beta\nu}^{\text{tree}} + G_{\mu\alpha}^{\text{tree}} i\tilde{\Sigma}^{\alpha\beta} G_{\beta\gamma}^{\text{tree}} i\tilde{\Sigma}^{\gamma\delta} G_{\delta\nu}^{\text{tree}} + \dots \quad (4.13)$$

For the summation, it is convenient, to decompose tree-level propagator and self-energy into transverse and longitudinal parts according to Equation (2.25). Then, the Dyson series (4.13) becomes

$$G_{\mu\nu} = \left(-g_{\mu\nu} + \frac{q_\mu q_\nu}{q^2}\right) G_T^{\text{tree}} \left(1 - i\tilde{\Sigma}_T G_T^{\text{tree}}\right)^{-1} - \frac{q_\mu q_\nu}{q^2} G_L^{\text{tree}} \left(1 - i\tilde{\Sigma}_L G_L^{\text{tree}}\right)^{-1}. \quad (4.14)$$

The irreducible two-point vertex function $\Gamma^{\mu\nu}(q^2)$ is the inverse of the propagator, defined by

$$\Gamma^{\mu\nu}(q^2) G_{\nu\rho} = -g^{\mu\rho}, \quad (4.15)$$

and can be readily obtained from Equation (4.14). According to Equation (4.12), the inverse of the tree-level propagator can be expressed in terms of $\tilde{\Gamma}^{\mu\nu}$, which yields

$$\Gamma^{\mu\nu} = \left(-g^{\mu\nu} + \frac{q^\mu q^\nu}{q^2}\right) [\tilde{\Gamma}_T + i\tilde{\Sigma}_T] - \frac{q^\mu q^\nu}{q^2} [\tilde{\Gamma}_L + i\tilde{\Sigma}_L]. \quad (4.16)$$

Using the same separation into transverse and longitudinal parts as before, the matrix elements of $\Gamma^{\mu\nu}$ in the Standard Model are given by

$$\Gamma_T^{\gamma\gamma} = iq^2(1 + \delta Z_A) + i(q^2 - M_{0,Z}^2)\delta Z_{ZA}^2 + i\Sigma_T^{\gamma\gamma}(q^2), \quad (4.17a)$$

$$\Gamma_L^{\gamma\gamma} = i\frac{q^2}{\xi_A}(1 + \delta Z_A) + i\left(\frac{q^2}{\xi_Z} - M_{0,Z}^2\right)\delta Z_{ZA}^2 + i\Sigma_L^{\gamma\gamma}(q^2), \quad (4.17b)$$

$$\Gamma_T^{ZZ} = i\left(q^2 - M_{0,Z}^2\right)(1 + \delta Z_Z) + iq^2\delta Z_{AZ}^2 + i\Sigma_T^{ZZ}(q^2), \quad (4.17c)$$

$$\Gamma_L^{ZZ} = i\left(\frac{q^2}{\xi_Z} - M_{0,Z}^2\right)(1 + \delta Z_Z) + i\frac{q^2}{\xi_A}\delta Z_{AZ}^2 + i\Sigma_L^{ZZ}(q^2), \quad (4.17d)$$

$$\Gamma_T^{\gamma Z} = iq^2\delta Z_{AZ}\sqrt{1 + \delta Z_A} + i\left(q^2 - M_{0,Z}^2\right)\delta Z_{ZA}\sqrt{1 + \delta Z_Z} + i\Sigma_T^{\gamma Z}(q^2), \quad (4.17e)$$

$$\Gamma_L^{\gamma Z} = i\frac{q^2}{\xi_A}\delta Z_{AZ}\sqrt{1 + \delta Z_A} + i\left(\frac{q^2}{\xi_Z} - M_{0,Z}^2\right)\delta Z_{ZA}\sqrt{1 + \delta Z_Z} + i\Sigma_L^{\gamma Z}(q^2), \quad (4.17f)$$

and $\Gamma_{\mu\nu}^{Z\gamma} = \Gamma_{\mu\nu}^{\gamma Z}$ due to the symmetry of the γZ -mixing. Equation (4.17) was derived without approximations and is valid to all orders of perturbation theory.

Equation (4.17) also motivates the particular choice of X in (2.19): If the off-diagonal elements in X had been defined using a square root, the factors δZ_{AZ}^2 and δZ_{ZA}^2 would be replaced by δZ_{AZ} and δZ_{ZA} , respectively. This would be counter-intuitive, as the γZ -mixing terms in $\Gamma_{\mu\nu}^{\gamma\gamma}$ and $\Gamma_{\mu\nu}^{ZZ}$ are clearly of two-loop order.

4.1.2. Fermionic Two-Point Functions

The terms in the Standard Model Lagrangian determining the tree-level propagator of a single fermion f read

$$\mathcal{L}_{fb} = \bar{f}_{0,i} (i\cancel{\partial} - m_{0,f}) f_{0,i}, \quad (4.18)$$

where $f_0 = f_0^L + f_0^R$. One needs to introduce renormalization constants for the left- and right-handed fields separately as given in Equation (2.19), which yields the expression

$$\mathcal{L}_{fb} = \bar{f} \left[i\cancel{\partial} \left(1 + \frac{1 - \gamma_5}{2} \delta Z_L^f + \frac{1 + \gamma_5}{2} \delta Z_R^f \right) - m_{0,f} \sqrt{1 + \delta Z_L^f} \sqrt{1 + \delta Z_R^f} \right] f \quad (4.19)$$

in terms of the renormalized fields. The remaining derivation of the fermion propagator is similar to the calculation of the bosonic propagator. The tree-level propagator $S_f^{(0)}(q)$ equals i times the inverse of the terms in the square brackets in Equation (4.19) and the corresponding equation in momentum space reads

$$i \left(S_f^{(0)}(q) \right)^{-1} = \cancel{q} \left(1 + \frac{1 - \gamma_5}{2} \delta Z_L^f + \frac{1 + \gamma_5}{2} \delta Z_R^f \right) - m_{0,f} \sqrt{1 + \delta Z_L^f} \sqrt{1 + \delta Z_R^f}. \quad (4.20)$$

As in case of the bosonic two-point functions, the propagator including the self energy insertion can be resummed in terms of a Dyson sum. Using $\Sigma^f(q)$ to

denote the self-energy function of the fermion and omitting the momentum dependence, it reads

$$S_f = S_f^{(0)} + S_f^{(0)} i \Sigma^f S_f^{(0)} + S_f^{(0)} i \Sigma^f S_f^{(0)} i \Sigma^f S_f^{(0)} + \dots = S_f^{(0)} \left[1 - i \Sigma^f S_f^{(0)} \right]^{-1}. \quad (4.21)$$

The self energy is a Dirac matrix and can be decomposed into vector, axial vector and scalar parts according to

$$\Sigma^f(q) = \not{q} \Sigma_V^f(q^2) + \not{q} \gamma_5 \Sigma_A^f(q^2) + m_{0,f} \Sigma_S^f(q^2). \quad (4.22)$$

The irreducible two-point vertex function Γ_f is the inverse of the propagator. Inserting Equations (4.20) to (4.22) yields

$$\begin{aligned} i\Gamma_f(q) &= i \left(S_f^{(0)}(q) \right)^{-1} + \Sigma^f(q) \\ &= \not{q} \left[1 + \frac{1 - \gamma_5}{2} \left(\delta Z_L^f + \Sigma_V^f(q^2) - \Sigma_A^f(q^2) \right) \right. \\ &\quad \left. + \frac{1 + \gamma_5}{2} \left(\delta Z_R^f + \Sigma_V^f(q^2) + \Sigma_A^f(q^2) \right) \right] \\ &\quad - m_{0,f} \left(\sqrt{1 + \delta Z_L^f} \sqrt{1 + \delta Z_R^f} - \Sigma_S^f(q^2) \right). \end{aligned} \quad (4.23)$$

For later use, it is convenient to group the terms of Equation (4.23) in terms of scalar, vector and axial vector parts. Using the vector and axial vector renormalization constants

$$\delta Z_V^f = \frac{\delta Z_L^f + \delta Z_R^f}{2} \quad \text{and} \quad \delta Z_A^f = \frac{\delta Z_R^f - \delta Z_L^f}{2} \quad (4.24)$$

as an abbreviation, the irreducible vertex function can be written as

$$\begin{aligned} i\Gamma_f(q) &= \not{q} \left(1 + \delta Z_V^f + \Sigma_V^f(q^2) \right) + \not{q} \gamma_5 \left(\delta Z_A^f + \Sigma_A^f(q^2) \right) \\ &\quad - m_{0,f} \left(\sqrt{1 + \delta Z_L^f} \sqrt{1 + \delta Z_R^f} - \Sigma_S^f(q^2) \right). \end{aligned} \quad (4.25)$$

4.1.3. Three-Point Functions

At leading order, the one-particle irreducible vertex functions are simply the Feynman rules for the interaction vertices. In the Standard Model, they are determined by the terms

$$\begin{aligned}
 & -e_0 Q_f \bar{f}_0 \gamma_\mu f_0 A_0^\mu + g_{0,Z} \bar{f}_0 \left(T_f^3 \gamma_\mu \frac{1-\gamma_5}{2} - s_0^2 Q_f \gamma_\mu \right) f_0 Z_0^\mu \\
 & = \bar{f} \gamma_\mu \left[-e_0 Q_f \left(1 + \delta Z_V^f + \delta Z_A^f \gamma_5 \right) \sqrt{1 + \delta Z_A} \right. \\
 & \qquad \qquad \qquad \left. + \frac{g_{0,Z}}{2} \left(v_f^* - a_f^* \gamma_5 \right) \delta Z_{ZA} \right] f A^\mu \tag{4.26} \\
 & + \bar{f} \gamma_\mu \left[\frac{g_{0,Z}}{2} \left(v_f^* - a_f^* \gamma_5 \right) \sqrt{1 + \delta Z_Z} \right. \\
 & \qquad \qquad \qquad \left. - e_0 Q_f \left(1 + \delta Z_V^f + \delta Z_A^f \gamma_5 \right) \delta Z_{AZ} \right] f Z^\mu
 \end{aligned}$$

in the Lagrangian density, in which the constants

$$v_f^* = T_f^3 \left(1 + \delta Z_V^f - \delta Z_A^f \right) - 2s_0^2 Q_f \left(1 + \delta Z_V^f \right), \tag{4.27a}$$

$$a_f^* = T_f^3 \left(1 + \delta Z_V^f - \delta Z_A^f \right) + 2s_0^2 Q_f \delta Z_A^f \tag{4.27b}$$

are used as abbreviations for vector- and axial vector coupling constants containing the fermionic renormalization constants. Equation (4.26) indicates that the off-diagonal renormalization constants δZ_{AZ} and δZ_{ZA} do not only induce a mixing of gauge boson propagators at higher loop order, but also play an important role in the renormalization of the coupling constants, as they affect the interaction vertices, too. Higher order corrections may be separated according to transformation behavior with respect to Lorentz transformations. Following the notation of Reference [3], the tensor structure of the vertex functions can be decomposed according to

$$\begin{aligned}
 \Lambda_\mu^{ffa}(q^2) & = \gamma_\mu \Lambda_V^{ffa}(q^2) + \gamma_\mu \gamma_5 \Lambda_A^{ffa}(q^2) \\
 & + \frac{(p+p')_\mu}{2\tilde{m}_f} \Lambda_S^{ffa}(q^2) + \gamma_5 \frac{(p-p')_\mu}{2\tilde{m}_f} \Lambda_P^{ffa}(q^2), \quad a = \gamma, Z, \tag{4.28}
 \end{aligned}$$

where $\Lambda_X^{ffa}(q^2)$ with $a = \gamma, Z$ and $X = V, A, S, P$ are used to parametrize the vector, axial vector, scalar and pseudo-scalar contributions, respectively. The irreducible fermion-photon and fermion-Z vertices in terms of $\Lambda_\mu^{ffa}(q^2)$ read

$$\begin{aligned} \Gamma_{1\text{PI},\mu}^{ff\gamma}(p, p') &= -ie_0 Q_f \gamma_\mu \left(1 + \delta Z_V^f + \delta Z_A^f \gamma_5\right) \sqrt{1 + \delta Z_A} \\ &\quad + i \frac{g_{0,Z}}{2} \gamma_\mu \left(v_f^* - a_f^* \gamma_5\right) \delta Z_{ZA} - ie_0 \Lambda_\mu^{ff\gamma}(q^2), \end{aligned} \quad (4.29)$$

$$\begin{aligned} \Gamma_{1\text{PI},\mu}^{ffZ}(p, p') &= +i \frac{g_{0,Z}}{2} \gamma_\mu \left(v_f^* - a_f^* \gamma_5\right) \sqrt{1 + \delta Z_Z} \\ &\quad - ie_0 Q_f \gamma_\mu \left(1 + \delta Z_V^f + \delta Z_A^f \gamma_5\right) \delta Z_{AZ} + i \frac{g_{0,Z}}{2} \Lambda_\mu^{ffZ}(q^2) \end{aligned} \quad (4.30)$$

and serve as a definition for the Λ_X^{ffa} -functions. The numerators of the coefficients of Λ_S^{ffX} and Λ_P^{ffX} are expressed in terms of the pole mass² \tilde{m} , as it avoids the occurrence of mass ratios when applying the Gordon identity. Since the vertex functions are loop corrections themselves, the choice of the pole mass instead of the bare or renormalized mass has no practical consequence at one-loop order. Comparing Equations (4.29) and (4.30) with Reference [2] yields the explicit one-loop expressions that are given in Appendix C.

The electromagnetic coupling constant is determined by the fermion–photon interaction. In order to renormalize the coupling constant or derive the electromagnetic coupling in an effective theory in terms of matching conditions, one has to calculate the fermion–photon interaction at zero momentum transfer. The corresponding Green function in position space defined by means of the functional integral reads

$$\begin{aligned} G^{ffa,\nu}(x_1, x_2, x_3) &= \frac{(-i)^2 i \delta^3}{\delta J_a^\nu(x_1) \delta \bar{\eta}_f(x_2) \delta \eta_f(x_3)} \\ &\quad \cdot \frac{\int \mathcal{D}[\dots] \exp \left\{ i \int d^4x [\mathcal{L} + \mathcal{L}_J] \right\}}{\int \mathcal{D}[\dots] \exp(iS)}, \quad a = \gamma, Z, \end{aligned} \quad (4.31)$$

²The definition of the pole mass is intricate in case of unstable particles and confined quarks do not possess a pole mass at all. The notation of Equations (4.29) and (4.30) is still valid, as the factor \tilde{m}_f^{-1} can be cancelled by an appropriate normalization of the vertex functions.

4. Parity Violating Interaction and the Weak Mixing Angle

where the source term Lagrangian in the exponential function in the numerator is defined as

$$\mathcal{L}_J = J_\gamma^\mu A_\mu + J_Z^\mu Z_\mu + \sum_f (\bar{\eta}_f f + \bar{f} \eta_f). \quad (4.32)$$

The function $G^{ff^a,\nu}(p, p')$ is used to denote the Fourier transform of the $ff\gamma$ -Green function in the following, p and p' refer to the incoming and outgoing fermion momenta, respectively, and

$$q = p - p' \quad (4.33)$$

is the momentum of the outgoing photon. The interaction described by (4.31) includes the one-particle irreducible fermion–photon vertex derived above, as well as the fermion– Z coupling paired with a γZ -mixing propagator. Due to charge universality, the particular choice of the charged fermion f is irrelevant. The family index i is omitted for brevity.

The Green function $G^{ff\gamma,\mu}(p, p')$ is represented by the sum of the Feynman diagrams shown in Figure 4.1. The white circular disks at the vertices are the one-particle irreducible functions denoted by $\Gamma_{1\text{PI},\mu}^{ff\gamma}(p, p')$ and $\Gamma_{1\text{PI},\mu}^{ffZ}(p, p')$. The filled blobs inserted in the external propagators denote all loop corrections including the reducible ones; that is, the attached propagators represent the two-point functions defined by the functional derivative (4.2). Translating the diagrams yields

$$\begin{aligned} G_\mu^{ff\gamma}(p, p') &= S_f(p') \Gamma_{1\text{PI}}^{ff\gamma,\nu}(p, p') S_f(p) G_{\nu\mu}^{\gamma\gamma}(q^2) \\ &+ S_f(p') \Gamma_{1\text{PI}}^{ffZ,\nu}(p, p') S_f(p) G_{\nu\mu}^{Z\gamma}(q^2) \end{aligned} \quad (4.34)$$

in terms of the irreducible vertex functions, where $G_{\mu\nu}^{aa}$ and S_f are defined in Section 4.1. Like before, it is easier to deal with the amputated vertex function. Multiplying with the inverse propagators of the external particles yields

$$\begin{aligned} \bar{u}(p') \Gamma_\mu^{ff\gamma}(p, p') u(p) \varepsilon^\mu &= \bar{u}(p') \Gamma_{1\text{PI},\mu}^{ff\gamma}(p, p') u(p) \varepsilon^\mu \\ &+ \bar{u}(p') \Gamma_{1\text{PI},\mu}^{ffZ}(p, p') u(p) \frac{G_T^{Z\gamma}(q^2)}{G_T^{\gamma\gamma}(q^2)} \varepsilon^\mu, \end{aligned} \quad (4.35)$$

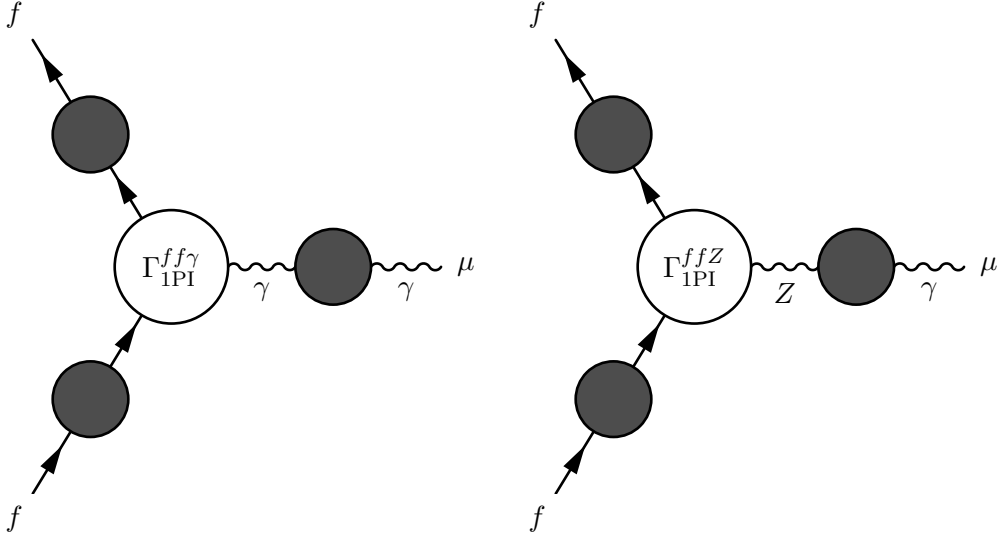


Figure 4.1.: Diagrammatic representation of the terms that make up the Green function $G^{ff\gamma,\mu}(p, p')$. The contribution of the irreducible ffZ -vertex arises due to the γZ -mixing.

where G_T^{ab} ($a, b = \gamma, Z$) are the transverse parts of the bosonic propagators. In the on-shell scheme, the renormalized γZ -propagator vanishes at zero momentum transfer, simplifying Equation (4.35). In the general case, however, the second term needs to be taken into account. Using the subscript T to denote the transverse parts of the irreducible vertex functions (4.16) and (4.17), too, the ratio of the propagators reads

$$\frac{G_T^{Z\gamma}(q^2)}{G_T^{\gamma\gamma}(q^2)} = -\frac{\Gamma_T^{Z\gamma}(q^2)}{\Gamma_T^{ZZ}(q^2)}. \quad (4.36)$$

The amputated vertex function $\Gamma_\mu^{ff\gamma}$ is obtained by inserting Equations (4.36), (4.17), (4.29) and (4.30) into (4.35).

4. Parity Violating Interaction and the Weak Mixing Angle

In order to compute the renormalization constant of the electromagnetic coupling, it is necessary to determine the projection $\bar{u}(p')\Gamma_\mu^{ff\gamma}(p,p')u(p)$ for on-shell fermions in the limit $p' \rightarrow p$. Sandwiching the first term of Equation (4.35) between Dirac spinors and making use of the Gordon identity yields³

$$\begin{aligned}\bar{u}(p)\Gamma_{1\text{PI},\mu}^{ff\gamma}(p,p)u(p) &= -ie\bar{u}(p)\gamma_\mu u(p) (V - \gamma_5 A) u(p), \\ V &= Q_f \left(1 + \delta Z_V^f\right) \sqrt{1 + \delta Z_A} - \frac{g_Z}{2e} v_f^* \delta Z_{ZA} + \Lambda_V^{ff\gamma}(0) + \Lambda_S^{ff\gamma}(0), \\ A &= -Q_f \delta Z_A^f \sqrt{1 + \delta Z_A} - \frac{g_Z}{2e} a_f^* \delta Z_{ZA} - \Lambda_A^{ff\gamma}(0).\end{aligned}\quad (4.37)$$

The projection of the second term in Equation (4.35) is similar, but also includes the propagator ratio,

$$\begin{aligned}\bar{u}(p)\Gamma_{1\text{PI},\mu}^{ffZ}(p,p)u(p) \frac{G_T^{Z\gamma}(0)}{G_T^{\gamma\gamma}(0)} &= -i\frac{g_Z}{2}\bar{u}(p)\gamma_\mu (V - \gamma_5 A) u(p) \frac{\Gamma_T^{Z\gamma}(0)}{\Gamma_T^{ZZ}(0)}, \\ V &= v_f^* \sqrt{1 + \delta Z_Z} - 2\frac{e}{g_Z} Q_f \left(1 + \delta Z_V^f\right) \delta Z_{AZ} + \Lambda_V^{ffZ}(0) + \Lambda_S^{ffZ}(0), \\ A &= a_f^* \sqrt{1 + \delta Z_Z} + 2\frac{e}{g_Z} Q_f \delta Z_A^f \delta Z_{AZ} - \Lambda_A^{ffZ}(0).\end{aligned}\quad (4.38)$$

4.2. Parity Violating Fermion–Fermion Interaction

With the derivation of the two- and three-point functions in the previous section, it is now possible to derive the parity violating interaction excluding box-graph contributions in the Standard Model. The first derivation of the parity violating interaction at one-loop order was done in Reference [29] for the scattering of electrons and quarks. In this section, the findings therein are generalized to fermion–fermion scattering with no particular choice for the scale μ . The result of this section also serves as a base for the derivation of matching conditions for

³Applying the Gordon identity also yields a term proportional to $\sigma_{\mu\nu}q^\nu$ which corresponds to the fermion's magnetic moment. This piece is irrelevant for the renormalization as it is UV finite and will not be discussed in the following.

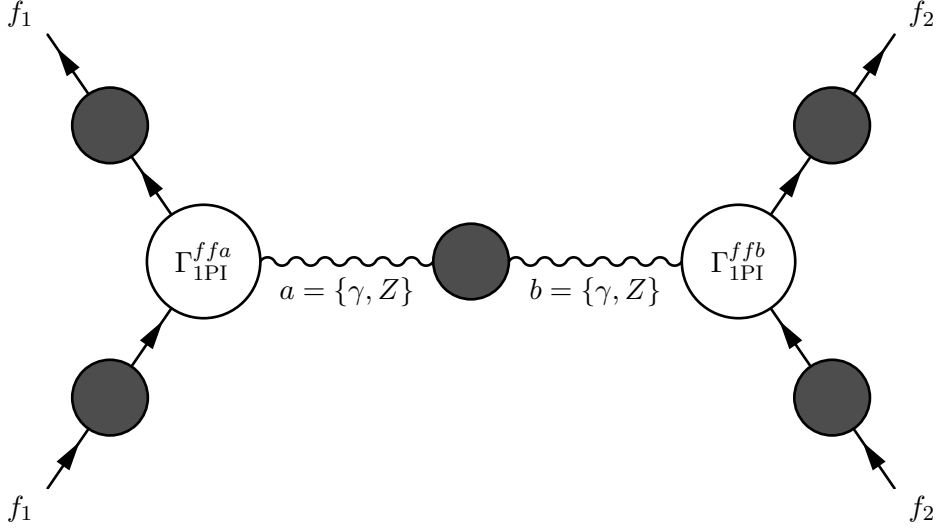


Figure 4.2.: One-particle reducible Feynman diagrams of neutral current fermion–fermion scattering. The dark grey blobs depict the sum of all reducible and irreducible self-energy diagrams.

the parameters describing electroweak phenomena in an effective model, which will be discussed in Chapter 5.

The parity violating amplitude of fermion–fermion scattering contains terms that are process dependent, that is they depend on the type of the scattering fermions, and universal terms that are the same for all external fermions. In order to separate the universal terms, box diagrams do not need to be treated explicitly in this section, as they only contribute to the process dependent terms. The contribution of these diagrams at zero momentum transfer will be abbreviated by $\square = \square_{\gamma\gamma} + \square_{\gamma Z} + \square_{ZZ} + \square_{WW}$, which is understood to also include crossed diagrams. Explicit expressions for the box diagrams can be found in Reference [29]. The remaining terms of the parity violating interaction are determined by the four Feynman diagrams that are obtained when

inserting photons and Z-bosons for the mediators in Figure 4.2. The parity violating interaction can be parametrized in terms of scalar functions $\tilde{C}_{1f_1}^{f_2}(q^2)$ and $\tilde{C}_{2f_1}^{f_2}(q^2)$ that depend on the squared momentum transfer and the type of the scattering fermions. Separating the Fermi constant G_F and a factor $\frac{i}{\sqrt{2}}$, the parity violating matrix element reads

$$\begin{aligned} \mathcal{M}_{\text{PV}}(q^2) = i \frac{G_F}{\sqrt{2}} & \left[\tilde{C}_{1f_1}^{f_2}(q^2) \bar{u}_1 \gamma_\mu u_1 \bar{u}_2 \gamma^\mu \gamma_5 u_2 \right. \\ & \left. + \tilde{C}_{2f_1}^{f_2}(q^2) \bar{u}_1 \gamma_\mu \gamma_5 u_1 \bar{u}_2 \gamma^\mu u_2 \right] + \mathcal{O}(q^2), \end{aligned} \quad (4.39)$$

where u_1 (u_2) is the spinor of fermion f_1 (f_2). This general structure will be reasoned in the following subsections. As indicated by the big O notation, there may be additional momentum transfer dependent terms that stem from the contraction of scalar and pseudo-scalar terms which do not fit the parametrization in terms of \tilde{C}_{1f_1} due to a differing Dirac structure; these do not contribute at zero momentum transfer as will be shown in Section 4.2.1. At zero momentum transfer, this parametrization corresponds to the effective contact interaction constants $C_{iq} = \tilde{C}_{iq}^e(0)$, $i = 1, 2$, $q = u, d$, introduced in Reference [29]. Without further specification of the fermions, the set of Feynman diagrams in Figure 4.2 is symmetric under the exchange $f_1 \leftrightarrow f_2$, so that the remainder of the section is restricted to the discussion of $\tilde{C}_{1f_1}^{f_2}(q^2)$.

4.2.1. Contribution of Scalar and Pseudo-Scalar Terms

It is not obvious that Equation (4.39) is a valid parametrization of the parity violating matrix element, as the vertex corrections (4.29) and (4.30) also contain scalar and pseudo-scalar terms in which the Lorentz index is carried by the fermion momenta. These terms are parametrized by the scalar functions Λ_S^{ffA} and Λ_P^{ffA} , respectively, where $A = \gamma, Z$. Additional treatment is required in order to derive the contribution of those pieces to the effective coupling $C_{1f_1}^{f_2}$ and show that no other terms exist beside $C_{1f_1}^{f_2}$. Since the scalar term does not contain a γ_5 -matrix, it may only contribute to the vertex correction of the

fermion f_1 , for which the vector terms are required. On the other hand, the pseudo-scalar term contributes to the vertex correction of the fermion f_2 only, because of the presence of γ_5 .

At one-loop order, the pseudo-scalar term can only contribute when contracted with a vector term $\bar{u}_1(p'_1)\gamma_\mu u_1(p_1)$. Using the Dirac equation and identical masses for initial and final fermions f_1 and f'_1 , one finds

$$\begin{aligned} & \bar{u}_1(p'_1)\gamma_\mu u_1(p_1)\bar{u}_2(p'_2)q^\mu\gamma_5 u_2(p_2) \\ & = \bar{u}_1(p'_1)(\tilde{m}_{f_1} - \tilde{m}_{f'_1})u_1(p_1)\bar{u}_2(p'_2)\gamma_5 u_2(p_2) = 0, \end{aligned} \quad (4.40)$$

where $q^\mu = p_1^\mu - p'_1{}^\mu = p_2'^\mu - p_2^\mu$ is the four-momentum transfer. It remains to derive the contribution of the scalar term to the low energy coupling constants. When terms of two-loop order are neglected, the Dirac structure of the only matrix element in which the scalar term can enter reads

$$\mathcal{M}_{SA} = \bar{u}_1(p'_1)q_\mu u_1(p_1)\bar{u}_2(p'_2)\gamma^\mu\gamma_5 u_2(p_2) = \bar{u}_1(p'_1)u_1(p_1)\bar{u}_2(p'_2)\not{q}\gamma_5 u_2(p_2), \quad (4.41)$$

in which the pseudo scalar term is contracted with the tree-level axial vector term as indicated by the subscript ‘‘SA’’. Equation (4.41) does not contribute to $C_{1f_1}^{f_2}$, which can be seen when calculating the square of the matrix element \mathcal{M}_{SA} and the product of \mathcal{M}_{SA} and

$$\mathcal{M}_{VA} = \bar{u}_1(p'_1)\gamma_\mu u_1(p_1)\bar{u}_2(p'_2)\gamma^\mu\gamma_5 u_2(p_2). \quad (4.42)$$

Using $\not{q}\gamma_5 = \not{p}_2'\gamma_5 + \gamma_5\not{p}_2$, Equation (4.41) can also be written as

$$\mathcal{M}_{SA} = 2\tilde{m}_{f_2}\bar{u}_1(p'_1)u_1(p_1)\bar{u}_2(p'_2)\gamma_5 u_2(p_2), \quad (4.43)$$

which yields

$$|\mathcal{M}_{SA}|^2 = -4\tilde{m}_{f_2}^2 \text{Tr}\{\rho_1\rho'_1\} \text{Tr}\{\rho_2\gamma_5\rho'_2\gamma_5\}, \quad (4.44)$$

where ρ_i and ρ'_i are the fermion density matrices of the incoming and outgoing fermions f_i and f'_i , respectively. The contribution to the asymmetry is obtained by inserting $\rho_2 = \gamma_5\not{s}_2(\not{p}_2 + m_{f_2})$ and $\rho'_2 = \not{p}'_2 + m_{f_2}$, where s_2 is the spin

four-vector of the incoming fermion f_2 . Two of the γ_5 -matrices cancel and the second trace becomes

$$\text{Tr}\left\{\not{\epsilon}_2 \left(\not{p}_2 + m_{f_2}\right) \gamma_5 \left(\not{p}'_2 + m_{f_2}\right)\right\}. \quad (4.45)$$

Since the number of independent four-vectors is less than four, the trace vanishes and $|\mathcal{M}_{SA}|^2$ does not contribute to the parity violating asymmetry. The product $\mathcal{M}_{SA}^\dagger \mathcal{M}_{VA}$ reads

$$\mathcal{M}_{SA}^\dagger \mathcal{M}_{VA} = 2\tilde{m}_{f_2} \text{Tr}\{\rho_1 \rho'_1 \gamma_\mu\} \text{Tr}\{\rho_2 \gamma_5 \rho'_2 \gamma^\mu \gamma_5\}, \quad (4.46)$$

where the contribution of the second trace vanishes when inserting the density matrix $\rho_2 = \gamma_5 \not{\epsilon}_2 (\not{p}_2 + m_{f_2})$ due to the same reason as before. This completes the proof that the scalar and pseudo scalar terms do not contribute to the parity violating asymmetry at one-loop order.

4.2.2. General Structure

As shown in Section 4.2.1, the only relevant terms that stem from the sum of the vertex functions on the second lines of Equations (4.29) and (4.30) are the vector and axial vector parts and read

$$\bar{u}_i(p'_i) \left[\gamma_\mu \Lambda_V^{ffX}(q^2) + \gamma_\mu \gamma_5 \Lambda_A^{ffX}(q^2) \right] u_i(p_i), \quad (4.47)$$

where $i = 1, 2$ denotes the fermion and $X = \gamma, Z$ the gauge boson. This allows decomposing the one-particle irreducible vertices in Equations (4.29) and (4.30) according to

$$\bar{u}(p') \Gamma_{\text{PI},\mu}^{ffa}(p, p') u(p) = \bar{u}(p') \left(\gamma_\mu \Gamma_{\text{PI},V}^{ffa}(q^2) + \gamma_\mu \gamma_5 \Gamma_{\text{PI},A}^{ffa}(q^2) \right) u(p) + \dots, \quad (4.48)$$

with

$$\Gamma_{\text{PI},V}^{ff\gamma}(q^2) = -ieQ_f \left(1 + \delta Z_V^f \right) \sqrt{1 + \delta Z_A} + i \frac{g_Z}{2} v_f^* \delta Z_{ZA} - ie \Lambda_V^{ff\gamma}(q^2), \quad (4.49a)$$

$$\Gamma_{1\text{PI},A}^{ff\gamma}(q^2) = -ieQ_f \delta Z_A^f \sqrt{1 + \delta Z_A} - i\frac{g_Z}{2} a_f^* \delta Z_{ZA} - ie\Lambda_A^{ff\gamma}(q^2) \quad (4.49b)$$

and

$$\Gamma_{1\text{PI},V}^{ffZ}(q^2) = i\frac{g_Z}{2} v_f^* \sqrt{1 + \delta Z_Z} - ieQ_f (1 + \delta Z_V^f) \delta Z_{AZ} + i\frac{g_Z}{2} \Lambda_V^{ffZ}(q^2), \quad (4.50a)$$

$$\Gamma_{1\text{PI},A}^{ffZ}(q^2) = -i\frac{g_Z}{2} a_f^* \sqrt{1 + \delta Z_Z} - ieQ_f \delta Z_A^f \delta Z_{AZ} + i\frac{g_Z}{2} \Lambda_A^{ffZ}(q^2), \quad (4.50b)$$

where the ellipsis in Equation (4.48) represents the terms that do not contribute to the parity violating interaction. It is convenient, to define an effective vertex to also account for normalization factors that stem from the LSZ theorem. As shown in Appendix D, the matrix element is obtained by amputating the Green function and inserting the LSZ factors. A fermion line with a single γ - or Z -interaction vertex denoted by $a = \gamma, Z$ becomes

$$\bar{u}(p') \left(1 - \frac{1}{2}\delta\mathcal{Z}_V + \frac{1}{2}\gamma_5\delta\mathcal{Z}_A\right) \Gamma_{1\text{PI},\mu}^{ffa}(p, p') \left(1 - \frac{1}{2}\delta\mathcal{Z}_V - \frac{1}{2}\gamma_5\delta\mathcal{Z}_A\right) u(p), \quad (4.51)$$

where $\delta\mathcal{Z}_V$ and $\delta\mathcal{Z}_A$ are given in Equation (D.23) in terms of fermionic self-energy functions. At one-loop order, the product of LSZ normalization factors and loop corrections may be neglected, which allows writing the fermion lines as

$$\bar{u}(p') \left(\gamma_\mu \check{\Gamma}_{1\text{PI},V}^{ffa}(q^2) + \gamma_\mu \gamma_5 \check{\Gamma}_{1\text{PI},A}^{ffa}(q^2)\right) u(p) + \dots \quad (4.52)$$

in terms of effective interaction vertices denoted by $\check{\Gamma}$ that are defined as

$$\check{\Gamma}_{1\text{PI},V}^{ff\gamma}(q^2) = \Gamma_{1\text{PI},V}^{ff\gamma}(q^2) + ieQ_f \delta\mathcal{Z}_V, \quad (4.53a)$$

$$\check{\Gamma}_{1\text{PI},A}^{ff\gamma}(q^2) = \Gamma_{1\text{PI},A}^{ff\gamma}(q^2) + ieQ_f \delta\mathcal{Z}_A \quad (4.53b)$$

and

$$\check{\Gamma}_{1\text{PI},V}^{ffZ}(q^2) = \Gamma_{1\text{PI},V}^{ffZ}(q^2) + i\frac{g_Z}{2} (-v_f \delta\mathcal{Z}_V + a_f \delta\mathcal{Z}_A), \quad (4.54a)$$

4. Parity Violating Interaction and the Weak Mixing Angle

$$\check{\Gamma}_{1\text{PI},A}^{ffZ}(q^2) = \Gamma_{1\text{PI},A}^{ffZ}(q^2) + i\frac{g_Z}{2}(-v_f\delta\mathcal{L}_A + a_f\delta\mathcal{L}_V). \quad (4.54b)$$

As before, the ellipses in Equation (4.52) represents terms not contributing to the parity violating interaction.

Using these definitions, the invariant amplitude that corresponds to the $\check{C}_{1f_1}^{f_2}$ -piece of Diagram 4.2 reads

$$\begin{aligned} \mathcal{M}_{\text{VA}}^{\text{PV}} &= -\bar{u}_1(p'_1)\gamma_\mu u_1(p_1) \bar{u}_2(p'_2)\gamma^\mu\gamma_5 u_2(p_2) \\ &\quad \cdot \sum_{a,b=\gamma,Z} \check{\Gamma}_{1\text{PI},V}^{f_1 f_1 a}(q^2) G_T^{ab}(q^2) \check{\Gamma}_{1\text{PI},A}^{f_2 f_2 b}(q^2), \end{aligned} \quad (4.55)$$

where the subscript VA refers to the vector-axial vector type of interaction. The $q^\mu q^\nu$ -terms in the gauge boson propagators drop out due to current conservation, so that the amplitude can be expressed in terms of the transverse parts of the propagators. In the limit $q^2 = 0$, the second line in Equation (4.55) can be written in terms of an effective coupling constant $C_{1f_1}^{f_2}$. Adopting the notation

$$\mathcal{M}_{\text{VA}}^{\text{PV}} = -i\frac{G_F}{\sqrt{2}} C_{1f_1}^{f_2} \bar{u}_1(p_1)\gamma_\mu u_1(p_1) \bar{u}_2(p_2)\gamma^\mu\gamma_5 u_2(p_2) \quad (4.56)$$

of Reference [29], the effective contact interaction strength $C_{1f_1}^{f_2}$ for arbitrary fermions f_1 and f_2 reads⁴

$$C_{1f_1}^{f_2} = -i\frac{\sqrt{2}}{G_F} \lim_{q^2 \rightarrow 0} \sum_{a,b=\gamma,Z} \check{\Gamma}_{1\text{PI},V}^{f_1 f_1 a}(q^2) G_T^{ab}(q^2) \check{\Gamma}_{1\text{PI},A}^{f_2 f_2 b}(q^2) + \square, \quad (4.57a)$$

$$C_{2f_1}^{f_2} = C_{1f_2}^{f_1}, \quad (4.57b)$$

where G_F is the Fermi constant and \square denotes the contribution of box diagrams as mentioned before. The parameters $C_{1f_1}^{f_2}$ and $C_{2f_1}^{f_2}$ also include the tree-level interaction and the second relation is a consequence of the symmetry mentioned above. The limit in Equation (4.57) must not be commuted with the sum, as

⁴The authors of Reference [29] restricted the discussion to $f_2 = e$ and omitted the superscript.

some terms in the sum are individually singular in $q^2 = 0$, but the poles cancel in the sum, eventually.

If one of the fermions is a quark, Equation (4.57) needs to be understood as a component of a scattering hadron. One has to be careful to not double count vertex corrections on the hadron side, as these may already be part of the experimentally determined form factor. A brief discussion is given at the end of Section 4.2.3. In the following, all contributions are treated as if the fermions were free particles.

4.2.3. $\overline{\text{MS}}$ -Coupling Parameters in the Standard Model

The calculation of $C_{1f_1}^{f_2}$ in the Standard Model can be simplified by inserting $\overline{\text{MS}}$ -renormalized loop expressions and dropping all renormalization constants, as these account for the UV-divergent pieces in the loop integrals, only. The definition of $C_{1f_1}^{f_2}$ includes a factor G_F^{-1} , which is introduced for convenience, to write the parity violating amplitude (4.55) in terms of the Fermi constant instead of the Z-boson mass. This way, the inverse Fermi constant cancels with the fundamental coupling constants that occur in Feynman rules up to loop corrections. The relation between coupling constants and the Fermi constant at one-loop order is conventionally given in terms of Δr . It was first derived in Reference [4] and the corresponding $\overline{\text{MS}}$ -expression $\Delta\hat{r}$ was given in Equation (2.33).

Here and in the following, a hat is used to denote $\overline{\text{MS}}$ -quantities, while the tilde symbol refers to OS-renormalized quantities as before. This allows writing

$$\frac{\sqrt{2}}{G_F} = 8 \frac{\tilde{M}_Z^2}{\tilde{e}^2} \hat{c}^2 \hat{s}^2 (1 - \Delta\hat{r}), \quad (4.58)$$

which is expressed in terms of the on-shell Z-mass and electromagnetic coupling constant and where $\Delta\hat{r}$ is given in Equation (2.33). In order to obtain a relation in terms of the corresponding $\overline{\text{MS}}$ -parameters, one has to express the OS mass in terms of the $\overline{\text{MS}}$ -mass via $\tilde{M}_Z^2 = \hat{M}_Z^2 - \Re\hat{\Sigma}_T^{ZZ}(\tilde{M}_Z^2)$, and use [7]

$$\frac{1}{\tilde{e}^2} = \frac{1}{\hat{e}^2} \left[1 - 2 \frac{\delta\hat{e}}{\hat{e}} \right]_{\overline{\text{MS}}} + \mathcal{O}(\delta e^2) \quad (4.59)$$

4. Parity Violating Interaction and the Weak Mixing Angle

to also rewrite the electromagnetic coupling in terms of its $\overline{\text{MS}}$ -definition. Equation (4.59) is valid at one-loop order only, but is sufficient within the present approximation. Eventually, Equation (4.58) becomes

$$\frac{\sqrt{2}}{G_F} = 8 \frac{\hat{M}_Z^2}{\hat{g}_Z^2} \left\{ 1 - \frac{\hat{\Sigma}_T^{WW}(0)}{\hat{M}_W^2} - \frac{\alpha}{4\pi s^2} \left[\left(\frac{7}{2\hat{s}^2} - 6 \right) \log \hat{c}^2 + 4 \log \frac{\mu^2}{M_Z^2} + 6 \right] + \mathcal{O}(\alpha^2) \right\}, \quad (4.60)$$

where the operator \mathfrak{R} was omitted, because $\hat{\Sigma}_T^{WW}$ is real valued at zero momentum transfer and the coupling constants were expressed in terms of $\hat{g}_Z^2 = \frac{\hat{e}^2}{\hat{c}^2 \hat{s}^2}$. Equations (4.58) and (4.60) account for radiative corrections to the muon decay at one-loop order. These diagrams do not enter the parity violating interaction, but need to be taken into account to make use of the Fermi constant, which is determined by measuring the muon's lifetime.

To facilitate the discussion of $C_{1f_1}^{f_2}$, the loop contributions are split up into four distinct pieces⁵:

- Omitting the arguments of the propagator and vertex functions, the first piece is

$$C_{1f_1}^{f_2(A)} = -i \frac{\sqrt{2}}{G_F} \left[\check{\Gamma}_{1\text{PI},V}^{f_1 f_1 Z} G_T^{ZZ} \check{\Gamma}_{1\text{PI},A}^{f_2 f_2 Z} \right]_{\text{tree-level}} \quad (4.61a)$$

and accounts for the tree-level expression including LSZ factors.

- The second piece contains all terms with a photon propagator but without γZ -mixing and reads

$$C_{1f_1}^{f_2(B)} = -8i \frac{\hat{M}_Z^2}{\hat{g}_Z^2} \check{\Gamma}_{1\text{PI},V}^{f_1 f_1 \gamma} G_T^{\gamma\gamma} \check{\Gamma}_{1\text{PI},A}^{f_2 f_2 \gamma}. \quad (4.61b)$$

⁵The second and fourth pieces are functions of q^2 , as they contain q^{-2} -terms that were mentioned above. However, the poles cancel in the sum, which is independent of q^2 .

4.2. Parity Violating Fermion–Fermion Interaction

The Fermi constant was expressed in terms of $\frac{\hat{M}_Z^2}{\hat{g}_Z^2}$ at tree-level only, since two-loop effects are neglected in the present calculation.

- Terms with a Z-vertex on either side but without the tree-level expression are combined in the third piece,

$$C_{1f_1}^{f_2(C)} = -8i \frac{\hat{M}_Z^2}{\hat{g}_Z^2} \left(\check{\Gamma}_{1\text{PI},V}^{f_1 f_1 Z} G_T^{ZZ} \check{\Gamma}_{1\text{PI},A}^{f_2 f_2 Z} - \left[\check{\Gamma}_{1\text{PI},V}^{f_1 f_1 Z} G_T^{ZZ} \check{\Gamma}_{1\text{PI},A}^{f_2 f_2 Z} \right]_{\text{tree-level}} \right). \quad (4.61c)$$

- The fourth piece includes all γZ -mixing contributions,

$$C_{1f_1}^{f_2(D)} = -8i \frac{\hat{M}_Z^2}{\hat{g}_Z^2} \left(\check{\Gamma}_{1\text{PI},V}^{f_1 f_1 \gamma} G_T^{\gamma Z} \check{\Gamma}_{1\text{PI},A}^{f_2 f_2 Z} + \check{\Gamma}_{1\text{PI},V}^{f_1 f_1 Z} G_T^{Z\gamma} \check{\Gamma}_{1\text{PI},A}^{f_2 f_2 \gamma} \right). \quad (4.61d)$$

These pieces are labelled with a superscript (x) , $x = A, B, C, D$ and sum up to the effective coupling $C_{1f_1}^{f_2}$,

$$C_{1f_1}^{f_2} = C_{1f_1}^{f_2(A)} + C_{1f_1}^{f_2(B)} + C_{1f_1}^{f_2(C)} + C_{1f_1}^{f_2(D)}. \quad (4.62)$$

Following the notation of Reference [29], the goal is to write the effective coupling $C_{1f_1}^{f_2}$ in the form

$$C_{1f_1}^{f_2} = -a_{f_2} \varrho \left[2T_{f_1}^3 - 4Q_{f_1} \varkappa \hat{s}^2 \right] + \square, \quad (4.63)$$

where the parameters ϱ and \varkappa are used to collect all one-loop order effects except for the box graph contributions that are denoted by \square . The parameter ϱ is defined as a coefficient of the vector coupling constant v_{f_1} instead of the weak isospin component $T_{f_1}^3$ for convenience, as the product of ϱ and \varkappa accounts for reducible two-loop effects that stem from a simultaneous one-loop correction of the overall amplitude and the diagrams contributing to \varkappa . However, a complete two-loop calculation is required to see if the product terms contained in Equation (4.63) correctly describe all two-loop effects that stem

4. Parity Violating Interaction and the Weak Mixing Angle

from reducible two-loop Feynman diagrams. At tree-level, one has $\varrho = \varkappa = 1$, which yields $C_{1f_1}^{f_2} = -2v_{f_1}a_{f_2}$ for the leading order coefficient when inserted into Equation (4.63). In the following, the four pieces will be calculated at one-loop order.

The first piece is obtained by calculating fermion–fermion scattering at tree-level including the appropriate LSZ factors given in Equation (4.54). In addition, Equation (4.60) needs to be inserted to account for the relation of the Fermi constant that enters via the definition (4.57) and the heavy gauge boson mass stemming from the propagator. Omitting terms of two-loop order, the first piece in $\overline{\text{MS}}$ reads

$$\begin{aligned}
C_{1f_1}^{f_2(A)} &= -i \frac{\sqrt{2}}{G_F} i \frac{\hat{g}_Z}{2} \left[v_{f_1} (1 - \delta\mathcal{Z}_V^{f_1}) + a_{f_1} \delta\mathcal{Z}_A^{f_1} \right] \left(-\frac{i}{\hat{M}_Z^2} \right) \\
&\quad \cdot i \frac{\hat{g}_Z}{2} \left[-a_{f_2} (1 - \delta\mathcal{Z}_V^{f_2}) - v_{f_2} \delta\mathcal{Z}_A^{f_2} \right] \\
&= -2v_{f_1}a_{f_2} \left\{ 1 - \frac{\alpha}{4\pi s^2} \left[4 \log \frac{\mu^2}{M_Z^2} + \left(\frac{7}{2\hat{s}^2} - 6 \right) \log \hat{c}^2 + 6 \right] \right. \\
&\quad \left. - \frac{\hat{\Sigma}_T^{WW}(0)}{M_W^2} - \delta\mathcal{Z}_V^{f_1} - \delta\mathcal{Z}_V^{f_2} + \frac{a_{f_1}}{v_{f_1}} \delta\mathcal{Z}_A^{f_1} + \frac{v_{f_2}}{a_{f_2}} \delta\mathcal{Z}_A^{f_2} \right\}.
\end{aligned} \tag{4.64a}$$

The electromagnetic tree-level interaction is parity conserving. Hence, the only contribution to the second piece stems from a vertex correction to the fermion line of fermion f_2 , which is encoded in $\Gamma_{1\text{PI},A}^{f_2 f_2 \gamma}$. Due to the presence of the inverse squared momentum transfer in the photon propagator, one needs to take into account the derivative of $\Gamma_{1\text{PI},A}^{f_2 f_2 \gamma}$, too. The LSZ factors in Equation (4.64a) stem from the effective ffZ -vertex (4.54); here, they appear again as part of the effective photon vertex (4.53). Inserting Equations (4.53), (4.29) and replacing the LSZ factors using (D.23) yields

$$C_{1f_1}^{f_2(B)} = -8i \frac{\hat{M}_Z^2}{\hat{g}_Z^2} (-ieQ_{f_1}) \frac{i}{q^2} ie \left[Q_{f_2} \hat{\Sigma}_A^{f_2}(\tilde{m}_{f_2}^2) - \hat{\Lambda}_A^{f_2 f_2 \gamma}(0) - q^2 \Lambda_A^{f_2 f_2 \gamma'}(0) \right].$$

Rewriting the trivial factors to facilitate the discussion with respect to the notation of Equation (4.63), the second piece becomes

$$C_{1f_1}^{f_2(B)} = -2 \left(-2s^2 Q_{f_1} \right) a_{f_2} \left(-2 \frac{\hat{c}^2}{T_{f_2}^3} \frac{\hat{M}_Z^2}{q^2} \right) \cdot \left[-Q_{f_2} \hat{\Sigma}_A^{f_2}(\tilde{m}_{f_2}^2) + \hat{\Lambda}_A^{f_2 f_2 \gamma}(0) + q^2 \Lambda_A^{f_2 f_2 \gamma'}(0) \right]. \quad (4.64b)$$

The first two terms in brackets in Equation (4.64b) on their own are not well-defined in the limit of vanishing momentum transfer, due to the inverse factor of the squared momentum. These terms appear as the corresponding Feynman diagrams are not individually gauge invariant and cancel with the corresponding singular terms in the γZ -mixing self-energy as will be shown later. The third piece obtains corrections from three different sources: each of the two vertices and the propagator; the sum of these three contributions is

$$\begin{aligned} C_{1f_1}^{f_2(C)} &= -8i \frac{\hat{M}_Z^2}{\hat{g}_Z^2} \left(i \frac{\hat{g}_Z}{2} v_{f_1} \right) \left(-\frac{i}{\hat{M}_Z^2} \right) \left(i \frac{\hat{g}_Z}{2} \hat{\Lambda}_A^{f_2 f_2 Z}(0) \right) \\ &\quad - 8i \frac{\hat{M}_Z^2}{\hat{g}_Z^2} \left(i \frac{\hat{g}_Z}{2} v_{f_1} \right) \left(-i \frac{\hat{\Sigma}_T^{ZZ}(0)}{\hat{M}_Z^4} \right) \left(-i \frac{\hat{g}_Z}{2} a_{f_2} \right) \\ &\quad - 8i \frac{\hat{M}_Z^2}{\hat{g}_Z^2} \left(i \frac{\hat{g}_Z}{2} \hat{\Lambda}_V^{f_1 f_1 Z}(0) \right) \left(-\frac{i}{\hat{M}_Z^2} \right) \left(-i \frac{\hat{g}_Z}{2} a_{f_2} \right), \end{aligned}$$

which can be combined to

$$C_{1f_1}^{f_2(C)} = -2v_{f_1} a_{f_2} \left[\frac{\hat{\Sigma}_T^{ZZ}(0)}{\hat{M}_Z^2} - \frac{1}{T_{f_2}^3} \hat{\Lambda}_A^{f_2 f_2 Z}(0) \right] - 2a_{f_2} \hat{\Lambda}_V^{f_1 f_1 Z}(0). \quad (4.64c)$$

The remaining piece is the one that contains the γZ -mixing self-energy. Due to the presence of the photon propagator, the expression at zero momentum transfer contains a derivative of the self-energy and the Z-boson's propagator.

4. Parity Violating Interaction and the Weak Mixing Angle

In addition, a term proportional to q^{-2} arises that corresponds to the singular terms in equation (4.64b). One finds⁶

$$\begin{aligned}
C_{1f_1}^{f_2(D)} &= -8i \frac{\hat{M}_Z^2}{\hat{g}_Z^2} (-ieQ_{f_1}) i \left[\frac{\hat{\Sigma}_T^{\gamma Z}(0)}{q^2 \hat{M}_Z^2} + \frac{\hat{\Sigma}_T^{\gamma Z}(0)}{\hat{M}_Z^4} + \frac{\hat{\Sigma}_T^{\gamma Z'}(0)}{\hat{M}_Z^2} \right] \left(-i \frac{\hat{g}_Z}{2} a_{f_2} \right) \\
&= -2 \left(-2\hat{s}^2 Q_{f_1} \right) a_{f_2} \cdot \left(-\frac{\hat{c}}{\hat{s}} \right) \left[\frac{\hat{\Sigma}_T^{\gamma Z}(0)}{q^2} + \frac{\hat{\Sigma}_T^{\gamma Z}(0)}{\hat{M}_Z^2} + \hat{\Sigma}_T^{\gamma Z'}(0) \right].
\end{aligned} \tag{4.64d}$$

Apart from box graphs, the four Equations (4.61a) to (4.61d) account for all loop corrections to the $\overline{\text{MS}}$ -renormalized parity violating interaction at one-loop order. Instead of summing all pieces and inserting explicit expressions for the self-energy functions and LSZ factors, it is more convenient, to group the different terms according to their contribution to the tree-level amplitude.

Due to the presence of the factor $v_{f_1} a_{f_2}$, the loop contributions in Equation (4.64a) and the terms in brackets in Equation (4.64c) can be absorbed into a global correction factor that is multiplied with the tree-level expression. On the other hand, Equations (4.64b) and (4.64d) may be understood as corrections to the weak mixing angle due to the charge factor Q_{f_1} that allows absorbing the expressions in the second term of the vector coupling constant $v_{f_1} = T_{f_1}^3 - 2\hat{s}^2 Q_{f_1}$. This facilitates combining all loop corrections derived above in two different constants, ϱ and \varkappa . With Equation (4.63) in mind, one finds

$$\begin{aligned}
\varrho &= 1 + \left(\frac{\hat{\Sigma}_T^{ZZ}(0)}{\hat{M}_Z^2} - \frac{\hat{\Sigma}_T^{WW}(0)}{M_W^2} \right) - \frac{\alpha}{4\pi s^2} \left[4 \log \frac{\mu^2}{M_Z^2} + \left(\frac{7}{2\hat{s}^2} - 6 \right) \log \hat{c}^2 + 6 \right] \\
&\quad - \delta \mathcal{L}_V^{f_1} + \frac{a_{f_1}}{v_{f_1}} \delta \mathcal{L}_A^{f_1} + \frac{\hat{\Lambda}_V^{f_1 f_1 Z}(0)}{v_{f_1}} - \delta \mathcal{L}_V^{f_2} + \frac{v_{f_2}}{a_{f_2}} \delta \mathcal{L}_A^{f_2} - \frac{\hat{\Lambda}_A^{f_2 f_2 Z}(0)}{T_{f_2}^3},
\end{aligned} \tag{4.65}$$

⁶The terms in brackets are the first two orders in the Laurent series of the γZ -propagator at one-loop order. The second term accounts for the derivative of the tree-level Z -propagator with respect to q^2 .

$$\begin{aligned} \varkappa = 1 - \frac{\hat{c}}{\hat{s}} & \left[\frac{\hat{\Sigma}_T^{\gamma Z}(0)}{q^2} + \frac{\hat{\Sigma}_T^{\gamma Z}(0)}{\hat{M}_Z^2} + \hat{\Sigma}_T^{\gamma Z'}(0) \right] \\ & - 2 \frac{\hat{c}^2}{T_{f_2}^3} \frac{\hat{M}_Z^2}{q^2} \left[-Q_{f_2} \hat{\Sigma}_{f_2}^A(\tilde{m}_{f_2}^2) + \Lambda_A^{f_2 f_2 \gamma}(0) + q^2 \Lambda_A^{f_2 f_2 \gamma'}(0) \right]. \end{aligned} \quad (4.66)$$

Equations (4.63), (4.65) and (4.66) are of limited use, as ϱ and \varkappa are no universal corrections, since they depend on the charges and weak isospins of the external fermions f_1 and f_2 . To obtain a more convenient form, in which terms that are independent of Q_f and T_f^3 are separated from the process dependent terms, one has to insert the explicit expressions of the loop functions occurring therein. As mentioned earlier, the sum of the q^{-2} -terms in the parameter \varkappa vanishes, when inserting the explicit one-loop expressions given in Equations (C.3), (C.12) and (C.18). The remaining terms are

$$\varkappa = 1 - \frac{\hat{c}}{\hat{s}} \frac{\hat{\Sigma}_T^{\gamma Z}(0)}{\hat{M}_Z^2} - \frac{\hat{c}}{\hat{s}} \hat{\Sigma}_T^{\gamma Z'}(0) - 2 \frac{\hat{c}^2}{T_{f_2}^3} \hat{M}_Z^2 \Lambda_A^{f_2 f_2 \gamma'}(0), \quad (4.67)$$

with the corresponding one-loop expressions given in Equations (C.3), (C.4) and (C.31). Using $Q_{f'} = Q_f - 2T_f^3$ to express the charge of the weak isospin partner f'_2 in terms of quantum numbers of fermion f_2 , the parameter \varkappa can be written as

$$\begin{aligned} \varkappa = 1 - \frac{\alpha}{2\pi s^2} & \left\{ \left(\frac{5}{2}c^2 + \frac{1}{12} \right) \log \frac{\mu^2}{\hat{M}_W^2} + \frac{7}{9} - \frac{s^2}{3} - \frac{1}{3} \sum_f N_f Q_f v_f \log \frac{\mu^2}{m_f^2} \right\} \\ & + \frac{\alpha}{4\pi s^2} \left\{ \frac{Q_{f_2} v_{f_2}}{9} \left(1 - 6 \log \frac{m_{f_2}^2}{\hat{M}_Z^2} \right) + \frac{Q_{f_2} - 2T_{f_2}^3}{18T_{f_2}^3} \left(1 - 6 \log \frac{m_{f_2}^2}{\hat{M}_W^2} \right) \right\}. \end{aligned} \quad (4.68)$$

In order to compute the parameter ϱ , it is helpful to derive the explicit one-loop expressions of the fermion residue first. It is determined by Equation (D.23), with the corresponding one-loop functions given in Equations (C.11), (C.12), (C.14) and (C.16). The axial vector piece $\delta\mathcal{L}_A^f$ is identical to the self-energy

4. Parity Violating Interaction and the Weak Mixing Angle

in Equation (C.12); neglecting the fermion mass compared to the mass of the heavy gauge bosons, the vector piece becomes

$$\delta\mathcal{Z}_V^f = \frac{\alpha}{4\pi} \left\{ Q_f^2 \left(4 + \log \frac{\mu^2}{\tilde{m}_f^2} + 2 \log \frac{\lambda^2}{\tilde{m}_f^2} \right) + \frac{v_f^2 + a_f^2}{4c^2 s^2} \left(-\frac{1}{2} + \log \frac{\mu^2}{\hat{M}_Z^2} \right) + \frac{1}{4s^2} \left(-\frac{1}{2} + \log \frac{\mu^2}{\hat{M}_W^2} \right) \right\} \quad (4.69)$$

The terms on the second line of Equation (4.65) cancel to some extent. Inserting Equations (4.69), (C.12) and (C.20) yields the f_2 -correction terms

$$-\delta\mathcal{Z}_V^{f_2} + \frac{v_{f_2}}{a_{f_2}} \delta\mathcal{Z}_A^{f_2} - \frac{1}{T_{f_2}^3} \hat{\Lambda}_A^{f_2 f_2 Z}(0) = \frac{\alpha}{4\pi} 2 \frac{c^2}{s^2} \log \frac{\mu^2}{\hat{M}_W^2} - \frac{\alpha}{4\pi} 2Q_{f_2}^2. \quad (4.70)$$

Similarly, the terms on the second line of Equation (4.65) that stem from fermion f_1 are determined by Equations (4.69), (C.12) and (C.19) and read

$$-\delta\mathcal{Z}_V^{f_1} + \frac{a_{f_1}}{v_{f_1}} \delta\mathcal{Z}_A^{f_1} + \frac{1}{v_{f_1}} \hat{\Lambda}_V^{f_1 f_1 Z}(0) = \frac{\alpha}{4\pi} \left(2 + \frac{4s^2 Q_{f_1}}{v_{f_1}} \right) \frac{c^2}{s^2} \log \frac{\mu^2}{\hat{M}_W^2} - \frac{\alpha}{4\pi} 2Q_{f_1}^2. \quad (4.71)$$

Combining Equations (4.70), (4.71) and (C.10) leads to the final result

$$\varrho = 1 + \frac{\alpha}{4\pi} \left\{ \frac{1}{c^2 s^2} \left(\frac{3}{4s^2} + \frac{5}{2} - 4s^2 \right) \log c^2 - \frac{7 + 16 \log \frac{\mu^2}{\hat{M}_Z^2}}{4s^2} + \frac{3}{4s^2} \frac{m_t^2}{\hat{M}_W^2} + \frac{16 - 19s^2}{4c^2 s^2} \log \frac{\mu^2}{\hat{M}_W^2} - \frac{4}{s^2} \log \frac{\mu^2}{\hat{M}_Z^2} + 4s^2 \frac{Q_{f_1}}{v_{f_1}} \frac{c^2}{s^2} \log \frac{\mu^2}{\hat{M}_W^2} - 2(Q_{f_1}^2 + Q_{f_2}^2) - \frac{3}{4s^2} \frac{c^2 \log \frac{\mu^2}{\hat{M}_W^2} - \xi \log \frac{\mu^2}{\hat{M}_H^2}}{c^2 - \xi} + \frac{3}{4c^2 s^2} \frac{\log \frac{\mu^2}{\hat{M}_Z^2} - \xi \log \frac{\mu^2}{\hat{M}_H^2}}{1 - \xi} \right\}, \quad (4.72)$$

where $\xi = \frac{\hat{M}_H^2}{\hat{M}_Z^2}$ and $\hat{M}_W = c\hat{M}_Z + \mathcal{O}(\alpha)$ were used. Equation (4.72) can be greatly simplified by combining the scale dependent logarithms, in which case the μ -dependency drops out almost entirely, with the term proportional to Q_{f_1} being the only remnant. Eventually, one finds the much simpler expression

$$\begin{aligned} \varrho = 1 + \frac{\alpha}{4\pi} \left\{ \frac{3}{4s^4} \log c^2 - \frac{7}{4s^2} + \frac{3}{4s^2} \frac{m_t^2}{M_W^2} + \frac{3\xi}{4s^2} \left[\frac{\log \frac{c^2}{\xi}}{c^2 - \xi} + \frac{\log \xi}{c^2(1 - \xi)} \right] \right\} \\ + \frac{\alpha c^2 Q_{f_1}}{\pi v_{f_1}} \log \frac{\mu^2}{M_W^2} - \frac{\alpha}{4\pi} 2(Q_{f_1}^2 + Q_{f_2}^2). \end{aligned} \quad (4.73)$$

It is clear that the first two terms of the parameter ϱ and the first line of Equation (4.68) are independent of the particular choice of the scattering fermions f_1 and f_2 , while the last term in Equation (4.73) and the second line in Equation (4.68) are not. The third term in Equation (4.73) depends on the charge and vector coupling of fermion f_1 , but may be rewritten as an f_1 -independent correction to \varkappa . It is reasonable to define universal parameters ρ and κ that are completely independent of f_1 and f_2 and keep all process dependent terms separate. To that end, the symbols ρ and κ are used to denote the expressions that were given in Reference [29]⁷. They read

$$\rho = 1 + \frac{\alpha}{4\pi} \left\{ \frac{3}{4s^4} \log c^2 - \frac{7}{4s^2} + \frac{3}{4s^2} \frac{m_t^2}{M_W^2} + \frac{3\xi}{4s^2} \left[\frac{\log \frac{c^2}{\xi}}{c^2 - \xi} + \frac{\log \xi}{c^2(1 - \xi)} \right] \right\}, \quad (4.74)$$

$$\kappa = 1 - \frac{\alpha}{2\pi s^2} \left\{ \left(\frac{7}{2}c^2 + \frac{1}{12} \right) \log \frac{\mu^2}{M_W^2} + \frac{7}{9} - \frac{s^2}{3} - \frac{1}{3} \sum_f N_f Q_f v_f \log \frac{\mu^2}{m_f^2} \right\} \quad (4.75)$$

⁷The choice $\mu = M_W$ was made in Reference [29]. Here, the terms proportional to $\log \frac{\mu^2}{M_W^2}$ (including the third term of Equation (4.73)) in κ are kept, as these reproduce the correct β -function-coefficient of the weak mixing angle.

and allow writing the effective coupling $C_{1f_1}^{f_2}$ similar to Equation (4.63), but with the process dependent terms separated. Appending the process dependent terms that do not stem from box diagrams at the end, it reads

$$C_{1f_1}^{f_2} = -a_{f_2}\rho \left[2T_{f_1}^3 - 4Q_{f_1}\kappa s^2 \right] + \square + 4a_{f_2}v_{f_1} \frac{\alpha}{4\pi} \left(Q_{f_1}^2 + Q_{f_2}^2 \right) + \frac{\alpha}{9\pi} Q_{f_1} a_{f_2} \left[Q_{f_2} v_{f_2} \left(1 - 6 \log \frac{m_{f_2}^2}{M_Z^2} \right) + \frac{Q_{f_2} - 2T_{f_2}^3}{2T_{f_2}^3} \left(1 - 6 \log \frac{m_{f_2}^2}{M_W^2} \right) \right]. \quad (4.76)$$

For the particular choice $f_1 = u$, $f_2 = e$ and $\mu = \hat{M}_W$, these process dependent terms in Equation (4.76) read

$$-\frac{\alpha}{4\pi} \left(1 + Q_u^2 \right) \left(1 - \frac{8}{3}s^2 \right) - \frac{\alpha}{9\pi} \left(1 - 4s^2 \right) \left(\frac{1}{6} - \log \frac{m_e^2}{\hat{M}_Z^2} \right). \quad (4.77)$$

The term proportional to Q_u^2 stems from a photonic correction of the quark vertex and naturally occurs along with the $Q_{f_1}^2$ -term of the charged lepton in a free-quark calculation. The obvious question is how one should use the result of a free-quark calculation to compute low energy observables of semileptonic processes that depend on the hadronic structure. Hadronic structure effects can not be calculated perturbatively and a comprehensive theoretical prediction of an observable requires experimental input in terms of form factors or particle distribution functions. An in-depth discussion of the combination of radiative corrections and form factors can be found in Reference [30]. After all, the correct treatment of the radiative corrections depends on the determination of the form factors, as various radiative corrections may or may not have been subtracted from the measured cross section before fitting the form factor functions. The Q_u^2 -term mentioned above is universal as it does not depend on leptonic properties and may be absorbed into the electromagnetic form factors of the scattering hadron. According to References [31, 32], the electromagnetic form factors of the proton given therein were obtained using the results of Reference [33] which include contributions of the photonic vertex correction that gives rise to the Q_u^2 -term. To not double count this correction, the term should be omitted which confirms the long known result [29].

4.3. The β -Function of the Weak Mixing Angle

Just as in the case of the electromagnetic coupling, the running of the weak mixing angle is governed by its renormalization group equation. The coefficients of the corresponding β -function are determined by the logarithms of the scale μ that contribute to the weak mixing angle. These are fixed by the renormalization scheme and can be obtained from the counter term associated with the weak mixing angle. Instead of calculating the counter term in a separate step, it is also possible to derive the β -function from the result of Section 4.2.3, in which all one-loop contributions to the weak mixing angle were collected in the effective constant κ . Differentiating Equation (4.75) with respect to μ^2 yields the β -function of the weak mixing angle in the $\overline{\text{MS}}$ -scheme,

$$\mu^2 \frac{d}{d\mu^2} \hat{s}^2 \kappa(\mu^2) = \frac{\alpha}{\pi} \left(\frac{1}{6} \sum_f N_f^c Q_f v_f - \frac{43}{24} + \frac{7}{4} s^2 \right). \quad (4.78)$$

The two rightmost terms are now expressed in terms of the squared sine s^2 instead of $c^2 = 1 - s^2$ and stem from W-boson loops in the γZ -self-energy function and vertex corrections.

The subscript f in Equation (4.78) indicates a sum over all Dirac fermions, but can be transformed into a sum over all chiral degrees of freedom, which is convenient for solving the differential equation. Since the weak isospin of the right-handed fermions vanishes, but the charges of left- and right-handed fermions are identical, the vector coupling constant v_f of a Dirac fermion is given by

$$v_f = T_f^3 - 2s^2 Q_f = \sum_{i=l_f, r_f} (T_i^3 - s^2 Q_i). \quad (4.79)$$

Here, the indices l_f and r_f denote the left- and right-handed chiral fermions of flavor f . In order to denote different particle types in this section and Section 4.4, the notation of Reference [17] is adopted. The different subscripts are summarized in Table 4.1. Rewriting the sum as a sum over chiral fermions allows combining the fermionic and bosonic terms and facilitates solving the β -function

4. Parity Violating Interaction and the Weak Mixing Angle

Particle	Subscript
Dirac fermion	f
Dirac quark	q
chiral fermion	i
chiral fermion or boson	p
chiral fermion or boson	i_q

Table 4.1.: Subscripts used to denote different particle types.

Field	γ_x
Real scalar	1
Complex scalar	2
Chiral fermion	4
Majorana fermion	4
Dirac fermion	8
Massless gauge boson	-22

Table 4.2.: Weight factors γ_x in the weak mixing angle's β -function.

in terms of the solution of the electromagnetic coupling. Using γ_p to denote particle type specific factors called weight factors in Reference [17], one finds

$$\hat{\beta}_{s^2} = -\frac{\alpha}{24\pi} \sum_p N_p^c \gamma_p (T_p^3 Q_p - s^2 Q_p^2). \quad (4.80)$$

Comparing Equations (4.78) and (4.80) yields $\gamma_i = 4$ for chiral fermions. The bosonic terms in Equation (4.78) can be obtained, when summing over a pair of massless gauge bosons ($\gamma_b = -22$) and one complex Goldstone boson ($\gamma_G = 2$, $T_G = +\frac{1}{2}$, $Q_G = +1$). The weight factors mentioned in Reference [17] are displayed in Table 4.2.

4.4. Solution of the Weak Mixing Angle's β -Function

The solution of the β -function of the weak mixing angle is simple from a technical point of view. One just needs to plug the β -function (4.80) into one of the first order solutions derived in Chapter 3. The obtained solution may then be used to rescale the weak mixing angle. However, the β -function is obtained using perturbation theory, which is not suitable for treating effects

of the strong interaction. As in the case of the electromagnetic coupling, the naive solution is ill-defined below the hadronization scale, if light quark effects are taken into account. In Chapter 3, the workaround was to make use of the optical theorem and experimental data in order to obtain a value of $\hat{\alpha}(\mu^2)$ above the hadronization scale and avoiding the non-perturbative region altogether. In order to treat the coupling parameters at low energies, a different ansatz is required. As described in References [17, 18], the coupling parameters can be constrained phenomenologically in the non-perturbative region, which is facilitated by relating the running of $\sin^2 \hat{\theta}_W$ to that of the electromagnetic coupling parameter. Using the solution of the latter, allows constraining the weak mixing angle indirectly in the non-perturbative region, too. To that end, the solution of the weak mixing angle in terms of the electromagnetic coupling is discussed in this section.

The β -function of the weak mixing was derived at one-loop order in the previous section. The fermionic contributions stem from the fermion loop in the γZ -mixing and can be deduced from the photonic self-energy. Some higher order corrections can be taken into account by replacing the color factor N_i with [18]

$$\begin{aligned}
 K_i &= N_i^c \left\{ \left(1 + \frac{3}{4} Q_i^2 \frac{\hat{\alpha}}{\pi} \right) + \frac{\hat{\alpha}_s}{\pi} + \left(\frac{\hat{\alpha}_s}{\pi} \right)^2 \left[\frac{125}{48} - \frac{11}{72} n_q \right] + \sum_{k=3}^4 \left(\frac{\hat{\alpha}_s}{\pi} \right)^k K_i^{(k)} \right\}, \\
 K_i^{(3)} &= \frac{10487}{1728} + \frac{55}{18} \zeta_3 - n_q \left(\frac{707}{864} + \frac{55}{54} \zeta_3 \right) - \frac{77}{3888} n_q^2, \\
 K_i^{(4)} &= \frac{2665349}{41472} + \frac{182335}{864} \zeta_3 - \frac{605}{16} \zeta_4 - \frac{31375}{288} \zeta_5 \\
 &\quad - n_q \left(\frac{11785}{648} + \frac{58625}{864} \zeta_3 - \frac{715}{48} \zeta_4 - \frac{13325}{432} \zeta_5 \right) \\
 &\quad - n_q^2 \left(\frac{4729}{31104} - \frac{3163}{1296} \zeta_3 + \frac{55}{72} \zeta_4 \right) + n_q^3 \left(\frac{107}{15552} + \frac{1}{108} \zeta_3 \right).
 \end{aligned} \tag{4.81}$$

The term independent of $\hat{\alpha}_s$ applies to all fermions, while the remaining terms stem from the strong interaction and need to be dropped for leptons. The bosons are treated at one-loop order, that is $K_b = 1$. K_i as defined above

4. Parity Violating Interaction and the Weak Mixing Angle

only accounts for non-singlet contributions, as these enter the electromagnetic coupling similarly. Singlet contributions are also present in the electromagnetic case but have a different structure and need to be treated separately. The singlet contributions may be parametrized in terms of σ according to [18]

$$\sigma = \frac{\hat{\alpha}_s^3}{\pi^3} \left[\frac{55}{216} - \frac{5}{9}\zeta_3 \right] + \frac{\hat{\alpha}_s^4}{\pi^4} \left[\frac{11065}{3456} - \frac{34775}{3456}\zeta_3 + \frac{55}{32}\zeta_4 + \frac{3875}{864}\zeta_5 - n_q \left(\frac{275}{1728} - \frac{205}{576}\zeta_3 + \frac{5}{48}\zeta_4 + \frac{25}{144}\zeta_5 \right) \right]. \quad (4.82)$$

This way, the renormalization group equation of the weak mixing angle becomes

$$\mu^2 \frac{d\hat{s}^2}{d\mu^2} = \frac{\hat{\alpha}}{\pi} \left[\sum_p \frac{K_p \gamma_p}{24} (s^2 Q_p^2 - T_p^3 Q_p) + \sigma \hat{s}^2 \left(\sum_q Q_q \right)^2 - \frac{\sigma}{2} \left(\sum_q T_q^3 \right) \left(\sum_q Q_q \right) \right]. \quad (4.83)$$

The singlet contributions are proportional to the vector coupling constants v_q of the virtual quarks; in order to relate the β -function of the weak mixing angle to that of the electromagnetic coupling the quark's vector coupling constants were already split up in Equation (4.83). Using the same separation of the bosonic terms into two massless gauge bosons and one Goldstone boson as explained in Section 4.3 allows writing the β -function of the electromagnetic coupling constant in a similar form,

$$\mu^2 \frac{d\hat{\alpha}}{d\mu^2} = \frac{\hat{\alpha}^2}{\pi} \left[\frac{1}{24} \sum_i K_i \gamma_i Q_i^2 + \sigma \left(\sum_q Q_q \right)^2 \right]. \quad (4.84)$$

Using Equations (4.83) and (4.84), it is straightforward to derive

$$\mu^2 \frac{d}{d\mu^2} \left(\frac{\hat{s}^2}{\hat{\alpha}} \right) = -\frac{1}{24\pi} \sum_p K_p \gamma_p T_p^3 Q_p - \frac{\sigma}{2\pi} \left(\sum_q T_q^3 \right) \left(\sum_q Q_q \right). \quad (4.85)$$

The solution of Equation (4.85) is not trivial, as the right-hand side still depends on the scale μ due to the presence of $\hat{\alpha}(\mu)$ and $\hat{\alpha}_s(\mu)$ within K_i and σ . When neglecting terms of order $\mathcal{O}(\hat{\alpha}^2)$ and $\mathcal{O}(\hat{\alpha}\hat{\alpha}_s)$ ⁸, the differential Equation (4.85) can be simplified by the introduction of five auxiliary coefficients $\lambda_1, \dots, \lambda_4$ and $\tilde{\sigma}$. The coefficients λ_i are independent of the coupling parameters and the scale μ and allow writing Equation (4.85) as

$$0 = \mu^2 \frac{d}{d\mu^2} \left(\frac{\hat{s}^2 - \lambda_1}{\hat{\alpha}} - \frac{3\lambda_3}{4\pi} \log \hat{\alpha} + \frac{\tilde{\sigma}}{\pi} \right) - \frac{\lambda_2}{3\pi} + \mathcal{O}(\hat{\alpha}^2, \hat{\alpha}\hat{\alpha}_s). \quad (4.86)$$

Using Equation (4.86) as an ansatz, the coefficients can be computed by inserting the derivatives of $\hat{\alpha}(\mu)$ and $\hat{s}^2(\mu)$ and expanding in powers of coupling constants $\hat{\alpha}$ and $\hat{\alpha}_s$. This yields a system of equations which eventually leads to

$$\begin{aligned} \lambda_1 &= \frac{\sum_q Q_q T_q^3}{2 \sum_q Q_q^2}, & \lambda_2 &= \frac{1}{8} \sum_i N_i \gamma_i (\lambda_1 Q_i^2 - T_i^3 Q_i), \\ \lambda_3 &= \frac{\sum_i N_i \gamma_i (\lambda_1 Q_i^4 - T_i^3 Q_i^3)}{\sum_i N_i \gamma_i Q_i^2}, & \tilde{\sigma} &= \frac{2\lambda_4}{\beta_0^{\text{QCD}}} \frac{\pi}{\hat{\alpha}_s} \sigma, \\ \lambda_4 &= \lambda_1 \left(\sum_q Q_q \right)^2 - \frac{1}{2} \left(\sum_q T_q^3 \right) \left(\sum_q Q_q \right). \end{aligned} \quad (4.87)$$

The expression of λ_1 is a simplification of

$$\lambda_1 = \frac{\sum_{i_q} N_{i_q} \gamma_{i_q} T_{i_q}^3 Q_{i_q}}{\sum_{i_q} N_{i_q} \gamma_{i_q} Q_{i_q}^2}, \quad (4.88)$$

in which the sum is taken over chiral quarks, as indicated by the index i_q . Rewriting the two sums as sums over Dirac quarks yields the result given in Equation (4.87). Due to the particular form of the coefficients λ_1 and λ_2 , the sum over quarks in λ_2 cancels, allowing to sum over chiral leptons $i \neq q$, only.

⁸Terms of order $\mathcal{O}(\hat{\alpha}\hat{\alpha}_s)$ have been neglected in the solution of the electromagnetic β -function, too.

This can be easily verified by inserting equation (4.88) into the definition of λ_2 . However, quarks still contribute to λ_2 via λ_1 in the sum over chiral leptons. The precise values of the coefficients in Equation (4.87) depend on the field content and change when integrating out a fermion. Explicit values can be found in Reference [17].

Since λ_2 is independent of μ , the differential Equation (4.86) can be readily integrated; without any additional approximation one finds the solution [17]

$$\begin{aligned} \hat{s}^2(\mu) = & \frac{\hat{\alpha}(\mu)}{\hat{\alpha}(\mu_0)} \hat{s}^2(\mu_0) + \lambda_1 \left(1 - \frac{\hat{\alpha}(\mu)}{\hat{\alpha}(\mu_0)} \right) \\ & + \frac{\hat{\alpha}(\mu)}{\pi} \left(\frac{\lambda_2}{3} \log \frac{\mu^2}{\mu_0^2} + \frac{3}{4} \lambda_3 \log \frac{\hat{\alpha}(\mu)}{\hat{\alpha}(\mu_0)} + \tilde{\sigma}(\mu_0) - \tilde{\sigma}(\mu) \right) + \mathcal{O}(\hat{\alpha}^3, \hat{\alpha}^2 \hat{\alpha}_s). \end{aligned} \quad (4.89)$$

The term $\mathcal{O}(\hat{\alpha}^3, \hat{\alpha}^2 \hat{\alpha}_s)$ in Equation (4.89) indicates the error that stems from the approximation made in Equation (4.86). However, as the β -function was derived without taking into account electroweak two-loop effects, there are also terms of order $\mathcal{O}(\alpha^2)$ that are missing in the solution (4.89). On the other hand, the $\mathcal{O}(\hat{\alpha}^2)$ -terms that stem from the two-particle irreducible purely electromagnetic two-loop diagrams are taken into account due to the two-loop solution $\hat{\alpha}(\mu)$ derived in Chapter 3. These are accompanied by two-loop terms that arise due to the resummation of one-particle irreducible terms. Either type of two-loop contributions can be identified by expanding Equation (4.89) in terms of $\hat{\alpha}$.

The solution (4.89) is particularly useful, as it expresses the running of the weak mixing angle in terms of the running of the electromagnetic coupling. That way, phenomenological constraints of hadronic effects in $\hat{\alpha}(\mu)$ can be indirectly applied to the weak mixing angle. Additional uncertainties because of non-perturbative effects arise from the singlet contribution and the parameters λ_i . The coefficients λ_i need to be changed at particle thresholds, which are not well-defined within perturbation theory.

5. Matching Conditions

5.1. Introduction

5.1.1. Concept

The effect of heavy particles on low-energy observables is often negligible and keeping those particles as degrees of freedom is an unnecessary complication. In MS-like renormalization schemes, this may be addressed by using an effective model, which does not contain the heavy fields. The parameters of the effective model are initially unknown, but can be linked to the parameters of the complete theory by the so called “matching”. The general procedure of integrating out heavy degrees of freedom is to introduce renormalization constants in the effective theory, which are determined by equating Green functions or observables of the effective and the complete theory, respectively. This follows the process of renormalization closely, but the matching conditions (in analogy to the renormalization conditions) depend on calculations in two different models. As a simple example, the matching condition that fixes the electromagnetic coupling constant in the effective theory reads

$$\bar{u}(p)\Gamma_{\mu}^{\prime f f \gamma}(p, p)u(p) = \bar{u}(p)\Gamma_{\mu}^{f f \gamma}(p, p)u(p) \quad (5.1)$$

for an arbitrary but fixed value of the momentum p . Here and in the following, primes are used to denote quantities of the effective theory. If the quantity is momentum dependent, the prime is used as a subscript to avoid confusion with the derivative with respect to the momentum. Equation (5.1) allows drawing two conclusions. First, if the Green function of the complete theory is properly renormalized, that is free of UV divergences, the Green function of the effective theory will be as well. Second, the matching procedure may be understood as a

5. Matching Conditions

generalization of renormalization; for instance, the renormalization condition for the electric charge in the on-shell scheme,

$$\bar{u}(p)\Gamma_\mu^{ff\gamma}(p,p)u(p) = -ieQ_f\bar{u}(p)\gamma_\mu u(p), \quad (5.2)$$

may be understood as matching the theory with the tree-level expression.

Equation (5.1) contains an ambiguity due to the presence of the mass scale μ that is introduced in dimensional regularization. At one-loop order, it appears in logarithms of the form

$$L_h := \log \frac{\mu^2}{M_h^2}, \quad (5.3)$$

where M_h refers to the mass of one of the heavy particles that are being integrated out. The particular choice of μ that has to be made in order to obtain a meaningful matching condition, is called matching scale. Its precise value is arbitrary, but it is advisable to choose a value of the order of M_h to prevent the occurrence of large logarithms. If the masses of the heavy particles span several orders of magnitude, large logarithms inevitably occur when removing all heavy particles at once. In this case, it might be better to integrate out the particles one at a time: Suppose there are two particles with masses $M_1 \gg M_2$. In a first step, one constructs an effective theory without the particle of mass M_1 and matches it with the complete theory at the scale $\mu_1 \sim M_1$. In a next step, the renormalization group equation (RGE) of the effective model can be used to evolve the effective parameters to a different scale $\mu_2 \sim M_2$. Now, the M_2 -particle can be removed by creating a second effective theory and matching it with the first one at the scale μ_2 . In this procedure, the large logarithms reappear when evolving the effective parameters from scale μ_1 to μ_2 . However, the benefit of this approach is that the large logarithms are automatically resummed when the β -function is solved analytically.

5.1.2. Published Calculations

The process of matching an effective theory with the one including all degrees of freedom has been worked out first in [34] and studied in the context of grand

unification in [35]. The calculations in these two publications were carried out for simple gauge groups only, raising the question, whether the direct application to the electroweak Standard Model (EWSM) is viable. In particular, the mass mixing between the fundamental fields B_μ and W_μ^3 that is induced by the vacuum expectation value of the Higgs,

$$\frac{v^2}{4}g_1g_2B_\mu W^{3\mu} = csM_Z^2B_\mu W^{3\mu}, \quad (5.4)$$

was not taken into account. Since Equation (5.4) describes a tree-level effect, it needs to be resummed in a Dyson series. This is crucially different from the γZ -mixing induced by loop diagrams, which can be treated perturbatively.

The matching conditions¹ for integrating out the W-boson or a heavy fermion in the $SU(2)\times U(1)$ product group of the EWSM were presented in References [9] and [17], citing the work of Hall [35]. The results for the effective coupling constants when removing the W-boson given in References [9, 17] read ($\mu = M_W$)

$$\frac{1}{\alpha} = \frac{1}{\alpha'} + \frac{1}{6\pi}, \quad (5.5a)$$

$$s^2 = 1 - \frac{\alpha}{\alpha'}(1 - s'^2) = s'^2 + \frac{\alpha}{6\pi}(1 - s'^2). \quad (5.5b)$$

In a more recent study [36], an effective low energy model was constructed by integrating out the top, Higgs, Z and W simultaneously. Omitting the top-quark contributions, the findings are

$$\frac{1}{\alpha} = \frac{1}{\alpha'} + \frac{1}{6\pi} - \frac{7}{4\pi}L_W \quad (5.6)$$

and confirm the result (5.5a). By integrating out the Z-boson, the weak mixing angle was removed from the theory and consequently, no equation analogous to (5.5b) was given in Reference [36]. However, a validation of Equation (5.5b) is desirable, as it is not clear whether the application of the methods described in References [34, 35] to the matching of the weak mixing angle can be justified.

¹In the following, the term ‘‘matching condition’’ will be used interchangeably for the defining relations like Equation (5.1) and its corresponding solutions like Equation (5.5).

5.1.3. Outline

The key ideas of the derivation of matching conditions based on Reference [35] are presented in Sections 5.2.1 to 5.2.3. In Section 5.2.4 the results are applied to integrating out the W-boson, reproducing the results given in Equation (5.5). This calculation is insufficient in describing all electroweak effects that are required for the matching of the weak mixing angle. The precise problem is briefly discussed in Section 5.2.5. Overcoming the inadequacy and deriving meaningful matching conditions requires a new ansatz that is discussed in the remainder of this chapter. Two similar calculations based on different effective models are presented in Sections 5.3 and 5.4, including precise definitions of the effective models and matching conditions for all relevant amputated two- and three-point functions.

5.2. Calculation in the Context of a Grand Unified Theory

The calculation outlined in Reference [35] was done in the context of a grand unified theory whose gauge group is spontaneously broken. The goal was to investigate the relation between the known interactions of the Standard Model and a hypothetical unified interaction that is described by a single simple gauge group. Additional assumptions like gauge invariance of certain terms in the effective theory were made, and it is not clear, if the prescription can be directly applied to the EWSM. The ideas and results of Reference [35] are outlined in the following subsections nonetheless, as they allow reproducing the matching condition (5.5b) published in Reference [9]. Different approaches that do not rely on the assumptions made in Reference [35] are discussed in Sections 5.3 and 5.4.

5.2.1. Heavy Particles at Zero Momentum Transfer

The effect of heavy particles at zero momentum transfer can be directly calculated in the Standard Model. The heavy particles appear as virtual particles in

the self-energies of the gauge bosons, which can be separated into transverse and longitudinal parts according to Equation (2.25). Calculating the matching condition for a gauge coupling requires the computation of the field renormalization constant of the associated gauge field; to this end, it is sufficient to take into account the coefficients of the metric tensor, only². Accordingly, the $q^\mu q^\nu$ -terms will be omitted in the following, so that the one-loop corrected propagator of a massless gauge boson reads

$$\frac{-ig_{\mu\nu}}{q^2} + \frac{-ig_{\mu\alpha}}{q^2} (i\Sigma^{\alpha\beta}) \frac{-ig_{\beta\nu}}{q^2} = \frac{-ig_{\mu\nu}}{q^2} \left(1 - \frac{\Sigma^T}{q^2}\right). \quad (5.7)$$

Any particle that couples to the mediating gauge boson, occurs in the self-energy and contributes to this correction, but the terms that stem from the heavy particle may be factorized. Using Σ_h^T to denote the contribution of the heavy particle and Σ_r^T for all remaining terms ($\Sigma^T = \Sigma_h^T + \Sigma_r^T$), the one-loop corrected propagator can be written as

$$\frac{-ig_{\mu\nu}}{q^2} \left(1 - \frac{\Sigma^T}{q^2}\right) = \frac{-ig_{\mu\nu}}{q^2} \left(1 - \frac{\Sigma_h^T}{q^2}\right) \left(1 - \frac{\Sigma_r^T}{q^2}\right) + \mathcal{O}(\Sigma_h^T \Sigma_r^T). \quad (5.8)$$

The correction $\frac{\Sigma_h^T}{q^2}$ can be expanded in $\frac{q^2}{M_h^2}$, where M_h is the mass of the heavy particle. For small values of q^2 it is dominated by the zeroth-order term of its Taylor expansion and the propagator (5.8) may be approximated as

$$\frac{-ig_{\mu\nu}}{q^2} \left[1 - (\Sigma_h^T)'(q^2=0)\right] \left(1 - \frac{\Sigma_r^T}{q^2}\right) + \mathcal{O}(\Sigma_h^T \Sigma_r^T) + \mathcal{O}\left(\frac{q^2}{M_h^2}\right), \quad (5.9)$$

assuming that $\Sigma_h^T(0) = 0$. In case of a massive gauge boson, the result is similar, but the calculation is more involved. The proper derivation including the mass is carried out in Section 5.3.

²This is justified by the results of the complete calculation in Section 5.3.

5.2.2. Effective Theory

The effective model does not contain the heavy field as a degree of freedom, but is constructed such that it includes the same correction of the propagator as shown in Equation (5.9). This is achieved with the “free” Lagrangian

$$\mathcal{L}_{\text{free}}^A = (1+l) \left[-\frac{1}{4} \left(\partial_\mu A_\nu^a - \partial_\nu A_\mu^a \right)^2 + \frac{1}{2} M_A^2 A_\mu^a A^{a\mu} - \frac{1}{2\xi^a} \left(\partial^\mu A_\mu^a \right)^2 \right] \quad (5.10)$$

of the gauge field A_μ^a , where the correction l is defined as $l = \left(\Sigma_h^T \right)' (q^2 = 0)$ at one-loop order. Using integration by parts and omitting surface terms, this may also be written as

$$\mathcal{L} = \frac{1+l}{2} A_\mu^a \left[g^{\mu\nu} \left(\partial^2 + M_A^2 \right) - \partial^\mu \partial^\nu \left(1 - \frac{1}{\xi^a} \right) \right] A_\nu^a. \quad (5.11)$$

Formally deriving the propagator in the effective theory shows that Equation (5.11) is in concordance with (5.9). The propagator is the tree-level expansion of the Green function

$$G_{\mu\nu}(x_1, x_2) = (-i)^2 \frac{\delta^2}{\delta J^\mu(x_1) \delta J^\nu(x_2)} \left. \frac{\int \mathcal{D}[\dots] \exp \left(i \int d^D x \left[\mathcal{L} + J^\mu A_\mu^a \right] \right)}{\int \mathcal{D}[\dots] \exp(iS)} \right|_{J^\mu=0}, \quad (5.12)$$

where $\mathcal{D}[\dots]$ denotes the functional integration over all fields of the effective theory. The argument of the exponential function in the numerator of Equation (5.12) can be rewritten as usual,

$$\begin{aligned} \int d^D x \left[\mathcal{L} + J^\mu A_\mu^a \right] &= \int d^D x \frac{1+l}{2} \tilde{A}_\mu^a \left[g^{\mu\nu} \left(\partial^2 + M_A^2 \right) - \partial^\mu \partial^\nu \left(1 - \frac{1}{\xi^a} \right) \right] \tilde{A}_\nu^a \\ &\quad + \frac{D}{2(1+l)} \int d^D x d^D x' J^\mu(x) \Delta_{\mu\nu}(x, x') J^\nu(x'), \end{aligned} \quad (5.13)$$

where D is the dimension of space-time, $\Delta_{\mu\nu}$ is the Green function of the bracket in Equation (5.11),

$$\left[g^{\mu\nu} \left(\partial^2 + M_A^2 \right) - \partial^\mu \partial^\nu \left(1 - \frac{1}{\xi^a} \right) \right] \Delta_{\mu\nu}(x, x') = -\delta^{(D)}(x, x'), \quad (5.14)$$

and

$$\tilde{A}_\mu^a = A_\mu^a - \frac{D}{1+l} \int d^D x' \Delta_{\mu\rho}(x, x') J^\rho(x'). \quad (5.15)$$

Due to translational invariance of the functional integral, the shifted field \tilde{A}_μ^a can be replaced by A_μ^a . Inserting the Lagrangian (5.13) into Equation (5.12) allows obtaining the Green function. Expanding the remaining exponential function yields

$$G_{\mu\nu}^{\text{tree}}(x_1, x_2) = -\frac{i}{2} \frac{D}{1+l} \left[\frac{\delta^2}{\delta J^\mu(x_1) \delta J^\nu(x_2)} \cdot \int d^D x d^D x' J^\mu(x) \Delta_{\mu\nu}(x, x') J^\nu(x') \right]_{J^\mu=0} \quad (5.16)$$

for the tree-level Green function. It can be evaluated using the solution of Equation (5.14), which reads

$$\Delta_{\mu\nu}(x, x') = \frac{1}{D} \int \frac{d^D p}{(2\pi)^D} e^{-ip(x-x')} \left[\frac{g_{\mu\nu}}{p^2 - M_A^2} - \frac{p_\mu p_\nu (1 - \xi^a)}{(p^2 - M_A^2)(p^2 - \xi^a M_A^2)} \right] \quad (5.17)$$

in terms of a D -dimensional Fourier integral. Inserting $\Delta_{\mu\nu}(x, x')$ into Equation (5.16) yields

$$G_{\mu\nu}^{\text{tree}}(x_1, x_2) = \int \frac{d^D p}{(2\pi)^D} e^{-ip(x_1-x_2)} \frac{1}{1+l} \cdot \left[\frac{-ig_{\mu\nu}}{p^2 - M_A^2} + \frac{ip_\mu p_\nu (1 - \xi^a)}{(p^2 - M_A^2)(p^2 - \xi^a M_A^2)} \right]. \quad (5.18)$$

The Fourier transform of this expression is the Feynman rule for a propagator in momentum space and in agreement with Equation (5.9) in Feynman gauge.

5. Matching Conditions

The Lagrangian in Equation (5.11) is not normalized canonically because of the leading factor $(1 + l)$. The canonical normalization can be restored by rescaling the field according to

$$A_\mu^a = \frac{A_\mu^{\prime a}}{\sqrt{1 + l}}, \quad (5.19)$$

where the prime denotes the quantity of the effective model. It is now evident that the constant l introduced as a correction factor carrying contributions of a heavy particle plays the role of a renormalization constant in the effective theory. To avoid confusion between the two closely related concepts of renormalization and matching, the renormalization constants in the effective theory will be called matching constants and denoted by a lowercase l , while Z is used for the renormalization constants of the Standard Model. Besides the bilinear terms, the gauge field also occurs in the interaction terms, which stem from the covariant derivative, the self-interaction and the gauge fixing. Replacing the field of the complete theory with that of the effective model in the covariant derivative gives a contribution to the interaction term,

$$\partial_\mu - igT^a A_\mu^a = \partial_\mu - igT^a A_\mu^{\prime a} \frac{1}{\sqrt{1 + l}}. \quad (5.20)$$

The standard form of the covariant derivative can be restored, too; this time by introducing an effective gauge coupling that is scaled with the inverse factor to cancel the corresponding normalization of the gauge field,

$$g = g' \sqrt{1 + l}. \quad (5.21)$$

Equation (5.21) is called the matching condition and relates the effective coupling g' to the coupling g of the parent theory. With the definition of the matching constant l , the coupling constant of the effective theory is solely determined by the self-energy function of the associated gauge field A_μ^a in the parent theory. This is similar to the renormalized electric charge in the Standard Model, which only depends on the self-energy function of the photon.

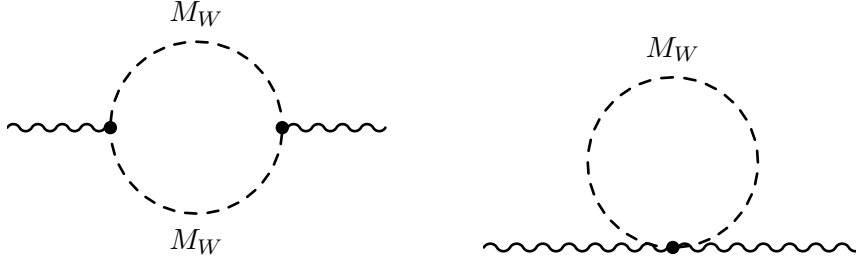


Figure 5.1.: Gauge boson self-energy diagrams excluding the Higgs-tadpole diagram. The dashed line represents any particle with mass M_W .

5.2.3. Application to the Fundamental Gauge Bosons of the Electroweak Sector

The self-energy of a gauge field was derived in Reference [35] by computing the diagrams with the topologies shown in Figure 5.1 in a general context. The part of the result that can be applied to integrating out the W-boson is³

$$l_A = -\frac{g^2}{48\pi^2} \text{Tr}(t_A t_A), \quad (5.22)$$

where A denotes the gauge field and g is the corresponding gauge coupling constant. The matrices t_A are the generators of the broken gauge group in the adjoint representation. Evaluating the trace yields

$$\begin{aligned} l_B &= 0, \\ l_{W^3} &= -\frac{g_2^2}{24\pi^2} \end{aligned} \quad (5.23)$$

for the U(1) and SU(2) gauge groups, respectively. The result $l_B = 0$ represents the fact that the B_μ -field does not couple directly to any of the fields with mass M_W .

³Note, that the definition of l in Reference [35] comes with a relative minus sign compared to the present definition.

5.2.4. Derivation of the Electromagnetic Coupling and the Weak Mixing Angle Via the Fundamental Gauge Couplings

The matching for the electromagnetic coupling constant can be obtained in terms of the vacuum polarization function by applying the results of Section 5.2.2 in the physical basis, that is the basis in which the mass matrix of the gauge bosons is diagonal. This calculation is carried out in Section 5.2.5. Since the electromagnetic coupling constant is defined in terms of the gauge couplings g_1 and g_2 that are associated with the gauge groups,

$$\alpha = \frac{e^2}{4\pi} = \frac{1}{4\pi} \frac{g_1^2 g_2^2}{g_1^2 + g_2^2}, \quad (5.24)$$

the matching can also be derived from the matching of the couplings g_1 and g_2 . The latter approach also allows deriving the matching for the weak mixing angle, which is defined as

$$s^2 = \frac{g_1^2}{g_1^2 + g_2^2}. \quad (5.25)$$

Inserting Equations (5.21) and (5.23) into the definition of α yields the matching condition [17]

$$\frac{1}{\alpha} = 4\pi \frac{\frac{g_1'^2}{1+l_{W3}} + \frac{g_2'^2}{1+l_B}}{g_1'^2 g_2'^2} = \frac{1}{\alpha'} + \frac{1}{6\pi} + \mathcal{O}(\alpha). \quad (5.26)$$

A similar calculation for the weak mixing angle also produces a matching condition of the weak mixing angle,

$$s^2 = s'^2 - c^2 s^2 (l_{W3} - l_B) + \mathcal{O}(\alpha^2) = s'^2 + \frac{\alpha}{6\pi} c^2 + \mathcal{O}(\alpha^2). \quad (5.27)$$

Equation (5.27) is the matching condition used in References [17, 18] to determine the weak mixing angle at low energies. As mentioned before, the calculation presented above is not sufficient for deriving the matching of the mixing angle of the EWSM, which will be briefly illustrated in Section 5.2.5.

5.2.5. Matching of Electromagnetic Coupling in Terms of the Photonic Self-Energy Function

To understand the shortcomings of the previous ansatz, the matching condition for the electromagnetic coupling constant is now derived using the self-energy of the photon directly. Following Section 5.2.2, the matching condition for the electromagnetic coupling constant reads

$$e = e' \sqrt{1 + l_e}, \quad l_e = \left[\frac{d}{dq^2} \Sigma_{T, M_W}^\gamma(q^2) \right]_{q^2=0}, \quad (5.28)$$

where $\Sigma_{M_W}^{\gamma, T}$ denotes the transverse part of the photon's self-energy that stems from a loop with a particle of mass M_W . The matching constant l_e is a power series in α , allowing to write the matching condition as

$$\frac{1}{e^2} = \frac{1}{e'^2} - \frac{l_e}{e^2} + \mathcal{O}(\alpha). \quad (5.29)$$

Dropping the fermionic part, the contribution to l_e from the $\overline{\text{MS}}$ -renormalized photon self-energy reads [2]

$$l_e = \frac{\alpha}{4\pi} \frac{d}{dq^2} \left[3q^2 \log \frac{M_W^2}{\mu^2} - (3q^2 + 4M_W^2) F(q^2, M_W, M_W) \right]_{q^2=0}, \quad (5.30)$$

where the function $F(q^2, M, M)$ is the UV-finite part of the two-point Passarino–Veltman function $B_0(q^2, M, M)$ with the Taylor expansion

$$F(q^2, M, M) = \frac{q^2}{6M^2} + \mathcal{O}\left(\frac{q^4}{M^4}\right). \quad (5.31)$$

With $\alpha = \frac{e^2}{4\pi}$, the matching condition for α reads

$$\frac{1}{\alpha(\mu)} = \frac{1}{\alpha'(\mu)} + \frac{1}{4\pi} \left[3 \log \frac{\mu^2}{M_W^2} + \frac{2}{3} \right]. \quad (5.32)$$

5. Matching Conditions

The matching scale is arbitrary to some extent and $\mu = M_W$ is a convenient choice, for which one finds [17]

$$\frac{1}{\alpha(M_W)} = \frac{1}{\alpha'(M_W)} + \frac{1}{6\pi}, \quad (5.33)$$

which confirms the results of the previous sections. The renormalization and accordingly the matching condition of the electric charge is not solely determined by the self-energy of the photon, but depends on the γZ -mixing, too [37]. This is the reason, why the scale dependent term in Equation (5.32) deviates from the result given in Reference [36]. The latter one also includes the γZ -self-energy contribution

$$-2\frac{s}{c}\frac{\hat{\Sigma}_T^{\gamma Z}(0)}{M_Z^2} = \frac{\alpha}{4\pi}4\log\frac{M_W^2}{\mu^2}, \quad (5.34)$$

which does not appear in the present calculation. Adding Equation (5.34) to the matching constant l_e yields the result of Reference [36], but is without justification at this point. The problem is that the present ansatz accounts for the self-energy of the investigated boson, only. This is sufficient if the gauge bosons of different gauge groups do not communicate like in the case of a simple gauge group which is the basis for the calculation in Reference [35]. As a consequence, the effect of γZ -mixing can not be reproduced by the results presented in Section 5.2.3.

The reason for the inadequacy of Reference [35] in the context of the EWSM is similar. The product group $SU(2)\times U(1)$ contains two different subgroups whose gauge bosons mix due to the interaction with the Higgs boson. The mixing is not accounted for as can be seen in Equation (5.23), where the matching for either subgroup is derived independently. To overcome this shortcoming, a different ansatz is discussed in Sections 5.3 and 5.4 based on two different effective models, in which the matching conditions are obtained by equating Green functions instead of self-energy functions. This follows the ideas of renormalization closely and guarantees that also all interactions between gauge bosons are taken into account.

5.3. Z as a Pseudo Gauge Boson

The ansatz described in Section 5.2 for the effective model does not include effective terms that describe the mixing between photon and Z-boson via a W^+W^- -loop. This mixing occurs at one-loop order in the EWSM due to the γZ -self-energy diagrams. Furthermore, the previous calculation also does not take into account vertex corrections, although the renormalization of the electromagnetic coupling constant and the weak mixing angle also depend on vertex functions. All these one-loop corrections have to be reproduced in the effective theory by means of effective interaction terms. Additionally, the matching of the weak mixing angle was calculated, presuming that $g_Z = \frac{e}{c_s}$ is a valid relation in the effective theory. However, in the effective theory, the coupling constant g_Z should be treated as an independent and elementary parameter at first. Calculating the matching conditions will then provide a relation to the physical parameters of the EWSM allowing to give a physical interpretation of the effective parameters.

In this section, a more versatile ansatz is used and matching conditions for all two- and three-point functions are derived. An effective model including the Z-boson but without charged current interactions is introduced in Section 5.3.1. The motivation for this model is to determine the matching conditions in the electroweak sector when integrating out the W-boson, but it may also serve as a basis for integrating out fermions, subsequently. The irreducible two- and three-point functions of the effective model are given in Section 5.3.2. In Section 5.3.3 the matching conditions of the field renormalization constants and electric charge are worked out and the matching of the weak mixing angle is determined in Section 5.3.5.

5.3.1. Lagrangian

In order to get rid of the shortcomings described above, one needs a more sophisticated ansatz for the derivation of matching conditions. The starting point is the electroweak Standard Model in terms of the physical fields as discussed in Section 2.1 and an ansatz for the effective model. The Lagrangian

5. Matching Conditions

of the effective model is obtained from the EWSM Lagrangian by omitting all terms that include a scalar, a W^\pm -field or a ghost-field. To compensate for the omitted interactions with the Higgs field, additional effective mass terms of the Z-boson and the fermions are introduced. The explicit expression for the effective Lagrangian reads

$$\begin{aligned} \mathcal{L}' = & \sum_f \left[\bar{f}' \left(i\cancel{\partial} - m'_{0,f} \right) f' - e' Q_f \bar{f}' A' f' + g'_Z \left(T_f^3 \bar{f}'^L \cancel{Z}' f'^L - s'^2 Q_f \bar{f}' \cancel{Z}' f' \right) \right] \\ & - \frac{1}{4} F'_{\mu\nu} F'^{\mu\nu} - \frac{1}{4} Z'_{\mu\nu} Z'^{\mu\nu} + \frac{1}{2} M'_{0,Z}{}^2 Z'_\mu Z'^\mu - \frac{1}{2\xi'_A} (\partial_\mu A'^\mu)^2 - \frac{1}{2\xi'_Z} (\partial_\mu Z'^\mu)^2, \end{aligned} \quad (5.35)$$

where primes denote effective fields and parameters. Additional non-diagonal terms that would mix the photon and the Z-field are not included, since the introduction of appropriate matching constants will allow for a non-diagonal matching of the fields in the effective theory to the corresponding fields in the EWSM (see Equation (5.37) below). The Lagrangian does not preserve the $SU(2) \times U(1)$ -symmetry of the Standard Model due to the lack of two components of the $SU(2)$ -vector field, that is W_μ^1 and W_μ^2 . Additionally, the Z-mass is not generated by a Higgs mechanism so that the Z_μ -field can not be a gauge field. Accordingly, ξ'_Z is not a gauge fixing parameter but merely an undetermined parameter of the model that has no practical relevance in the present use case. However, the effective photon field is still invariant under the local $U(1)$ -symmetry transformation

$$f'_i \rightarrow f'_i - ie' Q_{f_i} \delta\theta'^A f'_i, \quad A'_\mu \rightarrow A'_\mu + \partial_\mu \delta\theta'^A \quad (5.36)$$

so that the electric charge is conserved. Equation (5.35) describes only neutral current phenomena, that is all interactions are diagonal in flavor space. Charged current interactions like muon decay could be introduced by means of effective contact interactions of four fermions, but these interaction terms are not required for the matching of the electromagnetic coupling and the weak mixing angle. The Lagrangian is parametrized in terms of bare masses $m'_{0,f}$ and $M'_{0,Z}$, that may be expressed in terms of the pole masses or $\overline{\text{MS}}$ -masses, later on. It is also possible, to introduce a renormalized mass and mass counterterm, which is

briefly discussed in Section 5.3.3. Since the effective model does not exhibit a W-boson, the transition from the Standard Model to the effective one may be understood as the process of integrating out the W-bosons degree of freedom.

For now, the effective fields have no physical meaning as there is no link to the Standard Model's degrees of freedom. The relation between the fields of the EWSM and the effective theory is parametrized in terms of matching constants l'_X ; the defining equations are

$$\begin{aligned} \begin{pmatrix} A'_\mu \\ Z'_\mu \end{pmatrix} &= L \begin{pmatrix} A_\mu \\ Z_\mu \end{pmatrix}, \quad L = \begin{pmatrix} \sqrt{1+l_A} & l_{AZ} \\ l_{ZA} & \sqrt{1+l_Z} \end{pmatrix}, \\ f'^{L/R} &= f^{L/R} \sqrt{1+l'_{L/R}}. \end{aligned} \quad (5.37)$$

The off-diagonal elements in L are intentionally defined without a square root; the motivation for this was explained at the end of Section 4.1.1. Equation (5.37) allows expressing the effective Lagrangian in terms of the original fields and derive Green functions with respect to those fields.

5.3.2. Irreducible Vertex Functions

The derivation of the irreducible vertex functions is identical to the calculation in Section 4.1, due to the great similarity between the effective model and the neutral sector of the electroweak Standard Model. As a consequence, the previously obtained expressions can be adopted by replacing the Standard Model parameters with the effective ones and the counter terms δZ_X with the appropriate matching constants l_X of the effective theory. The self-energy and vertex functions also change since the fields missing in the effective model do not contribute. The matrix elements of the bosonic irreducible vertex function $\Gamma_I^{\mu\nu}$ in the effective model are given by

$$\Gamma_{I'T}^{\gamma\gamma} = iq^2(1+l_A) + i(q^2 - M'_{0,Z})^2 l_{ZA}^2 + i\Sigma_{I'T}^{\gamma\gamma}(q^2), \quad (5.38a)$$

$$\Gamma_{I'L}^{\gamma\gamma} = i\frac{q^2}{\xi'_A}(1+l_A) + i\left(\frac{q^2}{\xi'_Z} - M'_{0,Z})^2\right) l_{ZA}^2 + i\Sigma_{I'L}^{\gamma\gamma}(q^2), \quad (5.38b)$$

5. Matching Conditions

$$\Gamma_{iT}^{ZZ} = i \left(q^2 - M'_{0,Z}{}^2 \right) (1 + l_Z) + i q^2 l_{AZ}^2 + i \Sigma_{iT}^{ZZ}(q^2), \quad (5.38c)$$

$$\Gamma_{iL}^{ZZ} = i \left(\frac{q^2}{\xi'_Z} - M'_{0,Z}{}^2 \right) (1 + l_Z) + i \frac{q^2}{\xi'_A} l_{AZ}^2 + i \Sigma_{iL}^{ZZ}(q^2), \quad (5.38d)$$

$$\Gamma_{iT}^{\gamma Z} = i q^2 l_{AZ} \sqrt{1 + l_A} + i \left(q^2 - M'_{0,Z}{}^2 \right) l_{ZA} \sqrt{1 + l_Z} + i \Sigma_{iT}^{\gamma Z}(q^2), \quad (5.38e)$$

$$\Gamma_{iL}^{\gamma Z} = i \frac{q^2}{\xi'_A} l_{AZ} \sqrt{1 + l_A} + i \left(\frac{q^2}{\xi'_Z} - M'_{0,Z}{}^2 \right) l_{ZA} \sqrt{1 + l_Z} + i \Sigma_{iL}^{\gamma Z}(q^2), \quad (5.38f)$$

and $\Gamma_{\mu\nu}^{Z\gamma} = \Gamma_{\mu\nu}^{\gamma Z}$. Here, the prime is also introduced for the self-energy and amputated two-point functions to make its connection to the effective model explicit. Since $\Gamma_{\mu\nu}^{ab}$ and $\Sigma_{iT/L}^{ab}$ are not just constants, the prime is used as a subscript in order to avoid confusion with derivatives with respect to the momentum transfer which will be denoted by a superscript prime, later on. In analogy to Equation (4.25), the fermionic two point function reads

$$\begin{aligned} i\Gamma_f(q) = & -m'_{0,f} \left(\sqrt{1 + l_L^f} \sqrt{1 + l_R^f} - \Sigma_{if}^S(q^2) \right) \\ & + \not{q} \left(1 + l_V^f + \Sigma_{if}^V(q^2) \right) + \not{q}\gamma_5 \left(l_A^f + \Sigma_{if}^A(q^2) \right), \end{aligned} \quad (5.39)$$

where

$$l_V = \frac{l_L^f + l_R^f}{2} \quad \text{and} \quad l_A = \frac{l_R^f - l_L^f}{2} \quad (5.40)$$

are used to rewrite the left- and right-handed terms as vector and axial vector parts. It is convenient, to introduce the effective coupling constants

$$v_f^{**} = T_f^3 \left(1 + l_V^f - l_A^f \right) - 2s'^2 Q_f \left(1 + l_V^f \right), \quad (5.41a)$$

$$a_f^{**} = T_f^3 \left(1 + l_V^f + l_A^f \right) + 2s'^2 Q_f l_A^f \quad (5.41b)$$

to absorb some of the fermionic matching constants and where a double asterisk is used to avoid an ambiguity with respect to the definition in Equation (4.27). Finally, the irreducible fermion-photon and fermion-Z vertices in terms of

the effective vertex functions $\Lambda_{iX}^{ffa}(q^2)$ are defined like the vertex functions in Section 4.1.3 and read

$$\begin{aligned} \Gamma_{i1PI,\mu}^{ff\gamma}(p,p') &= -ie'Q_f\gamma_\mu\left(1+l_V^f+l_A^f\gamma_5\right)\sqrt{1+l_A}+i\frac{g_Z'}{2}\gamma_\mu\left(v_f^{**}-a_f^{**}\gamma_5\right)l_{ZA} \\ &\quad -ie'\left[\gamma_\mu\Lambda_{iV}^{ff\gamma}(q^2)+\gamma_\mu\gamma_5\Lambda_{iA}^{ff\gamma}(q^2)\right. \\ &\quad \left.+\frac{(p+p')_\mu}{2\tilde{m}_f}\Lambda_{iS}^{ff\gamma}(q^2)+\gamma_5\frac{(p-p')_\mu}{2\tilde{m}_f}\Lambda_{iP}^{ff\gamma}(q^2)\right], \end{aligned} \quad (5.42)$$

$$\begin{aligned} \Gamma_{i1PI,\mu}^{ffZ}(p,p') &= i\frac{g_Z'}{2}\gamma_\mu\left(v_f^{**}-\gamma_5a_f^{**}\right)\sqrt{1+l_Z}-ie'Q_f\gamma_\mu\left(1+l_V^f+l_A^f\gamma_5\right)l_{AZ} \\ &\quad +i\frac{g_Z'}{2}\left[\gamma_\mu\Lambda_{iV}^{ffZ}(q^2)+\gamma_\mu\gamma_5\Lambda_{iA}^{ffZ}(q^2)\right. \\ &\quad \left.+\frac{(p+p')_\mu}{2\tilde{m}_f}\Lambda_{iS}^{ffZ}(q^2)+\gamma_5\frac{(p-p')_\mu}{2\tilde{m}_f}\Lambda_{iP}^{ffZ}(q^2)\right]. \end{aligned} \quad (5.43)$$

The explicit one-loop expressions can be obtained from the formulae in Appendix C by omitting the terms that correspond to charged current interactions.

5.3.3. Matching Conditions of Two- and Three-Point Functions

Bosonic Two-Point Functions

Instead of equating two-point Green functions, it is easier to obtain the matching conditions by equating the irreducible vertex functions, which are the inverse of the Green functions. Then, the generic matching conditions read

$$\Gamma_{iP}^{ab}(0) = \Gamma_P^{ab}(0), \quad (5.44a)$$

$$\frac{d}{dq^2}\left[\Gamma_{iP}^{ab}(q^2)\right]_{q^2=0} = \frac{d}{dq^2}\left[\Gamma_P^{ab}(q^2)\right]_{q^2=0}, \quad (5.44b)$$

5. Matching Conditions

where $a, b = \gamma, Z$ and $P = T, L$ denote transverse and longitudinal parts. Due to the symmetry of Γ_l , Equation (5.44) includes twelve distinct equations. As the bosonic sector of the effective model is determined by seven parameters, five additional relations emerge. Since the system of Equations is overdetermined, explicit calculation will show, if the effective model is able to reproduce all effects of the EWSM. A violation of one of the excess equations proves that the effective model is not a valid ansatz for the description of the entire EWSM at low energy. The Implications are briefly discussed at the end of this section.

The bosonic irreducible two-point vertex functions of the EWSM and the effective theory are given in Equations (4.17) and (5.38), respectively. Inserting these expressions, the six equations that stem from the transverse parts become

$$M'_{0,Z}{}^2 l_{ZA}^2 = M_{0,Z}^2 \delta Z_{ZA}^2 - \overline{\Sigma}_T^{\gamma\gamma}(0), \quad (5.45a)$$

$$l_A + l_{ZA}^2 = \delta Z_A + \delta Z_{ZA}^2 + \overline{\Sigma}_T^{\gamma\prime}(0), \quad (5.45b)$$

$$M'_{0,Z}{}^2 (1 + l_Z) = M_{0,Z}^2 (1 + \delta Z_Z) - \overline{\Sigma}_T^{ZZ}(0), \quad (5.45c)$$

$$l_Z + l_{AZ}^2 = \delta Z_Z + \delta Z_{AZ}^2 + \overline{\Sigma}_T^{ZZ\prime}(0), \quad (5.45d)$$

$$M'_{0,Z}{}^2 l_{ZA} \sqrt{1 + l_Z} = M_{0,Z}^2 \delta Z_{ZA} \sqrt{1 + \delta Z_Z} - \overline{\Sigma}_T^{\gamma Z}(0), \quad (5.45e)$$

$$l_{AZ} \sqrt{1 + l_A} + l_{ZA} \sqrt{1 + l_Z} = \delta Z_{AZ} \sqrt{1 + \delta Z_A} + \delta Z_{ZA} \sqrt{1 + \delta Z_Z} + \overline{\Sigma}_T^{\gamma Z\prime}(0), \quad (5.45f)$$

where a superscript prime is used to abbreviate the derivatives and the notation

$$\overline{\Sigma}_{T/L}^{ab}(q^2) := \Sigma_{T/L}^{ab}(q^2) - \Sigma_{T/L}^{ab}(q^2) \quad (5.46)$$

is used for the difference between unrenormalized self-energy functions of the EWSM and the effective theory. So far, no assumptions about the renormalization of the EWSM theory were made. One could omit the renormalization constants on the right-hand sides of the above equations, but then the effective model needs to be renormalized additionally. It is easier, to derive the matching conditions using a renormalized version of the EWSM, in which case the effective theory “inherits” the renormalization prescription. The matching

conditions (5.45) need to be iteratively solved order by order, as the $(n+1)$ -loop self-energy functions depend on the n -loop matching constants. For completeness, the full analytic solution is given, nonetheless. Equations (5.45b), (5.45d), (5.45c) and (5.45e) are readily solved in terms of l_{AZ} ,

$$l_A = \overline{\Sigma}_T^{\gamma'}(0) + \delta Z_A + \delta Z_{ZA}^2 - l_{ZA}^2, \quad (5.47a)$$

$$l_Z = \overline{\Sigma}_T^{ZZ'}(0) + \delta Z_Z + \delta Z_{AZ}^2 - l_{AZ}^2, \quad (5.47b)$$

$$M_{0,Z}'^2 = \frac{M_{0,Z}^2(1 + \delta Z_Z) - \overline{\Sigma}_T^{ZZ}(0)}{1 + \overline{\Sigma}_T^{ZZ'}(0) + \delta Z_Z + \delta Z_{AZ}^2 - l_{AZ}^2}, \quad (5.47c)$$

$$l_{ZA} = z_1 \sqrt{1 + \overline{\Sigma}_T^{ZZ'}(0) + \delta Z_Z + \delta Z_{AZ}^2 - l_{AZ}^2}, \quad (5.47d)$$

$$z_1 = \frac{M_{0,Z}^2 \delta Z_{ZA} \sqrt{1 + \delta Z_Z} - \overline{\Sigma}_T^{\gamma Z}(0)}{M_{0,Z}^2(1 + \delta Z_Z) - \overline{\Sigma}_T^{ZZ}(0)}, \quad (5.47e)$$

which can be used in conjunction with (5.45f) to derive an equation for l_{AZ} . The quadratic equation has only one positive solution, which reads

$$l_{AZ} = -\frac{z_2 - z_1 \left(1 + \overline{\Sigma}_T^{ZZ'}(0) + \delta Z_Z + \delta Z_{AZ}^2\right)}{\sqrt{1 + z_3}},$$

$$z_2 = \overline{\Sigma}_T^{\gamma Z'}(0) + \delta Z_{AZ} \sqrt{1 + \delta Z_Z} + \delta Z_{ZA} \sqrt{1 + \delta Z_Z}, \quad (5.48)$$

$$z_3 = \overline{\Sigma}_T^{\gamma'}(0) + \delta Z_A + \delta Z_{ZA}^2$$

$$+ z_1^2 \left(1 + \overline{\Sigma}_T^{ZZ'}(0) + \delta Z_Z + \delta Z_{AZ}^2\right) - 2z_1 z_2.$$

The corresponding one-loop approximations

$$l_A = \delta Z_A + \overline{\Sigma}_T^{\gamma'}(0), \quad l_{ZA} = \delta Z_{ZA} - \frac{\overline{\Sigma}_T^{\gamma Z}(0)}{M_{0,Z}^2},$$

$$l_Z = \delta Z_Z + \overline{\Sigma}_T^{ZZ'}(0), \quad l_{AZ} = \delta Z_{AZ} + \overline{\Sigma}_T^{\gamma Z'}(0) + \frac{\overline{\Sigma}_T^{\gamma Z}(0)}{M_{0,Z}^2},$$

$$M_{0,Z}'^2 = M_{0,Z}^2 \left(1 - \overline{\Sigma}_T^{ZZ'}(0)\right) - \overline{\Sigma}_T^{ZZ}(0) \quad (5.49)$$

5. Matching Conditions

are much simpler and show immediately that the parameters of the effective theory and the Standard Model coincide at leading order and that the particle being integrated out contributes in the effective model indirectly by means of appropriate matching constants. The solution of the matching constant l_Z is given in terms of the derivative of the Z-boson's self-energy function instead of its value at zero momentum transfer. This is a consequence of the different masses $M'_{0,Z}$ and $M_{0,Z}$ that appear on the left-hand and right-hand side of Equation (5.45c), respectively. Equation (5.49) also makes clear that the particle being integrated out contributes in the effective model indirectly by means of appropriate matching constants and that the renormalization of the remaining fields in the effective model is “inherited” from the Standard Model: The terms that account for the renormalization, that is UV pieces as well as finite terms that occur due to the renormalization prescription, are adopted by the effective model. The renormalized mass $M'_Z = M_{0,Z} - \delta M'_Z$ is an exception to this observation, as M'_Z and $\delta M'_Z$ may be chosen freely and only the sum $M'_{0,Z}$ is fixed by the matching condition.

The matching conditions that are obtained when inserting the longitudinal parts of the two-point function into (5.44) read

$$M'^2_{0,Z} l^2_{ZA} = M^2_{0,Z} \delta Z^2_{ZA} - \overline{\Sigma}_L^{\gamma\gamma}(0), \quad (5.50a)$$

$$\frac{1+l_A}{\xi'_A} + \frac{l^2_{ZA}}{\xi'_Z} = \frac{1+\delta Z_A}{\xi_A} + \frac{\delta Z^2_{ZA}}{\xi_Z} + \overline{\Sigma}_L^{\gamma\gamma'}(0), \quad (5.50b)$$

$$M'^2_{0,Z} (1+l_Z) = M^2_{0,Z} (1+\delta Z_Z) - \overline{\Sigma}_L^{ZZ}(0), \quad (5.50c)$$

$$\frac{1+l_{Z'}}{\xi'_Z} + \frac{l^2_{AZ}}{\xi'_A} = \frac{1+\delta Z_Z}{\xi_Z} + \frac{\delta Z^2_{AZ}}{\xi_A} + \overline{\Sigma}_L^{ZZ'}(0), \quad (5.50d)$$

$$M'^2_{0,Z} l_{ZA} \sqrt{1+l_Z} = M^2_{0,Z} \delta Z_{ZA} \sqrt{1+\delta Z_Z} - \overline{\Sigma}_L^{\gamma Z}(0), \quad (5.50e)$$

$$\frac{l_{AZ}}{\xi'_A} \sqrt{1+l_A} + \frac{l_{ZA}}{\xi'_Z} \sqrt{1+l_Z} = \frac{\delta Z_{AZ}}{\xi_A} \sqrt{1+\delta Z_A} + \frac{\delta Z_{ZA}}{\xi_Z} \sqrt{1+\delta Z_Z} + \overline{\Sigma}_L^{\gamma Z'}(0). \quad (5.50f)$$

The renormalized longitudinal self-energy of the photon vanishes in the EWSM, but is kept, so that Equation (5.50a) is valid in the general case. Equa-

tions (5.50b) and (5.50d) can be solved for ξ'_A and ξ'_Z , but the solution is cumbersome when inserting the explicit expressions of the other matching constants. For brevity, only the two- and one-loop expansions are given,

$$\begin{aligned} \frac{1}{\xi'_A} &= \frac{1}{\xi_A} + \left(1 - \overline{\Sigma}_T^{\gamma\gamma'}(0) - \delta Z_A\right) \left(\overline{\Sigma}_L^{\gamma\gamma'}(0) - \frac{\overline{\Sigma}_T^{\gamma\gamma'}(0)}{\xi_A}\right) \\ &\quad + \left(\frac{1}{\xi_A} - \frac{1}{\xi_Z}\right) \frac{\overline{\Sigma}_T^{\gamma Z}(0)}{M_{0,Z}^2} \left(\frac{\overline{\Sigma}_T^{\gamma Z}(0)}{M_{0,Z}^2} - 2\delta Z_{ZA}\right) + \mathcal{O}(\alpha^3) \\ &= \frac{1}{\xi_A} + \overline{\Sigma}_L^{\gamma\gamma'}(0) - \frac{\overline{\Sigma}_T^{\gamma\gamma'}(0)}{\xi_A} + \mathcal{O}(\alpha^2), \end{aligned} \quad (5.51a)$$

$$\begin{aligned} \frac{1}{\xi'_Z} &= \frac{1}{\xi_Z} + \left(1 - \overline{\Sigma}_T^{ZZ'}(0) - \delta Z_Z\right) \left(\overline{\Sigma}_L^{ZZ'}(0) - \frac{\overline{\Sigma}_T^{ZZ'}(0)}{\xi_Z}\right) \\ &\quad + \left(\frac{1}{\xi_Z} - \frac{1}{\xi_A}\right) \left(\frac{\overline{\Sigma}_T^{\gamma Z}(0)}{M_{0,Z}^2} + \overline{\Sigma}_T^{\gamma Z'}(0)\right) \left(\frac{\overline{\Sigma}_T^{\gamma Z}(0)}{M_{0,Z}^2} + \overline{\Sigma}_T^{\gamma Z'}(0) + 2\delta Z_{AZ}\right) \\ &\quad + \mathcal{O}(\alpha^3) \\ &= \frac{1}{\xi_Z} + \overline{\Sigma}_L^{ZZ'}(0) - \frac{\overline{\Sigma}_T^{ZZ'}(0)}{\xi_Z} + \mathcal{O}(\alpha^2). \end{aligned} \quad (5.51b)$$

The solutions of the matching constants were derived using only a subset of the conditions (5.45) and (5.50). The system of equations is overdetermined due to the remaining matching conditions. This is a consequence of the effective model being less potent than the EWSM; it lacks a few parameters to be guaranteed to restore all the low energy properties of the EWSM. Inserting the solutions derived above into the remaining equations yields the five additional relations

$$\begin{aligned} \overline{\Sigma}_T^{\gamma\gamma'}(0) &= M_{0,Z}^2 \delta Z_{ZA}^2 - \frac{\left(M_{0,Z}^2 \delta Z_{ZA} \sqrt{1 + \delta Z_Z} - \overline{\Sigma}_T^{\gamma Z}(0)\right)^2}{M_{0,Z}^2 (1 + \delta Z_Z) - \overline{\Sigma}_T^{ZZ'}(0)} \\ &= \overline{\Sigma}_T^{\gamma Z}(0) \left(2\delta Z_{ZA} - \frac{\overline{\Sigma}_T^{\gamma Z}(0)}{M_{0,Z}^2}\right) + \mathcal{O}(\alpha^3), \end{aligned} \quad (5.52a)$$

5. Matching Conditions

$$\overline{\Sigma}_T^{ab}(0) = \overline{\Sigma}_L^{ab}(0), \quad a, b = \gamma, Z, \quad (5.52b)$$

$$\overline{\Sigma}_L^{\gamma Z'}(0) = \frac{\overline{\Sigma}_T^{\gamma Z'}(0)}{\xi_A} + \left(\frac{1}{\xi_A} - \frac{1}{\xi_Z} \right) \frac{\overline{\Sigma}_T^{\gamma Z}(0)}{M_{0,Z}^2} + \mathcal{O}(\alpha^2), \quad (5.52c)$$

where the second equation is a short notation for three independent conditions. Equation (5.52b) stems from (5.50f) and is given at one-loop order, only. Equation (5.52a) states that the photon remains massless when taking into account loop corrections and has to be fulfilled for the model to be physically meaningful. At one-loop order, it is trivially fulfilled due to $\Sigma_T^{\gamma\gamma}(0) = 0 + \mathcal{O}(\alpha^2)$. Equations (5.52) test the effective model to some extent, as a failure of one of the equations will hint at which of the EWSM properties can not be reproduced.

The one-loop expressions of the $\overline{\text{MS}}$ -renormalized effective parameters read

$$l_A = \delta Z_A - \frac{\alpha}{4\pi} \left(\frac{2}{3} + 3\Delta_W \right), \quad (5.53a)$$

$$l_{ZA} = \delta Z_{ZA} - \frac{\alpha}{4\pi} 2 \frac{c}{s} \Delta_W, \quad (5.53b)$$

$$l_{AZ} = \delta Z_{AZ} + \frac{\alpha}{4\pi} \left\{ \left(5 \frac{c}{s} + \frac{1}{6cs} \right) \Delta_W + \frac{1 + 2c^2}{3cs} \right\}, \quad (5.53c)$$

$$\frac{1}{\xi'_A} = 1 + \frac{\alpha}{4\pi} \left(\frac{2}{3} + 3\Delta_W \right), \quad (5.53d)$$

$$\frac{1}{\xi'_Z} = 1 + \overline{\Sigma}_L^{ZZ'}(0) - \overline{\Sigma}_T^{ZZ'}(0), \quad (5.53e)$$

$$\begin{aligned} l_Z = \delta Z_Z + \frac{\alpha}{4\pi} & \left[\left(3 - \frac{19}{6s^2} + \frac{1}{6c^2} \right) \Delta_W - \frac{4c^2}{3s^2} + \frac{(c^2 - s^2)^2}{6c^2 s^2} \right] \\ & + \frac{\alpha}{4\pi} \frac{1}{12c^2 s^2} \left[\frac{11}{3} + \frac{1 + \xi}{2(1 - \xi)} \log \xi - \log \frac{M_H M_{0,Z}}{M_W^2} \right. \\ & \quad + \frac{5 - \xi}{(1 - \xi)^3} (1 - \xi^2 + 2\xi \log \xi) \\ & \quad \left. + \frac{\xi^3 + 9\xi^2 - 9\xi - 1 - 6\xi(1 + \xi) \log \xi}{6(\xi - 1)^3} \right], \end{aligned} \quad (5.53f)$$

$$\begin{aligned}
 \frac{M'_{0,Z}}{M_{0,Z}^2} = & 1 - \frac{\alpha}{4\pi} \sum_f \frac{v_f^2 + a_f^2}{3c^2 s^2} \Delta_{\bar{f}} + \frac{\alpha}{4\pi} \frac{1}{2c^2 s^2} \sum_f \frac{m_f^2}{M_Z^2} \Delta_{\bar{f}} + \delta Z_Z - l_Z \\
 & - \frac{\alpha}{4\pi} \left[\left(4 + \frac{1}{c^2} - \frac{1}{s^2} \right) \Delta_W - \frac{\xi}{6c^2 s^2} \log \frac{M_H^2}{M_W^2} - \frac{1}{6c^2 s^2} \log \frac{M_Z^2}{M_W^2} \right. \\
 & \quad + \frac{1}{24c^2 s^2} \left(1 + \xi + 2\xi \frac{\log \xi}{1 - \xi} \right) \\
 & \quad \left. + \frac{5 - \xi}{6c^2 s^2} \left(1 + \frac{1 + \xi}{2(1 - \xi)} \log \xi - \log \frac{M_H M_Z}{M_W^2} \right) \right]
 \end{aligned} \tag{5.53g}$$

and are obtained by inserting the unrenormalized one-loop self-energies given in Appendix C and $\xi_A = \xi_Z = 1$ into Equations (5.49) and (5.51). For readability, the $\mathcal{O}(\alpha^2)$ -notation was omitted and l_Z used as an abbreviation in the expression of $M'_{0,Z}$. The one-loop approximations confirm Equations (5.52a) and (5.52b), but Equation (5.52c) is violated, as the left- and right-hand sides do not agree,

$$\frac{\alpha}{4\pi} \frac{1}{3cs} \neq \frac{\alpha}{4\pi} \frac{1}{3cs} \left[\left(\frac{1}{2} + 9c^2 \right) \Delta_W + 1 + 2c^2 \right]. \tag{5.54}$$

The disagreement in Equation (5.54) is not surprising, as the effective model defined in Section 5.3.1 is not a gauge theory due to the introduction of the Z-boson's mass without the Higgs mechanism. As a consequence, one has to expect that the effective model fails to reproduce the longitudinal degrees of freedom of the Standard Model that are associated with the masses of the heavy gauge bosons. A different choice of the parameters determined by the matching conditions (5.50a) to (5.50f) allows fulfilling Equation (5.52c), but one of the longitudinal matching conditions can not be met.

When contracting the longitudinal part of the Z-boson's propagator with fermion spinors, it vanishes if the two fermions interacting with the Z-boson have the same mass. Since the neutral interaction is not flavor changing, this is always the case when the fermions are on-shell. Consequently, the longitudinal part of the Z-boson's one-loop propagator can only give a contribution when coupled to off-shell fermions. This happens in box diagrams and at higher loop

order where the coupled fermions are virtual particles themselves. Both cases have been excluded in the calculation of the parity violating interaction, which means that the restriction of the effective model is of no concern for the present discussion.

Fermionic Two-Point Functions

Similar to the bosonic case, the fermionic constants of the effective model need to be fixed such that the propagators of the effective theory and the EWSM coincide in some limit of the fermion's momentum. Since the UV-divergent terms are independent of the momentum, any choice of the limit renders the effective model finite. The pole mass⁴ is a convenient choice for the matching point, even though the renormalized propagator does not have to be singular at the pole mass.

In that case, Standard Model and effective theory need to share the same value and derivative of the propagators at $q^2 = \tilde{m}_f^2$, where \tilde{m}_f is the pole mass of the fermion. In the most general case, the residue of the Dirac propagator is a matrix with an axial component (see also Appendix D), which yields independent matching conditions for the vector and axial vector parts. The matching of the propagators is achieved by imposing

$$i\Gamma_{if}(q^2)u(q)\Big|_{q^2=\tilde{m}_f^2} = i\Gamma_f(q^2)u(q)\Big|_{q^2=\tilde{m}_f^2}, \quad (5.55a)$$

$$\lim_{q^2 \rightarrow \tilde{m}_f^2} \frac{\not{q} + \tilde{m}_f}{q^2 - \tilde{m}_f^2} i\Gamma_{if}(q^2)u(q) = \lim_{q^2 \rightarrow \tilde{m}_f^2} \frac{\not{q} + \tilde{m}_f}{q^2 - \tilde{m}_f^2} i\Gamma_f(q^2)u(q). \quad (5.55b)$$

Due to the projection onto the Dirac spinor $u(q)$, the scalar and vector parts of the vertex function are combined. Accordingly, Equation (5.55) is a set of four distinct equations, two for the “scalar + vector” part and two for the axial part. However, the two axial matching conditions are identical, leaving three

⁴A pole mass does not exist for light quarks. This is of no concern in the following calculation, since the parity violating interaction does not depend on the quark masses. In a naive calculation, the quark masses enter the parity violating interaction via the running weak mixing angle, which can be worked around using phenomenologically constraints. [17, 18]

independent equations for the three effective parameters. It is convenient, to rewrite Equations (4.25) and (5.39) by grouping terms proportional to $\not{q} - \tilde{m}_f$, which yields

$$\begin{aligned} i\Gamma_{I_f}(q) &= \tilde{m}_f \left(1 + l_V^f + \Sigma_{I_V}^f(q^2) \right) - m'_{0,f} \left(\sqrt{1 + l_L^f} \sqrt{1 + l_R^f} - \Sigma_{I_S}^f(q^2) \right) \\ &\quad + \tilde{m}_f \gamma_5 \left(l_A^f + \Sigma_{I_A}^f(q^2) \right) \\ &\quad + \left(\not{q} - \tilde{m}_f \right) \left(1 + l_V^f + \Sigma_{I_V}^f(q^2) \right) + \left(\not{q} - \tilde{m}_f \right) \gamma_5 \left(l_A^f + \Sigma_{I_A}^f(q^2) \right) \end{aligned} \quad (5.56)$$

in case of the effective vertex. The $(\not{q} - \tilde{m}_f)$ -terms vanish when projected onto the Dirac spinor, so that the first matching condition (5.55a) can be readily solved. The solutions are

$$l_A^f = \delta Z_A^f + \bar{\Sigma}_A^f(\tilde{m}_f^2) \quad (5.57)$$

and

$$\frac{m'_{0,f}}{\tilde{m}_f} = \frac{\frac{m_{0,f}}{\tilde{m}_f} \left(\sqrt{1 + \delta Z_L^f} \sqrt{1 + \delta Z_R^f} - \Sigma_S^f(\tilde{m}_f^2) \right) + l_V^f - \delta Z_V^f - \bar{\Sigma}_V^f(\tilde{m}_f^2)}{\sqrt{1 + l_L^f} \sqrt{1 + l_R^f} - \Sigma_{I_S}^f(\tilde{m}_f^2)}, \quad (5.58)$$

where the notation (5.46) is used to abbreviate the difference between self-energy functions of the Standard Model and effective theory. The field renormalization constants and matching constants drop out of the matching condition of the fermion mass at the one-loop level,

$$\frac{m'_{0,f}}{\tilde{m}_f} = \frac{m_{0,f}}{\tilde{m}_f} - \bar{\Sigma}_V^f(\tilde{m}_f^2) - \bar{\Sigma}_S^f(\tilde{m}_f^2) + \mathcal{O}(\alpha^2). \quad (5.59)$$

The second condition (5.55b) requires a Taylor expansion of the terms on the first line of Equation (5.56) around $q^2 = \tilde{m}_f^2$ and one finds

$$l_V^f = \delta Z_V^f + \bar{\Sigma}_V^f(\tilde{m}_f^2) + 2\tilde{m}_f^2 \left[\bar{\Sigma}_V^{f'}(\tilde{m}_f^2) + \left(\frac{m_{0,f}}{\tilde{m}_f} \Sigma_f^{S'}(\tilde{m}_f^2) - \frac{m'_{0,f}}{\tilde{m}_f} \Sigma_{I_f}^{S'}(\tilde{m}_f^2) \right) \right]. \quad (5.60)$$

5. Matching Conditions

The one-loop order expression of Equation (5.60) is easily obtained by replacing the mass ratios $\frac{m_{0,f}}{\tilde{m}_f}$ and $\frac{m'_{0,f}}{\tilde{m}_f}$ with unity and the self-energy functions with the appropriate one-loop approximations.

Again, the mass may be chosen arbitrarily by introducing an appropriate mass counter term, as only the sum of the mass parameter and the mass counter term is physically meaningful. The field renormalization constants on the other hand are entirely determined by the renormalization scheme of the Standard Model.

Matching of the Electromagnetic Coupling Constant

When computing S-matrix elements within the effective model, it is insufficient to just cut off the external propagators; one also has to take into account the matching constants of the fields associated with the external particles as prescribed by the LSZ reduction formula. As in case of the renormalization constants, these matching constants are the residues of the corresponding on-shell particle propagators. Due to the matching conditions of the previous sections, these matching constants are identical to the associated renormalization constants of the Standard Model. Accordingly, they are not required for the matching of three- or four-point functions, even if the residues are not normalized to unity as in the OS scheme. For this reason, external lepton leg corrections are omitted in this section so that the matching condition for the electromagnetic coupling constant is determined by the vertex function, only. It reads

$$\bar{u}(p)\Gamma_{\mu}^{ff\gamma}(p,p)u(p) = \bar{u}(p)\Gamma_{\mu}^{\prime ff\gamma}(p,p)u(p), \quad p^2 = \tilde{m}_f^2, \quad (5.61)$$

for on-shell fermions at vanishing momentum transfer. The right-hand side of Equation (5.61) is defined by (4.35) and is the sum of Equations (4.37) and (4.38). Like before, the subscript prime denotes the quantity of the effective theory and can be obtained from Equations (5.42) and (5.43). Equation (5.61) contains two independent conditions, due to the presence of vector- and axial vector-terms in the three-point function. A discussion of the axial vector part of Equation (5.61) is postponed to the end of this section, as the vector part of

Equation (5.61) defines the electromagnetic coupling according to its definition as the coupling strength of parity conserving scattering at low energy. It reads

$$\begin{aligned}
 & e' \left[Q_f \left(1 + l_V^f \right) \sqrt{1 + l_A} - \frac{g_Z'}{2e'} v_f^{**} l_{ZA} + \Lambda_{V'}^{ff\gamma}(0) + \Lambda_{S'}^{ff\gamma}(0) \right] \\
 & + \frac{g_Z'}{2} \left[v_f^{**} \sqrt{1 + l_Z} - \frac{2e'}{g_Z'} Q_f (1 + l_V^f) l_{AZ} + \Lambda_{V'}^{ffZ}(0) + \Lambda_{S'}^{ffZ}(0) \right] \frac{\Gamma_{T'}^{Z\gamma}(0)}{\Gamma_{T'}^{ZZ}(0)} \\
 = & e \left[Q_f \left(1 + \delta Z_V^f \right) \sqrt{1 + \delta Z_A} - \frac{g_Z}{2e} v_f \delta Z_{ZA} + \Lambda_V^{ff\gamma}(0) + \Lambda_S^{ff\gamma}(0) \right] \\
 & + \frac{g_Z}{2} \left[v_f \sqrt{1 + \delta Z_Z} - \frac{2e}{g_Z} Q_f (1 + \delta Z_V^f) \delta Z_{AZ} + \Lambda_V^{ffZ}(0) + \Lambda_S^{ffZ}(0) \right] \frac{\Gamma_T^{Z\gamma}(0)}{\Gamma_T^{ZZ}(0)}
 \end{aligned} \tag{5.62}$$

and solving for e' requires the matching constants l_X of the effective theory that were derived in the previous sections.

The matching conditions derived before include the renormalization constants of the EWSM, but for matching with the $\overline{\text{MS}}$ -renormalized EWSM it is easier to drop the renormalization constants δZ_X and replace all corresponding one-loop functions with the appropriate $\overline{\text{MS}}$ -renormalized ones. Using $g_Z' = \frac{e'}{c's'} + \mathcal{O}(\alpha)$ and the equality of effective and EWSM coupling constants at tree-level⁵, the one-loop order expansion of Equation (5.62) reads

$$\begin{aligned}
 & e' \left[Q_f \left(1 + l_V^f + \frac{l_A}{2} \right) - \frac{v_f}{2cs} l_{ZA} + \Lambda_{V'}^{ff\gamma}(0) + \Lambda_{S'}^{ff\gamma}(0) \right] + \frac{e}{2cs} v_f \frac{\Gamma_{T'}^{Z\gamma}(0)}{\Gamma_{T'}^{ZZ}(0)} \\
 & = \hat{e} \left(Q_f + \hat{\Lambda}_V^{ff\gamma}(0) + \hat{\Lambda}_S^{ff\gamma}(0) \right) + \frac{e}{2cs} v_f \frac{\hat{\Gamma}_T^{Z\gamma}(0)}{\hat{\Gamma}_T^{ZZ}(0)} + \mathcal{O}(\alpha^2),
 \end{aligned} \tag{5.63}$$

where a hat is used to denote $\overline{\text{MS}}$ -renormalized quantities. Constants without primes or hats were used when the difference between effective and EWSM parameters is beyond one-loop precision. The terms involving the ratio of amputated two-point functions are identical due to the matching conditions

⁵While reasonable, these equalities were not yet proven and will be justified in Section 5.3.5.

5. Matching Conditions

of Section 5.3.3. Replacing the matching constants l_V^f , l_A and l_{ZA} with the solutions derived previously yields

$$\begin{aligned} \frac{e'}{\hat{e}} = & 1 - \frac{v_f}{2csQ_f} \frac{\hat{\Sigma}_T^{\gamma Z}(0) - \Sigma_{iT}^{\gamma Z}(0)}{\hat{M}_Z^2} + \frac{\hat{\Lambda}_V^{ff\gamma}(0) - \Lambda_{iV}^{ff\gamma}(0)}{Q_f} + \frac{\hat{\Lambda}_S^{ff\gamma}(0) - \Lambda_{iS}^{ff\gamma}(0)}{Q_f} \\ & - \frac{1}{2} \left(\hat{\Sigma}_T^{\gamma\gamma'}(0) - \Sigma_{iT}^{\gamma\gamma'}(0) \right) - \left(\hat{\Sigma}_V^f(\tilde{m}_f^2) - \Sigma_{iV}^f(\tilde{m}_f^2) \right) \\ & - 2\tilde{m}_f^2 \left(\hat{\Sigma}_V^{f'}(\tilde{m}_f^2) + \hat{\Sigma}_S^{f'}(\tilde{m}_f^2) - \Sigma_{iV}^{f'}(\tilde{m}_f^2) - \Sigma_{iS}^{f'}(\tilde{m}_f^2) \right) + \mathcal{O}(\alpha^2). \end{aligned} \quad (5.64)$$

Using the one-loop expressions of the self-energy and vertex functions given in Appendix C and neglecting terms of order $\mathcal{O}\left(\frac{m_f^2}{\hat{M}_W^2}\right)$ without using the big O notation explicitly, the $\overline{\text{MS}}$ -renormalized self-energy and vertex functions required for the matching of the electromagnetic coupling constant when integrating out the W-boson read

$$\hat{\Sigma}_T^{\gamma\gamma'}(0) - \Sigma_{iT}^{\gamma\gamma'}(0) = -\frac{\alpha}{4\pi} \left\{ \frac{4}{3} \sum_f N_f Q_f^2 \Delta + \left[\frac{2}{3} + 3 \log \frac{\mu^2}{\hat{M}_W^2} \right] \right\}, \quad (5.65a)$$

$$\hat{\Sigma}_V^f(\tilde{m}_f^2) - \Sigma_{iV}^f(\tilde{m}_f^2) = -\frac{\alpha}{4\pi} \left\{ Q_f^2 \Delta + \frac{v_f^2 + a_f^2}{4c^2 s^2} \Delta + \frac{1}{4s^2} \left[\frac{1}{2} - \log \frac{\mu^2}{\hat{M}_W^2} \right] \right\}, \quad (5.65b)$$

$$\hat{\Sigma}_V^{f'}(\tilde{m}_f^2) - \Sigma_{iV}^{f'}(\tilde{m}_f^2) = \hat{\Sigma}_S^{f'}(\tilde{m}_f^2) - \Sigma_{iS}^{f'}(\tilde{m}_f^2) = 0, \quad (5.65c)$$

$$\hat{\Sigma}_T^{\gamma Z}(0) - \Sigma_{iT}^{\gamma Z}(0) = \frac{\alpha}{4\pi} 2 \frac{c}{s} \hat{M}_Z^2 \log \frac{\mu^2}{\hat{M}_W^2}, \quad (5.65d)$$

$$\hat{\Lambda}_V^{ff\gamma}(0) - \Lambda_{iV}^{ff\gamma}(0) = \frac{\alpha}{4\pi} \left\{ -Q_f^3 \Delta - Q_f \frac{v_f^2 + a_f^2}{4c^2 s^2} \Delta \right. \quad (5.65e)$$

$$\left. + \frac{Q_{f'}}{4s^2} \left[\log \frac{\mu^2}{\hat{M}_W^2} - \frac{1}{2} \right] + \frac{3T_f^3}{2s^2} \left[\log \frac{\mu^2}{\hat{M}_W^2} - \frac{1}{6} \right] \right\}, \quad (5.65f)$$

$$\hat{\Lambda}_S^{ff\gamma}(0) - \Lambda_{fS}^{ff\gamma}(0) = 0, \quad (5.65g)$$

which eventually results in the final expression

$$\frac{e'}{\hat{e}} = 1 + \frac{\alpha}{4\pi} \left(\frac{1}{3} + \frac{7}{2} \log \frac{M_W^2}{\mu^2} \right) + \frac{\alpha}{4\pi} \frac{2}{3} \sum_f N_f Q_f^2 \Delta. \quad (5.66)$$

The final result being independent of the fermion f , confirms the charge universality of the pseudo gauge boson model that was proved by verifying the U(1)-gauge invariance in Section 5.3.1. The appearance of UV-singular and UV-finite terms is a consequence of matching an unrenormalized model with the renormalized SM. Equation (5.66) is similar to the renormalization of the electric charge in the SM, showing the close relation between matching and renormalization. The first term which stems from the contribution of the W-boson is free of a UV divergence, as the effective model was matched with the $\overline{\text{MS}}$ -renormalized SM, which is UV finite. Accordingly, the Δ -term stems from one-loop functions of the effective model. If one started with an $\overline{\text{MS}}$ -renormalized effective model, these Δ -terms would disappear. Equation (5.66) is general, but commonly only the UV-finite term is referred to as matching term.

The matching of the electric charge in the effective model allows obtaining the corresponding matching condition for the electromagnetic coupling constant α' . Dropping the UV-singular term to compare with published results and using the relation $\alpha' = \frac{e'^2}{4\pi}$, one finds

$$\frac{1}{\hat{\alpha}} = \frac{1}{\alpha'} + \frac{1}{6\pi} + \frac{7}{4\pi} \log \frac{\mu^2}{M_W^2}, \quad (5.67)$$

which confirms the matching condition (5.6) that was obtained from the results published in Reference [36].

Taking into account the axial part, Equation (5.61) contains two independent equations that seem to form an overdetermined set of equations for the electromagnetic coupling constant. The additional equation also appears in the charge renormalization of the Standard Model but is fulfilled automatically.

5. Matching Conditions

Using $\overline{\text{MS}}$ -renormalization of the Standard Model as before, the axial part of Equation (5.61) at one-loop order reads

$$Q_f l_A^f + \frac{a_f}{2cs} l_{ZA} + \Lambda_{fA}^{ff\gamma}(0) + \frac{a_f}{2cs} \left(\frac{\Sigma_{fT}^{\gamma Z}(0)}{M_Z^2} - l_{ZA} \right) = \Lambda_A^{ff\gamma}(0) + \frac{a_f}{2cs} \frac{\hat{\Sigma}_T^{\gamma Z}(0)}{M_Z^2}, \quad (5.68)$$

where the matching constants l_{ZA} on the left-hand side cancel immediately. The right-hand side is identical to $Q_f \hat{\Sigma}_A^f(\tilde{m}_f^2)$ in the Standard Model, which can be readily verified by inserting the appropriate loop functions. Replacing the remaining matching constant l_A^f on the left-hand side by (5.57) yields

$$Q_f \left(\hat{\Sigma}_A^f(\tilde{m}_f^2) - \Sigma_A^f(\tilde{m}_f^2) \right) + \Lambda_{fA}^{ff\gamma}(0) = Q_f \hat{\Sigma}_A^f(\tilde{m}_f^2). \quad (5.69)$$

The function $\Sigma_{fT}^{\gamma Z}(0)$ was omitted, as it vanishes in the effective model. Equation (5.69) can be verified with the aid of Appendix C, showing that the axial vector part of Equation (5.61) is fulfilled automatically and does not add an additional constraint to the matching of the electromagnetic coupling constant.

In general, the vertex correction also contains a scalar term that was split into a contribution to the vector piece and a term proportional to $\sigma_{\mu\nu} q^\nu$ by means of the Gordon identity. A matching of the $\sigma_{\mu\nu} q^\nu$ -term is not necessary, as the contribution induced by a virtual photon is identical in the Standard Model and the effective theory at one-loop order. The only difference arises from virtual heavy particles that are not present in the effective theory, but these contributions are of the order $\mathcal{O}\left(\frac{m_f}{M}\right)$, where M is the mass of the heavy particle, and can be neglected, accordingly.

5.3.4. Parity Violating Fermion–Fermion Interaction

In the previous sections, two- and three-point functions were matched with the ones obtained for the EWSM in Chapter 4, which also led to an expression of the effective charge in terms of the EWSM charge. In this section, the parity violating interaction is determined within the effective model; it is then used

to construct a matching condition for the weak mixing angle and the neutral current coupling strength g'_Z in Section 5.3.5. Due to the similarity to the EWSM, the calculation of the parity violating interaction in the effective pseudo gauge boson model follows closely the steps outlined in Section 4.2. However, there are two noteworthy differences. First, counter terms (called matching constants in the context of the effective model) need to be taken into account explicitly to incorporate the terms stemming from the matching. Second, the effective parameter $\Delta r'$ that accounts for the relation between Fermi constant and elementary coupling as well as Z-boson mass and which is defined by

$$1 - \Delta r' := \frac{\sqrt{2}}{G_F} \frac{g'_Z{}^2}{8\hat{M}_Z^2} \quad (5.70)$$

is kept as an unknown in the beginning. This is, because the relation between Fermi constant and coupling constants in the effective model is not yet known. It is defined in terms of the $\overline{\text{MS}}$ -mass of the Z-boson to obtain simpler expressions that do not involve the relation between the unrenormalized effective mass and the $\overline{\text{MS}}$ -mass. To simplify the calculation further, the tree-level equality

$$g'_Z = \hat{g}_Z + \mathcal{O}(\alpha) = \frac{\hat{e}}{\hat{c}\hat{s}} + \mathcal{O}(\alpha) \quad (5.71)$$

is used where applicable to omit terms of two-loop order. The relation (5.71) is reasonable but will be justified later, when calculating g'_Z explicitly. Matching the effective interaction with the SM expression allows giving a relation between G_F and g'_Z and determining $\Delta r'$, eventually. Consequently, $\Delta r'$ is explicitly contained in the low energy coupling piece $C_{1f_1}^{f_2(A)'}$, while its contribution to the remaining pieces $C_{1f_1}^{f_2(B)'}$ to $C_{1f_1}^{f_2(D)'}$ is of two-loop order and will be neglected. Otherwise, the corresponding definitions are identical to (4.61a) to (4.61d) except for the replacement of SM quantities by effective ones.

Following the prescription of the matching of the electromagnetic coupling in Section 5.3.3, $\overline{\text{MS}}$ -renormalization is used for the Standard Model. The matching constants of the effective theory are kept to account for the matching conditions of the two- and three-point functions. Due to the matching of the

5. Matching Conditions

two-point functions, the transverse parts of effective and SM propagators are identical. This simplifies the calculation of the parity violating interaction, since the one-loop corrections in $C_{1f_1}^{f_2(D)'}$ stem from the γZ -propagator only. Accordingly, this piece is identical to the one derived in the Standard Model, $C_{1f_1}^{f_2(D)'} = C_{1f_1}^{f_2(D)}$. The remaining pieces can not be taken over as easily and require a separate calculation. Using the matching constants derived before and omitting terms of two-loop order, the three other pieces in the effective model can be written as

$$C_{1f_1}^{f_2(A)'} = -2v_{f_1} a_{f_2} \left(1 - \Delta r'\right) \cdot \left(1 - \delta\mathcal{L}_V^{f_1'} - \delta\mathcal{L}_V^{f_2'} + \frac{a_{f_1}}{v_{f_1}} \delta\mathcal{L}_A^{f_1'} + \frac{v_{f_2}}{a_{f_2}} \delta\mathcal{L}_A^{f_2'}\right), \quad (5.72a)$$

$$C_{1f_1}^{f_2(B)'} = -2 \left(-2s^2 Q_{f_1}\right) a_{f_2} \frac{\alpha}{4\pi} \cdot \left\{ \frac{Q_{f_2} v_{f_2}}{9s^2} \left(1 - 6 \log \frac{m_f^2}{M_Z^2}\right) + 2 \frac{c^2}{s^2} \frac{M_Z^2}{q^2} \log \frac{\mu^2}{M_W^2} \right\}, \quad (5.72b)$$

$$C_{1f_1}^{f_2(C)'} = -2v_{f_1} a_{f_2} \left\{ \frac{\hat{\Sigma}_T^{ZZ}(0)}{M_Z^2} - \frac{\Lambda_{f_1 A}^{f_2 f_2 Z}(0)}{T_{f_2}^3} + l_V^{f_1} + l_V^{f_2} + l_Z - \frac{v_{f_2}}{T_{f_2}^3} l_A^{f_2} \right\} + 2a_{f_2} \left\{ T_{f_1}^3 l_A^{f_1} + 2cs Q_{f_1} l_{AZ} - \Lambda_{f_1 V}^{f_1 f_1 Z}(0) \right\}. \quad (5.72c)$$

Similarly to the calculation outlined in Section 4.2, the loop corrections to $C_{1f_1}^{f_2'}$ may be separated into three different groups: corrections to the overall amplitude denoted by ρ' , corrections to the weak mixing angle denoted by κ' and process dependent terms that can not be absorbed into a constant independent of the external fermions. Omitting terms of two-loop order, the effective low energy coupling can be written as

$$C_{1f_1}^{f_2'} = -a_{f_2} \rho' \left(2T_{f_1}^3 - 4Q_{f_1} \kappa' s'^2\right) + 4v_{f_1} a_{f_2} \frac{\alpha}{4\pi} \left(Q_{f_1}^2 + Q_{f_2}^2\right) + Q_{f_1} Q_{f_2} v_{f_2} a_{f_2} \frac{\alpha}{9\pi} \left(1 - 6 \log \frac{m_{f_2}^2}{M_Z^2}\right) + \square' + \mathcal{O}(\alpha^2), \quad (5.73)$$

$$\rho' = (1 - \Delta r') \left[1 + \frac{\hat{\Sigma}_T^{ZZ}(0)}{M_Z^2} + l_Z \right] + \mathcal{O}(\alpha^2), \quad (5.74)$$

$$\begin{aligned} \kappa' = 1 - \frac{c}{s} \left[\frac{\hat{\Sigma}_T^{\gamma Z}(0)}{q^2} + \frac{\hat{\Sigma}_T^{\gamma Z}(0)}{M_Z^2} + \hat{\Sigma}_T^{\gamma Z'}(0) \right] \\ + \frac{\alpha}{2\pi} \frac{c^2}{s^2} \frac{M_Z^2}{q^2} \log \frac{\mu^2}{M_W^2} + \frac{c}{s} l_{AZ} + \mathcal{O}(\alpha^2), \end{aligned} \quad (5.75)$$

where \square' denotes the box graph contribution in the effective model. Since the effective model does not contain the W-boson, the process dependent term containing $6 \log \frac{m_{f_2'}^2}{M_W^2}$ in Equation (4.76) is not reproduced; as a consequence, no universal matching condition can be found for the parameters ρ' and κ' ⁶. The missing term may be restored by introducing an effective contact interaction term in the Lagrangian. However, for the discussion of Møller scattering or charged lepton–quark scattering as required by the P2 and Q_{weak} experiments, this is not necessary, because the term vanishes due to the vanishing charge of the weak isospin partner, $Q_{f_2'} = 0$. When inserting l_{AZ} in terms of self-energy functions as given in Equation (5.49), most of the terms in κ' cancel yielding the expression

$$\kappa' = 1 + \frac{\alpha}{6\pi s^2} \sum_f N_f Q_f v_f \left(\Delta + \log \frac{\mu^2}{m_f^2} \right), \quad (5.76)$$

which does not contain terms that stem from the W-boson interactions. This is expected, as the effective model was constructed without W^\pm -fields.

5.3.5. Matching of the Weak Mixing Angle

With the parity violating interaction calculated in the previous section, it is now possible to derive the matching conditions for the weak mixing angle s' and the

⁶The same issue is raised by the missing W-box in the effective model. It needs to be added separately but will be ignored in the following.

5. Matching Conditions

effective coupling g'_Z . These are obtained by equating the low energy coupling constants $C_{1f_1}^{f_2}$ and $C_{1f_1}^{f'_2}$ of the Standard Model and the effective theory. Since the equality needs to be independent of f_1 and f_2 , one obtains two distinct equations,

$$\rho' = \rho, \quad (5.77a)$$

$$\kappa' s'^2 = \kappa s^2. \quad (5.77b)$$

Inserting the results (4.74), (4.75), (5.74) and (5.76) yields

$$s'^2 = s^2 - \frac{\alpha}{2\pi} \left\{ \left(\frac{7}{2}c^2 + \frac{1}{12} \right) \log \frac{\mu^2}{M_W^2} + \frac{7}{9} - \frac{s^2}{2} + \frac{1}{3} \sum_f N_f Q_f v_f \Delta \right\}, \quad (5.78)$$

$$\begin{aligned} \Delta r' = & \frac{\hat{\Sigma}_T^{WW}(0)}{M_W^2} - \frac{\alpha c^2}{\pi s^2} \log \frac{\mu^2}{M_W^2} + l_Z \\ & + \frac{\alpha}{4\pi s^2} \left[\log \frac{\mu^2}{M_Z^2} + \left(\frac{7}{2s^2} - l \right) \log c^2 + 6 \right]. \end{aligned} \quad (5.79)$$

The effective weak mixing angle (5.78) is similar to the κ -parameter in the Standard Model given in Equation (4.75) with two notable differences. First, the one-loop corrections in Equation (4.75) contain an inverse factor of s^2 , as κ is multiplied with s^2 when entering the effective coupling $C_{1f_1}^{f_2}$. Second, the fermionic terms contain only the UV-divergent terms but not the logarithmic ones. They account for the renormalization of the fermion loops that are present in the effective model, which is also the reason for the opposite sign in front of the sum. Dropping the fermionic renormalization terms yields what is conventionally called the matching condition,

$$s'^2 = s^2 - \frac{\alpha}{2\pi} \left\{ \left(\frac{7}{2}c^2 + \frac{1}{12} \right) \log \frac{\mu^2}{M_W^2} + \frac{7}{9} - \frac{s^2}{2} \right\}. \quad (5.80)$$

These terms are identical to the corresponding ones in the Standard Model that make up the W-boson contributions to the weak mixing angle at zero

momentum transfer. In the effective model they have to be part of the definition of the weak mixing angle as they are not dynamically reproduced by the theory by construction. The matching of the weak mixing angle at W -threshold in the pseudo gauge boson model differs from the matching condition published in Reference [17] that was given in Equation (5.5b). The numerical difference between Equations (5.80) and (5.5b) for $\mu = M_W$ is

$$\Delta s'^2 = \frac{\alpha}{6\pi} \left(\frac{4}{3} - \frac{s^2}{2} \right) + \mathcal{O}(\alpha^2) \approx 4.7 \cdot 10^{-4}, \quad (5.81)$$

which is obtained by inserting values of the Particle Data Group [38], $\alpha = 7.297 \cdot 10^{-3}$ and $s^2 = 0.231$. It is small compared to the numerical value of the weak mixing angle ($\Delta s'^2 \cdot s^{-2} \approx 0.2\%$), but almost seven times larger than the total theoretical error of $7 \cdot 10^{-5}$ published in Reference [18] for the weak mixing angle at low energies.

Combining Equations (2.33), (4.58), (5.70) and (5.79) allows relating the neutral current coupling constants g_Z and g'_Z ,

$$g_Z^2 = g_Z^2 \left\{ 1 + \frac{\alpha}{\pi} \frac{c^2}{s^2} \log \frac{\mu^2}{M_W^2} - l_Z + \mathcal{O}(\alpha^2) \right\}, \quad (5.82)$$

where the matching constant $l_Z = \hat{\Sigma}_T^{ZZ'}(0) - \Sigma_{T'}^{ZZ'}(0)$ can be obtained explicitly using Equation (C.6). The coupling constant (5.82) also contains UV singular terms hidden in the matching constant l_Z that are responsible for rendering the effective theory finite. Dropping the UV singular pieces, yields the matching condition for matching an effective theory that was $\overline{\text{MS}}$ -renormalized before the matching.

The results given above are obtained using the pseudo gauge boson model defined in Section 5.3.1. Section 5.4 discusses the matching of an effective model based on the same idea, but in the context of an effective contact interaction model similar to Fermi's four-fermion interaction theory. Therefore, the summary of the findings of this section and a comparison with the results of Reference [35] are postponed to Section 6.1, where the results of Section 5.4 will be included.

5.4. Contact Interaction Model

5.4.1. Lagrangian

The effective pseudo gauge boson model described in Section 5.3 was obtained by omitting the W^\pm - and Higgs-fields but keeping the Z-boson as a massive, pseudo gauge boson. The model is uncommon, but resembles the Standard Model in the neutral and electromagnetic sectors. In this section, a contact interaction model is discussed that is obtained by dropping the Z-boson, too, and introducing a four-fermion contact interaction term. As before, additional terms could be introduced to account for effective charged current interactions, but these are not required for the present discussion. The pseudo gauge boson model of Section 5.3 failed to restore all process dependent terms of the Standard Model. As explained before, this is not an issue, as the missing terms do not contribute to charged lepton scattering. The effective contact interaction model does not contain a Z-boson so that none of the process dependent terms will be dynamically reproduced. This is the reason, why the coupling in Fermi's four-fermion interaction theory carries fermion indices and why the matching conditions that will be derived later can not be expressed in terms of universal constants, only.

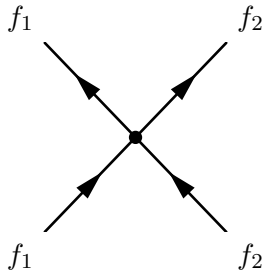
The definition of a weak mixing angle without Z-boson is not obvious. Here, it is introduced as part of an effective vector coupling in the neutral current that is proportional to the charge of the fermion, just like in the Standard Model. The Lagrangian can be written as

$$\begin{aligned} \mathcal{L}' = \sum_f \left[\bar{f}' (i\cancel{\partial} - m'_{0,f}) f' - e' Q_f \bar{f}' A' f' \right] \\ - \frac{1}{4} F'_{\mu\nu} F'^{\mu\nu} - \frac{1}{2\xi'_A} (\partial_\mu A'^\mu)^2 - K J'_{\text{NC}\mu} J'^\mu_{\text{NC}}, \end{aligned} \quad (5.83)$$

where the effective neutral current J'^μ_{NC} is defined by

$$J'^\mu_{\text{NC}} = \sum_f \left(T_f^3 \bar{f}'^L \gamma^\mu f'^L - s'^2 Q_f \bar{f}' \gamma^\mu f' \right). \quad (5.84)$$

Just like in the Standard Model, the part of the coupling proportional to the weak isospin⁷ applies to the left-handed fermions, solely. Again, primes are used to denote effective fields and constants and K is used to quantify the strength of the contact interaction. It has mass dimension -2 and the corresponding term in the Lagrangian is a dimension-6 operator. An additional coupling of the neutral current to the photon could be introduced at this point but determining its strength by matching yields a vanishing coupling constant, as the corresponding interaction vanishes in the Standard Model at one-loop order. The Feynman rule of the new interaction vertex is given by



$$\hat{=} -\frac{iK}{4}\gamma_\mu (v_{f_1}^{**} - a_{f_1}^{**}\gamma_5) \otimes \gamma^\mu (v_{f_2}^{**} - a_{f_2}^{**}\gamma_5), \quad (5.85)$$

and can be used to calculate the new Feynman diagrams induced by the contact interaction. The effective vector and axial vector coupling constants read

$$v_f^{**} = T_f^3 (1 + l_V^f - l_A^f) - 2s'^2 Q_f (1 + l_V^f), \quad (5.86a)$$

$$a_f^{**} = T_f^3 (1 + l_V^f - l_A^f) + 2s'^2 Q_f l_A^f, \quad (5.86b)$$

with

$$l_V^f = \frac{l_R^f + l_L^f}{2}, \quad l_A^f = \frac{l_R^f - l_L^f}{2} \quad (5.87)$$

in terms of l_L and l_R that are the matching constants of the effective theory defined as before. The special product symbol “ \otimes ” is used in the Feynman rule (5.85) to emphasize that the gamma matrices must not be contracted

⁷The model does not exhibit a SU(2)-symmetry and the weak isospin is introduced as an auxiliary parameter, only.

directly, but need to be wrapped between Dirac spinors associated with the fermion lines of the fermions f_1 and f_2 .

The remainder of this section is organized similar to the previous one. In Section 5.4.2 the two- and three-point functions of the model are determined. Section 5.4.3 is dedicated to the matching of two- and three-point functions and the electromagnetic coupling constant. The parity violating interaction within the contact interaction model is derived in Section 5.4.4 and the weak mixing angle and effective parameter K are obtained in Section 5.4.5.

5.4.2. Irreducible Vertex Functions

The derivation of the bosonic two-point function is simpler than the derivation in the Standard Model, as the propagator is not a two by two matrix. Apart from that, the steps that need to be carried out are the same. Consequently, the irreducible two-point vertex function in the effective model can be obtained from the first equation of the Standard Model result (4.17) by omitting the mixing terms,

$$\Gamma_{\mu\nu}^{\gamma\gamma} = \left(-g_{\mu\nu} + \frac{q_\mu q_\nu}{q^2} \right) \left[iq^2(1 + l_A) + i\Sigma_{T'}^{\gamma\gamma}(q^2) \right] - \frac{q_\mu q_\nu}{q^2} \left[i\frac{q^2}{\xi_A'}(1 + l_A) + i\Sigma_{L'}^{\gamma\gamma}(q^2) \right]. \quad (5.88)$$

The fermion propagator in terms of the fermionic self-energy functions Σ_{iX}^f does not change and is identical to Equation (5.39) when replacing the self-energy functions and counter terms with the ones of the contact interaction model. The derivation of the self-energy functions requires the evaluation of a new loop diagram that is induced by the contact interaction and is depicted in Figure 5.2. Omitting terms of two loop order by dropping all matching constants, the self-energy that corresponds to the loop diagram reads

$$\frac{i\Sigma_{f_1}^K}{\mu^{D-4}} = \sum_{f_2} \int \frac{d^D k}{(2\pi)^D} \text{Tr} \left\{ \frac{iK}{4} \gamma_\mu (v_{f_1} - a_{f_1} \gamma_5) i \frac{\not{k} - m_{f_2}}{k^2 - m_{f_2}^2} \gamma^\mu (v_{f_2} - a_{f_2} \gamma_5) \right\}, \quad (5.89)$$

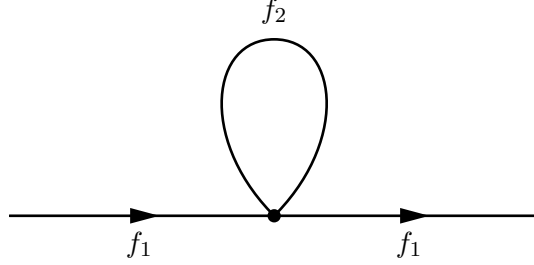


Figure 5.2.: Tadpole diagram in the effective theory that arises from the self interaction of a fermion line with a Z-boson in the Standard Model. The loop may contain any fermion that is part of the effective theory.

where the vector and axial vector coupling constants v_f^{**} and a_f^{**} were replaced with the Standard Model ones, as the difference is of two loop order. The solution of the loop integration is

$$-i\Sigma_{f_1}^K = i\frac{K}{4\pi^2} \sum_{f_2} (a_{f_1} a_{f_2} - v_{f_1} v_{f_2}) m_{f_2}^3 \left(\Delta + \log \frac{\mu^2}{m_{f_2}^2} + 1 \right) + \mathcal{O}(\alpha^2) \quad (5.90)$$

in four space-time dimensions, which gives a contribution to the scalar part of the fermionic self-energy function, only. The diagram in Figure 5.2 is a tadpole diagram in which the loop does not depend on the momentum of fermion f_1 . This is the reason why the corresponding self-energy function only depends on the mass of fermion f_2 . As a consequence, the loop merely induces a shift of the fermion mass m_{f_1} , which can be absorbed in a suitable matching constant. Since the goal of the matching is to reproduce the mass of the parent theory, one could get away with ignoring these tadpole diagrams altogether. For the sake of completeness, they are kept nonetheless, which means one has to distinguish m_f and m'_f for the masses in the SM and in the effective theory, respectively.

Due to the reduced field content compared to the Standard Model, the only vertex diagram that contributes in the effective contact interaction model is

5. Matching Conditions

the one with a virtual photon connecting incoming and outgoing fermion lines. Its structure is identical to the vertex (5.42) when omitting the matching constant l_{ZA} ,

$$\begin{aligned} \Gamma_{\text{IPI},\mu}^{ff\gamma}(p,p') &= -ie' Q_f \gamma_\mu \left(1 + l_V^f + l_A^f \gamma_5\right) \sqrt{1 + l_A} \\ &\quad - ie' \left[\gamma_\mu \Lambda_{V'}^{ff\gamma}(q^2) + \gamma_\mu \gamma_5 \Lambda_{A'}^{ff\gamma}(q^2) \right. \\ &\quad \left. + \frac{(p+p')_\mu}{2\tilde{m}_f} \Lambda_{S'}^{ff\gamma}(q^2) + \gamma_5 \frac{(p-p')_\mu}{2\tilde{m}_f} \Lambda_{P'}^{ff\gamma}(q^2) \right]. \end{aligned} \quad (5.91)$$

As before, the appropriate matching constants and loop functions of the contact interaction model have to be inserted.

5.4.3. Matching Conditions of Two and Three Point Functions

Bosonic Two-Point Functions

The effective model exhibits only one gauge boson propagator, so that there are only four matching conditions for the bosonic two-point functions as opposed to the twelve conditions in the EWSM; they read

$$\begin{aligned} \Gamma_{T/L}^{\gamma\gamma}(0) &= \Gamma_{T/L}^{\gamma\gamma}(0), \\ \Gamma_{T/L}^{\gamma\gamma'}(0) &= \Gamma_{T/L}^{\gamma\gamma'}(0). \end{aligned} \quad (5.92)$$

Inserting the transverse parts of the vertex functions yields

$$0 = -M_{0,Z}^2 \delta Z_{ZA}^2 + \bar{\Sigma}_T^{\gamma\gamma}(0), \quad (5.93a)$$

$$l_A = \delta Z_A + \delta Z_{ZA}^2 + \bar{\Sigma}_T^{\gamma\gamma'}(0), \quad (5.93b)$$

with the short notation (5.46). At one-loop order, the mixing counter term δZ_{ZA} does not contribute, so that the first equation is trivially fulfilled because of $\Sigma_{T'}^{\gamma\gamma}(0) = \Sigma_T^{\gamma\gamma}(0) = 0$. Using the derivative of the unrenormalized photonic self-energy function, the second equation becomes

$$l_A = \delta Z_A - \frac{\alpha}{4\pi} \left[3\Delta_W + \frac{2}{3} \right] + \mathcal{O}(\alpha^2) \quad (5.94)$$

when neglecting terms of two-loop order. Inserting the longitudinal parts of the vertex functions into equation (5.92) yields

$$0 = -M_Z^2 l_{ZA}^2 + \overline{\Sigma}_L^{\gamma\gamma}(0), \quad (5.95a)$$

$$\frac{1 + l_A}{\xi'_A} = \frac{1 + \delta Z_A}{\xi_A} + \frac{\delta Z_{ZA}^2}{\xi_Z} + \overline{\Sigma}_L^{\gamma\gamma'}(0), \quad (5.95b)$$

where the first condition is trivially fulfilled at one-loop order, too, and the second one reads

$$\frac{1}{\xi'_A} = \frac{1}{\xi_A} \left(1 + \frac{\alpha}{4\pi} \left[3\Delta_W + \frac{2}{3} \right] \right) + \mathcal{O}(\alpha^2) \quad (5.96)$$

when inserting Equation (5.94).

Fermionic Two-Point Functions

As mentioned in Section 5.4.2, the structure of the fermionic two-point function is the same as in Section 5.3 and consequently, the matching conditions are identical to Equations (5.57) to (5.60). Using the result of Section 5.4.2, the unrenormalized parts of the fermionic self-energy read

$$\Sigma_{IV}^f(\tilde{m}_f^2) = \frac{\alpha}{4\pi} Q_f^2 (\Delta_f + 2) + \mathcal{O}(\alpha^2), \quad (5.97a)$$

$$\Sigma_{IA}^f(\tilde{m}_f^2) = \mathcal{O}(\alpha^2), \quad (5.97b)$$

$$\begin{aligned} \Sigma_{IS}^f(\tilde{m}_f^2) = & -\frac{\alpha}{4\pi} Q_f^2 \left(6 + 4 \log \frac{\mu^2}{\tilde{m}_f^2} \right) \\ & - \frac{K}{4\pi^2} \sum_{f_2} (a_f a_{f_2} - v_f v_{f_2}) m_{f_2}^2 (\Delta_{f_2} + 1) + \mathcal{O}(\alpha^2). \end{aligned} \quad (5.97c)$$

The vanishing axial vector piece at one-loop order implies that the matching constant l_A is identical to the renormalized axial vector part of the self-energy function in the parent theory when neglecting higher order terms,

$$l_A^f = \delta Z_A^f + \Sigma_A^f(\tilde{m}_f^2) + \mathcal{O}(\alpha^2). \quad (5.98)$$

5. Matching Conditions

The differences of the derivatives of the fermionic self-energies vanish when neglecting the fermion mass compared to the heavy gauge boson mass so that inserting the self-energy functions into Equations (5.59) and (5.60) yields

$$\frac{m'_{0,f}}{\tilde{m}_f} = \frac{m_{0,f}}{\tilde{m}_f} - \frac{\alpha}{4\pi} \left\{ \frac{v_f^2 + a_f^2}{4c^2s^2} \left(\Delta_Z - \frac{1}{2} \right) + \frac{v_f^2 - a_f^2}{c^2s^2} \left(\Delta_Z + \frac{1}{2} \right) + \frac{1}{4s^2} \left[\Delta_W - \frac{1}{2} \right] \right\} \quad (5.99)$$

$$+ \frac{K}{4\pi^2} \sum_{f_2} (a_f a_{f_2} - v_f v_{f_2}) m_{f_2}^2 (\Delta_{f_2} + 1) + \mathcal{O}(\alpha^2),$$

$$l_V^f = \delta Z_V^f + \frac{\alpha}{4\pi} \left\{ \frac{v_f^2 + a_f^2}{4c^2s^2} \left(\Delta_Z - \frac{1}{2} \right) + \frac{1}{4s^2} \left[\Delta_W - \frac{1}{2} \right] \right\} + \mathcal{O}(\alpha^2). \quad (5.100)$$

Three-Point Functions

The effective three-point Green function $G_{/\mu}^{ff\gamma}(p, p')$ is similar to the Standard Model one, but due to the lack of γZ -mixing, it consists only of a term like the first one in Equation (4.34). Consequently, the amputated vertex function is similar to (4.35) when omitting the second term, implying $\Gamma_{/\mu}^{ff\gamma} \equiv \Gamma_{/1PI\mu}^{ff\gamma}$. The one particle irreducible vertex function was given in Equation (5.91), but the derivation of the vertex functions parametrising the loops requires the calculation of a new Feynman diagram shown in Figure 5.3. Using the generic notation V_1 , A_1 , V_2 and A_2 for the vector and axial vector couplings at the left- and right-hand side of the loop, the transverse part of the self-energy corresponding to the generic fermion loop reads

$$\Sigma_T^{\text{Of}}(q^2) = \frac{1}{16\pi^2} \frac{4}{3} \sum_f N_f \left\{ 6A_1A_2m_f^2\Delta_f + q^2 [A_1A_2 - (A_1A_2 + V_1V_2)\Delta_f] + \mathcal{O}(q^4) \right\} \quad (5.101)$$

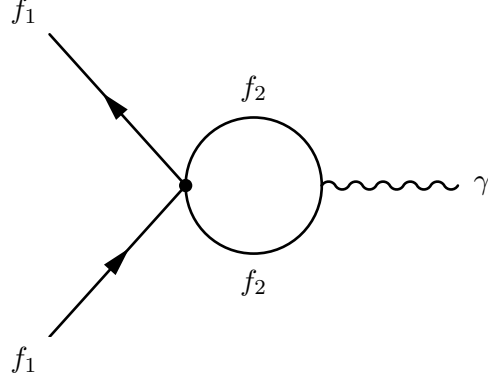


Figure 5.3.: New Feynman diagram contributing to the $ff\gamma$ -vertex in the effective contact interaction model.

when expanded at zero momentum transfer. The A_1A_2 -terms do not contribute to the Feynman diagram depicted in Figure 5.3 due to the coupling to the photon. Inserting $V_1 = \frac{iK}{4}$ and $V_2 = -ieQ_f$ allows writing the vertex function $\Lambda_V^{f_1f_1\gamma}$ as

$$\Lambda_V^{f_1f_1\gamma}(q^2) = \frac{\alpha}{4\pi} Q_{f_1}^3 \left(\Delta_{f_1} + 2 \log \frac{\lambda^2}{m_{f_1}^2} + 2 \right) - \frac{iK}{16\pi^2} \frac{Q_{f_1}}{3} \sum_f N_f (q^2 \Delta_f + \mathcal{O}(q^4)). \quad (5.102)$$

The photonic contribution is identical to the one in the Standard Model, but the terms induced by the heavy gauge bosons are missing. As before, the scalar and pseudo-scalar vertex functions do not contribute to the matching, allowing to write the one-loop expansion of the vector part of Equation (5.61) as

$$\begin{aligned} \frac{e'}{\hat{e}} = & 1 - \frac{\hat{\Sigma}_T^{\gamma\gamma'}(0) - \Sigma_{T'}^{\gamma\gamma'}(0)}{2} - \left(\hat{\Sigma}_V^f(\tilde{m}_f^2) - \hat{\Sigma}_{V'}^f(\tilde{m}_f^2) \right) \\ & + \frac{\hat{\Lambda}_V^{ff\gamma}(0) - \Lambda_{V'}^{ff\gamma}(0)}{Q_f} - \frac{v_f}{2csQ_f} \frac{\hat{\Sigma}_T^{\gamma Z}(0)}{M_Z^2} + \mathcal{O}(\alpha^2) \end{aligned} \quad (5.103)$$

5. Matching Conditions

when inserting the matching constants derived before and using $\overline{\text{MS}}$ -renormalization for the Standard Model. The Standard Model terms are identical to the right-hand side of Equation (5.63) and primes and hats are omitted when the difference is beyond the precision of one-loop order. Derivatives of the fermionic self-energies that are part of the matching constant l_V^f do not contribute, since the photonic terms are identical in the effective theory and Standard Model and all remaining terms are of order $\mathcal{O}\left(\frac{m_f^2}{M_W^2}\right)$. Inserting the individual differences

$$\hat{\Sigma}_T^{\gamma\gamma'}(0) - \Sigma_{T'}^{\gamma\gamma'}(0) = -\frac{\alpha}{4\pi} \left\{ \frac{4}{3} \sum_f N_f Q_f^2 \Delta + \left[3 \log \frac{\mu^2}{M_W^2} + \frac{2}{3} \right] \right\}, \quad (5.104a)$$

$$\begin{aligned} \hat{\Sigma}_V^f(\tilde{m}_f^2) - \hat{\Sigma}_{V'}^f(\tilde{m}_f^2) = & +\frac{\alpha}{4\pi} \left\{ -Q_f^2 \Delta + \frac{v_f^2 + a_f^2}{4c^2 s^2} \left(-\frac{1}{2} + \log \frac{\mu^2}{M_Z^2} \right) \right. \\ & \left. + \frac{1}{4s^2} \left[-\frac{1}{2} + \log \frac{\mu^2}{M_W^2} \right] \right\}, \end{aligned} \quad (5.104b)$$

$$\begin{aligned} \hat{\Lambda}_V^{ff\gamma}(0) - \Lambda_{V'}^{ff\gamma}(0) = & +\frac{\alpha}{4\pi} \left\{ -Q_f^3 \Delta + Q_f \frac{v_f^2 + a_f^2}{4c^2 s^2} \left(\log \frac{\mu^2}{M_Z^2} - \frac{1}{2} \right) \right. \\ & \left. + \frac{Q_{f'}}{4s^2} \left[\log \frac{\mu^2}{M_W^2} - \frac{1}{2} \right] + \frac{3T_f^3}{2s^2} \left[\log \frac{\mu^2}{M_W^2} - \frac{1}{6} \right] \right\} \end{aligned} \quad (5.104c)$$

and Equation (C.3) into (5.103) yields an expression for the effective electromagnetic coupling constant in terms of the $\overline{\text{MS}}$ -renormalized coupling,

$$\frac{e'}{\hat{e}} = 1 + \frac{\alpha}{4\pi} \left(\frac{1}{3} + \frac{7}{2} \log \frac{\mu^2}{M_W^2} \right) + \frac{\alpha}{6\pi} \sum_f N_f Q_f^2 \Delta. \quad (5.105)$$

Once again, the UV-singular term is a consequence of matching an unrenormalized theory with a renormalized one and accounts for the renormalization of the electric charge in the effective model. Omitting this term by assuming

$\overline{\text{MS}}$ -renormalization of the effective model, the matching condition for the fine structure constant reads

$$\frac{1}{\hat{\alpha}} = \frac{1}{\hat{\alpha}'} + \frac{1}{6\pi} + \frac{7}{4\pi} \log \frac{\mu^2}{M_W^2}. \quad (5.106)$$

Equation (5.106) is identical to the matching condition (5.67) derived in the context of a pseudo gauge Z-boson.

The axial vector part of the matching condition (5.61) yields an additional equation. The right-hand side is identical to the right-hand side of Equation (5.69), while the left-hand side is similar to the left-hand side of (5.69) but does not contain the mixing terms. At one-loop order, the axial matching condition reads

$$Q_f l_A^f + \Lambda_{fA}^{ff\gamma}(0) = Q_f \hat{\Sigma}_A(\tilde{m}_f^2). \quad (5.107)$$

Because of $l_A^f = \hat{\Sigma}_A^f(\tilde{m}_f^2)$ and since the axial vertex function $\Lambda_{fA}^{ff\gamma}$ vanishes in the contact interaction model, Equation (5.107) is fulfilled trivially.

5.4.4. Parity Violating Fermion–Fermion Interaction

Due to the lack of the Z-boson, the parity violating interaction in the contact interaction model is solely determined by Feynman diagrams including an effective contact vertex. At leading order, only the tree-level diagram contributes, which is identical to the diagram in the Feynman rule given in Equation (5.85). Including the LSZ factors, the terms of one of the fermion lines at one-loop order reads

$$\begin{aligned} & \bar{u}(p') \left(1 - \frac{1}{2} \delta \mathcal{Z}_V^f + \frac{1}{2} \delta \mathcal{Z}_A^f \gamma_5 \right) \gamma_\mu \left(v_f^{**} - a_f^{**} \gamma_5 \right) \left(1 - \frac{1}{2} \delta \mathcal{Z}_V^f - \frac{1}{2} \delta \mathcal{Z}_A^f \gamma_5 \right) u(p) \\ &= \bar{u}(p') \gamma_\mu \left[v_f^{**} - v_f \delta \mathcal{Z}_V^f + a_f \delta \mathcal{Z}_A^f - \gamma_5 \left(a_f^{**} - a_f \delta \mathcal{Z}_V^f + v_f \delta \mathcal{Z}_A^f \right) \right] u(p) \\ &= \bar{u}(p') \gamma_\mu \left(v_f - a_f \gamma_5 \right)_{s \rightarrow s'} \left[1 - \Sigma_V(\tilde{m}^2) - 2\tilde{m}^2 \left(\Sigma'_V(\tilde{m}^2) + \Sigma'_S(\tilde{m}^2) \right) \right] u(p). \end{aligned} \quad (5.108)$$

The last line is obtained by inserting the explicit expression (5.86) of the vector and axial vector counter terms and the LSZ factors in terms of the

5. Matching Conditions

self-energy functions as given in Equation (D.23)⁸. In addition, the axial vector piece $\Sigma_{iA}^f(\tilde{m}_f^2)$ was omitted since it vanishes in the effective contact interaction model. Here, the subscript “ $s \rightarrow s'$ ” is used to highlight that the vector and axial vector coupling constants v_f and a_f are still expressed in terms of the effective weak mixing angle, as only matching constants were written out explicitly. The vector part of the fermionic self-energy was given in Equation (5.97). Since the tadpole Diagram 5.2 does not contribute momentum dependent terms, the derivatives Σ_{iV}^f and Σ_{iS}^f are identical to the Standard Model expressions when omitting terms of order $\mathcal{O}\left(\frac{m_f}{M_W}\right)$. Using Equations (C.14) and (C.16) allows writing

$$\bar{u}(p')\gamma_\mu(v_f - a_f\gamma_5)_{s \rightarrow s'}u(p) \cdot \left[1 - \frac{\alpha}{4\pi}Q_f^2\left(\Delta_f + 2\log\frac{\lambda^2}{\tilde{m}_f^2} + 4\right)\right] \quad (5.109)$$

for the contribution of the fermion lines including the LSZ factors. Using Equation (5.109), the “vector-axial vector”-part of the entire tree-level matrix element becomes

$$\begin{aligned} & \frac{iK}{4}(v_{f_1}a_{f_2})_{s \rightarrow s'}\bar{u}(p'_1)\gamma_\mu u(p_1)\bar{u}(p'_2)\gamma^\mu\gamma_5 u(p_2) \\ & \cdot \left[1 - \frac{\alpha}{4\pi}\sum_{f=f_1, f_2}Q_f^2\left(\Delta_f + 2\log\frac{\lambda^2}{\tilde{m}_f^2} + 4\right)\right]. \end{aligned} \quad (5.110)$$

Using Equation (4.56) to define the effective coupling constant $C_{1f_1}^{f_2'}$ in the effective model, the tree-level diagram including LSZ factors yields the contribution

$$C_{1f_1}^{f_2(A)'} = -\frac{\sqrt{2}K}{G_F} \frac{1}{4}(v_{f_1}a_{f_2})_{s \rightarrow s'} \left[1 - \frac{\alpha}{4\pi}\sum_{f=f_1, f_2}Q_f^2\left(\Delta_f + 2\log\frac{\lambda^2}{\tilde{m}_f^2} + 4\right)\right]. \quad (5.111)$$

⁸The counter terms used in Equation (D.23) refer to the model itself and not the parent theory. Within the context of this section, one needs to apply the substitution $\delta Z_V \rightarrow l_V^f$ and $\delta Z_A \rightarrow l_A^f$.

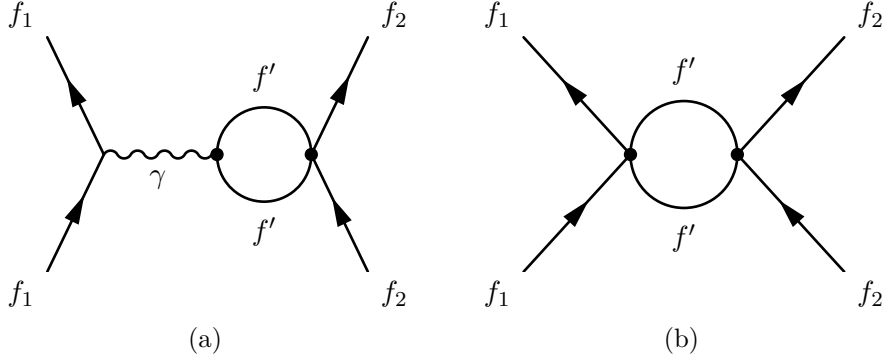


Figure 5.4.: Fermion loop diagrams contributing to the parity violating interaction in the effective interaction model.

The superscript “(A)” is used to separate the contributions of different diagrams and follows the definitions in Equations (4.61a) to (4.61d). The complete coupling $C_{1f_1}^{f_2'}$ is the sum of the individual pieces as written down in Equation (4.62).

For the following discussion, the loop diagrams are categorized as diagrams with or without a closed fermion loop. The two one-loop diagrams contributing to the parity violating interaction that include a closed fermion loop are shown in Figure 5.4. It was shown that Diagram 5.3 does not contribute to the matching of the electromagnetic coupling constant, as the self-energy vanishes at zero momentum transfer when the photon propagator is amputated. In case of Diagram 5.4a, the photon propagator is not amputated and accounts for a factor q^{-2} . This induces a contribution in terms of the derivative of the self-energy function $\Sigma_T^{\circ f}$ at zero momentum transfer. The series expansion of $\Sigma_T^{\circ f}$ was given in Equation (5.101) and readily allows obtaining the derivative. Following the notation of Section 4.2.3, this contribution counts towards the piece $C_{1f_1}^{f_2'(D)'}$, as the diagram is a remnant of the γZ -mixing in the Standard Model and can be obtained by replacing the Z -propagator with the effective contact interaction vertex. The longitudinal parts of the photon propagator and self-energy vanish because of current conservation and will be omitted

5. Matching Conditions

immediately; leaving out terms that do not belong to the “vector–axial vector”-part of the matrix element in addition, the Feynman diagram in Figure 5.4a translates to

$$\begin{aligned} & \bar{u}(p'_1) (-ieQ_{f_1} \gamma_\mu) u(p_1) \frac{-i}{q^2} (-i\Sigma_T^{\circ f}(q^2)) \bar{u}(p'_2) \left(\frac{iK}{4} a_{f_2} \gamma^\mu \gamma_5 \right) u(p_2) \\ &= -\frac{iK}{4} \frac{\alpha}{4\pi} Q_{f_1} a_{f_2} \frac{4}{3} \sum_{f'} N_{f'} (Q_{f'} v_{f'} \Delta_{f'}) \cdot \bar{u}(p'_1) \gamma_\mu u(p_1) \bar{u}(p'_2) \gamma_\mu \gamma_5 u(p_2), \end{aligned} \quad (5.112)$$

where the generic vector and axial vector couplings in Equation (5.101) were replaced by $A_1 = 0$, $V_1 = -ieQ_{f'}$ and $V_2 = v_{f'}$. Comparison with Equation (4.56) yields

$$C_{1f_1}^{f_2(D)'} = \frac{\sqrt{2}}{G_F} \frac{K}{4} \frac{\alpha}{4\pi} Q_{f_1} a_{f_2} \frac{4}{3} \sum_{f'} N_{f'} Q_{f'} v_{f'} \Delta_{f'} \quad (5.113)$$

for the corresponding contribution to the low energy coupling constant $C_{1f_1}^{f_2'}$. The second diagram with a fermion loop is depicted in Figure 5.4b and can be understood as the low energy version of the Z-boson’s self-energy diagram in the Standard Model and contributes to the piece $C_{1f_1}^{f_2(C)'}$, accordingly. The “vector–axial vector”-part of its matrix element reads

$$\begin{aligned} & \bar{u}(p'_1) \frac{-iK}{4} v_{f_1} \gamma_\mu u(p_1) (-i\Sigma_T^{\circ f}(q^2)) \bar{u}(p'_2) \frac{iK}{4} a_{f_2} \gamma^\mu \gamma_5 u(p_2) \\ &= -i \frac{G_F}{\sqrt{2}} \bar{u}(p'_1) \gamma_\mu u(p_1) \bar{u}(p'_2) \gamma^\mu \gamma_5 u(p_2) \cdot \frac{\sqrt{2}}{G_F} \frac{K^2}{8} \frac{v_{f_1} a_{f_2}}{16\pi^2} \sum_{f'} N_{f'} m_{f'}^2 \Delta_{f'}, \end{aligned} \quad (5.114)$$

where the generic axial vector coupling constants were replaced by $A_1 A_2 = a_{f'}^2 = \frac{1}{4}$. For convenience, the Fermi constant was introduced to separate the trivial factors in Equation (4.56) from the terms that are part of the low energy coupling constant $C_{1f_1}^{f_2'}$. The contribution to $C_{1f_1}^{f_2'}$ is given by the terms following the dot on the second line.

The one-loop diagrams contributing to the interaction that do not contain a closed fermion loop are obtained by adding virtual photon corrections to the

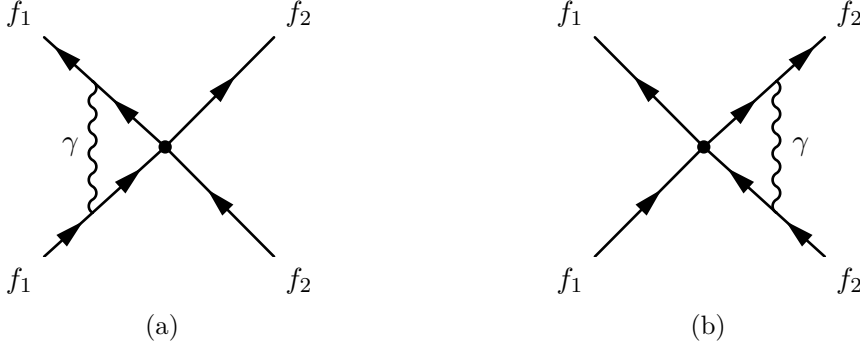


Figure 5.5.: Photonic corrections to the parity violating interaction in the contact interaction model. The diagrams with a photon connecting the fermions f_1 and f_2 are process dependent remnants of the γZ -box graphs in the Standard Model and will not be discussed.

tree-level diagram. The relevant Feynman diagrams are depicted in Figure 5.5. The similar diagrams with a photon between the left and right fermion lines are process dependent and can not be absorbed into the universal parameters ρ and κ , assuming a definition of the parameters similar to the corresponding one in the Standard Model and the model described in Section 5.3. These additional diagrams are linked to the γZ -box graphs in the Standard Model which have been excluded from the discussion. For this reason, only the photonic corrections shown in Figure 5.5 will be discussed in the following. It is sufficient to calculate only one of the associated matrix elements, as the diagrams are symmetric under the exchange of the external fermions. At one-loop order, the matrix element of Diagram 5.5a reads

$$\begin{aligned} \mu^{4-D} \int \frac{d^D k}{(2\pi)^D} \bar{u}(p'_1) (-ieQ_{f_1} \gamma_\mu) i \frac{\not{p}'_1 + \not{k} + m_{f_1}}{(p'_1 + k)^2 - m_{f_1}^2} \frac{-iK}{4} \gamma_\nu (v_{f_1} - a_{f_1} \gamma_5) \\ \cdot i \frac{\not{p}_1 + \not{k} + m_{f_1}}{(p_1 + k)^2 - m_{f_1}^2} (-ieQ_{f_1} \gamma^\mu) \frac{-i}{k^2} u(p_1) \bar{u}(p'_2) \gamma^\nu (v_{f_2} - a_{f_2} \gamma_5) u(p_2), \end{aligned} \quad (5.115)$$

5. Matching Conditions

where $p'_1 = p_1 - q$. Except for the coupling $\frac{iK}{4}$, the fermion line of fermion f_1 including the virtual photon is identical to the corresponding expression of the photonic vertex correction in a Standard Model calculation. This allows copying known results from the vertex function in Equation (C.17). Keeping “vector-axial vector”-terms only, one finds

$$i \frac{G_F}{\sqrt{2}} \bar{u}(p'_1) \gamma_\mu u(p_1) \bar{u}(p'_2) \gamma^\mu \gamma_5 u(p_2) \cdot \frac{\sqrt{2} K}{G_F} \frac{v_{f_1} a_{f_2}}{4} \frac{\alpha}{4\pi} Q_{f_1}^2 \left[\Delta_{f_1} + 2 \log \frac{\lambda^2}{m_{f_1}^2} + 2 \right] \quad (5.116)$$

for the contribution of Diagram 5.5a to the parity violating interaction. The expression for Diagram 5.5b can be obtained from Equation (5.116) by replacing the subscript f_1 inside the brackets with f_2 .

The piece $C_{1f_1}^{f_2(C) \prime}$ is made up of terms that correspond to the terms stemming from loop corrections of the neutral current interaction in the Standard Model. In the effective model, these are given by Equations (5.114) and (5.116) as well as the corresponding contribution of Diagram 5.5b. Combining all pieces, the low energy coupling constant becomes

$$C_{1f_1}^{f_2(C) \prime} = \frac{\sqrt{2} K}{G_F} \frac{v_{f_1} a_{f_2}}{4} \frac{\alpha}{4\pi} \left(-\frac{K}{8\pi\alpha} \sum_{f'} N_{f'} m_{f'}^2 \Delta_{f'} + V(f_1) + V(f_2) \right), \quad (5.117)$$

$$V(f) = Q_f^2 \left(\Delta_f + 2 \log \frac{\lambda^2}{m_f^2} + 2 \right).$$

The remaining part $C_{1f_1}^{f_2(B) \prime}$ vanishes in the effective contact interaction model, since the only axial vector coupling of a fermion to the photon at one-loop order is depicted in Figure 5.4a and counts towards $C_{1f_1}^{f_2(D) \prime}$. Hence, the effective low energy coupling in the contact interaction model is determined by Equations (5.111), (5.113) and (5.117). It reads

$$C_{1f_1}^{f_2 \prime} = -a_{f_2} \rho' \left(2T_{f_1}^3 - 4Q_{f_1} \kappa' s'^2 \right) + \frac{\sqrt{2} K}{G_F} \frac{v_{f_1} a_{f_2}}{8} \frac{\alpha}{\pi} \left(Q_{f_1}^2 + Q_{f_2}^2 \right) + \square' + \mathcal{O}(\alpha^2), \quad (5.118)$$

when using \square' to denote the γZ -box remnants and where the process independent parameters ρ' and κ' are defined as

$$\rho' = \frac{\sqrt{2}}{G_F} \frac{K}{8} \left(1 - \frac{K}{32\pi^2} \sum_f N_f m_f^2 \Delta_f \right), \quad (5.119a)$$

$$\kappa' = 1 + \frac{\alpha}{6\pi s^2} \sum_f N_f Q_f v_f \Delta_f. \quad (5.119b)$$

These parameters are meaningless without a proper definition of the coupling constants K and \hat{s}' which will be deduced by the matching in Section 5.4.5.

5.4.5. Matching of the Weak Mixing Angle

The process dependent terms in Equation (5.118) stem from a combination of photonic vertex corrections and LSZ factors. They are identical to the corresponding terms in the Standard Model that are given in Equation (4.76). In the Standard Model there are also terms resulting from vertex corrections including heavy gauge bosons, which are missing in the contact interaction model. As explained in section 5.4.1, this is the reason why the matching condition $C_{1f_1}^{f_2'} = C_{1f_1}^{f_2}$ can not be fulfilled with process independent constants K and s' ; the process dependent terms would need to be absorbed in either parameter. The missing correction induced by the W-boson in the Standard Model could be restored by introducing an effective flavor changing four-fermion interaction, but the missing Z-boson terms can only be reproduced with an additional effective contact interaction that depends on the fermion type. This is because the $ff\gamma$ -vertex with a virtual Z-boson degenerates to the Feynman Diagram 5.3 in the contact interaction model, which is the low energy analogue of the γZ -propagator at one-loop order. Consequently, it is impossible to separate the process dependent vertex correction and the universal propagator within the effective contact interaction model. In fact, a distinction of process dependent and universal contributions is only meaningful in the Standard Model, in which all degrees of freedom contribute to the low energy interaction.

5. Matching Conditions

When ignoring the issue regarding the process dependent terms, the correction κ' given in Equation (5.119) determines the matching condition of the weak mixing angle. Assuming the same set of fermions, it is identical to the matching condition obtained in the pseudo Z-boson model that was given in Equation (5.76). Accordingly, the matching condition of the weak mixing angle when matching the effective contact interaction model with the Standard Model is identical to the one derived in Section 5.3, with the final result given in Equation (5.78). The equality is a consequence of identical fermion contents and the lack of a W-boson in either effective model, as the weak mixing angle is corrected only by fermion and W-boson loops in the Standard Model at one-loop order.

The expression for the effective coupling strength K can be calculated by solving the matching condition that is obtained when equating the ρ -parameters and neglecting the process dependent terms. With the Standard Model expression given in Equation (4.74), one finds

$$K = 8 \frac{G_F}{\sqrt{2}} \rho + \frac{G_F \alpha}{\sqrt{2} \pi c^2 s^2} \sum_f N_f \frac{m_f^2}{M_Z^2} \Delta_f + \mathcal{O}(\alpha^3), \quad (5.120)$$

where one factor of the Fermi constant in the second term was replaced with its definition in terms of the electromagnetic coupling constant α . As before, the UV-divergent piece appears, since the contact interaction model was not renormalized beforehand. At leading order, the effective contact coupling is proportional to the Fermi constant showcasing the close relation to Fermi's four-fermion interaction theory. The coupling K accounts for the Z-boson propagator at zero momentum transfer and the square of the neutral coupling strength, $K \sim \frac{g_Z^2}{M_Z^2}$. While the matching of the weak mixing angle is identical in the contact interaction and pseudo Z-boson models, the matching of K and $g_Z'^2$ differs considerably. The obvious reason is that the Z-boson's propagator is missing in the contact interaction model.

Inserting the matching condition (5.120) into Equation (5.119) yields the effective parameter ρ' in terms of the Fermi constant, which is identical to the corresponding Standard Model parameter ρ given in Equation (4.74), by

construction. In a second step, $\rho' = \rho$, κ' and s' can be inserted into (5.118). Due to the matching, the product $\kappa' s'^2$ is identical to the corresponding expression in the Standard Model. Eventually, one finds

$$C_{1f_1}^{f_2'} = -a_{f_2}\rho \left(2T_{f_1}^3 - 4Q_{f_1}\kappa s^2 \right) + 4v_{f_1}a_{f_2}\frac{\alpha}{4\pi} \left(Q_{f_1}^2 + Q_{f_2}^2 \right) + \square' + \mathcal{O}(\alpha^2). \quad (5.121)$$

Equation (5.121) is almost identical to the Standard Model coupling (4.76), but the process dependent terms stemming from vertex corrections with a virtual heavy gauge boson are missing in the effective contact interaction model. As mentioned above, these terms can not universally be reproduced within the current model. In addition, the box graph contributions were not calculated in either model and could add to the deviation.

5.4.6. Matching at a Fermion Threshold

So far, the discussion was restricted to the matching of the effective models with the Standard Model. Since the effective models are incomplete in the heavy gauge boson sector, the transition from the Standard Model to one of the effective models can be considered as integrating out the degrees of freedom associated with (some of) the heavy gauge bosons. In order to obtain a prediction of the weak mixing angle at low energies, the remaining fermions are integrated out successively [17, 18]. The appropriate matching conditions for removing a fermion are different and require an additional calculation; the expression given in Reference [17] is valid for $\mu = m_f$, only, and reads

$$s'^2 = s^2 + \left(\frac{\alpha}{4\pi} \right)^2 \frac{15}{2} N_f v_f Q_f^3 + \mathcal{O}(\alpha^3) \quad (5.122)$$

when omitting higher order terms and QCD effects. The one-loop order term vanishes for $\mu = m_f$ so that the leading term beyond tree-level is of order $\mathcal{O}(\alpha^2)$. It stems from a fermion loop with a virtual photon inside the loop.

To obtain the matching condition for integrating out fermions in the effective contact interaction model, the model with a set of light fermions \mathcal{F}_l is

5. Matching Conditions

matched with the model with the same light fermions as well as a set of heavy fermions $\mathcal{F} = \mathcal{F}_l \cup \mathcal{F}_h$. Typically, the set \mathcal{F}_h will contain only a single fermion much heavier than all the light fermions. To stick with the notation used before, the two models will be referred to as child and parent theory, respectively. By construction, all terms that do not depend on a sum over all fermions in the effective model are identical in parent and child theory. This includes the contribution (5.111) to the low energy coupling constant, which contains a sum over the external fermions, solely. The only fermion loops that contribute to the parity violating interaction are depicted in Figure 5.4 and give rise to the two fermion sums in Equation (5.119). As before, the generic matching condition is (5.77). To comply with the previous expressions, the parent theory is $\overline{\text{MS}}$ -renormalized, while the child model remains unrenormalized. Inserting the corresponding parameters into Equation (5.77) yields

$$K \left(1 - \frac{K}{32\pi^2} \sum_{f \in \mathcal{F}} N_f m_f^2 \log \frac{\mu^2}{m_f^2} \right) = K' \left(1 - \frac{K'}{32\pi^2} \sum_{f \in \mathcal{F}_l} N_f m_f^2 \Delta_f \right), \quad (5.123a)$$

$$s^2 \left(1 + \frac{\alpha}{6\pi s^2} \sum_{f \in \mathcal{F}} N_f Q_f v_f \log \frac{\mu^2}{m_f^2} \right) = s'^2 \left(1 + \frac{\alpha}{6\pi s^2} \sum_{f \in \mathcal{F}_l} N_f Q_f v_f \Delta_f \right), \quad (5.123b)$$

where the primes denote quantities of the child theory. At leading order, the corresponding solutions in terms of K' and s'^2 are

$$K' = K - \frac{K^2}{32\pi^2} \sum_{f \in \mathcal{F}_h} N_f m_f^2 \log \frac{\mu^2}{m_f^2} + \frac{K^2}{32\pi^2} \sum_{f \in \mathcal{F}_l} N_f m_f^2 \Delta_f + \mathcal{O}(K^3), \quad (5.124a)$$

$$s'^2 = s^2 + \frac{\alpha}{6\pi} \sum_{f \in \mathcal{F}_h} N_f Q_f v_f \log \frac{\mu^2}{m_f^2} - \frac{\alpha}{6\pi} \sum_{f \in \mathcal{F}_l} N_f Q_f v_f \Delta_f + \mathcal{O}(\alpha^2). \quad (5.124b)$$

Omitting the UV-divergences that account for the renormalization of the child theory, the matching conditions are exclusively determined by a term stemming

from the heavy fermions that are missing in the child theory. In particular, the matching condition of the weak mixing angle for integrating out a single fermion f becomes

$$s'^2 = s^2 + \frac{\alpha}{6\pi} N_f Q_f v_f \log \frac{\mu^2}{m_f^2} + \mathcal{O}(\alpha^2). \quad (5.125)$$

Due to the scale dependent logarithm, Equation (5.125) reduces to the trivial matching condition $s'^2 = s^2$ at the fermion threshold and confirms Equation (5.122) at one-loop order.

6. Conclusion

6.1. Summary

This thesis dealt with the derivation of the parity violating interaction at zero momentum transfer. To that end, the scaling of coupling parameters according to the renormalization group equation and matching conditions of effective parameters were discussed. In particular, the matching condition of the weak mixing angle for integrating out the W-boson was discussed, and it was pointed out that the expression found in the literature needs to be corrected.

The electromagnetic coupling was discussed in Chapter 3. In the $\overline{\text{MS}}$ -renormalization scheme, the electromagnetic coupling parameter $\hat{\alpha}$ is accessible from first principles only, if the vacuum polarization function can be calculated perturbatively. This is not the case for energy scales at which hadronic effects play a role, as the strong interaction can not be treated perturbatively at low energies. This fundamental challenge can be avoided using the unsubtracted dispersion relation approach discussed in Section 3.1. The final result (3.8) with Equations (3.9), (3.24) and (3.25) can be used to obtain an expression for the vacuum polarization function just above the non-perturbative regime. The input are experimental data as described in Section 3.1 and a contour integral of perturbative expressions given in Section 3.1.1. In a second step, the electromagnetic coupling can be obtained using Equation (3.1).

In the following, the coupling at higher energy scales can be obtained using the solution of the renormalization group equation given in Equations (3.66) and (3.73), which is based on perturbative expressions of the vacuum polarization derived in Sections 3.1.1 and 3.2. Evolving to high energy scales requires incorporating the heavy particles via matching. The matching conditions were derived in a simple context in Section 3.5 with the result (3.75).

Chapter 4 discusses the parity violating interaction in the Standard Model, which is expressed in terms of low energy effective coupling constants. The final result (4.76) of Section 4.2 reproduces the long known expression of Reference [29] but is also valid for arbitrary fermions. The irreducible vertex functions discussed in Section 4.1 are an important ingredient for the parity violating interaction as well as the matching conditions derived later on. Finally, the renormalization group equation of the weak mixing angle and its solution were presented in Sections 4.3 and 4.4. The solution (4.89) expresses the weak mixing angle in terms of the running electromagnetic coupling. This allows making use of the treatment of non-perturbative effects entering the electromagnetic coupling in the context of the weak mixing angle without additional treatment and links Chapters 3 and 4.

In the main part of this thesis, Chapter 5, the matching conditions in the electroweak sector of the Standard Model were discussed in the $\overline{\text{MS}}$ -renormalization scheme. The matching conditions are the relation between the parameters of an effective model and the parameters of its parent theory and are used to switch from one model to the other, which corresponds to integrating out or incorporating heavy particles. The basic concept of matching was introduced in Section 5.1 and existing calculations were presented in Section 5.2. The main problems described there are the lack of a properly defined effective model and that the interaction between massive gauge bosons via the Higgs sector is not properly respected. The first issue might be fixable by specifying an effective model and clarifying how to use the matching conditions in the calculation of an observable, but the second issue is more fundamental and needs to be resolved in a new ansatz.

These deficiencies are overcome by the explicit introduction of two different effective models in Sections 5.3 and 5.4. The first one in Section 5.3 resembles the electroweak sector of the Standard Model but introduces an artificial pseudo gauge boson. The second model, on the other hand, is a four-fermion contact interaction model that does not comprise a Z-boson at all. In either case the matching conditions were derived by equating irreducible vertex functions and observables with the corresponding expressions in the Standard Model derived in Chapter 4.

The final results for the matching of the weak mixing angle at the W-boson threshold are identical due to the same fermionic field content and the lack of the W-boson in either model; the explicit expression was given in Equation (5.78). The difference between the matching condition for integrating out the W-boson derived in this thesis and the one used in the literature [17, 18] was given in Equation (5.81). The deviation is almost seven times larger than the total theoretical uncertainty of the weak mixing angle at low energies and requires a correction of its calculation.

Finally, in Section 5.4.6, the matching condition for integrating out a fermion in the contact interaction model was derived and found to be in agreement with the known expressions presented in Section 3.5.

The main drawback of the contact interaction model is that it does not allow introducing a process independent weak mixing angle as it can not reproduce the process dependent terms induced by the Z-boson in the Standard Model. The model of Section 5.3 on the other hand needs to introduce a pseudo gauge boson and does not restore the longitudinal properties of the Standard Model, even though the longitudinal part of the pseudo boson's propagator exists. Nonetheless, both models are applicable in the context of the parity violating asymmetry and other theories with a different set of parameters leading to different matching conditions could be used, too. In any case, a complete calculation of the observables is needed for a proper theoretical prediction, as the coupling parameters are not observable and need to be paired with the outcome of loop calculations to compensate the scale dependence.

6.2. Discussion of the Electromagnetic Matching Condition

The findings of Chapter 5 suggest that taking into account electroweak effects at two-loop order makes the simple ansatz of Section 3.5 inappropriate. In particular, the W-boson will appear in vertex corrections at two-loop order, which seems to require the treatment of all loop diagrams and not just the corrections to the vacuum polarization function. At least, this is the reason, why

the two effective models can be expected to yield different matching conditions when accounting for electroweak two-loop effects, as the contact interaction vertex will appear in the matching of the weak mixing angle. However, an explicit calculation of all vertex corrections for the derivation of the matching condition of the electromagnetic coupling is probably still not necessary. The fact that the renormalization of the electric charge in QED depends only on the field renormalization of the photon field is guaranteed by the Ward identity. As a consequence, vertex corrections can be ignored as they cancel with external leg corrections. In the EWSM, the Ward identity is slightly different and causes the charge renormalization to also depend on the γZ -mixing self-energy [3]. This is the reason, why Equation (5.34) had to be manually added to (5.32) to obtain the correct dependence on $\log \frac{\mu}{M_W}$. And at higher loop orders, the γZ -mixing self-energy will also contain finite terms that require a rigorous treatment, even if the matching scale $\mu = M_W$ is kept.

An effective model will not exhibit the same symmetries as the EWSM, but most probably needs to restore the Ward identity for two reasons. First, the Ward identity follows from a symmetry of the functional integration and not from specific model properties. Second, the Ward identity ensures that the photon remains massless at higher loop order, which must be the case in an effective model, too. Consequently, the application of the Ward identity will probably allow skipping the calculation of vertex corrections at higher loop order, too, but a more detailed discussion of the topic is required.

6.3. Outlook

As pointed out in Section 6.1, the matching condition of the weak mixing angle for integrating out the W-boson needs to be corrected. This will alter the numerical value of the weak mixing angle right below the W-threshold and subsequently the running of the weak mixing angle at lower energy scales. In particular, this also will lead to a small change of the weak mixing angle at zero momentum transfer that was published in References [17, 18] and requires a recalculation thereof.

In the light of the findings of Chapter 5, a discussion about a suitable effective model for the matching of the weak mixing angle and the electromagnetic coupling is due. The contact interaction model described in Section 5.4 seems natural but requires the introduction of a process dependent weak mixing angle and other models that were not discussed in this thesis might be suitable, as well.

An aspect that was not discussed but is relevant for the P2 experiment is the effect of the hadronic structure of the proton. Using a compound target particle requires a treatment of the hadronic structure which is parametrized in terms of form factors at low energy. Form factors can not be calculated from first principles and need to be determined in an experiment. Accordingly, they may or may not contain all sorts of radiative corrections depending on the data analysis performed after the measurement. In order to avoid double counting of certain effects, one has to exclude all diagrams from the calculations in this thesis that are already part of the form factors.

In the long run, a discussion of electroweak two-loop effects is very much desirable. These will increase the theoretical precision even further but also discriminate between the effective models proposed in Chapter 5. In addition, the discussion of electroweak two-loop diagrams will explicitly show that the published ansatz for the calculation of the electromagnetic matching conditions requires a modification as mentioned before.

A. Illustration of the RG-Running and Matching Conditions in a Simple Model

The general steps that are required in order to evolve a coupling parameter from one energy scale to another were laid out in Section 2.5.4. These steps are illustrated in the following in case of an effective QED that incorporates electrons and muons.

The electromagnetic coupling constant is derived from experimental data obtained at zero momentum transfer below the creation threshold of the electron, where no logarithms of the type $\log \frac{\mu^2}{m^2}$ occur in the $\overline{\text{MS}}$ -scheme. Accordingly, the PDG value corresponds to an $\overline{\text{MS}}$ -determination of $\hat{\alpha}(\mu_0)$ with no active particle. The initial scale μ_0 can be selected freely; $\mu_0 = m_e$ will be used in the following.¹ The steps 2 and 3 described at the end of Section 2.5.4 need to be executed two times due to the crossing of two particle thresholds. In the following, 2a, 3a, 2b and 3b are used as numeration for the recurring steps. In order to keep the equations simple, they are expressed in terms of $a = \frac{\alpha}{\pi}$ instead of α .

1. As explained above, the initial value is given by experimental value of the electromagnetic coupling, $\hat{\alpha}(\mu_0 = m_e) = \frac{\alpha_{\text{PDG}}}{\pi} = \frac{\alpha}{\pi}$.
- 2a. This step is not required, as the initial value $\hat{\alpha}(\mu_0 = m_e) = a$ is already given at threshold.

¹Since the β -function vanishes below the electron threshold, $\hat{\alpha}(\mu)$ is constant for $\mu \leq m_e$. This implies that any other choice μ'_0 with $\mu'_0 < m_e$ is identical to $\mu_0 = m_e$.

A. Illustration of the RG-Running and Matching Conditions in a Simple Model

- 3a. The finite parts of the vacuum polarization at zero momentum transfer do not vanish at two-loop order, which leads to a discontinuity in \hat{a} . Using the results of Section 3.5 and the notation introduced in Section 2.3, one has

$$\hat{a}^{\text{P}}(m_e) = \hat{a}^{\text{c}}(m_e) + \frac{15}{16} (\hat{a}^{\text{c}}(m_e))^3 = a + \frac{15}{16} a^3. \quad (\text{A.1})$$

- 2b. The solution of the two-loop β -function in QED reads²

$$a(\mu) = a(\mu_0) - a^2(\mu_0)\beta_0 \log \frac{\mu^2}{\mu_0^2} + a^3(\mu_0) \left(\beta_0^2 \log^2 \frac{\mu^2}{\mu_0^2} - \beta_1 \log \frac{\mu^2}{\mu_0^2} \right). \quad (\text{A.2})$$

Replacing $a(\mu_0)$ by $\hat{a}^{\text{P}}(m_e)$ and neglecting terms of order $\mathcal{O}(\alpha^4)$ yields

$$\hat{a}^{\text{c}}(m_\mu) = a + \frac{15}{16} a^3 + \frac{a^2}{3} \log \frac{m_\mu^2}{m_e^2} + a^3 \left(\frac{1}{9} \log^2 \frac{m_\mu^2}{m_e^2} + \frac{1}{4} \log \frac{m_\mu^2}{m_e^2} \right) + \mathcal{O}(\alpha^4), \quad (\text{A.3})$$

where the coefficients $\hat{\beta}_0$ and $\hat{\beta}_1$ were replaced by the appropriate numerical values $-\frac{1}{3}$ and $-\frac{1}{4}$ of the effective one-particle QED, respectively, and the threshold value $\hat{a}^{\text{P}}(m_e)$ was expressed in terms of a by inserting Equation (A.1).

- 3b. The matching condition of the muon is the same as the one of the electron given in Equation (A.1) yielding

$$\hat{a}^{\text{P}}(m_\mu) = a + \frac{a^2}{3} \log \frac{m_\mu^2}{m_e^2} + a^3 \left(\frac{1}{9} \log^2 \frac{m_\mu^2}{m_e^2} + \frac{1}{4} \log \frac{m_\mu^2}{m_e^2} + \frac{15}{8} \right) + \mathcal{O}(\alpha^4), \quad (\text{A.4})$$

where the two individual matching constants $\frac{15}{16}$ of the electron and muon have been combined.

²It can be derived from the three-loop solution given in Equation (3.71).

-
4. The final result for $\hat{\alpha}(\mu_f)$ with an arbitrary scale $\mu_f \geq m_\mu$ is obtained by inserting $\hat{\alpha}^P(m_\mu)$ into Equation (A.2). It reads

$$\begin{aligned}
\hat{\alpha}(\mu_f) = & a + \frac{a^2}{3} \log \frac{m_\mu^2}{m_e^2} + a^3 \left(\frac{1}{9} \log^2 \frac{m_\mu^2}{m_e^2} + \frac{1}{4} \log \frac{m_\mu^2}{m_e^2} + \frac{15}{8} \right) \\
& + \frac{2}{3} a^2 \log \frac{\mu_f^2}{m_\mu^2} + \frac{4}{9} a^3 \log \frac{\mu_f^2}{m_\mu^2} \log \frac{m_\mu^2}{m_e^2} \\
& + a^3 \left(\frac{4}{9} \log^2 \frac{\mu_f^2}{m_\mu^2} + \frac{1}{2} \log \frac{\mu_f^2}{m_\mu^2} \right) + \mathcal{O}(\alpha^4), \quad \text{for } \mu_f \geq m_\mu.
\end{aligned} \tag{A.5}$$

This time, the RGE-coefficients $\hat{\beta}_0$ and $\hat{\beta}_1$ were replaced by the values $-\frac{2}{3}$ and $-\frac{1}{2}$ according to the field content of the full two-particle QED. Equation (A.5) can be simplified by expressing all logarithms in the form $\log \frac{\mu_f^2}{m_{e,\mu}^2}$, which also separates the individual logarithmic contributions of the electron and muon,

$$\begin{aligned}
\hat{\alpha}(\mu_f) = & a + \frac{a^2}{3} \left(\log \frac{\mu_f^2}{m_e^2} + \log \frac{\mu_f^2}{m_\mu^2} \right) + \frac{a^3}{4} \left(\log \frac{\mu_f^2}{m_e^2} + \log \frac{\mu_f^2}{m_\mu^2} \right) \\
& + \frac{a^3}{9} \left(\log \frac{\mu_f^2}{m_e^2} + \log \frac{\mu_f^2}{m_\mu^2} \right)^2 + a^3 \frac{15}{8} + \mathcal{O}(\alpha^4), \quad \text{for } \mu_f \geq m_\mu.
\end{aligned} \tag{A.6}$$

The final result (A.6) obtained via RGE evolution and matching of effective theories is the same as the expression of the electromagnetic coupling one obtains when calculating in the full theory and deriving $\hat{\alpha}(\mu_f)$ directly as in Equation (2.42): Dyson resumming Equation (2.39) yields

$$\hat{\alpha}(\mu) = \alpha \left[1 + \hat{\Pi}(q^2 = 0, \mu^2) \right] \tag{A.7}$$

for the relation between $\overline{\text{MS}}$ -renormalized and OS coupling parameters, where $\hat{\Pi}$ consists of contributions of irreducible diagrams, only. The two-loop vacuum

A. Illustration of the RG-Running and Matching Conditions in a Simple Model

polarization function of QED including electrons and muons is given by (see Section 3.2)

$$\hat{\Pi}(q^2 = 0, \mu^2) = \frac{\hat{\alpha}(\mu^2)}{\pi} \left(-\frac{1}{3} - \frac{\hat{\alpha}(\mu^2)}{4\pi} \right) \left(\log \frac{m_e^2}{\mu^2} + \log \frac{m_\mu^2}{\mu^2} \right) + \frac{15}{8} \frac{\hat{\alpha}^2(\mu^2)}{\pi^2}. \quad (\text{A.8})$$

Inserting Equation (A.8) into (A.7) yields an implicit equation for $\hat{\alpha}(\mu)$, as $\hat{\Pi}$ is given in terms of $\hat{\alpha}(\mu)$ instead of α . It can be solved by iteratively replacing every occurrence of $\hat{\alpha}(\mu)$ with the right-hand side of Equation (A.7) and neglecting terms of order $\mathcal{O}(\alpha^4)$. The result of that iterated process coincides with the previously determined expression (A.6).

B. Feynman Rules

The Feynman rules including the corresponding sign conventions are taken from Reference [2]. Since an explicit calculation of most of the Feynman diagrams can be avoided when using the self-energy functions given in Appendix C, only a couple of Feynman rules are needed throughout this thesis. For completeness, the ones that are used in this thesis are collected below, with the notation adjusted according to Section 2.3.

The Feynman rule (B.3) describes a self-energy insertion into one of the gauge boson propagators or the γZ -mixing; hence, the expression on the right-hand side includes only the blob without the attached propagators. The coupling of the blob to the attached propagators is part of the self-energy $\Sigma_{\mu\nu}^{ab}$, too. The tensor structure of $\Sigma_{\mu\nu}^{ab}$ and its decomposition in terms of the transverse and longitudinal self-energy functions is given in Equation (2.25).

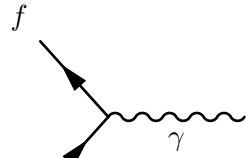
The single additional Feynman rule required for calculations in the effective contact interaction model in Section 5.4 is not listed and can be found in Equation (5.85).

$$\begin{array}{c} \mu \\ \text{~~~~~} \\ \gamma \\ \text{~~~~~} \\ \nu \end{array} \quad \hat{=} \quad \frac{-ig_{\mu\nu}}{q^2 - M^2} \quad (\text{B.1})$$

$$\begin{array}{c} \text{-----} \\ \blacktriangleright \\ f \end{array} \quad \hat{=} \quad i \frac{\not{q} + m_f}{q^2 - m_f^2} \quad (\text{B.2})$$

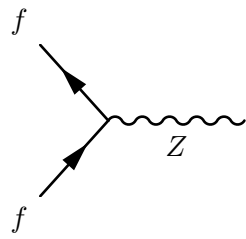
$$\begin{array}{c} \mu \quad \nu \\ \text{~~~~} \quad \text{~~~~} \\ a \quad \text{[blob]} \quad b \\ \text{~~~~} \quad \text{~~~~} \end{array} \quad \hat{=} \quad i\Sigma_{\mu\nu}^{ab} \quad (\text{B.3})$$

B. Feynman Rules



A Feynman diagram showing a fermion line (solid line with arrows) entering from the bottom left and exiting from the top left. A wavy line representing a photon, labeled with the Greek letter γ , is emitted from the vertex where the fermion line changes direction.

$$\cong -ieQ_f\gamma_\mu \quad (\text{B.4})$$



A Feynman diagram showing a fermion line (solid line with arrows) entering from the bottom left and exiting from the top left. A wavy line representing a Z boson, labeled with the letter Z , is emitted from the vertex where the fermion line changes direction.

$$\cong iM_Z\sqrt{\sqrt{2}G_F}\gamma_\mu(v_f - a_f\gamma_5) \quad (\text{B.5})$$

C. One-Loop Functions at Zero Momentum Transfer

This appendix contains a list of one-loop functions and their derivatives evaluated at zero momentum transfer or $q^2 = \tilde{m}_f^2$, which are used in the calculations throughout this thesis. As before, the mass parameter \tilde{m}_f is the on-shell mass of the fermion f . Except for the derivatives of the vertex functions, the expressions were derived from the complete formulas provided by Reference [2]¹ with the help of `Package-X` [39]. The derivative of the axial part of the fermion-fermion-photon vertex functions was calculated from scratch with the aid of `FeynCalc` [40], `FeynHelpers` [41] and `Package-X`. To facilitate the notation of the Z-boson's self-energy, the ratio of Higgs- and Z-mass is abbreviated as $\xi = \frac{M_H^2}{M_Z^2}$. Additionally, the notation $\tilde{f} = f$ if $f \neq \nu_l$ and $\tilde{f} = l$ if $f = \nu_l$ of Reference [2] is adopted.

Terms in brackets stem from W-bosons or the Higgs sector and do not appear in the effective model of Section 5.3, that is the self-energies in the effective theory are obtained by dropping all brackets. Hats indicate $\overline{\text{MS}}$ -renormalization as before. The unrenormalized quantities can be obtained when reintroducing the UV-divergent terms by means of the substitution $\log \frac{\mu^2}{M_X^2} \rightarrow \Delta_X$, where Δ_X is defined in Equation (2.21). Some of the series expansions of Passarino-Veltman base functions needed for the evaluation of the self-energies are given in Section C.4.

¹There is a typo in the axial part of the self-energy in Reference [2]. The terms that stem from the Z-boson loop need an additional factor of -1 . Moreover, the V-A term on the first line of Equation (5.30) should read $v_\sigma - a_\sigma \gamma_5$ instead of $v_\sigma^- a_\sigma \gamma_5$ and there is a closing parenthesis missing on the second line of the Zff -Feynman rule, right after the first $Q^{i\sigma}$.

C.1. Bosonic Self-Energies

The transverse parts of the self-energies, their derivatives with respect to the momentum transfer and the corresponding longitudinal parts that are identical to the transverse parts read

$$\hat{\Sigma}_T^{\gamma\gamma}(0) = \hat{\Sigma}_L^{\gamma\gamma}(0) = \hat{\Sigma}_L^{\gamma\gamma'}(0) = 0, \quad (\text{C.1})$$

$$\hat{\Sigma}_T^{\gamma\gamma'}(0) = \frac{\alpha}{4\pi} \left\{ \frac{4}{3} \sum_f N_f Q_f^2 \log \frac{\mu^2}{m_f^2} - \left[3 \log \frac{\mu^2}{M_W^2} + \frac{2}{3} \right] \right\}, \quad (\text{C.2})$$

$$\hat{\Sigma}_T^{\gamma Z}(0) = \hat{\Sigma}_L^{\gamma Z}(0) = \frac{\alpha}{4\pi} \left[2 \frac{M_W^2}{cs} \log \frac{\mu^2}{M_W^2} \right], \quad (\text{C.3})$$

$$\begin{aligned} \hat{\Sigma}_T^{\gamma Z'}(0) = \frac{\alpha}{4\pi} \left\{ -\frac{2}{3cs} \sum_f N_f Q_f v_f \log \frac{\mu^2}{m_f^2} \right. \\ \left. + \left[\left(3 \frac{c}{s} + \frac{1}{6cs} \right) \log \frac{\mu^2}{M_W^2} + \frac{1+2c^2}{3cs} \right] \right\}, \end{aligned} \quad (\text{C.4})$$

$$\frac{\hat{\Sigma}_T^{ZZ}(0)}{M_Z^2} = \frac{\hat{\Sigma}_L^{ZZ}(0)}{M_Z^2} - \frac{\alpha}{4\pi} \frac{1}{2c^2 s^2} \sum_f \frac{m_f^2}{M_Z^2} \log \frac{\mu^2}{m_f^2}, \quad (\text{C.5})$$

$$\begin{aligned} \hat{\Sigma}_T^{ZZ'}(0) = \frac{\alpha}{4\pi} \sum_f \frac{v_f^2 + a_f^2}{3c^2 s^2} \log \frac{\mu^2}{m_f^2} \\ + \frac{\alpha}{4\pi} \left[\left(3 - \frac{19}{6s^2} + \frac{1}{6c^2} \right) \log \frac{\mu^2}{M_W^2} - \frac{4c^2}{3s^2} + \frac{(c^2 - s^2)^2}{6c^2 s^2} \right] \\ + \frac{\alpha}{4\pi} \frac{1}{12c^2 s^2} \left[\frac{11}{3} + \frac{1+\xi}{2(1-\xi)} \log \xi - \log \frac{M_H M_Z}{M_W^2} \right. \\ + \frac{5-\xi}{(1-\xi)^3} (1 - \xi^2 + 2\xi \log \xi) \\ \left. + \frac{\xi^3 + 9\xi^2 - 9\xi - 1 - 6\xi(1+\xi) \log \xi}{6(\xi-1)^3} \right]. \end{aligned} \quad (\text{C.6})$$

The remaining longitudinal self-energy functions that were not specified in the equations above, that is all longitudinal parts that differ from the respective transverse part, are

$$\hat{\Sigma}_L^{\gamma Z'}(0) = \frac{\alpha}{4\pi} \left[\frac{1}{3cs} \right], \quad (\text{C.7})$$

$$\begin{aligned} \frac{\hat{\Sigma}_L^{ZZ}(0)}{M_Z^2} = \frac{\alpha}{4\pi} & \left[\left(4 + \frac{1}{c^2} - \frac{1}{s^2} \right) \log \frac{\mu^2}{M_W^2} - \frac{\xi}{6c^2s^2} \log \frac{M_H^2}{M_W^2} \right. \\ & - \frac{1}{6c^2s^2} \log \frac{M_Z^2}{M_W^2} + \frac{1}{24c^2s^2} \left(1 + \xi + 2\xi \frac{\log \xi}{1-\xi} \right) \\ & \left. + \frac{5-\xi}{6c^2s^2} \left(1 + \frac{1+\xi}{2(1-\xi)} \log \xi - \log \frac{M_H M_Z}{M_W^2} \right) \right] \end{aligned} \quad (\text{C.8})$$

$$\hat{\Sigma}_L^{ZZ'}(0) = \frac{\alpha}{4\pi} \left[\frac{\xi^3 - 3\xi^2 - 9\xi + 11 + 6\xi(3-\xi) \log \xi}{24c^2s^2(1-\xi)^3} - \frac{c^2 - s^2}{3s^2} \frac{M_Z^2}{M_W^2} \right]. \quad (\text{C.9})$$

A particular important quantity is the difference of the Z- and W-boson's transverse self-energies that enters at many places in the renormalization prescriptions. For instance, it is part of the ρ -parameter required by the parity violating interaction as can be seen in Equation (4.65). The terms cancel to some extent so that the difference is less complex than the individual pieces. Using $M_W = cM_Z$, which is sufficient for the one-loop calculation, confirms the result given in Reference [42],

$$\begin{aligned} \frac{\hat{\Sigma}_T^{ZZ}(0)}{M_Z^2} - \frac{\hat{\Sigma}_T^{WW}(0)}{M_W^2} = \frac{\alpha}{4\pi} & \left\{ \frac{1}{c^2s^2} \left(\frac{17}{4s^2} - 7 + 2s^2 \right) \log c^2 \right. \\ & + \frac{1}{c^2} \left(\frac{13}{4} - 4s^2 \right) \log \frac{\mu^2}{M_W^2} + \frac{17}{4s^2} + \frac{3}{4s^2} \frac{m_t^2}{M_W^2} \\ & \left. - \frac{3}{4s^2} \frac{c^2 \log \frac{\mu^2}{M_W^2} - \xi \log \frac{\mu^2}{M_H^2}}{c^2 - \xi} + \frac{3}{4c^2s^2} \frac{\log \frac{\mu^2}{M_Z^2} - \xi \log \frac{\mu^2}{M_H^2}}{1 - \xi} \right\}. \end{aligned} \quad (\text{C.10})$$

C.2. Fermionic Self-Energies

Using λ as an infinitesimal photon mass to regularize the infrared divergences, the fermionic self-energies read

$$\hat{\Sigma}_f^V(\tilde{m}_f^2) = +\frac{\alpha}{4\pi} \left\{ Q_f^2 \left(2 + \log \frac{\mu^2}{\tilde{m}_f^2} \right) + \frac{v_f^2 + a_f^2}{4c^2 s^2} \left(-\frac{1}{2} + \log \frac{\mu^2}{M_Z^2} \right) + \frac{1}{4s^2} \left[-\frac{1}{2} + \log \frac{\mu^2}{M_W^2} \right] \right\}, \quad (\text{C.11})$$

$$\hat{\Sigma}_f^A(\tilde{m}_f^2) = -\frac{\alpha}{4\pi} \left\{ \frac{v_f a_f}{2c^2 s^2} \left(-\frac{1}{2} + \log \frac{\mu^2}{M_Z^2} \right) + \frac{1}{4s^2} \left[-\frac{1}{2} + \log \frac{\mu^2}{M_W^2} \right] \right\}, \quad (\text{C.12})$$

$$\hat{\Sigma}_f^S(\tilde{m}_f^2) = -\frac{\alpha}{4\pi} \left\{ Q_f^2 \left(6 + 4 \log \frac{\mu^2}{\tilde{m}_f^2} \right) + \frac{v_f^2 - a_f^2}{4c^2 s^2} \left(2 + 4 \log \frac{\mu^2}{M_Z^2} \right) \right\}, \quad (\text{C.13})$$

$$\hat{\Sigma}_f^{V'}(\tilde{m}_f^2) = +\frac{\alpha}{4\pi} \left\{ -\frac{Q_f^2}{\tilde{m}_f^2} \left(3 + \log \frac{\lambda^2}{\tilde{m}_f^2} \right) + \frac{v_f^2 + a_f^2}{4c^2 s^2} \frac{1}{3M_Z^2} + \frac{1}{4s^2} \left[\frac{1}{3M_W^2} \right] \right\}, \quad (\text{C.14})$$

$$\hat{\Sigma}_f^{A'}(\tilde{m}_f^2) = -\frac{\alpha}{4\pi} \left\{ \frac{v_f a_f}{2c^2 s^2} \frac{1}{3M_Z^2} + \frac{1}{4s^2} \left[\frac{1}{3M_W^2} \right] \right\}, \quad (\text{C.15})$$

$$\hat{\Sigma}_f^{S'}(\tilde{m}_f^2) = +\frac{\alpha}{4\pi} \left\{ 2 \frac{Q_f^2}{\tilde{m}_f^2} \left(2 + \log \frac{\lambda^2}{\tilde{m}_f^2} \right) - \frac{v_f^2 - a_f^2}{4c^2 s^2} \frac{2}{M_Z^2} \right\}. \quad (\text{C.16})$$

C.3. Vertex Functions

The photonic vertex corrections are infrared divergent in general and need to be combined with bremsstrahlung diagrams to cancel the singularities. The infinitesimal photon mass is again parametrized by λ and f' denotes the weak isospin partner of the fermion f . Note, that there is a mistake in the photonic contributions of Reference [2]. The correct expressions can be obtained using the exact vertex correction given in Section C.3.2.

C.3.1. Function Values at Zero Momentum Transfer

$$\begin{aligned} \Lambda_V^{ff\gamma}(0) = \frac{\alpha}{4\pi} \left\{ Q_f^3 \left(\Delta_f + 2 \log \frac{\lambda^2}{m_f^2} + 2 \right) Q_f \frac{v_f^2 + a_f^2}{4c^2 s^2} \left(\Delta_Z - \frac{1}{2} \right) \right. \\ \left. + \frac{Q_{f'}}{4s^2} \left[\Delta_W - \frac{1}{2} \right] + \frac{3T_f^3}{2s^2} \left[\Delta_W - \frac{1}{6} \right] \right\} \end{aligned} \quad (\text{C.17})$$

$$\Lambda_A^{ff\gamma}(0) = -\frac{\alpha}{4\pi} \left\{ Q_f \frac{2v_f a_f}{4c^2 s^2} \left(\Delta_Z - \frac{1}{2} \right) + \frac{Q_{f'}}{4s^2} \left[\Delta_W - \frac{1}{2} \right] + \frac{3T_f^3}{2s^2} \left[\Delta_W - \frac{1}{6} \right] \right\} \quad (\text{C.18})$$

$$\begin{aligned} \Lambda_V^{ffZ}(0) = \frac{\alpha}{4\pi} \left\{ v_f Q_f^2 \left(\Delta_f + 2 \log \frac{\lambda^2}{m_f^2} + 2 \right) v_f \frac{v_f^2 + 3a_f^2}{4c^2 s^2} \left(\Delta_Z - \frac{1}{2} \right) \right. \\ \left. + \frac{v_{f'} + a_{f'}}{4s^2} \left[\Delta_W - \frac{1}{2} \right] + 3T_f^3 \frac{c^2}{s^2} \left[\Delta_W - \frac{1}{6} \right] \right\} \end{aligned} \quad (\text{C.19})$$

$$\begin{aligned} \Lambda_A^{ffZ}(0) = -\frac{\alpha}{4\pi} \left\{ a_f Q_f^2 \left(\Delta_f - 2 \log \frac{m_f^2}{\lambda^2} + 2 \right) a_f \frac{3v_f^2 + a_f^2}{4c^2 s^2} \left(\Delta_Z - \frac{1}{2} \right) \right. \\ \left. + \frac{v_{f'} + a_{f'}}{4s^2} \left[\Delta_W - \frac{1}{2} \right] + 3T_f^3 \frac{c^2}{s^2} \left[\Delta_W - \frac{1}{6} \right] \right\} \end{aligned} \quad (\text{C.20})$$

$$\Lambda_S^{ffZ}(0) = \mathcal{O} \left(\frac{m_f^2}{M_W^2} \right) \quad (\text{C.21})$$

C.3.2. Derivative of the Axial Fermion-Fermion-Photon-Vertex

Previously, only the vertex functions evaluated at zero momentum transfer were given. For the parity violating interaction at one-loop order, one also needs the derivative with respect to the momentum transfer of the axial piece of the $ff\gamma$ -vertex correction evaluated at zero momentum transfer, $\Lambda_A^{ff\gamma'}(0)$. The expressions in Reference [2] are not suitable to obtain the derivative at $q^2 = 0$, as they are defined in the limit $m_f^2 \ll q^2$, only. The results of Reference [37]

C. One-Loop Functions at Zero Momentum Transfer

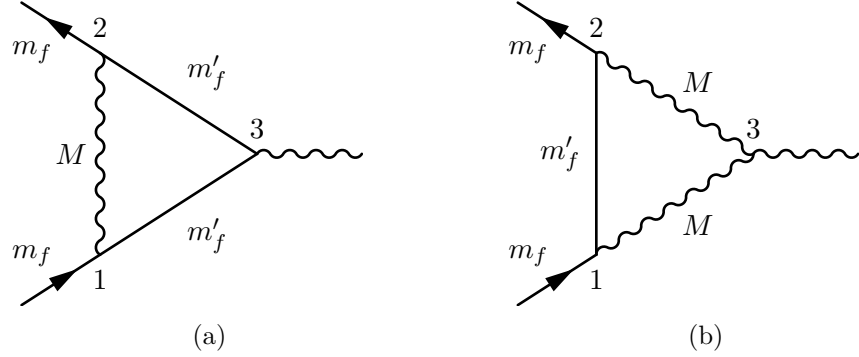


Figure C.1.: Feynman diagrams that contribute to the axial vertex corrections $\Lambda_A^{ff\gamma}$ and Λ_A^{ffZ} . The Arabic numbers index the vertices in order to facilitate the generic notation $g_i^\pm, i = 1, 2, 3$, for the corresponding coupling constants.

are exact in the momentum transfer, but were obtained by neglecting light fermion masses, which is insufficient for computing the derivative. A calculation from scratch for the axial piece $\Lambda_A^{ff\gamma}(q^2)$ and its derivative at zero momentum transfer is presented in the following. All results are written in terms of a photon as external gauge boson, but the calculation is generic and can also be used in a neutral current calculation when substituting the coupling constant appropriately.

There are only two types of Feynman diagrams contributing to $\Lambda_A^{ff\gamma}(0)$, one with a virtual W- or Z-boson that is attached to the incoming and outgoing fermions and one with two virtual W-bosons that form a triple gauge boson vertex with the external gauge boson. They are displayed in Figure C.1 and the functions $\Lambda_{A(a)}^{ff\gamma}$ and $\Lambda_{A(b)}^{ff\gamma}$ will be used to denote their individual contributions to the axial vertex function,

$$\Lambda_A^{ff\gamma} = \Lambda_{A(a)}^{ff\gamma} + \Lambda_{A(b)}^{ff\gamma}. \quad (\text{C.22})$$

Using C_i and C_{ij} to denote the scalar Passarino–Veltman functions as defined in Reference [37] and omitting their arguments $(m_f^2, q^2, m_f^2, M, m'_f, m'_f)$ for the

sake of readability, the expression for the generic fermion–fermion–gauge–boson vertex Diagram C.1a can be written as

$$\begin{aligned}
\mathcal{M}_{C.1a} &= -ie\bar{u}(p_2)\gamma_\mu\gamma_5u(p_1) \cdot X \\
X &= -i\frac{g_1^+g_2^+g_3^+ - g_1^-g_2^-g_3^-}{16\pi^2e} \left[2C_{00} - 1 - q^2(C_0 + C_1 + C_2 + C_{12}) \right. \\
&\quad \left. + m^2(C_0 + 2C_1 + 2C_2 + C_{11} + C_{22} + 2C_{12}) \right] \\
&\quad + \frac{im_f'^2}{16\pi^2e} C_0 (g_1^+g_2^+g_3^- - g_1^-g_2^-g_3^+).
\end{aligned} \tag{C.23}$$

A notation similar to the one of Reference [37] is used: g_i^- (g_i^+), $i = 1, 2, 3$, denote the generic left (right) handed couplings associated with the loop vertices. The parameter M refers to the mass of the gauge boson within the loop and m_f' is the mass of the fermions f weak isospin partner when $M = M_W$, and identical to m_f otherwise. The matrix element (C.23) represents the contribution of a single Feynman diagram, only. In order to obtain $\Lambda_{A(a)}^{ff\gamma}$, one has to sum over all possible virtual gauge bosons inside the loop. A diagram with a virtual photon does not contribute to the axial fermion-fermion-photon vertex, as QED is not parity violating. In case of a fermion-fermion-photon vertex with a virtual Z-boson inside the loop, the coupling constants read

$$g_1^- = g_2^- = ie\frac{T_f^3 - s^2Q_f}{cs}, \quad g_1^+ = g_2^+ = -ie\frac{s^2Q_f}{cs}, \quad g_3^+ = g_3^- = -ieQ_f; \tag{C.24}$$

if the virtual boson is a W-boson, they read

$$g_1^- = g_2^- = \frac{ie}{\sqrt{2}s}, \quad g_1^+ = g_2^+ = 0, \quad g_3^+ = g_3^- = -ieQ_f. \tag{C.25}$$

For identical incoming and outgoing fermions, the Passarino–Veltman functions obey the relations

$$C_1(m_f^2, q^2, m_f^2, M, m_f', m_f') \equiv C_2(m_f^2, q^2, m_f^2, M, m_f', m_f'), \tag{C.26a}$$

$$C_{11}(m_f^2, q^2, m_f^2, M, m_f', m_f') \equiv C_{22}(m_f^2, q^2, m_f^2, M, m_f', m_f'), \tag{C.26b}$$

C. One-Loop Functions at Zero Momentum Transfer

which can be used to further simplify Equation (C.23). The Passarino–Veltman functions can be easily Taylor expanded in the squared momentum transfer with the help of `Package-X`. Inserting Equations (C.24) and (C.25), one finds

$$\begin{aligned} \Lambda_{A(a)}^{ff\gamma}(q^2) = & -\frac{\alpha}{4\pi} \left\{ \frac{Q_f v_f a_f}{2c^2 s^2} \left(\Delta_Z - \frac{1}{2} \right) + \frac{Q_{f'}}{4s^2} \left[\Delta_W - \frac{1}{2} \right] \right\} \\ & - \frac{\alpha}{4\pi} q^2 \left\{ \frac{Q_f v_f a_f}{2c^2 s^2} \frac{1}{9M_Z^2} \left(1 - 6 \log \frac{m_f^2}{M_Z^2} \right) \right. \\ & \left. + \frac{Q_{f'}}{4s^2} \frac{1}{9M_W^2} \left[1 - 6 \log \frac{m_f'^2}{M_W^2} \right] \right\} + \mathcal{O} \left(\frac{m_f, m_f'}{M_W}, \frac{q^4}{M_W^4} \right). \end{aligned} \quad (\text{C.27})$$

Similarly to Equation (C.23), the Feynman diagram in Figure C.1b evaluates to the matrix element

$$\begin{aligned} \mathcal{M}_{C.1b} = & -ie\bar{u}(p_2)\gamma_\mu\gamma_5 u(p_1) \cdot X \\ X = & -\frac{i}{16\pi^2 e} \left[6C_{00} - 1 - q^2 (C_1 + C_2 + C_{12}) \right. \\ & \left. + m^2 (C_1 + C_2 + C_{11} + C_{22} + 2C_{12}) \right] (g_1^- g_2^- - g_1^+ g_2^+) g_3, \end{aligned} \quad (\text{C.28})$$

but this time with $C_{i,j} \equiv C_{i,j}(m_f^2, q^2, m_f^2, m_f', M, M)$. Inserting the coupling constants

$$g_1^- = g_2^- = \frac{ie}{\sqrt{2}s}, \quad g_1^+ = g_2^+ = 0, \quad g_3 = -ie, \quad (\text{C.29})$$

eventually leads to²

$$\Lambda_{A(b)}^{ff\gamma}(q^2) = -\frac{\alpha}{4\pi} \frac{T_f^3}{2s^2} \left[\left(3\Delta_W - \frac{1}{2} \right) - \frac{5q^2}{9M_W^2} \right] + \mathcal{O} \left(\frac{m_f, m_f'}{M_W} \right) + \mathcal{O} \left(\frac{q^4}{M_W^4} \right). \quad (\text{C.30})$$

²The Feynman rule for g_3 depends on the orientation of the gauge bosons, that is the direction of flow of the charge. This is determined by the isospin of fermion f so that $2T_f^3$ is used to parametrize Equation C.30.

Adding Equations (C.27) and (C.30) confirms Equation (C.18) and yields the derivative

$$\Lambda_A^{ff\gamma'}(0) = -\frac{\alpha}{4\pi} \left\{ \frac{Q_f v_f a_f}{18c^2 s^2 M_Z^2} \left(1 - 6 \log \frac{m_f^2}{M_Z^2} \right) + \frac{Q_{f'}}{36s^2 M_W^2} \left[1 - 6 \log \frac{m_{f'}^2}{M_W^2} \right] - \left[\frac{5T_f^3}{18s^2 M_W^2} \right] \right\} \quad (\text{C.31})$$

of the axial part of the vertex correction at zero momentum transfer.

C.4. Passarino–Veltman Functions

Primes denote derivatives with respect to the first argument and λ and f' have the same meaning as before. The parameter M is used to denote the masses of the heavy gauge bosons M_W and M_Z . In case of $M = M_Z$, one also has $m_{f'} = m_f$. If $M = M_W$, the difference $m_f \neq m_{f'}$ in the B_0 - and B_1 -functions becomes relevant when taking into account terms of order $\mathcal{O}\left(\frac{m_f^2}{M_W^2}\right)$. Polynomial terms in the photon mass λ are omitted without indication.

$$B_0(m_f^2, m_f, \lambda) = \Delta + \log \frac{\mu^2}{m_f^2} + 2 \quad (\text{C.32})$$

$$B_0'(m_f^2, m_f, \lambda) = -\frac{1}{2m_f^2} \left(2 + \log \frac{\lambda^2}{m_f^2} \right) \quad (\text{C.33})$$

$$B_0(m_f^2, m_{f'}, M) = \Delta + \log \frac{\mu^2}{M^2} + 1 + \frac{m_f^2 + 2m_{f'}^2 \log \frac{m_{f'}^2}{M^2}}{2M^2} + \mathcal{O}\left(\frac{m_f^4, m_{f'}^4}{M^4}\right) \quad (\text{C.34})$$

$$B_0'(m_f^2, m_{f'}, M) = \frac{1}{2M^2} + \mathcal{O}\left(\frac{m_f^2, m_{f'}^2}{M^4}\right) \quad (\text{C.35})$$

$$B_1(m_f^2, m_f, \lambda) = -\frac{1}{2} \left(\Delta + \log \frac{\mu^2}{m_f^2} + 3 \right) \quad (\text{C.36})$$

$$B'_1(m_f^2, m_f, \lambda) = \frac{1}{2m_f^2} \left(3 + \log \frac{\lambda^2}{m_f^2} \right) \quad (\text{C.37})$$

$$B_1(m_f^2, m_{f'}, M) = -\frac{1}{2} \left(\Delta + \log \frac{\mu^2}{M^2} + \frac{1}{2} \right) + \mathcal{O} \left(\frac{m_f^2, m_{f'}^2}{M^2} \right) \quad (\text{C.38})$$

$$B'_1(m_f^2, m_{f'}, M) = -\frac{1}{6M^2} + \mathcal{O} \left(\frac{m_f^2, m_{f'}^2}{M^4} \right) \quad (\text{C.39})$$

C.5. Propagators

For completeness, the transverse parts of the one-loop gauge boson propagators in terms of the bosonic self-energies are given in this section. The relation between polarization components and the propagator can be read off Equation (2.25).

$$G_T^{\gamma\gamma}(q^2) = \frac{i}{q^2} \left(1 - \frac{\Sigma_T^{\gamma\gamma}(q^2)}{q^2} \right) \quad (\text{C.40})$$

$$G_T^{\gamma Z}(q^2) = -\frac{i}{q^2} \frac{\Sigma_T^{\gamma Z}(q^2)}{q^2 - M_Z^2} \quad (\text{C.41})$$

$$G_T^{ZZ}(q^2) = \frac{i}{q^2 - M_Z^2} \left(1 - \frac{\Sigma_T^{ZZ}(q^2)}{q^2 - M_Z^2} \right) \quad (\text{C.42})$$

D. LSZ Reduction Formula for Fermions in the EWSM

This appendix is dedicated to the derivation of the LSZ reduction formula for fermions and the corresponding normalization factors in a theory in which left- and right-handed fermions have different interactions. The LSZ theorem was first published in Reference [43] and gives a relation between Green functions and S-matrix elements in a quantum field theory. The calculation in the following subsections is based on Reference [44].

D.1. In- and Out-fields

The incoming and outgoing states that are used to describe scattering amplitudes are defined as free-particle states with the physical mass m and normalized to unity. They are created by the fields ψ_i and ψ_o , where the subscripts are used to denote incoming and outgoing fields. The fields are normalized by the requirement that the corresponding particle wave functions are properly normalized and need to obey the Dirac equation

$$(i\cancel{\partial} - \tilde{m}) \psi_{i/o}(x) = 0. \quad (\text{D.1})$$

The normalization condition reads

$$\langle 0 | T \{ \psi_{i/o}(x) \bar{\psi}_{i/o}(y) \} | 0 \rangle = \int \frac{d^4 k}{(2\pi)^4} e^{-ik(x-y)} iS_f(k), \quad (\text{D.2})$$

where

$$iS_f(k) = i \frac{\cancel{k} + \tilde{m}}{k^2 - \tilde{m}^2} \quad (\text{D.3})$$

is the unperturbed momentum space propagator and \tilde{m} is the on-shell mass. The fields ψ_i and ψ_o can be constructed from the interacting field ψ that adheres to the Dirac equation

$$(i\not{\partial} - m_0) \psi(x) = j(x), \quad (\text{D.4})$$

where m_0 is the bare fermion mass and $j(x)$ describes the coupling of the interacting field to other fields or external sources. Using the retarded and advanced propagators

$$S_{\text{ret}}(x, y) = \theta(x^0 - y^0) \int \frac{d^4k}{(2\pi)^4} e^{-ik(x-y)} S_f(k), \quad (\text{D.5a})$$

$$S_{\text{adv}}(x, y) = \theta(y^0 - x^0) \int \frac{d^4k}{(2\pi)^4} e^{-ik(x-y)} S_f(k), \quad (\text{D.5b})$$

the in- and out-fields can be written as

$$\mathcal{Z}^{-\frac{1}{2}} \psi_i(x) := \psi(x) - \int d^4y S_{\text{ret}}(x, y) (j(y) + (m_0 - \tilde{m}) \psi(y)), \quad (\text{D.6a})$$

$$\mathcal{Z}^{-\frac{1}{2}} \psi_o(x) := \psi(x) - \int d^4y S_{\text{adv}}(x, y) (j(y) + (m_0 - \tilde{m}) \psi(y)) \quad (\text{D.6b})$$

in terms of a yet undetermined normalization constant \mathcal{Z} . Technically, the constant \mathcal{Z} is closely related to the field renormalization constant that is introduced in quantum field theories to hide UV-singularities and renormalizing ψ directly affects \mathcal{Z} , as can be read off Equation (D.6) and as will be shown explicitly in Section D.3. However, the physical reason for either normalization is very different. By construction, the fields defined by Equation (D.6) solve (D.1) and \mathcal{Z} can be adjusted so that the condition (D.2) is fulfilled, too, which proves that (D.6) are in fact the in- and out-fields introduced in the beginning. The normalization \mathcal{Z} is allowed to carry an axial structure and the parametrization and shortcuts

$$\sqrt{\mathcal{Z}} = \sqrt{1 + \delta\mathcal{Z}_V + \delta Z_A \gamma_5} = 1 + \frac{1}{2} \delta\mathcal{Z}_V + \frac{1}{2} \delta\mathcal{Z}_A \gamma_5 + \mathcal{O}(\delta^2), \quad (\text{D.7a})$$

$$\sqrt{\mathcal{Z}^\dagger} = 1 + \frac{1}{2} \delta\mathcal{Z}_V - \frac{1}{2} \delta\mathcal{Z}_A \gamma_5 + \mathcal{O}(\delta^2) \quad (\text{D.7b})$$

with perturbatively small real valued numbers $\delta\mathcal{L}_V$ and $\delta\mathcal{L}_A$ will be used in the following. The matrix structure needs to be respected, because it implies $\psi_{i/o}(x)\mathcal{Z} \neq \mathcal{Z}\psi_{i/o}(x)$. Due to the use of the retarded and advanced propagators, ψ_i and ψ_o obey the limiting behavior

$$\psi(x) \xrightarrow{t \rightarrow -\infty} \mathcal{Z}^{-\frac{1}{2}}\psi_i, \quad (\text{D.8a})$$

$$\psi(x) \xrightarrow{t \rightarrow +\infty} \mathcal{Z}^{-\frac{1}{2}}\psi_o \quad (\text{D.8b})$$

by means of weak operator convergence.¹ The in- and out-fields can be Fourier expanded using creation and annihilation operators,

$$\psi_{i/o}(x) = \frac{1}{(2\pi)^3} \sum_s \int \frac{d^3p}{2E_p} \left[u^s(p) a_{i/o}^s(p) e^{-ipx} + v^s(p) b_{i/o}^{s\dagger}(p) e^{+ipx} \right], \quad (\text{D.9a})$$

$$\bar{\psi}_{i/o}(x) = \frac{1}{(2\pi)^3} \sum_s \int \frac{d^3p}{2E_p} \left[\bar{v}^s(p) b_{i/o}^s(p) e^{-ipx} + \bar{u}^s(p) a_{i/o}^{s\dagger}(p) e^{+ipx} \right], \quad (\text{D.9b})$$

where $u^s(p)$ and $v^s(p)$ are Dirac spinors in terms of the physical mass and $a_{i/o}^s$ and $b_{i/o}^s$ obey the anticommutation relations,

$$\left\{ a_{i/o}^s(p), a_{i/o}^{s'\dagger}(p') \right\} = \left\{ b_{i/o}^s(p), b_{i/o}^{s'\dagger}(p') \right\} = 2E_p (2\pi)^3 \delta^{(3)}(\mathbf{p} - \mathbf{p}') \delta_{ss'}, \quad (\text{D.10})$$

with all other anticommutators equal to zero. The inverse of Equation (D.9) regarding the particle creators and annihilators reads

$$a_{i/o}^{s\dagger}(p) = \int d^3x \psi_{i/o}^\dagger(x) u^s(p) e^{-ipx}, \quad (\text{D.11a})$$

$$a_{i/o}^s(p) = \int d^3x u^{s\dagger}(p) \psi_{i/o}(x) e^{+ipx}. \quad (\text{D.11b})$$

and will be required to express one-particle state in terms of the in- and out-fields.

¹See References [43] and [44] for details.

D.2. Reduction Formula

With the in- and out-fields constructed in the previous section, it is now possible to derive the reduction formula. To that end, consider the scattering amplitude

$$S_{p,\alpha\rightarrow\beta} = {}_o\langle\beta|(ps),\alpha\rangle_i, \quad (\text{D.12})$$

where $|(ps),\alpha\rangle_i$ and ${}_o\langle\beta|$ are in- and out-states, respectively, (ps) denotes a single fermion with momentum p and spin s and α and β refer to an unspecified state of many particles. Using Equation (D.11), the amplitude $S_{p,\alpha\rightarrow\beta}$ can be written as

$$\begin{aligned} {}_o\langle\beta|(ps),\alpha\rangle_i &= {}_o\langle\beta - (ps)|\alpha\rangle_i + {}_o\langle\beta| \left(a_i^{s\dagger}(p) - a_o^{s\dagger}(p) \right) |\alpha\rangle_i \\ &= {}_o\langle\beta - (ps)|\alpha\rangle_i + \int d^3x {}_o\langle\beta| \left(\psi_i^\dagger(x) - \psi_o^\dagger(x) \right) e^{-ipx} u^s(p) |\alpha\rangle_i. \end{aligned} \quad (\text{D.13})$$

The term ${}_o\langle\beta - (ps)|\alpha\rangle_i$ is the scattering amplitude in which the fermion (ps) is removed from the final state denoted by β . The state ${}_o\langle\beta - (ps)|$ is unequal zero only if β contains a fermion with momentum p and spin s . In that case, $S_{p,\alpha\rightarrow\beta}$ describes a forward scattering process which would be represented by disconnected Feynman diagrams. Hence, the first term on the right-hand side of Equation (D.13) will be omitted in the following. Replacing the in- and out-fields using the asymptotic condition (D.8) yields

$$\begin{aligned} S_{p,\alpha\rightarrow\beta} &\sim - \left(\lim_{t\rightarrow+\infty} - \lim_{t\rightarrow-\infty} \right) \int d^3x {}_o\langle\beta|\psi^\dagger(x)\sqrt{\mathcal{L}}e^{-ipx}u^s(p)|\alpha\rangle_i \\ &= - \int d^4x {}_o\langle\beta|\frac{\partial}{\partial x^0} \left(\bar{\psi}(x)\gamma_0\sqrt{\mathcal{L}}u^s(p)e^{-ipx} \right) |\alpha\rangle_i, \end{aligned} \quad (\text{D.14})$$

where the tilde sign indicates that the forward scattering term is missing. The expression on the last line is obtained with the aid of the fundamental theorem of calculus. As $u^s(p)e^{-ipx}$ solves the Dirac equation, its time derivative is

$$\gamma_0\sqrt{\mathcal{L}}\frac{\partial}{\partial x^0}u^s(p)e^{-ipx} = \sqrt{\mathcal{L}^\dagger}(\gamma\nabla - im)u^s(p)e^{-ipx}. \quad (\text{D.15})$$

Using integration by parts and omitting surface terms allows combining the differential operators. One finds

$$\begin{aligned} \int d^4x \left[\left(\frac{\partial}{\partial x^0} \bar{\psi}(x) \right) \gamma_0 \sqrt{\mathcal{L}} + \bar{\psi}(x) \sqrt{\mathcal{L}^\dagger} (\gamma \nabla - im) \right] u^s(p) e^{-ipx} \\ = -i \int d^4x \bar{\psi}(x) \sqrt{\mathcal{L}^\dagger} \left(i \overleftarrow{\not{\partial}} + m \right) u^s(p) e^{-ipx}, \end{aligned} \quad (\text{D.16})$$

where the derivative $\overleftarrow{\not{\partial}}$ acts on $\bar{\psi}(x)$ only. Inserting Equation (D.16) into (D.14) expresses the scattering amplitude in terms of an expectation value of the fermion field $\psi(x)$,

$$S_{p,\alpha \rightarrow \beta} \sim i \int d^4x \langle \beta | \bar{\psi}(x) | \alpha \rangle_i \sqrt{\mathcal{L}^\dagger} \left(i \overleftarrow{\not{\partial}} + m \right) u^s(p) e^{-ipx}. \quad (\text{D.17})$$

Using the Fourier transform $\bar{\psi}(x) = \int \frac{d^4q}{(2\pi)^4} e^{-iqx} \bar{\psi}(q)$ of the fermion field yields the momentum space expression

$$S_{p,\alpha \rightarrow \beta} \sim -i \langle \beta | \bar{\psi}(-p) | \alpha \rangle_i \sqrt{\mathcal{L}^\dagger} (\not{p} - m) u^s(p). \quad (\text{D.18})$$

The calculation outlined above can also be applied to removing a fermion from the out-state. Repeating the same steps when starting with $\langle \beta | \psi(p) | \alpha \rangle_i$ leads to the similar result

$$S_{\alpha \rightarrow p, \beta} \sim -i \bar{u}^s(p) (\not{p} - m) \sqrt{\mathcal{L}} \langle \beta | \psi(-p) | \alpha \rangle_i. \quad (\text{D.19})$$

Equations (D.18) and (D.19) can be repeatedly applied until all particles in the initial and final states are represented by field operators sandwiched between vacuum states. Such a projection $\langle 0 | \psi_1 \dots \psi_n | 0 \rangle$ is a Green function of the theory, so that the reduction formula gives a relation between S-matrix elements and Green functions, eventually. It remains to derive an expression for the LSZ factors \mathcal{L} , which is done in Section D.3.

D.3. Normalization

The normalization constant \mathcal{Z} in Equation (D.6) accounts for self interactions of the interacting field as can be seen in Equation (D.8). Accordingly, it is fully determined by the two-point functions of the in- and out-fields and the interacting fields. Equation (D.8) implies the relation

$$\langle 0|T\{\psi(x)\bar{\psi}(y)\}|0\rangle_{\text{on-shell}} = \mathcal{Z}^{-\frac{1}{2}} \langle 0|T\{\psi_{i/o}(x)\bar{\psi}_{i/o}(y)\}|0\rangle_{\text{on-shell}} \mathcal{Z}^{\dagger-\frac{1}{2}} \quad (\text{D.20})$$

for large x^0 and y^0 , but since the two-point function only depends on the difference of x and y , the equation is universally valid and can be used to determine the normalization constant \mathcal{Z} . Inserting the propagators of the free and interacting theories yields

$$\frac{1}{\not{p} - \tilde{m}} = \sqrt{\mathcal{Z}} \frac{1}{\not{p} - m_0 + \Sigma(\not{p})} \sqrt{\mathcal{Z}^\dagger}, \quad (\text{D.21})$$

where $\Sigma(\not{p})$ is the renormalized self-energy of the interacting theory and \tilde{m} and m_0 are the on-shell and bare mass, respectively. Since (D.21) is a matrix equation, it is convenient to project either side onto a Dirac spinor, as the resulting equation is still sufficient to solve for \mathcal{Z} . Taking the inverse on either side and projecting onto the spinor $u(p, \tilde{m})$ yields

$$\frac{1}{\not{p} - \tilde{m}} \mathcal{Z}^{\dagger-\frac{1}{2}} (\not{p} - m_0 + \Sigma(\not{p})) \mathcal{Z}^{-\frac{1}{2}} u(p, \tilde{m}) = u(p, \tilde{m}). \quad (\text{D.22})$$

This expression can be solved for $\delta\mathcal{Z}_V$ and $\delta\mathcal{Z}_A$ when inserting Equation (D.7). The calculation similar to the one outlined in Section 5.3.3 and yields

$$\delta\mathcal{Z}_V = \Sigma_V(\tilde{m}^2) + \delta Z_V + 2\tilde{m}^2 \left(\Sigma'_V(\tilde{m}^2) + \Sigma'_S(\tilde{m}^2) \right), \quad (\text{D.23a})$$

$$\delta\mathcal{Z}_A = \Sigma_A(\tilde{m}^2) + \delta Z_A, \quad (\text{D.23b})$$

where δZ_V and δZ_A are the vector and axial vector renormalization constants, respectively. If one decides to not renormalize the fields ($\delta Z_V = \delta Z_A = 0$), the LSZ factors (D.23) will pick up the leftover UV-poles, so that the scattering matrix elements are finite even though the Green functions are not.

D.4. Amputation of Green Functions

Equations (D.18) and (D.19) give a relation between S-matrix elements and Green functions of the interacting theory. The S-matrix element is obtained by multiplying the corresponding Green function with the LSZ factors

$$-i\sqrt{\mathcal{Z}^\dagger}(\not{p} - \tilde{m}) u^s(p, \tilde{m}) \quad (\text{D.24a})$$

for each incoming fermion and

$$-i\bar{u}^s(p, \tilde{m})(\not{p} - \tilde{m})\sqrt{\mathcal{Z}} \quad (\text{D.24b})$$

for each fermion in the final state. The external fermion lines of the Green functions represent the fermion propagators, so that the product of a Green function and LSZ factors contains terms of the form

$$\frac{1}{\not{p} - m_0 + \Sigma(\not{p})}\sqrt{\mathcal{Z}^\dagger}(\not{p} - \tilde{m})u^s(p, \tilde{m}) = \mathcal{Z}^{-\frac{1}{2}}u^s(p, \tilde{m}), \quad (\text{D.25a})$$

$$\bar{u}^s(p, \tilde{m})(\not{p} - m)\sqrt{\mathcal{Z}}\frac{1}{\not{p} - m_0 + \Sigma(\not{p})} = \bar{u}^s(p, \tilde{m})\mathcal{Z}^{\dagger-\frac{1}{2}}. \quad (\text{D.25b})$$

The right-hand sides are immediate consequences of Equation (D.21). Accordingly, an S-matrix element is obtained by multiplying the corresponding amputated Green function with the right-hand sides of Equations (D.25a) and (D.25b) for incoming and outgoing fermions, respectively.

Bibliography

- [1] D. Becker et al., „The P2 Experiment“, *The European Physical Journal A* **54**, 208 (2018) 10.1140/epja/i2018-12611-6.
- [2] M. Böhm, H. Spiesberger, and W. Hollik, „On the One-Loop Renormalization of the Electroweak Standard Model and Its Application to Leptonic Processes“, *Fortsch. Phys.* **34**, 687 (1986) 10.1002/prop.19860341102.
- [3] M. Böhm, A. Denner, and H. Joos, *Gauge Theories of the Strong and Electroweak Interaction* (Vieweg+Teubner Verlag, 2001).
- [4] A. Sirlin, „Radiative Corrections in the $SU(2)_L \times U(1)$ Theory: A Simple Renormalization Framework“, *Phys. Rev. D* **22**, 971 (1980) 10.1103/PhysRevD.22.971.
- [5] W. F. L. Hollik, „Radiative Corrections in the Standard Model and their Role for Precision Tests of the Electroweak Theory“, *Fortsch. Phys.* **38**, 165 (1990) 10.1002/prop.2190380302.
- [6] A. Sirlin, „Role of $\sin^2 \theta_W(m_Z)$ at the Z^0 Peak“, *Phys. Lett. B* **232**, 123 (1989) 10.1016/0370-2693(89)90568-6.
- [7] G. Degrossi, S. Fanchiotti, and A. Sirlin, „Relations Between the On-Shell and \overline{MS} Frameworks and the M_W - M_Z Interdependence“, *Nucl. Phys. B* **351**, 49 (1991) 10.1016/0550-3213(91)90081-8.
- [8] M. Peskin and D. Schroeder, *An Introduction to Quantum Field Theory*, Advanced book program (Addison-Wesley Publishing Company, 1995).
- [9] J. Erler, „Calculation of the QED Coupling $\alpha(M_Z)$ in the Modified Minimal Subtraction Scheme“, *Phys. Rev. D* **59**, 054008 (1999) 10.1103/PhysRevD.59.054008, arXiv:hep-ph/9803453 [hep-ph].

- [10] A. Czarnecki and W. J. Marciano, „Polarized Moller Scattering Asymmetries“, *Int. J. Mod. Phys.* **A15**, 2365 (2000) 10.1016/S0217-751X(00)00243-0, 10.1142/S0217751X00002433, arXiv:hep-ph/0003049 [hep-ph].
- [11] T. Appelquist and J. Carazzone, „Infrared Singularities and Massive Fields“, *Phys. Rev.* **D11**, 2856 (1975) 10.1103/PhysRevD.11.2856.
- [12] B. A. Ovrut and H. J. Schnitzer, „Gauge Theories With Minimal Subtraction and the Decoupling Theorem“, *Nucl. Phys.* **B179**, 381 (1981) 10.1016/0550-3213(81)90011-0.
- [13] W. Bernreuther and W. Wetzel, „Decoupling of Heavy Quarks in the Minimal Subtraction Scheme“, *Nucl. Phys.* **B197**, [Erratum: *Nucl. Phys.*B513 758(1998)], 228 (1982) 10.1016/0550-3213(82)90288-7, 10.1016/S0550-3213(97)00811-0.
- [14] W. Bernreuther, „Decoupling of Heavy Quarks in Quantum Chromodynamics“, *Annals Phys.* **151**, 127 (1983) 10.1016/0003-4916(83)90317-2.
- [15] G. Rodrigo and A. Santamaria, „QCD Matching Conditions at Thresholds“, *Phys. Lett.* **B313**, 441 (1993) 10.1016/0370-2693(93)90016-B, arXiv:hep-ph/9305305 [hep-ph].
- [16] W. Bernreuther, „Threshold Effects on the QCD Coupling $\alpha_{\overline{\text{MS}}}$ “, in *Proceedings: Workshop on QCD at LEP: Determinations of α_s from Inclusive Observables*, Aachen, Germany, Apr 11, 1994 (1994), pp. 39–46, arXiv:hep-ph/9409390 [hep-ph].
- [17] J. Erler and M. J. Ramsey-Musolf, „The Weak Mixing Angle at Low Energies“, *Phys. Rev.* **D72**, 073003 (2005) 10.1103/PhysRevD.72.073003, arXiv:hep-ph/0409169 [hep-ph].
- [18] J. Erler and R. Ferro-Hernández, „Weak Mixing Angle in the Thomson Limit“, *JHEP* **03**, 196 (2018) 10.1007/JHEP03(2018)196, arXiv:1712.09146 [hep-ph].

-
- [19] K. G. Chetyrkin, J. H. Kühn, and M. Steinhauser, „Three-Loop Polarization Function and $\mathcal{O}(\alpha_s^2)$ Corrections to the Production of Heavy Quarks“, Nucl. Phys. **B482**, 213 (1996) 10.1016/S0550-3213(96)00534-2, arXiv:hep-ph/9606230 [hep-ph].
- [20] N. Cabibbo and R. Gatto, „Electron-Positron Colliding Beam Experiments“, Phys. Rev. **124**, 1577 (1961) 10.1103/PhysRev.124.1577.
- [21] M. Davier, A. Hoecker, B. Malaescu, and Z. Zhang, „Reevaluation of the Hadronic Vacuum Polarisation Contributions to the Standard Model Predictions of the Muon $g - 2$ and $\alpha(m_Z^2)$ Using Newest Hadronic Cross-Section Data“, Eur. Phys. J. **C77**, 827 (2017) 10.1140/epjc/s10052-017-5161-6, arXiv:1706.09436 [hep-ph].
- [22] F. Jegerlehner and R. Szafron, „ ρ^0 - γ Mixing in the Neutral Channel Pion Form Factor F_π^e and its Role in Comparing e^+e^- with τ Spectral Functions“, Eur. Phys. J. **C71**, 1632 (2011) 10.1140/epjc/s10052-011-1632-3, arXiv:1101.2872 [hep-ph].
- [23] A. O. G. Kallen and A. Sabry, „Fourth Order Vacuum Polarization“, Kong. Dan. Vid. Sel. Mat. Fys. Med. **29**, [555(1955)], 1 (1955) 10.1007/978-3-319-00627-7_93.
- [24] B. A. Kniehl, „Two-Loop QED Vertex Correction From Virtual Heavy Fermions“, Phys. Lett. **B237**, 127 (1990) 10.1016/0370-2693(90)90474-K.
- [25] S. A. Larin, T. van Ritbergen, and J. A. M. Vermaseren, „The Large Quark Mass Expansion of $\Gamma(Z^0 \rightarrow \text{Hadrons})$ and $\Gamma(\tau^- \rightarrow \nu_\tau + \text{Hadrons})$ in the Order α_s^3 “, Nucl. Phys. **B438**, 278 (1995) 10.1016/0550-3213(94)00574-X, arXiv:hep-ph/9411260 [hep-ph].
- [26] C. Patrignani et al. (Particle Data Group), „Review of Particle Physics“, Chin. Phys. **C40**, 100001 (2016) 10.1088/1674-1137/40/10/100001.

- [27] K. G. Chetyrkin, B. A. Kniehl, and M. Steinhauser, „Decoupling Relations to $\mathcal{O}(\alpha_s^3)$ and their Connection to Low-Energy Theorems“, Nucl. Phys. **B510**, 61 (1998) 10.1016/S0550-3213(98)81004-3, 10.1016/S0550-3213(97)00649-4, arXiv:hep-ph/9708255 [hep-ph].
- [28] K. G. Chetyrkin, B. A. Kniehl, and M. Steinhauser, „Strong Coupling Constant with Flavor Thresholds at Four Loops in the MS Scheme“, Phys. Rev. Lett. **79**, 2184 (1997) 10.1103/PhysRevLett.79.2184, arXiv:hep-ph/9706430.
- [29] W. J. Marciano and A. Sirlin, „Radiative Corrections to Atomic Parity Violation“, Phys. Rev. **D27**, 552 (1983) 10.1103/PhysRevD.27.552.
- [30] M. J. Musolf, T. W. Donnelly, J. Dubach, S. J. Pollock, S. Kowalski, and E. J. Beise, „Intermediate-Energy Semileptonic Probes of the Hadronic Neutral Current“, Phys. Rept. **239**, 1 (1994) 10.1016/0370-1573(94)90040-X.
- [31] J. C. Bernauer, „Measurement of the Elastic Electron-Proton Cross Section and Separation of the Electric and Magnetic Form Factor in the Q^2 Range from 0.004 to 1 (GeV/c)²“, PhD thesis (Johannes Gutenberg-Universität, Institut für Kernphysik, 2010).
- [32] J. C. Bernauer et al. (A1), „Electric and Magnetic Form Factors of the Proton“, Phys. Rev. C **90**, 015206 (2014) 10.1103/PhysRevC.90.015206, arXiv:1307.6227 [nucl-ex].
- [33] L. C. Maximon and J. A. Tjon, „Radiative Corrections to Electron-Proton Scattering“, Phys. Rev. C **62**, 054320 (2000) 10.1103/PhysRevC.62.054320, arXiv:nuc1-th/0002058.
- [34] S. Weinberg, „Effective Gauge Theories“, Phys. Lett. **91B**, 51 (1980) 10.1016/0370-2693(80)90660-7.
- [35] L. J. Hall, „Grand Unification of Effective Gauge Theories“, Nucl. Phys. B **178**, 75 (1981) 10.1016/0550-3213(81)90498-3.

-
- [36] S. P. Martin, „Matching Relations for Decoupling in the Standard Model at Two Loops and Beyond“, *Phys. Rev. D* **99**, 033007 (2019) 10.1103/PhysRevD.99.033007, arXiv:1812.04100 [hep-ph].
- [37] A. Denner, „Techniques for Calculation of Electroweak Radiative Corrections at the One-Loop Level and Results for W -Physics at LEP-200“, *Fortsch. Phys.* **41**, 307 (1993) 10.1002/prop.2190410402, arXiv:0709.1075 [hep-ph].
- [38] R. L. Workman et al. (Particle Data Group), „Review of Particle Physics“, *PTEP* **2022**, 083C01 (2022) 10.1093/ptep/ptac097.
- [39] H. H. Patel, „Package-X: A Mathematica Package for the Analytic Calculation of One-Loop Integrals“, *Comput. Phys. Commun.* **197**, 276 (2015) 10.1016/j.cpc.2015.08.017, arXiv:1503.01469 [hep-ph].
- [40] V. Shtabovenko, R. Mertig, and F. Orellana, „New Developments in FeynCalc 9.0“, *Comput. Phys. Commun.* **207**, 432 (2016) 10.1016/j.cpc.2016.06.008, arXiv:1601.01167 [hep-ph].
- [41] V. Shtabovenko, „FeynHelpers: Connecting FeynCalc to FIRE and Package-X“, *Comput. Phys. Commun.* **218**, 48 (2017) 10.1016/j.cpc.2017.04.014, arXiv:1611.06793 [physics.comp-ph].
- [42] W. J. Marciano and A. Sirlin, „Radiative Corrections to Neutrino-Induced Neutral-Current Phenomena in the $SU(2)_L \times U(1)$ Theory“, *Phys. Rev. D* **22**, [Erratum: *Phys. Rev. D* **31**, 213(1985)], 2695 (1980) 10.1103/PhysRevD.31.213, 10.1103/PhysRevD.22.2695.
- [43] H. Lehmann, K. Symanzik, and W. Zimmermann, „On the Formulation of Quantized Field Theories“, *Nuovo Cim.* **1**, 205 (1955) 10.1007/BF02731765.
- [44] J. D. Bjorken and S. D. Drell, *Relativistic Quantum Fields* (1965).

